Technische Universität München
TUM School of Life Sciences

TUM

Separation of the major whey proteins α-Lactalbumin and β-Lactoglobulin by means of selective precipitation and continuous centrifugal separation

Nicole Haller

Acknowledgement

Content

Abbreviations and Symbols

Abbreviation	Meaning	Unit
A_p	Particle area	μm^2
a_z	Centrifugal acceleration	$m\ s^{-2}$
AC	Affinity chromatography	
ACE	Angiotensin-converting enzyme	
AEC	Anion exchange chromatography	
Ala	Alanine	
ANOVA	Analysis of variance	
Asn	Asparagine	
ATR	Attenuated total reflectance	
Arg	Arginine	
Asp	Aspartic acid	
BAMLET	Bovine α-lactalbumin made lethal to tumour cells	
BCAA	Branched chain amino acid	
BSA	Bovine serum albumin	
c_F	Frictional coefficient	
C_t	Protein concentration after heat treatment	$g\ L^{-1}$
C_W	Solids weight fraction	
c_0, c_1, c_2, c_3	Constants used for curve fitting	
C_0	Initial protein concentration	$g\ L^{-1}$
$CaCl_2$	Calcium chloride	
CEC	Cation exchange chromatography	
CF	Concentration factor	
CFD	Computational fluid dynamics	
Cys	Cysteine	
$d_{XX,3}$	Percentile of volume-based particle size distribution	μm
d_p	Particle diameter	μm
D	Denatured state	
DD	Degree of denaturation	%
DEM	Discrete element method	
DF	Diafiltration	

Abbreviation	Meaning	Unit
DIW	De-ionized water	
DSC	Differential scanning calorimetry	
DTT	Dithiothreitol	
EDTA	Ethylene-diamine-tetraacetic acid	
EtOH	Ethanol	
F	Specific adhesion force	N
$f(\phi)$	Solids flux function	
F_A	Linkage forces	N
F_B	Buoyant force	N
F_C	Acceleration force	N
F_F	Frictional force	N
F_G	Gravity force	N
FTIR	Fourier-transform infrared spectroscopy	
g	Acceleration of gravity	$m\ s^{-2}$
Gly	Glycine	
Gln	Glutamine	
Glu	Glutamic Acid	
GMO	Genetically modified organism	
GMP	Glycomacropeptide	
GRAS	Generally regarded as safe	
h_0	Initial suspension height in batch settling test	cm
H_0	Suspension height	mm
H_∞	Equilibrium sediment bed height	mm
HAMLET	Human α-lactalbumin made lethal to tumour cells	
HCl	Hydrogen chloride	
His	Histidine	
HIV	Human immunodeficiency virus	
IEC	Ion exchange chromatography	
IEP	Isoelectric point	
IgG	Immunoglobulin G	
Ile	Isoleucine	
k	Consistency index	Pa s

Abbreviation	Meaning	Unit
k_{x-xx}	Velocity constant of denaturation	s^{-1}
kDa	Kilo Dalton	
Leu	Leucine	
LF	Lactoferrin	
Lys	Lysine	
m_p	Particle mass	g
MF	Microfiltration	
MGS	Molten globule state	
MWCO	Molecular weight cut-off	kDa
n	Reaction order	
n	Flow index	
N	Native state	
NaCl	Sodium chloride	
NaOH	Sodium hydroxide	
N.d.	No data	
NMR	Nuclear magnetic resonance	
OD	Optical density	
p	Pressure	$kg\ m^{-1}\ s^{-2}$
p	Statistical significance	
$P_y(\phi)$	Compressive yield stress	Pa
PAGE	Polyacrylamide gel electrophoresis	
PCA	Principal component analysis	
PEI	Polyetherimide	
PEG	Polyethylene glycol	
PES	Polyethersulfone	
Perm.	Permeate	
Phe	Phenylalanine	
Pro	Proline	
q_0	Number-based distribution density of particle size	
Q_0	Cumulative number-based distribution of particle size	
q_3	Volume-based distribution density of particle size	

Abbreviation	Meaning	Unit
Q_3	Cumulative volume-based distribution of particle size	
$R(\phi)$	Hindered settling factor	
R_{max}	Radius from central axis to the sample bottom	mm
RD	Resolubilization degree	
Re	Reynolds number	
Ret.	Retentate	
RP-HPLC	Reverse phase high performance liquid chromatography	
SD	Standard deviation	
SDS	Sodium dodecyl sulfate	
SEM	Scanning electron microscopy	
Ser	Serine	
SH	Sulfhydryl	
t	Time	s
T	Transmission	
TFA	Trifluoroacetic acid	
TFF	Tangential flow filtration	
Thr	Threonine	
TR-IR	Time-resolved infrared	
Try	Tryptophane	
U	Unfolded state	
u_p	Particle settling velocity	$m\ s^{-1}$
u_{St}	Stokes settling velocity	$m\ s^{-1}$
UFDF	Ultrafiltration in diafiltration mode	
UV	Ultraviolet	
V_p	Particle volume	m^3
WPC	Whey protein concentrate	
WPI	Whey protein isolate	
$w\ v^{-1}$	Weight/volume	$kg\ L^{-1}$
$w\ w^{-1}$	Weight/weight	$kg\ kg^{-1}$
x	Particle diameter	µm
X_P	Precipitated fraction	

Greek symbols	Meaning	Unit
α-La	α-Lactalbumin	
β-Lg	β-Lactoglobulin	
Δn	Differential speed of scroll	rpm
γ	Shear rate	s^{-1}
η_f	Viscosity of the fluid	$N\ s\ m^{-2}$
η_{sep}	Separation efficiency	%
ρ_f	Fluid density	$g\ cm^{-3}$
ρ_p	Particle density	$g\ cm^{-3}$
ρ_s	Suspension density	$g\ cm^{-3}$
ϕ	Volume fraction	
ϕ_s	Volume fraction of solids	
τ	Shear stress	Pa
τ_0	Yield shear stress	Pa
ω	Angular velocity	s^{-1}

1 General Introduction

Since several decades, whey proteins and thereof derived products became one of the most important and lucrative branches in dairy industry. Even if the trend of vegan dietary is rapidly emerging, forecast reports predict that the global whey protein market size will keep on growing over the next years. It is projected to reach 15.7 billion USD by 2026. There are several reasons that are driving the market growth, one of them is the continuously rising demand for performance and sports nutrition, as well as nutritional supplements. Another one is the growing birth rates especially in the Asian Pacific area with an increasing demand for infant nutrition, but also the local rising awareness about the high nutritional value of whey proteins.

Generally, liquid whey is a low-cost byproduct from cheese manufacturing. By its concentration, demineralization and spray drying, the sales price of the product is increased tremendously. It was recognized that a separation of the whey protein bulk into the single whey protein fractions is the subsequent step to create an even higher value and turns it into a premium product. This allows a more directed use of the single whey proteins and enables exploiting the full nutritional or techno-functional potential of the individual protein fraction.

Over the last decades, many different separation processes have been proposed addressing the target of an effective isolation of the individual whey protein fractions. However, all of them are showing distinct deficiencies, either in terms of the final product purity, the overall yield or production costs, which is often related to a missing scalability of the process.

This thesis proposes an innovative process for the separation of the major whey protein fractions, named α-Lactalbumin (α-La) and β-Lactoglobulin (β-Lg). The process basically consists of two production steps. The first one is a selective thermal aggregation of one of the major whey protein fractions, while the counterpart remains native and soluble in the liquid phase. The second step is the separation of the aggregated fraction from the liquid phase by using a continuous decanter centrifuge. The selective aggregation of each of the major fractions, α-La and β-Lg, respectively, was followed by subsequent centrifugal separation, which was investigated as an own topic. The aim was to develop a new, efficient, and scalable process, which delivers high purity protein fractions.

This thesis is based on published research articles. The following introductive chapter provides the fundamentals base and summarizes the current state-of-art knowledge. After the description of the theoretical background, the published research articles will examine specific parts of the proposed process. The thesis concludes with an overall discussion covering the published results separately presented as individual publications in one context and evaluating to what extent the targets have been met.

1.1 Whey proteins

Historians assume that already more than 8,000 years ago in the region of Southwest Asia, the first cheese was manufactured initiated by natural fermentation of stored milk in the warm climate, resulting in the separation in a coagulated casein curd and liquid whey (Fox et al., 2017). The concept of cheese making spread globally. However, the yellowish remainder liquid, the whey, was ever since regarded as a waste stream. It was dumped in rivers, used to fed pigs or other livestock or spread as fertilizer (Tunick, 2008). With the industrial mass production of cheese, the amount of whey exploded and became a severe environmental pollution issue (Guo, 2019). In the early twentieth century, efforts were taken focusing on the utilization and preservation of whey. In the 1970s the membrane filtration technique enabled the breakthrough by recovering the whey proteins in the form of whey protein concentrate (WPC) and whey protein isolate (WPI) (Smithers, 2008).

There are two categories of whey, the sweet whey being a byproduct of rennet-coagulated cheese, and the acid whey, which is the byproduct of acid-coagulated cheese. The sweet whey has a pH value of at least 5.6. while acid whey has a pH below 5.1. Acid whey does typically not contain glycomacropeptide (GMP), which is formed by enzymatic degradation using rennet. Apart from this difference, the composition of the two whey types is quite similar, as can be seen in Tab. 1-1.

Tab. 1-1: Typical composition of sweet and acid whey (Tunick, 2008).

	Sweet whey	Acid whey
Protein (g L^{-1})	6-10	6-8
Lactose (g L^{-1})	46-52	44-46
Minerals (g L^{-1})	2.5-4.7	4.3-7.2
pH	>5.6	<5.6

The protein fraction is considered the most precious component in whey. The main proteins are named α-Lactalbumin (α-La), β-Lactoglobulin (β-Lg), immunoglobulin G (IgG), bovine serum albumin (BSA), and lactoferrin (LF). These five proteins make up approximately 85% of bovine and human whey proteins, respectively.

Comparing the composition of whey proteins in human and bovine milks, some distinct differences are seen. Firstly, the bovine milk has double the amount of caseins than human milk does. Secondly, the protein β-Lg is absent in human milk, but it is the main protein fraction in bovine whey. Further, human mother's milk shows a significantly higher content of α-La and LF than bovine whey. The complete composition is listed in Tab. 1-2.

Tab. 1-2: Concentration of protein fractions of bovine and human milk (Layman et al., 2018).

	Human milk %	Bovine milk %
Whey proteins		
α-La	36	17
β-Lg	0	52
IgG	17	10
HSA/BSA	6	5
LF	25	1.5
other	10	14.5
Percent of total protein	60	20
Caseins		
β-casein	68	36
κ-casein	20	14
α_{s1}-casein	12	40
α_{s2}-casein	0	10
Percent of total protein	40	80

For infant nutrition, mother's breast milk is certainly the golden standard. However, for various reasons, it is often required to rely on commercially available infant formulations that are based on bovine milk. The composition of infant formulas is under continuous modification with the overall goal to reach the golden standard of human mother's milk. In that course, the overall protein content was reduced, specifically the casein fraction, and the proportion of α-La was increased in order to approach the human's milk amino acid profile (Lien, 2003). In studies comparing infants fed with standard formula to infants fed with formula with added α-La and lowered protein content, the neonates being fed with the α-La enriched formula had growth and development outcomes more similar to breast-fed infants (Lönnerdal and Lien, 2003; Petersen et al., 2020; Trabulsi et al., 2011). Moreover, β-Lg is suspected to cause cow's milk allergy, as this protein is not meant to be consumed by infants and thus it is recognized as allergen triggering a respective immune response (Järvinen et al., 2001; Selo et al., 1999)

1.1.1   α-Lactalbumin

Naturally, α-La is produced in the epithelial cells of the mammary gland, where it supports the formation of lactose synthase, which catalyzes the conversation of glucose and galactose into lactose (Brew and Hill, 1975).

α-La is a globular protein consisting of 123 amino acid residues with a respective molecular weight of 14.2 kDa (Permyakov, 2020). The X-ray crystallography structure of α-La is depicted in Fig. 1-1. This protein consists of two domains, the α- and

β-domain, being connected via the calcium binding loop. The name of both domains originates from the predominant secondary structural motif in the respective domain. The α-domain comprises three α-helices (residues 5–11, 23–34, and 86–99) and two 3_{10}-helices (residues 17–21 and 115–119) shown in blue. The smaller β-domain is composed of antiparallel β-sheets (residues 40–43, 47–50, and 55–56) shown in green, a series of loops, and a 3_{10}-helix (76–82). It contains eight cysteines (shown in yellow), which form four disulfide bonds and are mainly determining the native structure (Chang and Li, 2002). One disulfide bridge is located in the β-subdomain, two disulfide bonds are in the α-subdomain, and one bridges the α- and β-subdomains.
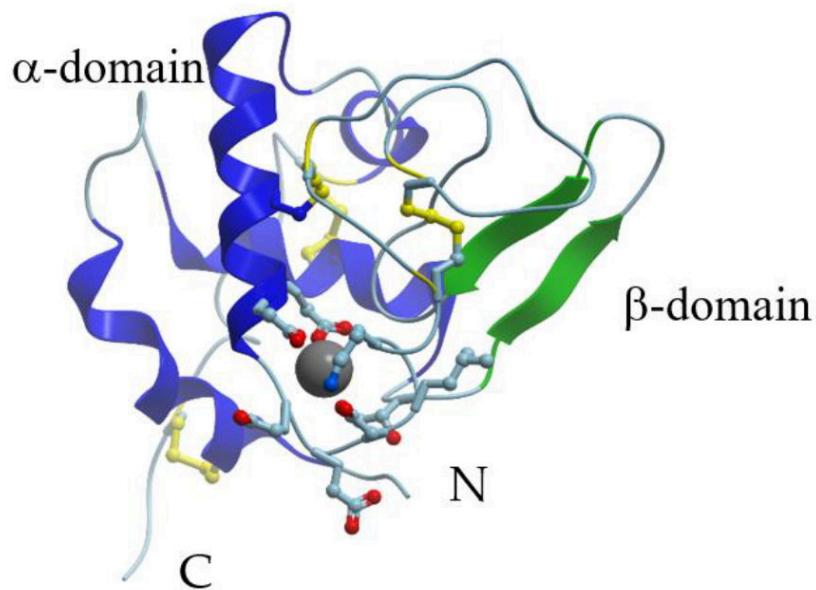
Fig. 1-1 X-ray structure of human α-La showing division in α- and β-domain. Dark grey sphere represents bound calcium ion, α-helices are shown in blue, β-sheets in green, and disulfide bridges in yellow (Permyakov, 2020).

α-La is categorized a metalloprotein, because it has natively bound a calcium ion (dark gray sphere) connecting two molecular domains (Hiraoka et al., 1980). It is this structural element of α-La that allows for a targeted weakening of its globular structure to enable its selective thermal precipitation under mild conditions, thus avoiding or minimizing aggregation of other whey proteins. This is applied as a key processing aspect in this work. The primary calcium-binding site is formed by Asp82, Asp84, Asp87, Asp88, and Lys79 (Permyakov et al., 1981). The calcium-bound form is called the holo-α-La, while the calcium-depleted form is referred to as apo-α-La. There is also a weaker, secondary calcium-binding site, formed by Thr38, Gln39, Asp83, and Leu81, which has a lower relevance for the protein conformation (Chandra et al., 1998). The primary calcium-binding site of α-La is capable of binding several other cations, such as Cd^{2+}, Mg^{2+}, Mn^{2+}, Pb^{2+}, Sr^{2+}, Na^+, and K^+ (Noyelle and van Dael, 2002; Veprintsev et al., 1996; Aramini et al., 1996). Additionally, the protein possesses several Zn^{2+}-binding sites, the strongest one being

located near the N-terminus. At this site, also interactions with Al^{3+}, Co^{2+}, Hg^{2+}, and other cations were reported (Berliner et al., 1987; Noyelle and van Dael, 2002; Permyakov and Berliner, 2000; van Dael et al., 1992; Veprintsev et al., 1996). Naturally, the cation-binding capability is suspected to be related to a temperature regulation of α-La and potentially other functions in the mammary gland. In food technologies, this property could be exploited for food fortification (Barone et al., 2021).

Generally, hydrophobic residues (Leu, Val, Ile, Ala, Gly, Phe, and Pro) are buried inside of a protein, while hydrophilic residues (Ser, Thr, Cys, Asn, Gln, Arg, His, Glu and Asp) are exposed to the solvent. As shown in Fig. 1-2, the most hydrophobic residues on the protein surface are located between the α- and β-domains. Therefore, this area is called hydrophobic box. The isoelectric point (IEP) of α-La is between 4.2 to 4.5 (Bramaud et al., 1997b; Kronman et al., 1964).
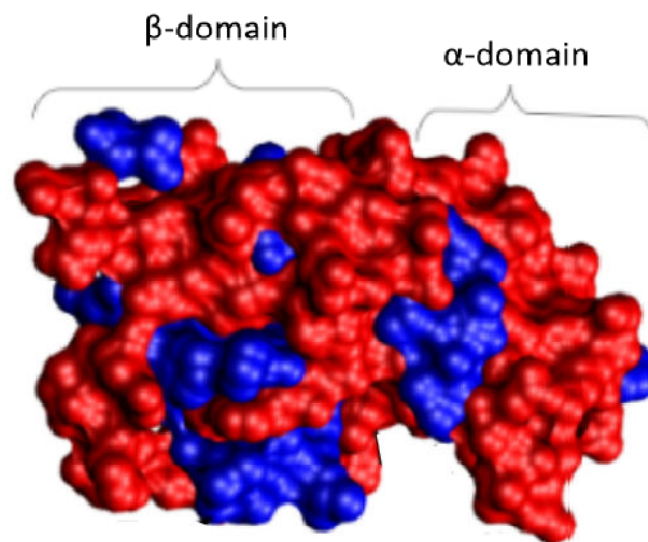
Fig. 1-2 Hydrophilic (red) and hydrophobic (blue) surface residues of α-La (Pansri, 2012).

In various studies, diverse beneficial effects and potential medical applications of isolated α-La have been described, which are listed in the following.

- Improvement of gut development and immunity in infants (Boscaini et al., 2019; Heine et al., 1991).
- Stimulating the growth of beneficial bacteria in the intestinal tract (Layman et al., 2018; Lönnerdal and Lien, 2003).
- Regulation of sleep: reduce the time for infants to fall asleep, lengthen the deep sleep periods and the overall time of sleeping. (Aparicio et al., 2007)
- Improvement of mood and brain measures by tryptophan intake through α-La (Markus et al., 2000; Markus et al., 2005).
- Glutathione (synthesized from cysteine, glutamate, and glycine) plays a major role in protection of cells against oxidative stress. Studies showed that

- supplementation with Cys-rich whey proteins increased blood levels of glutathione and improved the quality of life among HIV-positive individuals (Grey et al., 2003; Jaziri et al., 1992; Micke et al., 2002).
- α-La has a high level of branched-chain amino acids (BCAA, Leu, Ile, Val), which is essential for muscle contraction and also provides material for *de novo* synthesis of skeletal muscle protein. Studies prove that whey protein intake together with resistant exercise lead to increased muscle mass and strength, as well as to an enhanced recovery (Huang et al., 2017; Phillips et al., 2009; Snijders et al., 2015; Tipton et al., 2007).
- An innovative way of cancer treatment by human/bovine α-La made lethal to tumor cells (HAMLET/BAMLET) (Delgado et al., 2015a; Gustafsson et al., 2005; Hoque et al., 2016).
- Protective effect in epileptogenesis (Russo et al., 2012).

1.1.2 β-Lactoglobulin

β-Lg is the predominant bovine whey protein and presumably the one that was studied most extensively. It belongs to the group of lipocalins and is able to bind hydrophobic compounds such as vitamins and fatty acids. Though, the true biological role is still speculative, but is likely related to this property (Mandalari et al., 2009; Perez et al., 1992; Puyol et al., 1995).

Bovine β-Lg is a globular protein consisting of 162 amino acids with a respective molecular weight of 18.3 kDa (Qin et al., 1998). The secondary structure of β-Lg is composed of 50% β-sheet, 15% α-helix, and 15-20% reverse turn (Creamer et al., 1983; Sawyer and Kontopidis, 2000). The nine β-strands labelled A to I, are arranged to form a barrel-like globular structure, called a calyx (Fig. 1-3).

β-Lg contains five cysteine residues, forming disulfide bridges between Cys66-Cys160 and Cys106-Cys119, respectively (Papiz et al., 1986). The disulfide bonds link strands G to H and strand D to the C-terminal. The fifth thiol residue, Cys121 is a free thiol group that lies buried in the center of β-Lg structure and is not accessible under physiological conditions (Burova et al., 1998; Qin et al., 1998).

Fig. 1-3 Crystal structures of bovine β-Lg (Oliveira et al., 2001).

About a dozen genetic variants of β-Lg have been detected in vertebrates, with the A and B variants being the most common (Godovac-Zimmermann et al., 1996). These two variants differ in two amino acid residues. Variant A has Asp64 and Val118, while variant B has Gly64 and Ala118. These two different amino acids are located on a flexible surface loop and in the hydrophobic core, thus not causing any differences in tertiary structure at neutral pH of the two genetic variants (Sawyer and Kontopidis, 2000). However, some differences between the two variants were reported for thermal denaturation temperature and reaction rate (Manderson et al., 1999; O'Kennedy et al., 2006), susceptibility to chemicals (Bouhallab et al., 2004; Boye et al., 2004), affinity for aliphatic compounds (Loch et al., 2013), and differences in IEP (Yan et al., 2013).

Under physiological conditions, β-Lg mainly appears as non-covalently bound dimers (McKenzie, 1967). The A-variant tends to grow to tetramers between pH 3.5 and 5.5, which may even form octamers at low temperatures (Sawyer and James, 1982; Timasheff and Townend, 1964). Below pH 3.5 and above 7.5 it exists as a monomer (Gottschalk et al., 2003). High-resolution X-ray structural studies showed that at low pH values, the EF loop (residues 85-90) blocks the access to the calyx similar like a lid (Oliveira et al., 2001). Whereas at pH values from 7.1 to 8.2, it adopts a conformation where the access to the calyx is open (Qin et al., 1998). This conformational change is known as the Tanford transition and has functional implications for the reversible binding and release of ligands (Tanford et al., 1959).

Different values for the IEP can be found in literature, ranging from 5.2 to 5.4 (Nozaki et al., 1959; Reithel and Kelly, 1971). Electrostatic potential contours show that the positive and negative domains of the β-Lg dimer are located on opposite sides with approximately equal strength. This is exemplarily shown for different pH

values between 4.0 to 5.2 and ionic strength of 0.0045 M in Fig. 1-4. With the net charge being close to zero, many proteins exhibit a diminished solubility near the isoelectric point. This phenomenon is often referred to as isoelectric precipitation, corresponding to the loss of aggregation-inhibiting repulsion. Interestingly, for β-Lg the maximum aggregation occurs instead at a pH of 4.6, where the net charge is significantly positive. However, the main driver are the highly asymmetric electrostatic potential contours at pH 4.6 (Majhi et al., 2006).
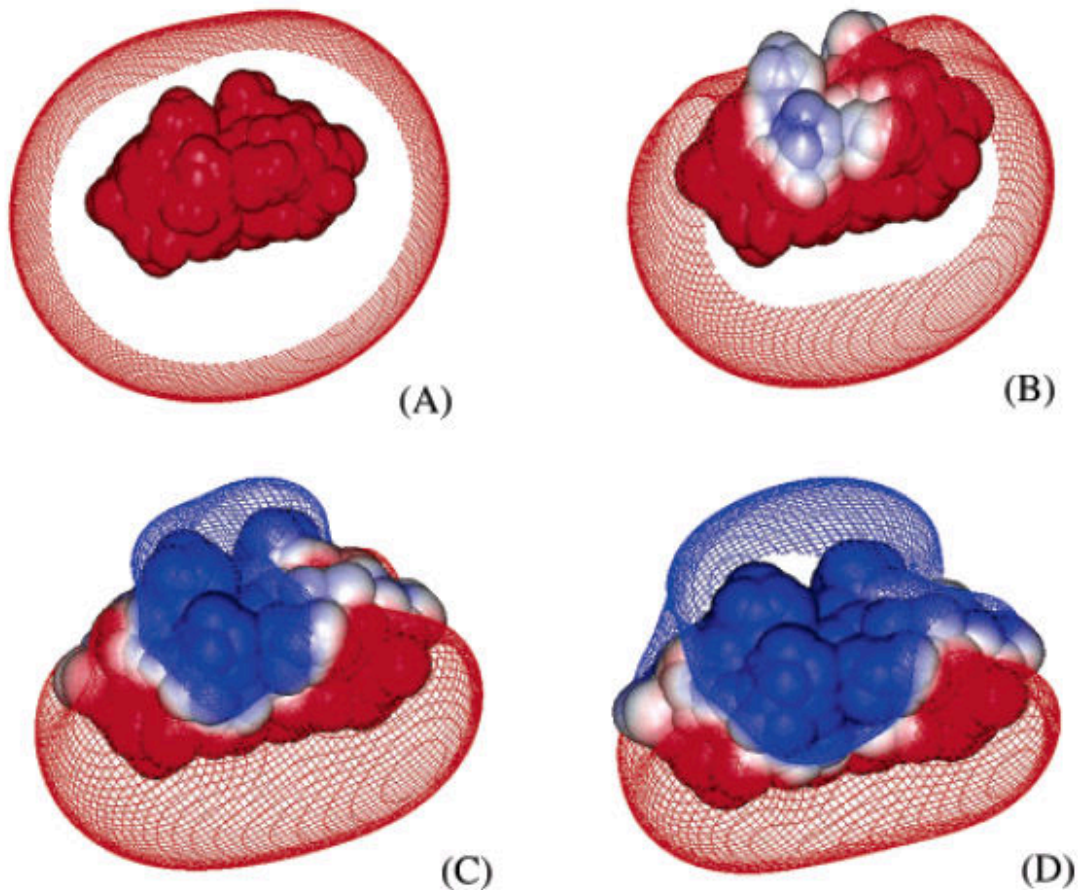
Fig. 1-4 Electrostatic potential contours positive charge in red and negative charge in blue around the β-Lg dimer at ionic strength 0.0045 M, and at pH (A) 4.0, (B) 4.6, (C) 5.0, and (D) 5.2 (Majhi et al., 2006).

The protein β-Lg in an isolated form shows several medicinal and physiological activities, which are listed in the following.

- Various peptides derived from proteolytic digestion β-Lg with pepsin, trypsin or chymotrypsin inhibit the angiotensin-converting enzyme (ACE) activity (Mullally et al., 1997). This inhibition contributes to a proper regulation of blood pressure in humans (Ortiz-Chao et al., 2009).
- β-Lg is a rich source of Cys, which appears to stimulate the glutathione synthesis, an anticarcinogenic tripeptide that protects against intestinal cancer (McIntosh et al., 1995).

- Chemically modified β-Lg was shown to inhibit HIV (Neurath et al., 1997; Wyand et al., 1999).
- β-Lg was found to bind to human ileostomy glycoproteins, which significantly reduces the level of adhesion of different bacteria like *Klebsiella* and *E. coli* (Ouwehand et al., 1997).
- A peptide derived from β-Lg was reported to exhibit greater hypocholesterolemic activity in comparison with that of available medicine (Nagaoka et al., 2001).
- β-Lg enhances intestinal uptake of retinol, triglyceride, and long-chain fatty acids and may play a role in the absorption and subsequent metabolism of fatty acids (Kushibiki et al., 2001).
- Finally, it is a rich source of BCAA, which stimulate muscle protein synthesis, and is appreciated as sportive nutrition (Tipton et al., 2007).

However, the real value of β-Lg is mostly seen in its impressive techno-functional properties, making it an indispensable source in food industry. β-Lg has excellent heat-set gelation characteristics, providing water-binding capabilities and a controllable texturization of formulated foods (Mulvihill and Kinsella, 1988). It has a great foamability that is comparable to egg white proteins (Foegeding et al., 2006). Microparticulates produced from β-Lg can be used as a fat-replacer for yoghurt, ice cream, and cheese (Ipsen, 2017; Koxholt et al., 1999; Sturaro et al., 2015; Torres et al., 2018).

1.2 Thermal denaturation of whey proteins

There is a broad fundament of knowledge available on the selective thermal denaturation of the main whey proteins, which is in this thesis used as a steppingstone to develop an innovative separation method of α-La and β-Lg. To better understand the methodologic approach described in the results section, the basics of the whey proteins´ thermal reactivity are comprehensively summarized in this chapter.

In general, the reaction scheme of a protein exposed to heat-treatment is described in the following three-step model.

$$N \leftrightarrow U \rightarrow A$$

N being the native state, where the protein is in its naturally correct conformation. Upon heating, the protein starts to unfold (U) and loses some structural parts of its initial native conformation. Sometimes this state is also referred to as the molten globule state (MGS). This (partial) unfolding is – to a certain extent – reversible. With continuation of heating, the molecule will completely and irreversibly lose the native structure, known as denatured state (D). This is often accompanied with intermolecular aggregation. The extent of the aggregation is determined by the protein's thermodynamic reactivity.

The terms "aggregation" and "precipitation" are often used interchangeably in literature. Without attempting to resolve this ambiguity, in this thesis, the term aggregation is used when relating to an irreversible, chemical binding reaction, such as intermolecular disulfide bridging. The term precipitation shall relate to generally reversible crowding reactions of molecules, as e.g., isoelectric precipitation, when protein concentrations are exceeding the solubility limit, and hydrophobic interactions that occur when hydrophobic inner surfaces are exposed under certain conditions.

1.2.1 Unfolding and precipitation mechanism of α-Lactalbumin

Due to its four stabilizing disulfide bonds, α-La presents an excellent heat stability under physiological conditions and neutral pH (Havea et al., 2000). At an acidic pH, the bound Ca^{2+}-ion is released from α-La, which shifts the equilibrium towards the apo-form. An additional calcium-complexing agent, such as EDTA (Bernal and Jelen, 1984), sodium hexametaphosphate (Alomirah and Alli, 2004), lactic acid (Lucena et al., 2007), or citrate (Bramaud et al., 1997b) prevents the re-transition to holo-state. In the calcium-free apo-form, the hydrophobic parts of the α-La protein are easier accessible, which is further promoted by gentle heating up to 60 °C (Bonnaillie and Tomasula, 2012). Under these conditions, α-La forms precipitates, most likely caused by a combination of hydrophobic and electrostatic interactions (Pedersen et al., 2006). The formed precipitates enable a size-based separation either by microfiltration (MF) or centrifugation (Gésan-Guiziou et al., 1999; Lucena et al., 2007; Toro-Sierra et al., 2013).

The calcium-bound holo-α-La has a significantly higher stability compared to the calcium-depleted apo-form (Vanderheeren and Hanssens, 1994; Veprintsev et al., 1997). The thermal unfolding of apo-α-La starts at temperatures as low as 10 °C, while the unfolding of the holo-form requires temperature of at least 60 °C (De Wit and Klarenbeek, 1984; Permyakov et al., 1985). The unfolding results in a small decrease in the α-helix content leading to a partial exposure of inner-laying Try residues and other hydrophobic parts. Furthermore, in the calcium-depleted form, α-La has a higher sensitivity to pH and ionic conditions due to uncompensated negative charge-charge interactions at the cation binding site, what results in an overall reduced molecular stability against adverse milieu or processing conditions (Griko and Remeta, 1999). All of these smaller structural changes are generally reversible upon cooling, as long as the four disulfide bridges remain intact.

Heating the isolated protein up to 85 °C at a neutral pH does not lead to any (irreversible) aggregation (Bertrand-Harb et al., 2002). However, it is assumed that a reorganization of the disulfide bridges can appear at that temperature, which remains after cooling (McGuffey et al., 2005). Interestingly, when α-La is heated together with other proteins comprising a free thiol group, it can lead to an irreversible denaturation of α-La (Calvo et al., 1993). The reactivity and thus the tendency to

irreversibly aggregate increases significantly in the presence of reactive proteins containing free SH-groups, such as β-Lg at elevated temperatures (Boye and Alli, 2000; Schokker et al., 2000).

α-La is a popular model protein for folding studies, because of its ability to transition into a MGS. In this state, the protein is still compact, the radius of gyration increases to 17.2 Å, which is only about 10% larger compared to the native molecule (Kataoka et al., 1997). The MGS is further characterized by a flexible tertiary structure with simultaneous presence of most secondary structure (Dolgikh et al., 1981; Kuwajima, 1996). The MGS is of high interest, because the transition from the MGS to the native state (apo and holo) is fully reversible. A high stability of the MGS was observed under the following conditions (Kuwajima, 1996):

- Addition of a strong denaturant such as guanidine hydrochloride or urea (Gast et al., 1998; Redfield et al., 1999; Smith et al., 2005)
- In the acid-denatured state, which is fully stabilized at pH 2.0, often called the A-state (Alexandrescu et al., 1993; Rösner and Redfield, 2009)
- In the apo-form at low ionic strength (Griko and Remeta, 1999; Xie et al., 1993; Yutani et al., 1992)

1.2.2   Unfolding and aggregation mechanism of β-Lactoglobulin

The thermal behaviour of β-Lg at physiological conditions is schematically shown in Fig. 1-5. At room temperature, β-Lg mainly exists as a non-covalently linked dimer. Upon heating up to 55 °C, it dissociates into monomers and small conformational changes may occur. By long-term heating at a temperature between 60 to 70 °C, β-Lg may transition into the MGS. Other studies reported the existence of a MGS under different conditions, e.g., at pH 6.7 and temperatures between 70 to 130 °C (Qi et al., 1997), at pH 2.6 and 1 h of heating at 80 °C (Tavel et al., 2010), or after the exposure to a pressure 600 MPa at 50 °C for more than 1 h (Yang et al., 2001). However, up to date it is controversially discussed whether this molecular state of β-Lg should be termed MGS or not (Dickinson and Matsumura, 1994; Ptitsyn and Uversky, 1994; Qi et al., 1997). At temperatures above 65 °C partial unfolding of monomers leads to the exposure of usually buried inner hydrophobic groups and the free thiol group at Cys121. At temperatures between 75 to 85 °C large aggregates are formed by intermolecular hydrophobic interactions and thiol/disulfide exchange reactions. At temperatures higher than 85 °C, the disulfide bridging is the predominant polymerization mechanism, resulting in smaller sized aggregates. At temperatures above 125 °C a breakdown of the chemical structure occurs, resulting in complete denaturation of the protein.

Structure	Temperature	Time	Result
(N)(○)	20°C	———	Native dimer
↓↑			Dissociation at conc. ≤ 25 mg/ml
2x (R)	55°C	———	Monomers
↓			
(S)	60 - 70°C	≥ 15 min	Molten globule $\Delta H^{\ddagger}$ =142 kJ/mol
↓			
(S)(S)	65-75°C	5-10 min	Partial unfolding $\Delta H^{\ddagger}$ = 280 kJ/mol Dimerization by thiol-oxidation
↓			
Large aggregates	75 - 85°C	5- 10 min	Disulphide and hydrophobic aggregation
↓			
Small aggregates	85 - 105°C	≈10 min and fast cooling	Only disulphide aggregation
↓			
Physical and Chemical reactions	> 125°C	5- 10 min	Disulphide breakdown and Complete unfolding
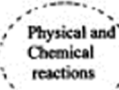
Fig. 1-5 Schematic presentation of the proposed thermal behavior of β-Lg at pH > 6.8 between 20 and 150 °C (De Wit, 2009).

Under selected conditions (20 to 90 g L^{-1} in water at pH 7.0, 78 °C), a heat-treatment of pure β-Lg and β-Lg in WPI for at least 30 min results in the generation of non-native monomers (Kehoe et al., 2011). The difference lies in the exposure of the Cys119 as a free thiol group instead of the Cys121, which causes larger hydrodynamic conformation, a low solubility at acidic pH values, as well as a significantly lower reactivity in a second heating cycle (Croguennec et al., 2003).

Generally, the heat-induced aggregation of β-Lg can be interpreted as a two-step reaction scheme. Fig. 1-6 shows the temperature influence on the β-Lg denaturation kinetic rate in the temperature range from 68 to 96 °C. There is a sharp bend in the Arrhenius plot around 80 °C. Below 80 °C the β-Lg denaturation reaction is unfolding limited, which means that aggregation is faster than unfolding of the protein occurs. Above 80 °C all β-Lg molecules are rapidly unfolding, and the aggregation is the rate limiting reaction step. The unfolding reaction is mostly described as a first order reaction, while the aggregation reaction step is reported to have a reaction order of 1.5 (Anema, 2000; Dannenberg and Kessler, 1988; Le Bon et al., 1999; Petit et al., 2016; Tolkach, 2008). It is also noteworthy that beside the temperature, the calcium concentration is another important influencing factor on the kinetic rates, which can be seen in Fig. 1-6 as well. The increase of the reaction rate can be explained by the reduction of the negative net charge of β-Lg by the

positively charged Ca^{2+}-ions, which results in lowered intermolecular repulsive forces.
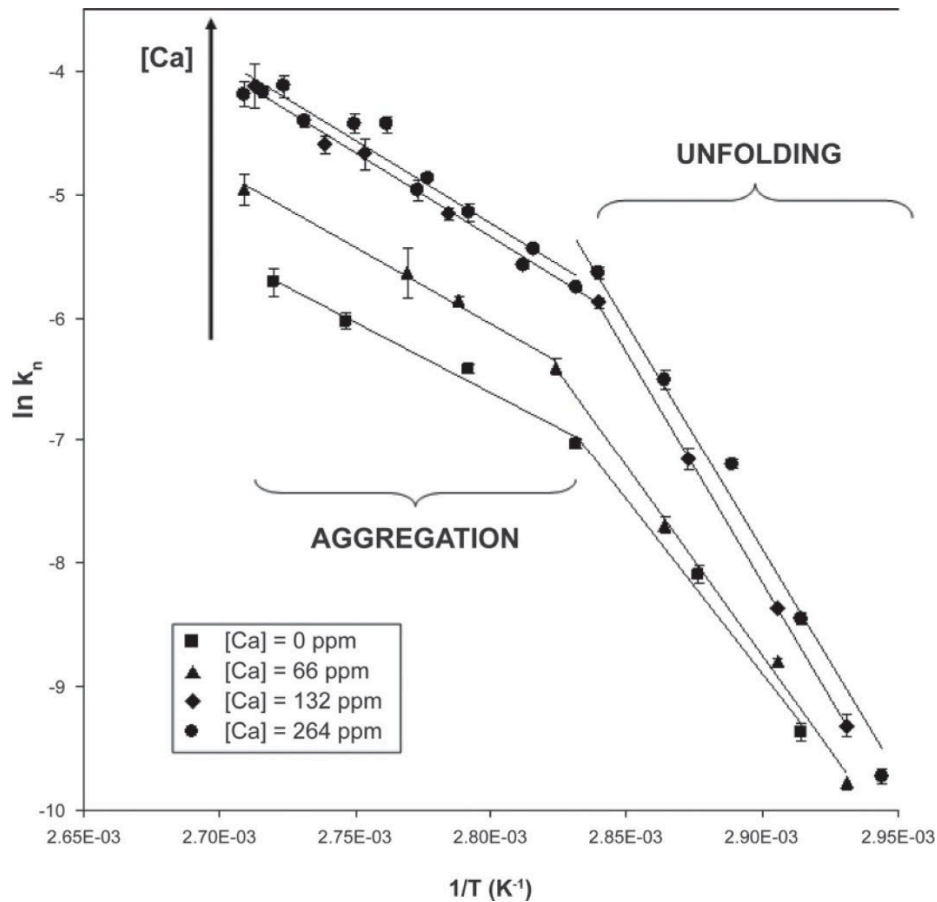
Fig. 1-6 Arrhenius plot for the β-lg denaturation reaction with 1.5 reaction order at various Ca concentrations. The solid lines correspond to the linear regressions of experimental data and k_n being the denaturation reaction rate ($g^{1-n} \cdot L^{n-1} \cdot s^{-1}$) (Petit et al., 2011).

1.2.3 Denaturation kinetics of whey protein mixtures

The respective whey proteins naturally do not exist as pure fractions but occur as mixtures of several proteins. A heat treatment of such a protein mixture can lead to a deviant denaturation and aggregation behaviour compared to the heating of an isolated fraction. As described in chapter 1.2.1, α-La alone does not tend to form aggregates, when heated above 75 °C at a neutral pH. However, if proteins with a reactive free thiol group, such as β-Lg, are present, α-La gets involved in the thiol-disulfide exchange reactions as well (Gezimati et al., 1997). This causes an irreversible incorporation of α-La into the β-Lg aggregates and the loss of its native form. This means that a heat treatment aiming to form stable β-Lg aggregates, will always sacrifice a certain amount of the native α-La. The main influencing factors of the degree of denaturation (DD) are temperature, heat holding time, and total protein concentration. However, also the environmental conditions, such as pH, calcium and lactose content affect the overall denaturation result.

Tolkach et al. (2005) extensively studied the denaturation kinetics of α-La and β-Lg when heating whey protein concentrate.

The general kinetic equation with the reaction order n ($n \neq 0$) is described as

$$\left(\frac{C_t}{C_0}\right)^{1-n} = 1 + (n-1) \cdot k \, t \tag{1.1}$$

Where C_t is the protein concertation after heating, C_0 is the initial protein concentration, k (s^{-1}) is the velocity constant, and t the treatment time. The reaction order n was determined by calculation of maximal regression coefficient R^2, and resulted in a reaction order of 1 for α-La and 1.5 for β-Lg.

The velocity constant of α-La's thermal denaturation $k_{\alpha-La}$ can be described as

$$k_{\alpha-La} = - \, ln\left(\frac{C_{\alpha-La,t}}{C_{\alpha-La,0}}\right) \cdot \frac{1}{t} \tag{1.2}$$

with $C_{\alpha-La,0}$ and $C_{\alpha-La,t}$ being the concentrations of native α-La in g L^{-1} before and after heat treatment for holding times t.

The concentration-independent velocity constant of the thermal denaturation of β-Lg is $k_{\beta\text{-}Lg}$, which can be calculated with the following equation

$$k_{\beta-Lg} = k_{\beta-Lg/1.5} \cdot C_{\beta-Lg,0}^{0.5} \tag{1.3}$$

with $k_{\beta\text{-}Lg/1.5}$ being the concentration-independent velocity constant of thermal denaturation of β-Lg.

In Fig. 1-7 the influence of the heating temperature on the velocity constant of β-Lg (left) and α-La (right) are shown, respectively. On the right axes of these Arrhenius plots the time to reach a certain DD (99.5% for β-Lg and 25% for α-La) are given. The different curves represent various protein concentrations that were investigated. The higher the protein concentration, the shorter is the time required to meet the targeted DD. This finding is supported by various other studies (Dissanayake et al., 2013a; Fitzsimons et al., 2007; Wolz and Kulozik, 2015). It is remarkable that β-Lg denatures much faster than α-La does. Also, other research articles confirmed that in the early stages of heating, the formed aggregates contained relatively more β-Lg than α-La, whereas in the later stages they contained equal amounts of both proteins (Dalgleish et al., 1997). These observations suggest that α-La has a kind of lag-phase until it is "activated" by β-Lg (Schokker et al., 2000). Moreover, the underlying binding mechanisms seem to change. The prevalence of non-covalent bonding was reported to be much higher, when α-La is involved in the aggregation compared to β-Lg being heated alone (Havea et al., 2001; McSwiney et al., 1994a; Mulvihill and Donovan, 1987).
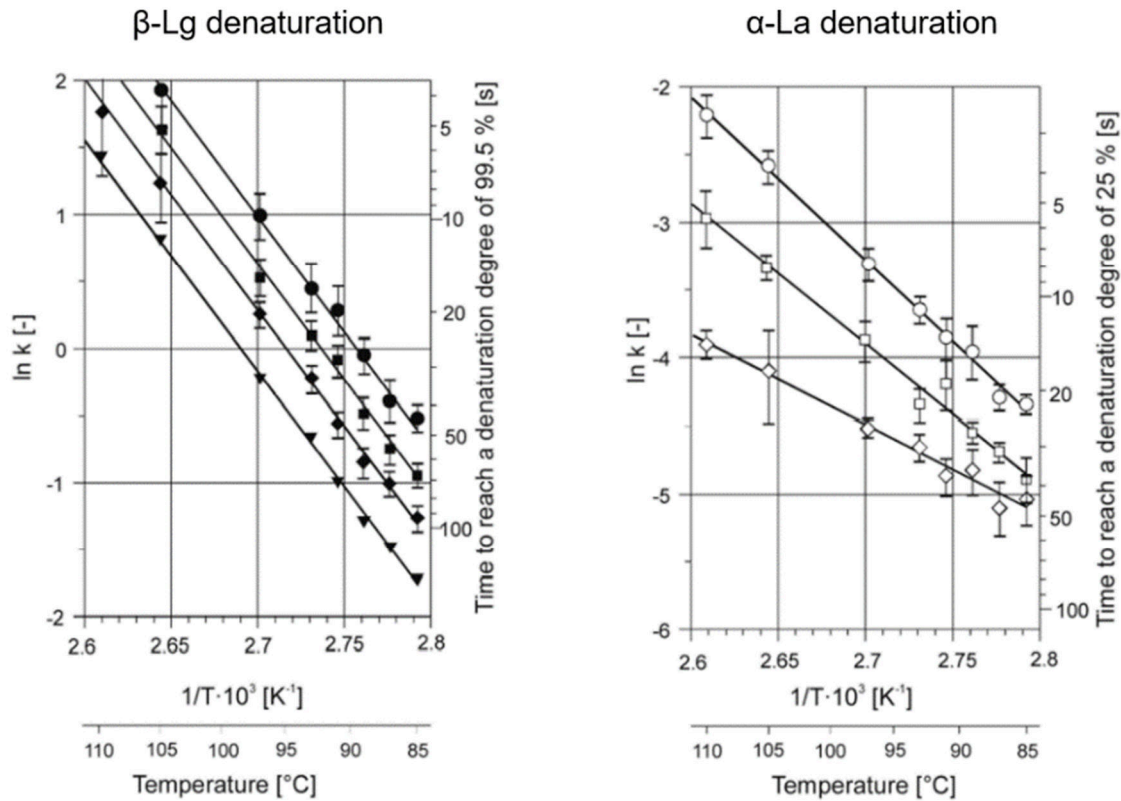
Fig. 1-7 Influence of the heating temperature on the velocity constant of β-Lg (left) and α-La denaturation (right) according to Arrhenius equation at different total protein concentrations: (●/○) = 20 g L^{-1}; (■/□) = 10 g L^{-1}; (♦/◊) = 5 g L^{-1}; (▼) = concentration independent velocity constant. Environmental parameters: pH 7.5, calcium content 0.55 g L^{-1}, lactose content 0.5 g L^{-1}. Modified from Tolkach et al. (2005).

Using this knowledge, it is possible to apply a heat treatment resulting in a high DD of β-Lg, while keeping α-La native to a maximum extent. This approach is commonly called a selective thermal aggregation of one specific protein and served as a fundament for the process developed in this thesis. Besides the target of a high selectivity in the aggregation step, another objective was to produce aggregates or precipitates that present suitable characteristics for centrifugal separation.

In fact, not only the DD can be controlled via the applied heating conditions, but also the form and specifically the size of the generated aggregates can be directed (see Fig. 1-8). Spiegel (1999b) described the dependency of the aggregate structure on the applied heating temperature. A low temperature (in this case < 85 °C) in the unfolding-limited range results in a loose and porous structure. The higher the heating temperature, the more rigid and condensed the structure gets. The reason that the aggregate structure is temperature-depend, is that different molecular binding mechanisms are involved in the aggregate formation depending on the applied temperature. Especially the importance of non-covalent interactions varies with temperature (Galani and Apenten, 1999; Iametti et al., 1995). Galani and Apenten (1999) reported that the contribution of non-covalent interactions to the overall aggregation mechanism has a higher importance at temperatures above

15

90 °C. It is assumed that the formation of non-covalent bonding precedes the thiol-disulfide exchange, making the latter reaction easier by creating a non-polar environment and prolonging the contact time between the molecules (Schokker et al., 2000). This is also supposed to be the reason for this more rigid and compact structure of the aggregates, when heated at higher temperatures.

In terms of sizes, the smallest aggregates are found when heated in the range of kinetic transition area. In the unfolding- and aggregation-limited temperature range, the aggregate size was significantly higher, and reached sizes up to 100 μm (Spiegel, 1999b). In general, it can be noted that such aggregates are highly favorable for separation by centrifuge.
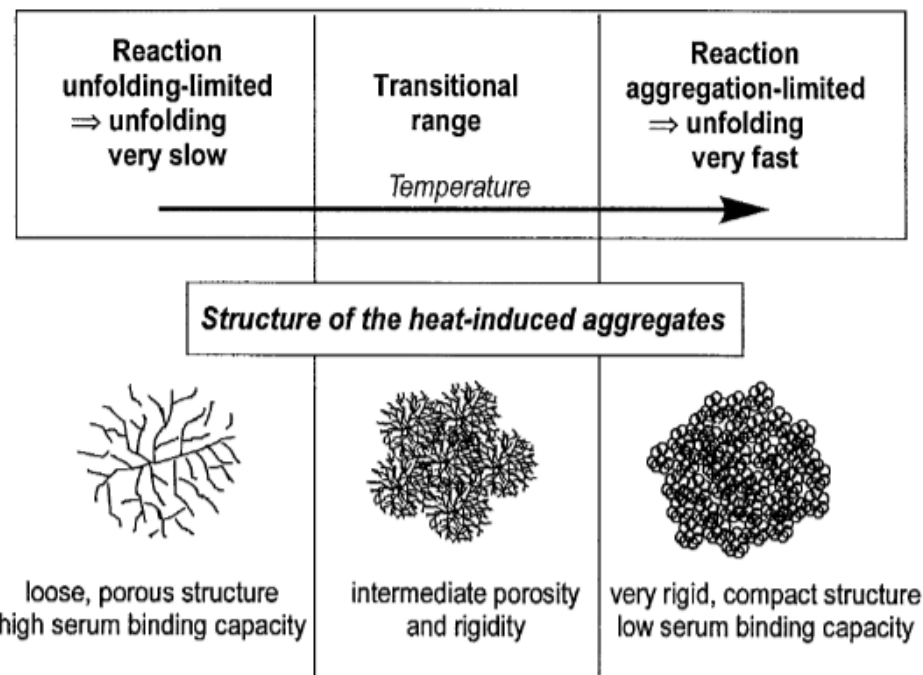
Fig. 1-8 Structure of heat-induced whey protein aggregates in dependency of temperature. Modified from Spiegel (1999b).

Regarding the structure of α-La precipitates and how it can be influenced, only little is known. Bonnaillie and Tomasula (2012) investigated the precipitate formation by confocal fluorescence microscopy and reported a growth of the particles with progressing incubation time. Furthermore, they reported that the heating temperature is not only influencing the speed of the precipitation, also the resulting size seems to be affected. In the investigated range between 50 and 70 °C, the final precipitate sizes seemed largest at 60 °C. The suspected sizes of the precipitates based on the microscopic images were about 200 to 300 μm. However, when determined in a particle size analyzer, no particles above 50 μm were detected. This is an indication that the precipitates are volatile and might only be loosely connected. No further data is published how the applied environmental conditions influence the structure of α-La precipitates, as the available studies mainly focus on achieved yields and precipitate composition.

1.3   Resolubilization of precipitated α-Lactalbumin

Shortly after finding that α-La forms precipitates under acidic conditions, the possibility of its resolubilization by a subsequent pH increase was reported (Bramaud et al., 1997a; Kronman et al., 1964). A variety of different research groups targeted the optimization of this process. Pierre and Fauquant (1986) adjusted the pH to 7.0 and added 0.03 M CaCl$_2$ and received a fraction containing 64% α-La. Pearce (1987) reported a maximum solubilization yield of 80% with a pH adjustment in the range of pH 6.5 to 8.0. Bramaud et al. (1997a) observed that the initially turbid solution became clear and proteins were solubilized, when the pH returned to 7.5 or higher. They achieved the best solubilization yield of 80% of α-La with a purity of 80%, after dispersion in a 0.1 mol L^{-1} CaCl$_2$ solution and adjustment to a pH 8.0. Whereas another study using similar resolubilization conditions (0.1 mol L^{-1} CaCl$_2$ with an adjustment to pH 7.5) yielded only 11 to 43% of α-La, with purities ranging from 68 to 73% (Alomirah and Alli, 2004). Toro-Sierra et al. (2013) produced α-La fractions with 91% purity and an overall yield between 60 to 80%, relying on resolubilization using pH 8.0 and a stoichiometric amount of calcium to the amount of α-La molecules present in the starting whey protein solution. All these studies show significant discrepancies in yields and purities, which presumably originate from the highly different methods used for precipitation (rather than for the resolubilization step).

In recent years, the efforts in the investigation of protein folding kinetics rocketed, which is especially attributed to the remarkable progress in analytical technologies. The origin of protein folding theory is often ascribed to the Levinthal paradox, which states that the time needed to find the native structure by randomly searching among all possible conformations would be far too long to be biologically relevant. In conclusion, Levinthal (1969) proposed that this process has to follow a specific pathway or set of pathways encoded in the amino acid sequence in order to fold in a finite time.

In regard to α-La, time-resolved infrared (TR-IR) spectroscopy studies suggest that the thermally unfolded apo-α-La likely initially transitions to a MGS, followed by either parallel or sequential folding pathways to resume the native holo-α-La state (Hsu et al., 2021). And indeed, monitoring α-La's refolding by a stopped-flow small-angle X-ray scattering, showed that the folding intermediate has the same radius of gyration and overall shape as the equilibrium MGS at a pH of 2.0 (Arai et al., 2002). Structural analysis by nuclear magnetic resonance (NMR) spectroscopy revealed that the MGS of α-La comprises a structured α-helical domain and a disordered β-sheet domain (Kuwajima, 1996; Peng et al., 1995).

For the transition from the MGS to the native folding, two models have been proposed: On the one hand, a 'nonspecific' approach, often referred to as the jigsaw puzzle model. In this model, the correct folding depends on the formation of a sufficient number of native-like contacts regardless of which amino acids are involved,

i.e., there is no preferential starting point for folding, and each folding attempt may follow a different path (Harrison and Durbin, 1985; Sali et al., 1994). On the other hand, a 'specific' approach, in which the native folding of a protein depends on the formation of a specific subset of the native structure, often called the nucleation-condensation (Fersht, 1995; Itzhaki et al., 1995). The nucleation-condensation model assumes that the overall structure condenses around an element of structure, the nucleus, that itself consolidates during the condensation.

Literature indicates that the binding of Ca^{2+} to the calcium-binding site of α-La helps with initiating the folding nucleus at the interface between the α- and β-domain (Chedad and van Dael, 2004; Troullier et al., 2000). This is because metal ions lower the energy barrier between the MGS and the transition state, mainly by decreasing the difference of entropy between the two states (Bushmarina et al., 2006). The study of Kuhlman et al. (1997) supports this hypothesis and demonstrates that the native C-helix is crucial for the formation of the calcium-binding site. In case the C-helix is sterically hindered, e.g., by intermolecular crosslinks, the link between the α- and β-domains is impaired.

It is noteworthy that most published data concerning the folding mechanism of α-La has been obtained from monitoring the refolding process of denatured α-La with intact and native disulfide bonds. Chang (2002) used the technique of disulfide scrambling to obtain detailed insights in the refolding pathways of completely unfolded α-La. When the native disulfide bonds are formed, the intermediates comprise partially native-like structures and will likely proceed directly to form the native α-La. The results revealed two major types of these intermediates with native disulfide bonds. One type takes on a native-like α-helical domain, and the other one comprises a structured β-sheet calcium binding domain. Additional stop/go folding experiments with the purified folding intermediates have demonstrated that the formation of the α-helical domain is about 65% more efficient than that of the β-sheet domain (Chang, 2002). The formation of non-native disulfide bonds may lead to a kinetic trap, which are stabilized by non-native interactions and formed structures. Nevertheless, the results indicate that a reshuffling of the disulfide bridges is possible.

However, heating to temperature higher than 80 °C leads to irreversible structural changes. At both, acid and alkaline pH, the cooled samples showed a loss of β-turns compared to native reference (Boye et al., 1997). Furthermore, they reported on an increased β-sheet formation in the samples heated and cooled under acidic conditions. This was attributed to intensified intermolecular interactions due to increased hydrophobicity upon unfolding, which finally resulted in the formation of intermolecular β-sheets. Even disulfide shuffling to a non-native Cys61-Cys73 disulfide bond was observed when samples were heated at temperatures of 80 °C for 120 min (Wijesinha-Bettoni et al., 2007).

In summary, it can be stated that, firstly, it is possible to resolubilize α-La after it has been precipitated and separated, as proven by several research works. However, the studies only claimed that α-La was soluble, but no investigations of the true molecular state of α-La has been performed so far. Secondly, *in vitro* folding studies demonstrate that α-La can transition to an unfolded state without losing the capability to convert back to the original native conformation. The herein presented thesis aims to close the gap of knowledge, if precipitated, mechanically separated and resolubilized α-La resumes its previous native conformation or if there are irreversible deviations in the structure that allow for a soluble folding variant of α-La.

1.4 Centrifugal separation and alternative whey protein fractionation methods

As the separation of protein particles with a continuously working centrifuge is the centerpiece of this thesis, the theoretical basics of centrifugation shall be briefly summarized in this chapter. Centrifugal separation relies on the physical principle of sedimentation, and belongs to the three types of mechanical separation, which include also filtration and flotation.

Settling is the process of suspended particles falling through the liquid and is driven by gravity or centrifugal acceleration. Sedimentation is the final result of the settling process, i.e., the deposition of particles in a suspension. If the size of particles is less than 5 μm they undergo Brownian motion (Majekodunmi, 2015). For these small particles, the sedimentation velocity in the earth's gravitational field is very small, and sedimentation can only be observed by artificially increasing the gravitational field by means of centrifugation.

Assuming that there is a single spherical particle in an infinite fluid medium, it's movement will be induced by an external forces field, which may be the gravitational or centrifugal field. The gravitational force F_G is defined as the product of the particle mass m_p and the acceleration of gravity g, being 9.81 m s^{-2}:

$$F_G = m_p\, g \tag{1.4}$$

m_p can be substituted with the product of the particle density ρ_p and its volume V_p.

$$m_p = \rho_p\, V_p \tag{1.5}$$

Most assumptions consider the particle to be a sphere, whose volume is calculated using the particle diameter d_p.

$$V_p = \frac{\pi}{6}\, d_p^3 \tag{1.6}$$

When the particle is in the settling process, the F_G is opposed by two forces, the frictional resistance F_F against a particle moving through liquid, and the buoyant force F_B. A buoyant force F_B will arise because the particle displaces a volume of fluid equal to its V_p and is given by

$$F_B = -V_p \, \rho_f \, g \tag{1.7}$$

with ρ_f being the fluid density.

The frictional resistance F_F is given as

$$F_F = -\frac{\rho_p}{2} \, u_p^2 \, A_p \, c_F(Re_p) \tag{1.8}$$

where, u_p is the settling velocity of the particle, A_p is the particle area, and c_F is the frictional coefficient, which is a function of the particles Reynolds number Re_p.

When the particle settles in a liquid in a gravitational field, the following force balance can be applied:

$$F_G + F_B + F_F = 0 \tag{1.9}$$

This results in a definition of the steady-state settling velocity of the particle as

$$u_p^2 = \frac{4}{3} \frac{(\rho_p - \rho_f)}{\rho_f} \frac{g \, d_p}{c_F(Re_p)} \tag{1.10}$$

At low particle Reynolds numbers (Re_p < 0.5, creeping flow), c_F can be approximated by the following equation

$$c_F = \frac{24}{Re_p} \tag{1.11}$$

with

$$Re_p = \frac{u_p \, d \, \rho_f}{\eta_f} \tag{1.12}$$

With η_f being the fluid viscosity. Combining (1.10), (1.11), and (1.12), the Stokes settling velocity u_{St} can be simplified as

$$u_{St} = \frac{(\rho_p - \rho_f)}{18 \, \eta_f} g \, d_p^2 \tag{1.13}$$

In a centrifugal field, it is not only the gravitational force, but also the centrifugal force that affects the particle. The centrifugal acceleration a_Z is defined as the product of the circular radius of the particle r and the squared angular velocity ω

$$a_Z = r \, \omega^2 \tag{1.14}$$

Under laminar flow conditions and with negligible Coriolis forces and radial acceleration, the settling velocity of a particle in a centrifugal field, can still be described with the Stokes equation:

$$u_{St} = \frac{(\rho_p - \rho_f)}{18 \, \eta_f} r \, \omega^2 \, d_p^2 \tag{1.15}$$

In centrifuge parlance the term "g" or "g-force" is often used to describe the multiple of gravitation, by which the acceleration in the centrifuge is greater than that of gravity alone.

The previously described calculations are applicable to a single particle settling. With an increasing number of particles, the relative distance from one to another is reduced, which facilitates particle-particle interactions. These interactions include, but are not limited to electrostatic forces, Van-der-Waals forces, and steric

effects (Hogg, 2005). These interactions may result in settling enhancing or hindering effects, mainly depending on the effective particle concentration.

Fig. 1-9 shows the empirical settling velocity of monodisperse particles (several particles of the same size) in dependence of the solid's concentration as described in Bhatty (1986). The monodisperse suspension consisted of glass ballotini with a nominal diameter of 0.1 cm. At low concentrations, when a free settling takes place, the velocity can be appropriately described with the Stokes equation. At solids concentration above 1% the empiric settling velocity is higher than the theoretical Stokes velocity. This phenomenon is attributed to the formation of particle clusters (Bhatty, 1986). These are particles agglomerates that form and dissociate in a dynamical manner, which is favored by attractive particle-particle interactions. The intermediately higher particle size results in a faster settling. The settling rate reaches a maximum at a solid content of 10% w w^{-1}. The calculated Re numbers ranged from 0.016 to 2.48, depending on cluster size. According to Bhatty (1986) the highest cluster stability was observed at Re < 0.6. Even though, some stable cluster formed even at Re up to 1.48, which was explained by strong interparticle forces.

Other authors found the maximum settling velocity to be around 2 to 5% w v^{-1} (Johne, 1966; Kaye and Boardman, 1962). With further increase of the solid concentration, the settling rate decreases constantly and steeply. The reasons are an increasing suspension density, a discrepancy from Newtonian flow behavior, and increased buoyant forces due to higher amounts of displaced liquid (Bickert and Stahl, 1997).
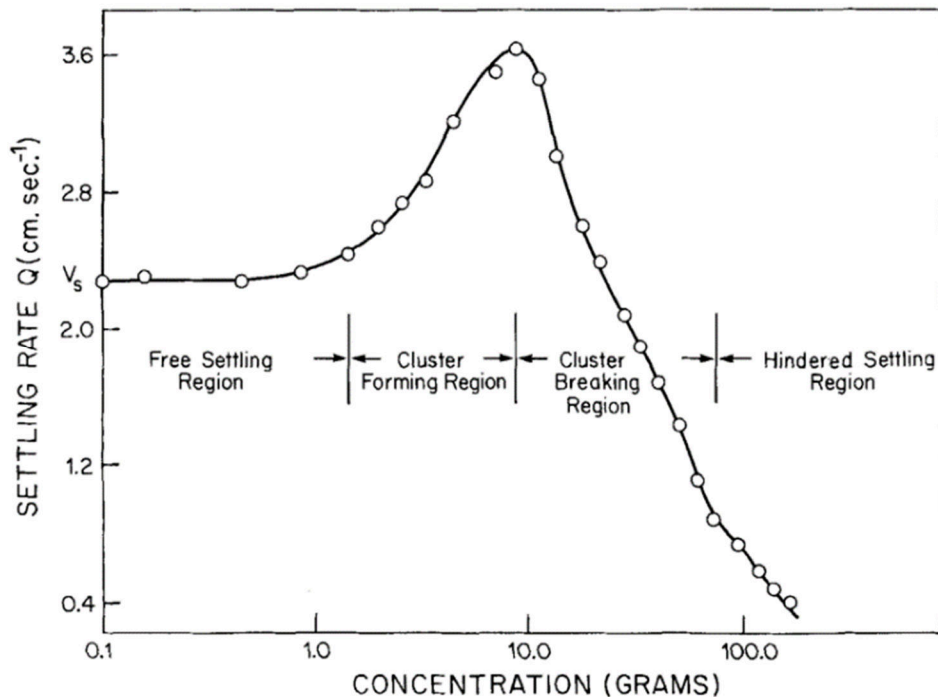
Fig. 1-9 Settling rate of a monodisperse suspension in dependence of particle concentration (Bhatty, 1986).

Generally, in polydisperse suspensions the same mechanisms as for monodisperse systems apply. However, additional segregation effects may occur between the different particle size classes, depending on the particle size distribution, i.e., the number of particles in the respective size classes. As long as a broad variety of settling velocities can be observed, which is directly related to the respective particle size class (a particle swarm), this settling type is called swarm sedimentation (Mirza and Richardson, 1979). Effectively, this means the larger particles sink rapidly, the smaller ones remain in the supernatant for a longer time before they settle. This leads to a gradient of the solids concentration with the highest concentration on the bottom of the settling vessel.

When a certain solids concentration is exceeded, no more segregation effects will occur. Instead, all particles will settle with an approximate same velocity, which is visible with a sharp borderline between the suspension and the cleared supernatant. This settling type is called zone settlement (Stahl, 2004). This phenomenon is attributed to an increase in particle-particle interactions and a rise in the apparent viscosity of the system, as well as a higher relevancy of the drag forces.

In some applications, a so-called flocculant is added to the suspension to induce a zone settlement. The flocculation enables the settlement of all particles at a time in order to maximize the clarification of the supernatant, including the smallest particles, which would not settle on their own (Gregory and O'Melia, 1989; Thomas et al., 1999). The surface properties of protein-based particles and the respective particle-particle interactions (van der Waals forces, electrostatic attraction or repulsion, hydrophobic effects) can be modified by pH adjustments, addition of salts, or additives like flocculants in order to improve the separation results.

That said, the necessity arises to include the solids concentration in the calculation of the sedimentation velocity. One of the most frequently used approximations is the equation of Richardson and Zaki (1954), which provides a relation for the empirical particle settling velocity based on the Stokes velocity with respect to the solids volume fraction ϕ.

$$u_p = u_{St} \left(1 - \phi\right)^{4.65} \tag{1.16}$$

1.4.1 Continuous centrifuges

Centrifuges usually comprise a rotating vessel filled with the suspension to be separated. Accelerations that are up to 10^6 higher than gravity can be achieved with specific types of centrifuges. There are types of centrifuges that can be either operated continuously or in batch mode. Tubular centrifuges, basket type centrifuges and rotating buckets run discontinuously, while disc centrifuges and decanters are fully continuous in operation. The continuous way of working is related to a mechanism that allows the sediment to be discharged from the solid centrifugal bowl, while the centrifuge continues running.

So-called decanters are not only used in mining industry (Merkl and Steiger, 2012) and wastewater management (Veeken and Hamelers, 1999), but also find a broad range of applications in the food industry, e.g., olive oil extraction (Altieri et al., 2013), casein fractionation (Schubert et al., 2018), juice extraction of diverse fruits (Beveridge and Harrison, 1995), fractionation of egg yolk (Ulrichs et al., 2015), the isolation of steviol glycosides (Arslan Kulcan and Karhan, 2021) and many more.

In practice, decanter centrifuges provide excellent performance levels when handling slurries with amounts of solids higher than 10% and they are often the only choice for solids concentrations above 40% (Records and Sutherland, 2001).

For scaling up from laboratory data to pilot or industrially sized centrifuges, often the so-called Σ-theory is used. Ambler (1959) introduced this mathematical approach to compare the settling behavior between different forms of sedimentation type centrifuges. The thereof derived Σ-value is the calculated equivalent area of a settling tank theoretically capable of doing the same amount of work in a unit gravitational field. In recent years, the interest in numerical models, such as computational fluid dynamics (CFD) and discrete element method (DEM) simulations have increased (Menesklou et al., 2021). The development of numerical methods and modelling of centrifuges appears to be complex and time intensive. However, if successfully validated, they are powerful tools to provide detailed insights and have better accuracy in result prediction. This will be taken up in the overall discussion of results.

1.4.2 Separation principles in decanter centrifuges

The design of a typical counter-current decanter centrifuge can be seen in Fig. 1-10. The outer housing or casing contains the bowl, which is the separation room. The bowl usually consists of a cylindrical and a conical part. The suspension enters the decanter via the feed tube. The suspension passes into the rotating bowl through holes located in the feed pipe. By the rotation of the bowl, respective centrifugal forces are generated and accelerate the particles to sediment at the inner wall of cylindrical part of the bowl. This part is also called the compression zone, where the sediment consolidates and builds up a sediment cake.
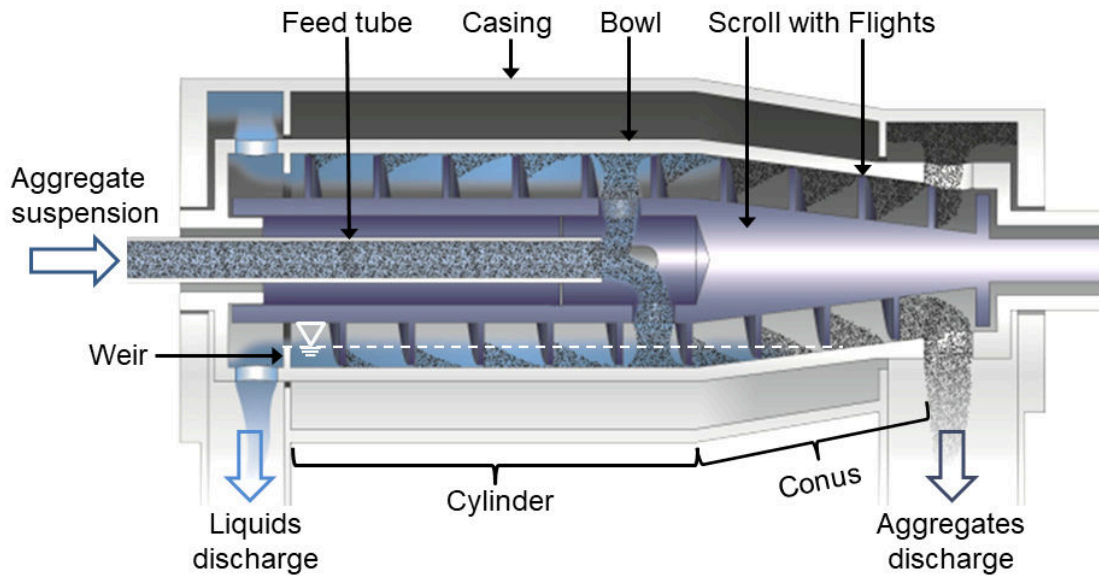
Fig. 1-10 Schematic design of a counter-current decanter centrifuge.

The conveyor scroll rotates with a slightly higher differential speed than the bowl and transports the sediment towards the conical part of the bowl. While its transport up the conical inclination, the sediment is further dewatered as it leaves the liquid pond. The sediment is finally discharged at the highest point of the conical part. The supernatant, also called centrate, is discharged at the opposite end of the bowl. Here, a weir serves as a barrier and defines the height of the liquid level in the bowl. The weir can usually be adjusted in its height. The effects are schematically shown in Fig. 1-11. A higher weir will extend the residence time of particles in the centrifuge and can therefore increase the clarity of the supernatant. However, at the same time, the higher weir reduces the sediment drying zone, i.e., the length of the conical bowl part, which can negatively affect the dryness of discharged sediment. A lower weir can reduce the centrates clarity and simultaneously increase the discharged sediments dryness (Records and Sutherland, 2001). Soluble proteins will remain in the centrate, as they are too small to sediment. Nevertheless, as the sediment cannot be discharged completely dry, a small portion of soluble protein may be discharged as part of the interstitial and vicinal water of the sediment.
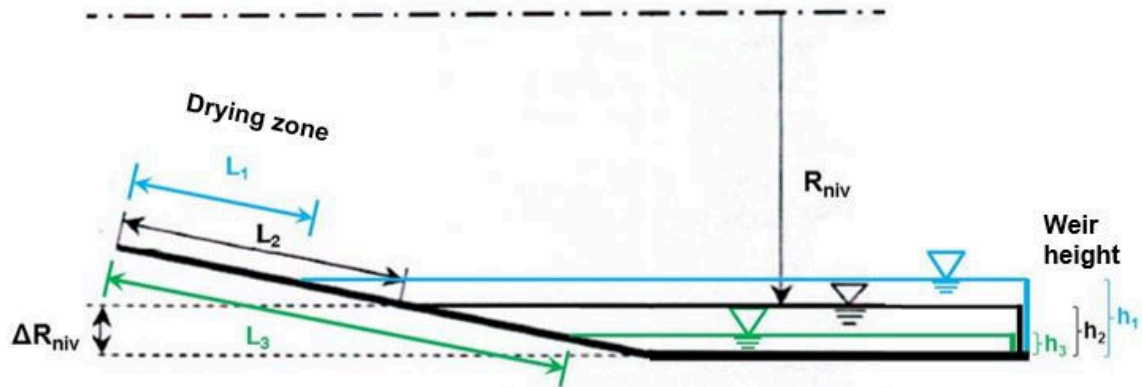
Fig. 1-11 Effects of different weir heights on the filling level in a decanter centrifuge.

It needs to be emphasized that not only external factors, e.g., the decanter configuration, like the weir height, impact the dewatering of the sediment. The major influencing factor derives intrinsically from the particles themself. The particles density, size, form, and structure do significantly influence the sediment that is formed out of this type of particles. Generally, the particle properties predetermine both the feasible extent of sediment dewaterability and its flowability, i.e., how easily the sediment is conveyed up the conical bowl part to the discharge port.

The main portion of the sediment dewatering takes place in the cylindrical bowl, when the sediment cake is exposed to compressive forces induced by the centrifugal acceleration in combination with the sediment weight itself. The strength of the particle network will influence the solids content obtainable in a dewatering process. Ways for determination of the network strength are often based on the work of Buscall and White (1987), which is nowadays seen as the fundamental theory of compressive rheology (Kretser et al., 2003). They introduced the compressive yield stress $P_y(\phi)$ for the characterization of the network strength, and the hindered settling factor $R(\phi)$ to describe the network permeability by means of an interphase drag parameter. Various authors developed characterization approaches involving these two parameters. In essence, depending on the solids volume fraction to be investigated, a gravitational sedimentation (Cacossa and Vaccari, 1994; Grassia et al., 2008, 2011; Howells et al., 1990; Lester et al., 2005; Usher and Scales, 2005; van Deventer et al., 2011), an analytical centrifugation (Angle et al., 2017; Curvers et al., 2009; Loginov et al., 2014; Skinner et al, 2015; Usher et al., 2013), a compression-permeability cell test (Höfgen et al., 2019; Landman and White, 1994; Stickland et al., 2005), or combination thereof (Gladman et al., 2006; Loginov et al., 2017) are the methods of choice. The compression-permeability cell test comprises a chamber filled with pre-thickened sediment of known height and concentration, where pressure is applied by a porous piston, while recording the permeating liquid.

Moreover, several authors have demonstrated that the surface properties of colloidal particles in suspension are closely linked to the flow behavior of thereof originating sediments (Channell and Zukoski, 1997; Leong et al., 1993; Scales et al., 2000). In practice, the flow characteristics of sediments are often determined by rheological investigation. Exposing a sample to oscillatory shear stress will indicate its viscoelastic properties, typically using the shear modulus and loss angle for description (Ward and Hoare, 1990). Additionally, an investigation of the sediment adhesiveness can reveal whether the sediment has a tendency to stick to the conveyor and thus impairing a continuous solids discharge or not (Friedman et al., 1963). These characterizations allow to draw conclusions for the flowability of the sediment.

Basically, the sediments discharged from a decanter can reach from a paste-like sludge to coarse or even crystalline dry particulates (Records and Sutherland, 2001). The sludge-like sediments often show a high compressibility. The density difference between particle and liquid is usually quite low, and usually no individual particles or agglomerates are visible. In order to maximize the dewatering, it is advisable to enlarge the sediment cake height for exhaustive compression and to use low conveyor differential speed, especially if the sediments tends to have a shear-thinning behavior (Erk and Luda, 2003). On the other side, the coarse or granular particulates mainly rely on interstitial drainage, and profit from a longer residence time on the beach. This can be realized by a reduced throughput, a lower conveyor differential speed or the reduction of weir height (Stiborsky et al., 2003).

The steady removal of the sedimented solids from the centrifuge bowl enables a continuous one-step processing of suspensions over a wide range of flow rates.

1.4.3 Alternative whey protein fractionation methods

In the last few decades, many approaches were published aiming at developing a process for whey protein separation that delivers a maximum protein fraction purity, high yields, that keeps the proteins in their native state, and being at the same time simple to operate and easy to scale-up, as well as cost efficient. The suggested processes exploit different attributes of the whey proteins, including their variation in sizes, their denaturation properties, the ionic nature of proteins, or other of their specific physical properties. In the following, most relevant published separation approaches are presented, and their advantages and drawbacks are briefly summarized.

An impressive number of studies describe the separation of the major whey proteins by diverse preparative chromatographic application, such as ion-exchange chromatography (IEC) and affinity chromatography (AC). IEC can be further distinguished into anion (AEC) and cation exchange chromatography (CEC) and makes use of the ionic properties of proteins. A charged protein will bind to oppositely

charged ligands of a resin. Therefore, proteins will be retained by AEC at a pH above their IEP, and they will be retained by CEC below their IEP. With consciously chosen elution conditions, it is possible to separately release the individual bound proteins from the resin and recover them in highly pure fractions. Contrary to IEC, in AC (almost) solely the target protein is captured by a specific complementary binding substance, which results in an incomparable selectivity of the process.

Examples for AEC processes for fractionation of the individual whey proteins are Carrère et al. (1996), Flashner et al. (1983), Kristiansen et al. (1998), Kunz and Lönnerdal (1989), Manji et al. (1985), Outinen et al. (1996), Pedersen et al. (2003), Santos et al. (2012). Studies using CEC for whey protein fractions include, but are not limited to Doultani et al. (2004), El-Sayed and Chase (2009), Hahn et al. (1998), Turhan and Etzel (2004). Also combinations of AEC and CEC are described, which target a complete fraction of all whey proteins Gerberding and Byers (1998), Voswinkel and Kulozik (2014), Ye et al. (2000). The use of AC for whey protein separation was studied by Gurgel et al. (2000), Ounis et al. (2008), Vyas et al. (2002), and Wang and Swaisgood (1993).

All approaches for IEC and AC have in common the attainment of highly pure whey protein fractions (most were above 90%), an attribute for which the preparative chromatography has been appreciated for decades in biotechnological and pharmaceutical processing. The reported recovery rates, however, varied from about 50% (Gurgel et al., 2000; Santos et al., 2012; Vyas et al., 2002) to more than 90% (El-Sayed and Chase, 2009; Skudder, 1985).

Most mentioned studies presented the process only on a lab scale basis but did not provide any data for pilot or production scale. The scale-up of packed bed chromatography columns, however, is a challenging task. A common phenomenon is an increased compression of packed beds in production scale columns. This compression can deform individual resin particles, thus changing the surface area available and reducing the porosity of the packed bed and its effective binding capacity (Colby et al., 1996). A common recommendation is to maintain the bed height and increase the resin volume by increasing the diameter of the packed column. The problematic issues are on the one hand, the extremely high prices for these large-scale columns as well as the enormous volumes of resin, and on the other hand, the challenge of column packing, which requires trained personnel.

The introduction of membrane-based ion-adsorbers opened new possibilities of whey protein separation. The functional groups are immobilized on a membrane, which can be assembled in different designs, like spiral-wound, tubular hollow fibers, pleated sheets, or stacked-disc (Nath et al., 2022). This set-up results in low backpressures, up to 20-fold higher flow rates compared to column-based processes and allows to load the adsorber without pre-filtration of the sample (Goodall et al., 2008). Respective studies using membrane-based chromatography include Adisaputro et al. (1996), Bhattacharjee et al. (2006a), Goodall et al. (2008), Kim et

al. (2003), Saufi and Fee (2009, 2011), Splitt et al. (1996), Voswinkel and Kulozik (2011, 2013, 2014), and Weinbrenner and Etzel (1994).

These studies show consistently high purities and good yields for all whey protein fractions, and some even claimed no reduction in binding capacity over several cycles. However, it should be emphasized that the initial binding capacities of membrane adsorbers currently available on the market are much lower than the ones achieved with packed columns with similar geometries. Another drawback of the membrane chromatography is the requirement of several pass cycles for a sufficient adsorption of the molecules to the ligands, as well as increased dilution effects while elution. Additionally, the used membranes tend to have a short lifetime, and need to be replaced frequently. Also challenges like a non-uniform flow distribution across the membrane still needs to be overcome to allow for proper scale-up. In conclusion, although preparative chromatography can provide effective protein purification, they typically have unacceptable economics at large scale.

Membranes are not only employed as matrix in chromatography, traditionally they are used for filtration, mainly tangential flow filtration (TFF). The membrane has a defined pore size, often referred to as molecular weight cut-off (MWCO), which allows a precise size-based separation. By adaption of the membrane area and respective hardware sizing, this separation method is also suitable for industrial scale. Another benefit of TFF is that the nativity and structure of the proteins are usually not affected by this processing technique. Several authors demonstrated that certain whey proteins can be separated without any further pre-treatment using TFF. A list of respective studies with a summary of the achieved purities and yields for α-La and β-Lg fraction is shown in Tab. 1-3.

The results for separation of α-La and β-Lg by filtration without any pre-treatment are quite limited in terms of achieved purities and yields. The challenge is the marginal small size difference between α-La and β-Lg, with 14.2 kDa and 18.3 kDa, respectively. In average, purities of around 30% were achieved, the yields being even worse. With such unsatisfactory results, it cannot be claimed an effective process for whey protein fractionation.

A noteworthy exception is the study of Cheang and Zydney (2003). They demonstrated that purities higher than 90% for both fractions and yields of more than 90% for β-Lg and higher than 95% for α-La are achievable by using a stirred cell filtration device with a 30 kDa MWCO. They used optimized environmental conditions to promote β-Lg's presence as a dimer in order to enhance a size-based separation. However, this result took a total of 16 diafiltration (DF) steps, implicating elevated costs for DF media, and an enormous time consumption. Furthermore, the capabilities to upscale a stirred filtration cell are highly limited, which disqualifies this process from an operational and economical point of view.

Tab. 1-3 Summary of published studies using TFF for separation of major whey protein fractions without whey protein pre-treatment.

Reference	Filter MWCO, material	Process design	Purity	Yield
Lucas et al. (1998)	150 kDa, ZrO$_2$ coated with PEI	1x CF TFF	N.d.	α-La (perm.): 14%
Muller et al. (2003a)	300 kDa, ceramic	9x CF No DF TFF	α-La (perm.): 44% β-Lg, BSA, IgG (ret.): N.d.	α-La (perm.): 53%
Muller et al. (2003b)	50 kDa, ceramic	7x CF No DF TFF	α-La (perm.): 65% No data: β-Lg (ret.): N.d.	α-La (perm.): 28%
(Bhattacharjee et al., 2006b)	30 kDa, PES	30 min run time TFF	β-Lg (perm.): 75% BSA, Lf, IgG (ret.): N.d.	N.d.
Almécija et al. (2007)	300 kDa tubular ceramic membrane	4x DF at pH 4	N.d.	α-La (ret.): 100% β-Lg (perm.): 100%
Metsämuuronen and Nyström (2009)	30 kDa, regenerated cellulose	1x CF TFF	N.d.	α-La (perm.): 26%
Marella et al. (2011)	50 kDa, PVDF	5x CF No DF TFF	α-La (perm.): 63% β-Lg (ret.): N.d.	α-La (perm.): 34%
Holland et al. (2012)	100 kDa, regenerated cellulose	2x CF TFF	α-La (perm.): 80% β-Lg (ret.): N.d.	α-La (perm.): 10%
Arunkumar and Etzel (2013)	300 kDa, charged regenerated cellulose	3-stage rectification	α-La (perm.): 95% β-Lg (ret.): 73%	N.d.

N.d.: No data, perm.: permeate, ret.: retentate, DF: diafiltration, CF: concentration factor, PEI: polyetherimide, PES: polyethersulfone

A strategy to overcome the limitations of protein sizes being too similar for proper size-based separation is either an increase or a reduction of the size of one of the two major whey proteins.

A way to decrease the size of one protein component is the use of selective hydrolysis. On the one hand, it was demonstrated that β-Lg has a higher resistance to hydrolysis compared to α-La during the digestion of WPI using pepsin, acid protease A and protease M. Depending on the enzyme used, about 99% of α-La were hydrolyzed, while β-Lg remained almost completely unhydrolyzed (Jakopović et al., 2019). On the other hand, β-Lg has a higher susceptibility to tryptic hydrolysis compared to α-La. By investigating the influence of hydrolysis temperature and pH on the selective hydrolysis of β-Lg in WPI, Cheison et al. (2011) reported a recovery of up to 68% of pure α-La. Konrad and Kleinschmidt (2008) reported on a complete digestion of β-Lg with practically no degradation of α-La. The hydrolyzed β-Lg was removed by ultrafiltration in diafiltration mode (UFDF) using a 10 kDa MWCO membrane, which resulted in an α-La fraction with up to 95 % purity, but with an unsatisfactory yield of only 15%. Lisak et al. (2013) optimized the environmental conditions for β-Lg degradation using chymotrypsin outside the enzyme optimum and were able to maximize the recovery of α-La to 81% with nearly 99% purity. However, in this study, the hydrolysis reaction was stopped by addition of an inhibitor molecule, which necessitates an additional step to remove the inhibitor-enzyme-complex. In conclusion, the selective hydrolysis itself is an efficient process showing good controllability and scalability. However, the separation of the hydrolyzed peptides from the unaffected protein appears to be the bottleneck in the process, as can be seen by the low recovery rate from Konrad and Kleinschmidt (2008). The reason is presumably, that the introduced size difference between peptides and proteins is not sufficient to allow for an efficient separation by means of UFDF. Apart from that, one component is irreversibly sacrificed as it is degraded into peptides. One of the ambitions in this study, however, is to realize the recovery of both protein fractions in their native (soluble) states.

A way to increase the protein size is to make use of the interaction of whey proteins with specific complexing agents. For example, chitosan builds complexes with β-Lg, while more than 80% of the other proteins remain soluble (Casal et al., 2006). The complexes can be separated by filtration or centrifugation. In a subsequent solubilization step using acetic acid, more than 90% of the β-Lg can be recovered from the chitosan complexes (Montilla et al., 2007). However, this solubilization necessitate a subsequent multi-step DF to remove the acetic acid. This additional step makes the process highly time and cost intensive. Additionally, NMR spectroscopy could not confirm the nativity of β-Lg after this process (Montilla et al., 2007).

The size of a protein fraction can also be increased by salting-out procedures. With the addition of high concentrations of NaCl and preferably at pH 2, nearly all whey

proteins except β-Lg can be salted out of acid or cheese whey and WPI (Mailliart and Ribadeau-Dumas, 1988). After recovery by centrifugation, the β-Lg fraction requires extensive DF for removal of salts. With this approach Maté and Krochta (1994) achieved a β-Lg recovery rate of 65% and a purity of 95%. The process itself appears to be simple and achieved good purity. However, salting out works best with highly pure WPI, which requires intensive purification efforts before the actual separation process starts (Konrad et al., 2000). Additionally, an enormous energy and time consumption is expected for subsequent removal of the salts by dialysis or UFDF.

Another strategy to increase the size difference between two protein fractions is a selective thermal aggregation of one of the involved proteins. This method exploits the protein's specific molecular properties under particular heat and environmental conditions to initiate an agglomeration reaction, which affects selectively only one of the protein fractions. While the precipitation of α-La is mainly based on (reversible) hydrophobic interactions (chapter 1.2.1), β-Lg can form stably linked aggregates via disulfide bridges (chapter 1.2.2). The resulting size (and density) difference enables a mechanical separation of the aggregated fraction. The precipitation of α-La is supposed to be reversible, which would leverage the recovery of both protein fractions, α-La and β-Lg, in their native states.

Prospecting a scalable process, most authors described the use TFF as the method of choice for separating the precipitated fraction from the soluble proteins. Several studies proofed the feasibility to separate aggregated β-Lg (Kiesner et al., 2000; Tolkach, 2008) and precipitated α-La (Gésan-Guiziou et al., 1999; Toro-Sierra et al., 2013) from the respective soluble proteins by means of membrane filtration.

Toro-Sierra et al. (2013) achieved purities above 90% for both fractions, the yields were varying between 60 to 97%. The study also described that the permeation was lower than expected, which required the execution of more DF steps than anticipated to achieve the targeted results. The low permeate was attributed to fouling issues of the highly adhesive precipitates. In fact, it is repeatedly reported that whey protein aggregates promote fouling and are one of the main drivers in declining permeate flux (Barukčić et al., 2015; Marshall et al., 1997; Mourouzidis-Mourouzis and Karabelas, 2008; Steinhauer et al., 2015; Tarapata et al., 2022). The prominent fouling tendency is likely the root cause of the fluctuating results and could be an indication for poor repeatability of the process, which is a challenging behavior when working on industrial scale.

Compared to TFF, which requires multiple DF steps in order to achieve acceptable separation results, centrifugation is considered to be a straightforward one-step separation method. Another benefit of centrifugation is that no consumables, such as filters, are required, which lowers the required operational expenditure, specifically on large scale applications. Last but not least, it can be expected that the final

solids content in the TFF will be dramatically lower as for the fractions derived from a centrifugation. This is not only valid for the retentate fraction compared to the sediment, but also for the permeate compared to the supernatant. The retentate of a TFF needs to be a fluidlike liquid to allow a proper processing and recovery from the filter and plant. In comparison, the sediment of a centrifuge can reach solids content of 50% or higher without any restrictions in recovery. The permeate from a TFF process in DF mode, appears to be highly diluted because of the additional amounts of DF media added. For further processing of the target component in the permeate, an additional concentration step is often indispensable. On the other side, the supernatant is usually not diluted with any additional liquid in centrifugal separation.

Several authors used a batch-wise centrifugation for the separation of the precipitated α-La (Bonnaillie and Tomasula, 2012; Bramaud et al., 1997a; Fernández et al., 2011; Lucena et al., 2007). All in all, the separation results were promising. The process of Bonnaillie and Tomasula (2012) yielded a precipitated fraction with 99% α-La recovery and 58% α-La purity, and a soluble β-Lg fraction with 74% recovery, and 75.5% purity using a bench-top centrifuge with 2,000 g for 60 min. Fernández et al. (2012) explored the possibilities to perform washing steps of the precipitated fraction after the initial separation. It was found that two washing steps can remove up to 92% of β-Lg from the precipitate, with a loss of only 5% of α-La. The subsequent solubilization yielded 75% of α-La. These studies can be considered as a proof of concept that selectively precipitated of α-La can efficiently be separated from soluble β-Lg by means of centrifugation. However, the use of batch-wise centrifuges is considered a bottleneck for any scale-up prospects. Therefore, this thesis targets to adapt and modify the process in a way to make it applicable for industrial scale whey protein separation. This was realized by transferring the centrifugation step from a batch-wise mode into a continuously running separation process using a decanter.

2 Objective and Outline

With the exploration of new fields of application as well as intensification of established products, such as nutraceuticals and sportive nutrition, the demand for pure fractions of the individual major whey protein is continuously rising. Since several years, the development of cost-efficient and scalable separation methods delivering maximum yield and purity of the individual whey protein fractions has become one of the focus areas in food research and dairy industry. Up to date, all of the suggested process are showing distinct deficiencies, either in terms of the final product purity, the overall yield or production costs, which is often related to a missing scalability of the process.

The objective of this thesis was to develop an innovative process for separation of the major whey proteins, α-La and β-Lg, with high yield and purities. The proposed process consists of no more than two production steps. The first step is a selective thermal aggregation of one of the major whey protein fractions, while the counterpart remains native and soluble in the liquid phase. The second one is the separation of the aggregated fraction in a single step from the liquid phase using a continuous decanter centrifuge, which is more efficient than a multistep DF procedure based on MF.

The field of selective thermal aggregation of whey proteins has been intensively studied by various research groups around the globe, one of them being the Chair of Bioprocess and Food Technology at the Technical University of Munich. Here, extensive technological work has been performed by Dannenberg (1986), Beyer (1990), Plock (1994), Kennel (1994), Spiegel (1999a), Tolkach (2008), Toro-Sierra (2016). All of them delivered the fundaments of this thesis. These pre-works provided knowledge on how the various influencing factors affect the aggregation of one target protein component in whey, while keeping the other major protein as untouched as possible. Thus, the first aim was to transfer the available knowledge of selective thermal aggregation to the process designed in the frame of this thesis.

The selective thermal aggregation was followed by continuous centrifugal separation, which was investigated as an own topic. This separation method was chosen to overcome the limitations of membrane filtration, which are a low permeability due to membrane fouling, the requirement of several DF steps to achieve acceptable separation efficiencies, and the costly consumption of filters. Indeed, there are no other studies available in literature on the separation of whey protein aggregates by a continuous centrifugation.

Within this process design, two different routes were explored: On the one hand, the selective thermal aggregation of β-Lg, keeping α-La native, followed by the continuous centrifugal separation. On the other hand, the selective precipitation of α-La, followed by centrifugal separation and as a third step the resolubilization of

the α-La precipitates, as the underlying binding mechanisms rely on reversible principles.

The idea was to start with an extensive characterization of the particle properties as well as their behavior as a sediment. Batch settling test in the gravitational field and compressibility experiments were conducted to predict potential challenges in continuous centrifugation, specifically for the sediment discharge. The analyses were performed for α-La precipitates and β-Lg aggregates side by side. Extremely differing behaviors were observed, which could be traced back to the respectively underlying molecular binding mechanisms of the precipitates and aggregate.

The characterization of the particles led to the conclusion that different decanter types might be required for efficient separation processes. While the β-Lg aggregates showed good separability in a regular counter-current decanter, the α-La precipitate separation was more challenging with this model. It was investigated if the co-current decanter is the appropriate centrifuge type for separation of α-La precipitates in order to receive two high purity fractions. Another key question was if the fragile α-La precipitates would maintain their physical integrity along the separation process, despite high mechanical stress and shear forces. This was especially challenged by testing the feasibility to wash α-La-enriched sediment after initial separation from the β-Lg supernatant.

Regarding β-Lg aggregate separation, the counter-current decanter showed promising results and turned out to be the tool of choice. However, there was still potential to improve the centrate purity, as the suspension contained small aggregate fragments that did not sediment. The hypothesis was that a variation of the suspension pH might induce flocculation, which leads to an agglomeration of the primary aggregates and finally results in higher clarification of the centrate. Additionally, it was investigated whether the modification of pH leads to any side effects on the sediment dewaterability or affects nativity of α-La in the supernatant.

In the last article, an insightful molecular assessment of resolubilized α-La was performed, which was received after selective thermal precipitation and centrifugal separation. The question was whether or to which extent the original native state of α-La, after having been exposed to thermal, chemical, and mechanical stress, can be re-established. The underlying idea was that a complete refolding of α-La to the original conformation would enable to receive both protein fractions, β-Lg from the centrate and α-La, in native state.

3 Separation of whey protein aggregates by means of continuous centrifugation

Summary and Contribution of the Doctoral Candidate

The aim of this work was to investigate the suitability of a decanter centrifuge for whey protein particle separation. Firstly, a detailed characterization of the two types of whey protein particles, α-La precipitate and β-Lg aggregates, was performed, respectively. The α-La precipitates were non-covalently stabilized, built irregularly shaped particles with a tendency to form loose clumps, and had a median size of 12 µm. The β-Lg aggregates, stabilized by disulfide bonds, were rigid, had an elongated shape with several branches, and had a median size of 109 µm, with a distinctly lower density than the α-La precipitates. This characterization data was used for calculation of theoretical settling velocities and were compared to *in vitro* batch settling experiments. After a short lag phase, the α-La precipitates seemed to flocculate, which led to a settling-enhancing zone sedimentation. Even the calculated Stokes velocity was exceeded by many times over. Although the β-Lg aggregates were significantly larger in size than the α-La precipitates, their sedimentation velocity stayed far below the one of the α-La precipitates. In consolidation experiments, the α-La precipitates showed a high compressibility, whereas the β-Lg aggregates were highly resistant to compressive forces, which is attributed to the stabilization via disulfide bonds resulting in rigid and firm particles.

The critical part was the transfer of obtained sedimentation and consolidation insights to the lab-scale decanter centrifugation process. The beneficial sedimentation effects of the α-La precipitates were not reproducible in the decanter. A potential root cause is that the centrifugal forces resulted in particle breakdown. Moreover, the high adhesiveness of sludge-like sediment impaired the discharge. Under all investigated conditions, a 70% clarification of the supernatant and a dry solids content of 25% in sediment were the best achieved results. It was concluded that another discharge mechanism of the decanter would improve the separation results.

The β-Lg aggregates were discharged without any difficulties as a free-flowing powder from the decanter. The sediment dryness of maximal 40% was attributed to enclosed liquid through thermal aggregation process, which is also reflected in the low particle density. A clarification of 90% was achieved with highest applied g-force level. This study is the proof of principle that the separation of whey protein particles can be conducted with decanter centrifuges.

The doctoral candidate contributed substantially to conception, design and execution of experiments based on preceded critical literature review. The doctoral candidate conducted major parts of the data analysis, interpretation, and discussion. She wrote and revised the majority of the manuscript.

Separation of whey protein aggregates by means of continuous centrifugation[1]

Nicole Haller[a], Ulrich Kulozik[a,b]

[a]Chair for Food and Bioprocess Engineering, Technical University of Munich, Weihenstephaner Berg 1, 85354 Freising, Germany

[b]ZIEL – Institute for Food & Health, Weihenstephaner Berg 1, 85354 Freising, Germany

Abstract

This study investigates the applicability of decanter centrifuges for high efficient separation of valuable proteins from whey. Thus, two different types of protein aggregates, α-La and β-Lg, were produced by means of selective thermal aggregation. The two aggregate suspensions were investigated for their particle characteristics, sedimentation and consolidation behavior, and were finally separated in a lab-scale decanter. They showed severe differences in particle size distribution, particle shape, and in the underlying molecular binding mechanisms, all affecting their separability. In scale-down experiments, the non-covalently stabilized α-La aggregates presented sedimentation enhancing flocculation, and a high compressibility of the cake. However, the beneficial sedimentation effects were not observed in the decanter, as the centrifugal forces resulted in particle breakdown. Moreover, the high adhesiveness of sludge-like sediment impeded the discharge. Under best investigated conditions, a clarification around 70% of the supernatant and a dry solids content of 25% in sediment was achieved. Contrary to that, the β-Lg aggregates, stabilized by disulfide bonds, were rigid aggregates comprising a median size of 109 μm with irregular shapes. They presented low compressibility in scale-down testing but were discharged as a free-flowing powder from the decanter. The sediment dryness of maximal 40% was attributed to enclosed liquid through thermal aggregation process, which is also reflected in the low particle density. This

---

[1] Adapted original manuscript. Adaptions of the manuscript refer to numbering of sections, figures, tables and equations, abbreviations, units, spelling, format, and style of citation. All references have been merged into a joint list of publications to avoid redundancies. Footnotes were added to provide additional information that is not included in original publication.

study demonstrates the successful application of a decanter for the separation of whey proteins and contributes to the understanding of aggregate separability by means of continuous centrifuges.

Keywords: α-Lactalbumin, β-Lactoglobulin, Whey protein aggregates, Decanter centrifuge, Sedimentation, Consolidation

3.1 Introduction

The two major proteins α-La (MW = 14.2 kDa) and β-Lg (MW = 18.0 kDa) represent the main proteins in whey. In recent years, the fractionation of these whey proteins got more into industrial focus. This can be ascribed to their specific technological properties, nutritional values, and reported biopharmaceutical activities. α-La stimulates serotonin uptake (Booij et al., 2006; Markus et al., 2005), shows antibacterial and anti-tumor activities (Håkansson et al., 2000; Pellegrini et al., 1999; Rammer et al., 2010), and it is a great source for infant food formulations (Heine et al., 1991; Lien, 2003; Trabulsi et al., 2011). On the other side, various studies report about β-Lg's excellent gelling, foaming or water-binding properties, which are even superior to egg white protein (Abd El-Salam et al., 2009; Dombrowski et al., 2017; Pearce, 1991), as well as its ACE inhibiting activity (Hernández-Ledesma et al., 2007; Hernández-Ledesma et al., 2008), and many more.

However, the isolation of individual whey proteins is still a challenging task at industrial scale in terms of purity, yield, and throughput (Chatterton et al., 2006). A range of fractionation processes are described in literature, beyond other membrane filtration, size exclusion or IEC (Mehra and Kelly, 2004; Neyestani et al., 2003; Outinen et al., 1996; Turhan and Etzel, 2004). However, all have limitation in throughput and low purities or yields in common. An alternative to these single step separation approaches is the combination of a controlled thermal pre-treatment with a subsequent mechanical separation. A selective thermal aggregation of one candidate molecule renders a protein mixture separable based on size and/or density. Relevant processes are reported for α-La precipitation (Bramaud et al., 1995; Lucena et al., 2006; Fernández et al., 2012; Maubois et al., 1987; Pearce, 1983; Tolkach and Kulozik, 2008;), and β-Lg aggregation (Dannenberg and Kessler, 1988; Erabit et al., 2014; Griffin et al., 1993; Hillier and Lyster, 1979; Roefs and Kruif, 1994), respectively.

Subsequently to induction of a size and density difference, the two fractions can be separated by high-throughput mechanical separation methods, e.g., crossflow filtration or continuous centrifugation, like scroll decanter centrifuges. For this type of centrifuge, the main fields of applications are sewage water treatment, removal of plant residues in oil and juice production, and in brewery industry (Records and

Sutherland, 2001; Stahl, 2004; Wakeman, 2007). All these applications fulfill thickening tasks of high dry substance containing slurries or sludges, often comprising big sized aggregates. In contrast to that, only a small number of reports for continuous centrifugal separation of protein precipitates are available, e.g., for isoelectric precipitated soy protein (Bell and Dunnill, 1982), acid casein curd (Munro and van Til, 1988), and salt precipitated yeast homogenate (Maybury et al., 2000). Separation of protein precipitates is a challenging task, as they are often small and irregularly shaped particles, presenting low density differences to the liquid phase. Also, particle breakdown is likely to occur due to high shear forces especially in the feed zone of the centrifuge. Moreover, the rheological behavior, mainly showing nonlinear viscoelastic properties, often creates difficulties in solids discharge.

While the commercial demand for pure whey protein fractions is constantly rising, basic information for development of relevant separation processes is still lacking. Up to date, continuous centrifugal separation of whey protein precipitates has not been reported in literature yet. The aim of this study was to investigate the suitability of decanter centrifuges to be used as high accuracy separation plant for whey proteins by using low feed concentrations. Thus, as a first step, a detailed characterization of the specific particle properties of both aggregate types, α-La and β-Lg, was performed. This was followed by investigation of their settling, and the sediment consolidation behavior, which can be used as indications for sediment dewaterability in centrifugal separation. Finally, trials in a lab-scale decanter centrifuge were conducted based on the previous findings.

Theoretical considerations

The particle volume fraction ϕ can be calculated based on the solids weight fraction C_w by the following equation:

$$\phi = 1/[\frac{(1-C_w)\rho_p}{\rho_s} + 1]$$
(3.1)

With ρ_p: density of particle, ρ_s: density of suspension.

Considerations concerning sedimentation of particles

For low particle concentrations settling under laminar flow conditions, the sedimentation velocity u can be appropriately described according to Stokes' law:

$$u_{St} = \frac{(\rho_s-\rho_f)\cdot g}{18\cdot\eta_l} \cdot x^2$$
(3.2)

With η_f: dynamic viscosity of fluid, x: particle diameter, ρ_f: density of fluid, g: gravitational acceleration.

With increasing solids concentration, however, the sedimentation velocity is impaired due to settling hindrance effects. These effects comprise an increase in particle-particle interactions and a rise in the apparent viscosity of the system, as well as a higher relevancy of the drag forces. This necessitates the inclusion of the

solids fraction for the determination of sedimentation velocity. One of the most frequently used approximations is the equation of Richardson and Zaki (1954), which provides a relation for the empirical particle settling velocity u_p with respect to the solids volume fraction ϕ.

$$\frac{u_p}{u_{St}} = (1 - \phi)^{4.65} \tag{3.3}$$

The most common method for sedimentation analysis is the batch settling test, which provides important information for future transfer to centrifugal separation. The fundamentals of batch settling tests under gravity were published by Coe (1916) and Kynch (1952). Recording the liquid-suspension interface height as a function of time, results in a settling curve comprising three distinct parts: a constant settling period, hindered settling period and a compression zone. The constant settling period is the initial linear portion of the curve, where (almost) no particle hindrance effects appear. As the interface moves downwards, the concentration of particles increases, while the respective available volume is continuously shrinking. This implements a slowdown of sedimentation velocity, referred to as the hindered settling period. The sedimentation phase stops as soon as all particles entered the sediment layer on the bottom of the vessel (detailed information on compression is provided in the next passage). This, however, implements that all conceivable concentrations of solids ϕ_i are attained in one single experiment.

The Kynch theory comprises the assumption that the local solids concentration is the solely driving force for hindrance in settling velocity. Thereof a mass continuity equation of the solid phase can be introduced as

$$\frac{d\phi_s}{dt} + \frac{d(u_s\phi_s)}{dx} = 0 \tag{3.4}$$

For a proper description of the settling process in dependency of solids concentration ϕ, the (solids) flux function can be defined as follows.

$$f(\phi) = u(\phi)\phi \tag{3.5}$$

An approximation for local solids concentration ϕ in a batch settling test is given by

$$\phi = \frac{\phi_0 h_0}{h(t)} \tag{3.6}$$

With ϕ_0 and h_0 as initial concentration and suspension height, and $h(t)$ as interface height at time point t.

Considerations concerning dewatering properties of sediment

At the end of the settling phase, the position of the interface between the particle-free supernatant and the sediment stays constant. The sediment is a continuous network of particles at the bottom of the vessel, which exhibits a certain network strength P_y mainly depending on its structure, i.e., the number, strength and arrangement of interparticular connections. The particle network will remain in this original form until an applied stress dp exceeds the compressive yield stress P_y

resulting in a collapse of the network followed by its consolidation. Thereby, sediments of compressible solids comprise a concentration gradient with the highest packing density at the bottom of the vessel., i.e., there the solids volume fraction ϕ_i is maximal. Incompressible solids would lead to a homogeneous solids concentration and permeability that is insensitive to the applied pressure.

The dewatering properties of a buildup sediment can be described by determination of the compressive yield stress $P_y(\phi)$, which is a function of the local solids volume fraction (Buscall and White, 1987). In literature several numerical solutions are presented, which use iterative algorithms to model the equilibrium solids volume fraction distribution in the sediment (Curvers et al., 2009; Usher et al., 2013; Loginov et al., 2017). Alternatively, an approximative calculation of the maximal particle volume fraction, ϕ_{base}, and respective compressive yield stress $P_y(\phi_{base})$ at the tube base is provided by Buscall and White (1987) and was experimentally proven by Usher et al. (2013) to fit the results properly.

$$\phi_{base} = \frac{\phi_0 H_0\left[1-\frac{1}{2R_{max}}(H_\infty+a\frac{dH_\infty}{da})\right]}{\left(H_\infty+a\frac{dH_\infty}{da}\right)\left(1-\frac{H_\infty}{R_{max}}\right)+\frac{H_\infty^2}{2R_{max}}} \tag{3.7}$$

The subscript 0 refers to initial conditions of volume fraction ϕ and suspension height H, while H_∞ indicates equilibrium sediment bed height, a is the acceleration, and R_{max} the radius from central axis to the sample bottom.

$$P_y(\phi_{base}) = \Delta\rho a \phi_0 H_0(1 - \frac{H_\infty}{R_{max}}) \tag{3.8}$$

With

$$a = \omega_i^2 R_{max} \tag{3.9}$$

3.2 Materials and methods

3.2.1 Production of aggregate suspensions

For production of whey protein solution, WPI powder (Davisco, Le Seur, Minnesota, US) was used as starting material. WPI had a protein content of 94% based on dry matter and comprised 18% α-La, 44% β-Lg A, 30% β-Lg B, and 8% minor proteins.

3.2.1.1 Production of α-La aggregates

WPI powder was dissolved in de-ionized water (DIW) to a final protein concentration of 150 g L^{-1} and was kept under gentle agitation using a three-blade stirrer (Heidolph Elektro GmbH & Co. KG, Schwabach, Germany) with rotation speed of 350 rpm for 12 h at 4°C, for complete rehydration of the proteins. Environmental conditions were adjusted to a pH value of 3.4 using trisodium citrate dihydrate and

citric acid monohydrate (Bernd Kraft GmbH, Duisburg, Germany) to a citrate content of 60 g L^{-1}, as previously described by Toro-Sierra et al. (2013). Heat treatment was conducted with a vessel containing the protein solution in a water bath while stirring the solution to ensure ideal mixing. Upon reaching the target temperature of 50 °C, the temperature was kept at 50 °C ± 0.5 °C for 120 min, followed by a fast cooling phase with ice water. If required, the suspension was diluted with DIW to desired protein concentration.

3.2.1.2 Production of β-Lg aggregates

WPI was dissolved in DIW to a protein content of 25 g L^{-1} in batches of 15 L. Solution was homogenously mixed using a three-blade stirrer with rotation speed of 350 rpm for 12 h at 4 °C. Ionic calcium (CaCl$_2$ 2 H$_2$O, Sigma Aldrich, St. Louis, United states) content was set to 0.55 g L^{-1}, and confirmed by a flame photometer (Elex 6361, Eppendorf, Hamburg, Germany). Afterwards lactose was added to an amount of 0.5 g L^{-1}. Consequently, the pH was adjusted to 7.5 using 1 M HCl (Tolkach et al., 2005). For heat treatment a pilot scale tubular counter-current heat exchanger plant was used (GEA TDS GmbH, Ahaus, Germany), comprised of a heating, holding, and cooling section. The product with an initial temperature of 20 °C was heated to 92 °C with a constant heating rate of 2 K s^{-1}. The temperature was kept constant for 23 s. Cooling rate was respective to heating rate. The product flow rate was 120 L h^{-1}.

3.2.2 Protein analytics

3.2.2.1 Quantification of major proteins

Quantification of native whey proteins was executed by RP-HPLC. Samples were diluted to fit the calibration range, followed by pH adjustment to 4.6 using 0.1 M and 0.01 M HCl or NaOH. Non-native proteins precipitated and were separated using a syringe filter of 0.45 μm (Chromafil RC-45/25, Macherey-Nagel GmbH & Co. KG, Dueren, Germany). The analysis was performed using an Agilent 1100 series chromatograph (Agilent Technologies Inc., Santa Clara, CA, USA). Separation of the proteins was done with a PLRP-S 300-Å 8-μm column (Latek Labortechnik-Geräte GmbH & Co., Eppelheim, Germany). Elution was performed using a mixture of eluent A [1% trifluoroacetic acid (TFA) in water] and eluent B (80% acetonitrile and 0.05% TFA in water) at a flow rate of 1.0 mL min^{-1} at 40 °C.

The DD represents the ratio of remaining native protein concentration after heat treatment $C_{p,t}$ to initial concentration of native protein prior to heating $C_{p,0}$ and was calculated for each protein p separately (p = α-La, β-Lg).

$$DD = \left(1 - \frac{C_{p,t}}{C_{p,0}}\right) \cdot 100\% \qquad (3.10)$$

3.2.2.2 Analysis of stabilizing forces in aggregates

To analyze the stabilizing mechanisms of the aggregates formed, polyacrylamide gelelectrophoretic (PAGE) analysis was performed, adding different reactants to the sample buffer as described by Leeb et al. (2018). In short, disintegration of non-covalent interactions was achieved by adding 1% w v^{-1} SDS and 6 M urea to the glycine/Tris sample buffer. Complete dissociation by disruption of disulfide bonds was induced by addition of 1.54 mg mL^{-1} dithiothreitol (DTT). 10 µL of the samples in respective buffer system were transferred to gel pockets (Mini Protean Stainfree gels, Bio-Rad Laboratories Inc., Hercules, CA, USA) and voltage of 300 V was applied for electrophoretic separation. Evaluation of gels was conducted in the GelDoc XR+ scanning system equipped with the Software Image Lab Version 5.1 (Bio-Rad Laboratories Inc., Hercules, CA, USA).

3.2.3 Characterization of aggregates suspensions

3.2.3.1 Particle size measurement

Particle size distribution of the aggregates was determined by laser diffraction using a Malvern Mastersizer 2000 equipped with a Malvern Hydro 2000S sample dispersion unit (Malvern Instruments GmbH, Herrenberg, Germany). Refractive index of the dispersant (softened water) was set at 1.33, with an absorption of 0.001, and the refractive index of protein was set at 1.41. Each sample applied to dispersion unit was measured twice within 2 min. Aggregate size stayed stable within the measurement time. Sample application to dispersion unit was done twice for each sample.

3.2.3.2 Density

All measurements were performed using a temperature controlled oscillating U-tube density meter (DMA 4100 M, Anton Paar, Graz, Austria). Measurements were performed in triplicate.

3.2.3.3 Viscosity

Dynamic viscosities of liquid phases were determined by rheometric measurements using the rheometer MCR302 (Anton Paar GmbH, Graz, Austria) equipped with a cone-plate geometry (diameter = 50 mm, angle = 2°, distance = 0.213 mm). Measuring and evaluation was conducted in the software RHEOPLUS/32 V3.61. Shear rate was increased from 1 to 100 s^{-1} within 33 measurement points, the shear rate of 100 s^{-1} was held for another 10 points, followed by a downwards ramp to 1 s^{-1} again. All liquids showed Newtonian flow behavior.

3.2.3.4 Determination of mass fraction

Dry matter content was measured by a microwave moisture/solids analysis system (CEM Smart Turbo, CEM GmbH, Kamp-Lintfort, Germany). Samples were given on pre-dried pads, put on top of the integrated weighing machine. The sample was dried at 105 °C by focused microwaves and reduction of weight was used for calculation of dry matter content. All measurements were performed in triplicate.

3.2.4 Analysis of sedimentation and consolidation behavior

3.2.4.1 Settling Behavior

Batch settling tests can supply information for distinction between types of sedimentation behavior and for determination of sedimentation velocities. In this test suspensions with initial concentration of $\phi = 0.02$ were transferred to 500 mL measuring cylinders. The distance between two graduation lines was 2 mm. The suspensions were consciously mixed before the settling tests started. The height of the interface was monitored as a function of time from visual measurements.

3.2.4.2 Sediment consolidation behavior

A helpful tool for analysis of sediment consolidation behavior are analytical centrifuges, like the Lumifuge (LUM GmbH, Berlin, Germany), which was used in this study. Herein, light (wavelength 870 nm) is transmitted through the samples in dependence of time and position in the cuvette while centrifugation, thus enabling a high-resolution tracking of the sediment bed height (Lerche and Sobisch, 2007; Sobisch and Lerche, 2000). From the data obtained, a function of the particle network resistance to deformation can be determined, the compressive yield stress $P_y(\phi)$.

Throughout all measurements rectangular polycarbonate cells with diameter of 10 mm were used. The inserted sample volume was 1.4 mL with a respective sample height $H_0 = 18$ mm. In the transmission profiles, the interface between air and liquid is visible as a sharp increase, the sediment-liquid interphase is indicated by a sharp decrease of the transmission (Fig. 3-1). The sediment bed height is the difference between the bottom of the cuvette ($R_{max} = 130$ mm) and the sediment-liquid interface. The experiment was designed as a multistep centrifugal consolidation method as previously described by Curvers et al. (2009) and Loginov et al. (2014). Thus, a sequence of increasing rotational speeds ω (300 to 3,600 rpm) was programmed and each step was executed until an equilibrium sediment bed height $H_\infty(\omega)$ was achieved. Sample temperature was previously adjusted to 20 °C and was maintained during centrifugation.
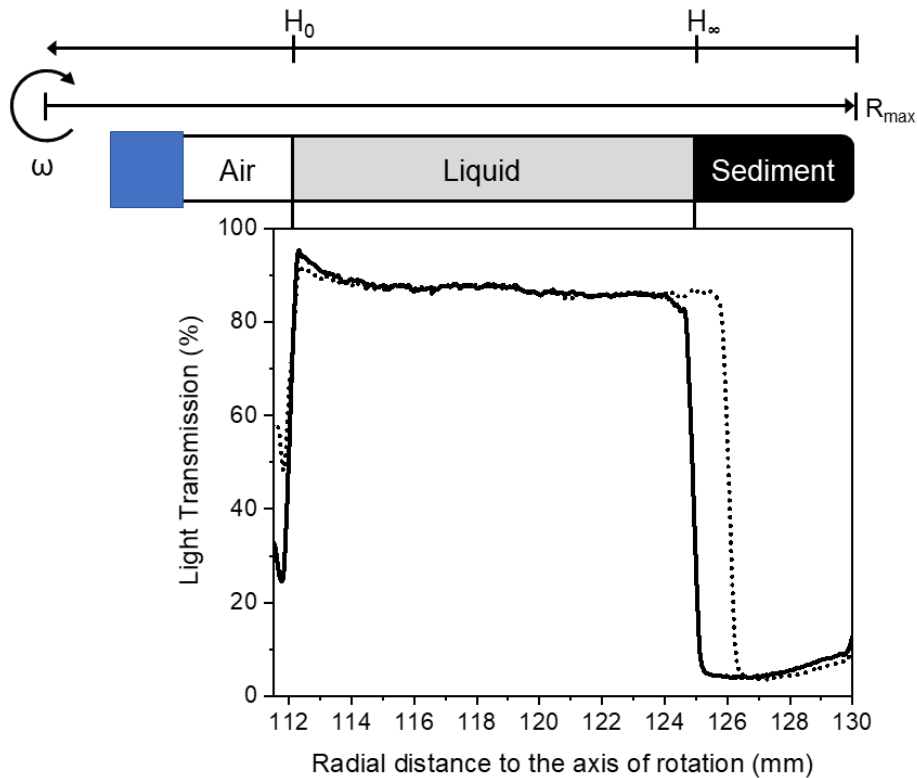
Fig. 3-1 Exemplary light transmission profiles at two rotational speeds for β-Lg suspension 2% (w w^{-1}), at the end of a constant speed period, and drawing for indication of the air-liquid and liquid-sediment interfaces to give the coordinates for R_{max}, H_0, H_∞.

3.2.4.3 Texture analysis of sediment

A Texture Analyzer TAXT Plus (Stable Micro Systems Ltd, Godalming, England) was used to investigate interaction of sediments towards product touching parts of the decanter, for prediction of stickiness between sediment and material, respectively. Therefore, an in-house manufactured measurement geometry (dimensions of semi-circle: diameter = 55 mm) was used, imitating half a flight of decanter scroll. For manufacture stainless steel with similar alloy as in the pilot scale decanter was used.

All experiments were conducted in a controlled temperature room at 20 °C. Compression of sediments was performed, measuring the resulting force-time curve. Same volume of sediment samples was given in a beaker glass (diameter = 90 mm, height = 70 mm) and was placed on the table of the Texture Analyzer. Then the crosshead descended at the rate of 1 mm s^{-1}. A force of 0.1 g was defined as trigger force, when head accelerates to 2 mm s^{-1} and conducts total deformation depth of 9 mm. When the compression stroke was completed, geometry abruptly reversed direction and started its upward stroke at 2 mm s^{-1}. Five to six measurements were conducted for each sample. The adhesiveness was defined as the integrated negative area in the pull phase, as described in Friedman et al. (1963).

3.2.5 Separation process

The separation of aggregates from soluble protein phase was performed using a laboratory-scale decanter centrifuge based on counter-flow principle (MD80, Lemitec GmbH, Berlin, Germany). A sectional view of the decanter is provided in Fig. 3-2, and the working principle is briefly explained in the following. The aggregate suspension is pumped through an inlaying pipe to the middle of the cylindrical part of the bowl, where it enters the separation room. The centrifugal force is generated by rotation and accelerates the particles to sediment at the inner wall of the bowl. The conveyor scroll transports the sediment cake towards the conical part of the bowl, and finally discharges the sediment via the conus. The liquid phase flows over the weir on the counterpart, is collected by an impeller disc, and is discharged as the so-called centrate. Applicable g-forces lay between 10 to 4,400 g, with differential speeds of the scroll between 0 to 150 rpm.
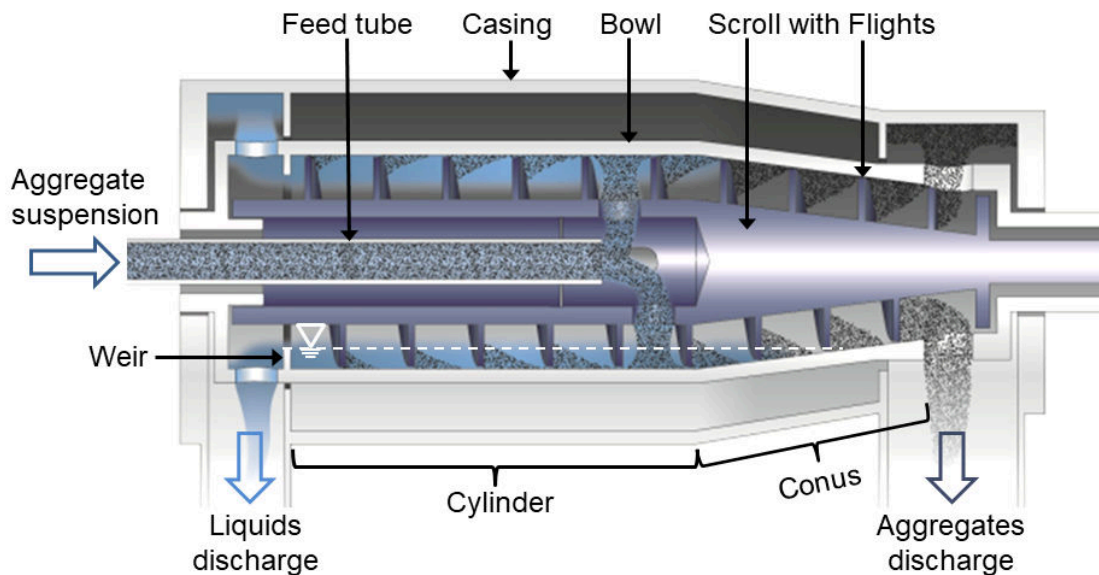
Fig. 3-2 Schematic sectional view of a counter-current decanter centrifuge [modified image from Lemitec GmbH, Berlin, Germany].

3.2.5.1 Operation and sampling

The suspensions were pumped at a flow rate of 12 L h^{-1} by a hose pump (Verderlab VL1000, Verder Deutschland GmbH, Haan, Germany) from a stirred feed vessel (three-blade stirrer, 200 rpm) into the decanter. Samples of centrate and sediment were taken after constant separation conditions were reached. After a change of process conditions, i.e., increase of g-force, at least 4 complete bowl throughputs were awaited, before sampling was performed. Samples were immediately cooled in an ice bath to prevent microbiological deterioration. After centrifugal separation, samples were forwarded to analysis. The dry substance content of the sediments were measured with the method described above for determination of solid mass

fractions. The centrates were analyzed by photospectrometry (Jenway 6305, Cole Parmer, Staffordshire, UK) for determination of clarification. Thus, the transmission at a wavelength of 600 nm was measured in the obtained centrate, the slurry, and an ideally cleared reference sample, which was rendered particle-free by excessive batch centrifugation (15 min, 6,000 g) and additional purification through a syringe filter of 0.1 µm. The clarification was calculated according to (3.11).

$$Clarification = \frac{(T_{Slurry} - T_{Reference}) - (T_{Centrate} - T_{Reference})}{(T_{Slurry} - T_{Reference})} \cdot 100\% \qquad (3.11)$$

3.3 Results and discussion

3.3.1 Characterization of aggregate suspensions

As described above, α-La and β-Lg aggregates were produced by means of selective thermal aggregation, according to conditions described in chapter 3.2.1. Tab. 3-1 lists the obtained denaturation results determined by RP-HPLC analysis and calculated according to (3.10). Regarding α-La denaturation, a DD of almost 98% was achieved, thereby losing only 3% of β-Lg's nativity. The heat denaturation for generation of β-Lg aggregates resulted in a denaturation of β-Lg of 94%, accompanied by α-La aggregation of 12%. As described by Tolkach et al. (2005a) a higher β-Lg denaturation is always at the expense of a further loss of α-La. We therefore decided to focus on a high preservation of α-La fraction in this heating procedure, thereby accepting remaining residues of native β-Lg in the final solution, which could be removed, e.g., by IEC at a later stage.

Tab. 3-1 Characterization results of α-La and β-Lg suspensions including DD (mean value ± SD of 10 independent experiments), particle density and viscosity of liquid phase.

	α-La aggregation	β-Lg aggregation
DD of target component	97.8% ± 0.7%	94.1% ± 0.9%
DD of non-target component	2.6% ± 2.1%	12.2% ± 2.9%
Particle density	1358 kg m^{-3}	1268 kg m^{-3}
Viscosity (20°C)	1.5 mPa s	1.1 mPa s

After selective thermal aggregation, a detailed characterization of the obtained particle suspension was performed by particle size measurement, PAGE analysis for elucidation of stabilizing mechanisms, determination of particle density (see Tab. 3-1), measuring of viscosity of the particle-free liquid phase (see Tab. 3-1), and microscopic analysis of aggregate shape. Fig. 3-3 depicts the sum distribution of aggregate sizes together with indicated the volume-based diameter for percentiles of 1%, 50%, and 99% of the distribution, respectively. The α-La aggregates (grey diamonds) showed a narrow particle size distribution with a $d_{0.5}$ of 11.6 µm.

β-Lg aggregates (black squares) were distinctly larger and showed a broader size distribution range. Moreover, a small pre-shoulder is visible at ca. 10 µm, which makes up less than 4% on a volume-based distribution. The $d_{0.5}$ of β-Lg aggregates was at 109 µm, but also aggregates with sizes up to 500 µm were detected.
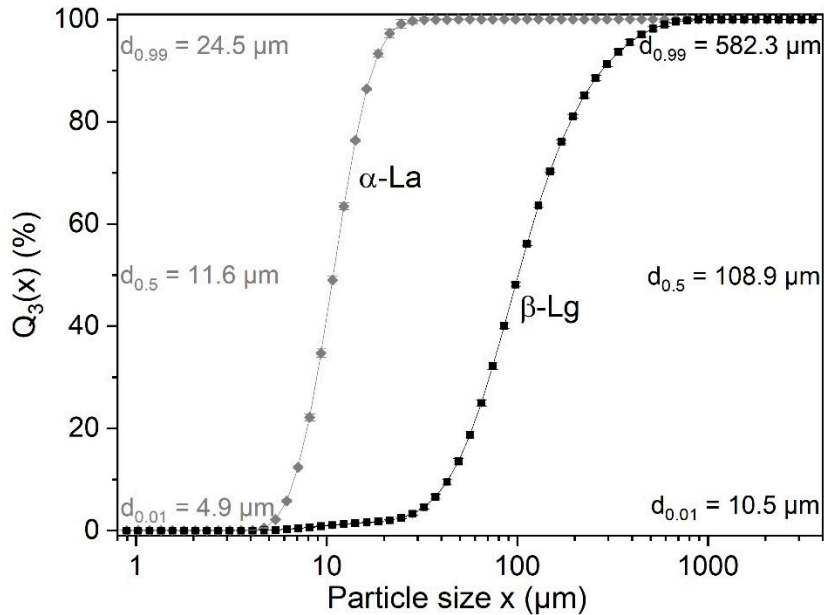
Fig. 3-3 Particle size sum distribution of selectively aggregated α-La and β-Lg with indicated $d_{0.5}$.

The aggregate shape was investigated by means of light microscopy. In Fig. 3-4 representative images are given for α-La aggregates (a) and β-Lg aggregates (b). α-La built small, irregularly shaped particles, with sizes around 12 µm, which agrees with laser diffraction analysis. The single particles formed loose clumps, which seemed to be reversible after disturbance. β-Lg aggregates (Fig. 3-4b) showed shapes of elongated, partially branched single strands, with chord lengths of over 100 µm. They presented a rigid and stable conformation.
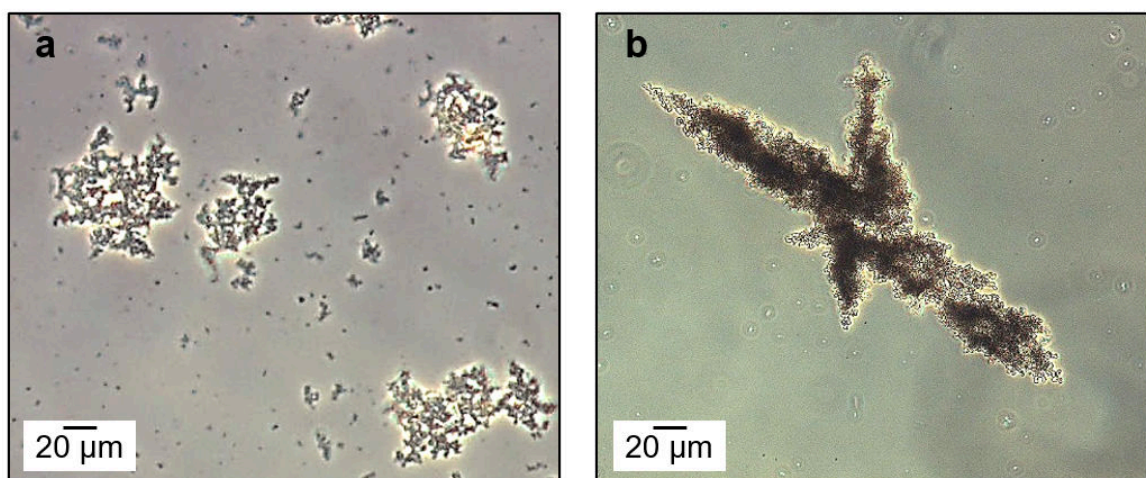
Fig. 3-4 Microscopic images of α-La aggregates (a) and β-Lg aggregates (b).

Elucidation of intermolecular stabilizing mechanisms was conducted applying PAGE analysis under non-reducing (sample buffer + SDS, Fig. 3-5a) and reducing conditions (sample buffer + SDS + DTT, Fig. 3-5b). For denatured β-Lg (lane 2) no band was visible under non-reducing conditions, however, in an reducing environment the band appeared. This finding proves that the β-Lg aggregates were stabilized via disulfide bridges, which got disintegrated by DTT and enabled the penetration into the gel. Under non-reducing conditions, the aggregates were withheld in the gel pockets. The stabilization of β-Lg aggregates via disulfide bridging is proved, e.g., by De Wit (2009) and Nicolai et al. (2011). They described the β-Lg aggregate formation as a combination of radical-like thiol-disulfide exchange reactions and hydrophobic interactions that also creates the polymer strand appearance, which was observed in microscopic analysis. The weak β-Lg band of supernatant sample (lane 3) presents the remaining 6% of β-Lg that were consciously not denatured by the chosen thermal heating conditions, according to the aim of minimal heat impact on the α-La fraction, as described above. Evaluation of the thermal denaturation of α-La showed an aggregate disruption already under non-reducing conditions, as the α-La band is visible in lane 6. This indicates α-La aggregate stabilization via non-covalent bonds. Based on studies of Bramaud et al. (1995, 1997a, 1997b), the predominant interaction for α-La aggregate stabilization are hydrophobic interactions. When the calcium ion is depleted from the binding site, the two domains of α-La slightly drift away, thus loosening the tertiary structure. Upon unfolding, hydrophobic residues, hidden in the inner core of the molecule, get exposed and interact with each other, leading to the formation of α-La aggregates (Schultz, 2000).
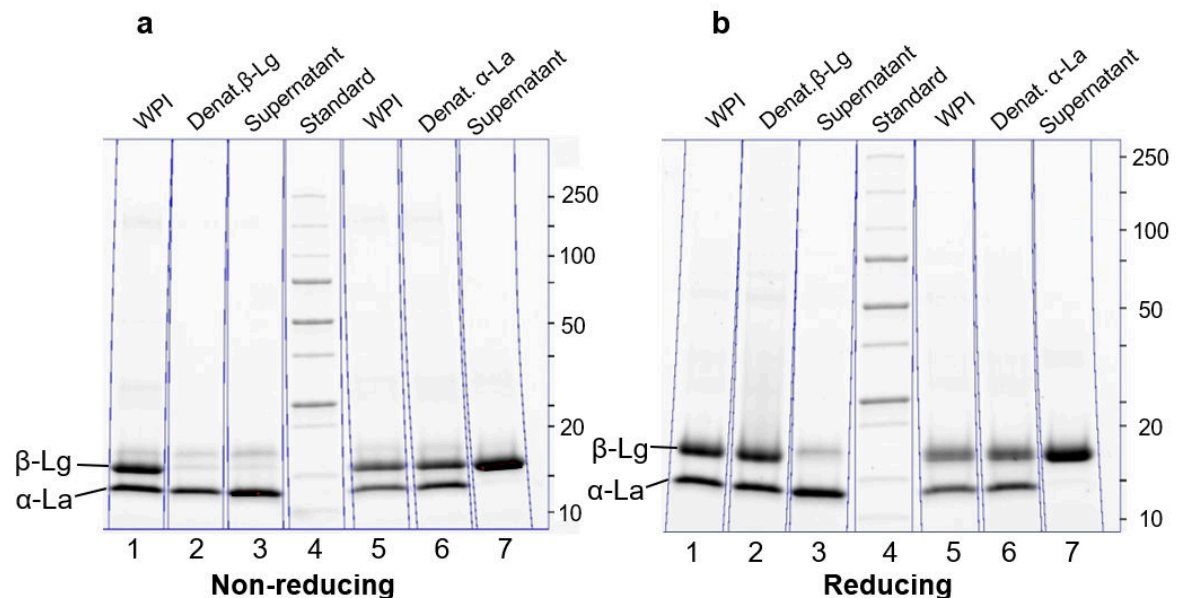
Fig. 3-5 SDS-PAGE with non-reducing (a) and reducing (a) environmental conditions, lane 1 and 5 present the starting WPI solution before heat treatment, lane 2 and 6 show the suspension after thermal treatment for β-Lg and α-La, respectively, lane 3 and 7 present the corresponding supernatant.

3.3.2 Investigation of sedimentation behavior

For the batch settling test, height of the clear liquid interface was noted at regular intervals for a total duration of 900 min. The resulting settling curves for both aggregate suspensions are illustrated in Fig. 3-6.
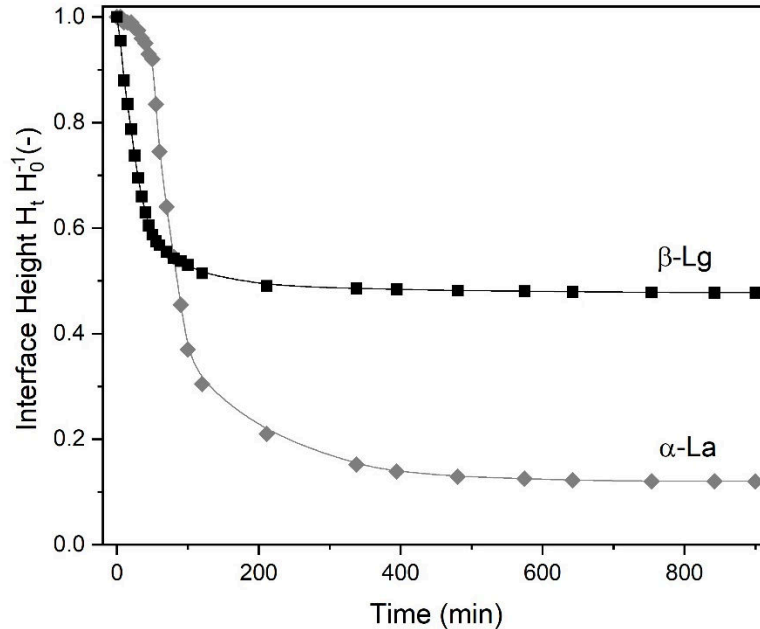
Fig. 3-6 Batch settling curves (ϕ = 0.02) of α-La aggregates and β-Lg aggregates.

Sedimentation of β-Lg aggregates started straight away and within an hour nearly all particles were settled down. The progression of interface lowering slowed down, as the local aggregate concentration rose towards the bottom of the cylinder. At higher aggregate concentrations particle-particle interactions become more prominent, the viscosity increases, and the drag forces of displaced liquid reduce sedimentation velocity. In comparison to that, α-La aggregate settlement showed an initial period with hardly any change in the level of interface. A so-called lag phase represents either a time span where suspension recovers from previous disturbance, or, and what is more probable in this case, in which loosely connected flocs comprising several aggregate units are formed. Probably, a steric entanglement of the aggregates might occur as the calcium-free apo-form is known for its loose and swollen state, which facilitates twisting of the helix-rich regions of the protein (Permyakov and Berliner, 2000). After flocculation, a rapid settling period started with comparable sedimentation velocity than the β-Lg aggregates. At the end of settling phase, the sediment of α-La reached a higher packing density than the sediment of β-Lg aggregates. This lack of compactability of β-Lg aggregates is presumably due to the high degree of particle misfit because of their irregular form and high rigidity.

As mentioned above, sedimentation velocity changes in dependence of local solids concentration. The experimental values for the $u(\phi)$ function are distracted from the

absolute values of the gradients of the settling curves from Fig. 3-6. The respective solids void fractions ϕ are derived from (3.1). Thus, Fig. 3-7 presents the experimental sedimentation velocities (filled symbols) and compares it with the theoretic velocities according to the equation of Richardson and Zaki ((3.3), hollow symbols). The sedimentation velocities according to the Richardson and Zaki equation were determined for the 1% of smallest particles ($d_{0.01}$) in α-La and β-Lg suspensions. The sedimentation velocities close to $\phi = 0$ present the Stokes velocities (3.2), respectively. Necessary data (density, particle size, viscosity) for calculation was derived from aggregate characterization described in chapter 3.3.1.
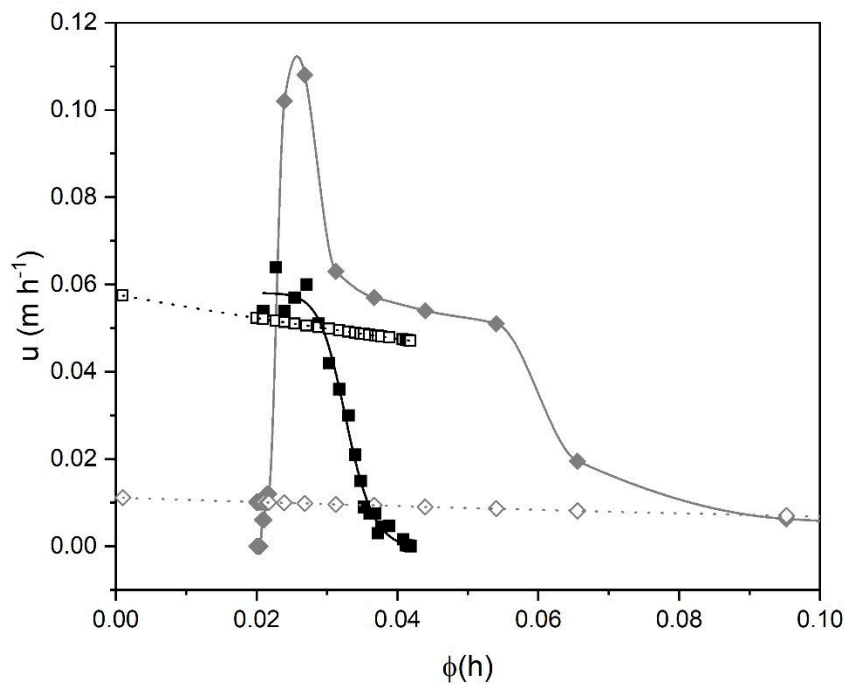
Fig. 3-7 Sedimentation velocities for α-La (grey diamonds) and β-Lg (black squares) aggregates derived from batch settling experiments (filled symbols) and calculated by Richardson & Zaki equation (hollow symbols).

The lag phase in α-La aggregate sedimentation is assigned to an initial period with nearly no settling velocity. This phase is followed by a rapid settling period, reaching maximal velocity of 0.11 m h^{-1}. Afterwards, two plateau phases can be estimated in sedimentation velocity, finally converging towards zero. A similar shape of slope was reported by Bargieł and Tory (2013) for flocculated suspensions. After an initial floc formation phase, the experimental settling velocity can exceed the Stokes velocity by many times over. A characteristic phenomenon for flocculated suspensions is the so-called zone sedimentation, meaning that all particles build a single zone and present the same settling velocity. Thus, the velocity of the interface is steady (plateau at 0.06 m h^{-1}), but changes with time as other settling hindrance factors gain more importance. A further increase in the solids void fraction progressively decelerates sedimentation velocity, finally fitting well to calculated values.

Regarding the settling of β-Lg aggregates, the approximation with the Stokes equation for the $d_{0.01}$ results in a good accordance with experimental data up to $\phi = 0.03$. The distinct drop of $u(\phi)$ is, however, poorly described by the Richardson & Zaki approach, as the boundary conditions neglect the particle shape. As the β-Lg aggregates exhibit high rigidity and present irregular shapes, soon a porous sediment ($\phi = 0.04$) is reached that only allows for compaction by application of external forces.

3.3.3 Compressibility of sediments

Investigation of sediment compressibility during centrifugal acceleration is a helpful tool to gain information about overall sediment structure and to predict dewaterability. By relating the values of equilibrium sediment bed height $H_{\infty,i}$ to their respective logarithmic centrifugal acceleration a_i, a linear dependency is obtained. Fig. 3-8 illustrates this dependency for α-La and β-Lg aggregate suspensions containing mass fractions of 1% and 2%, respectively. All curves show a decrease of H_∞ at respective higher centrifugal accelerations. An increase in centrifugal acceleration provokes higher compressional forces, which are reflected in the networks' resistance. Already observed in the batch settling test, the α-La aggregates build up a distinctly more compact sediment compared to β-Lg.
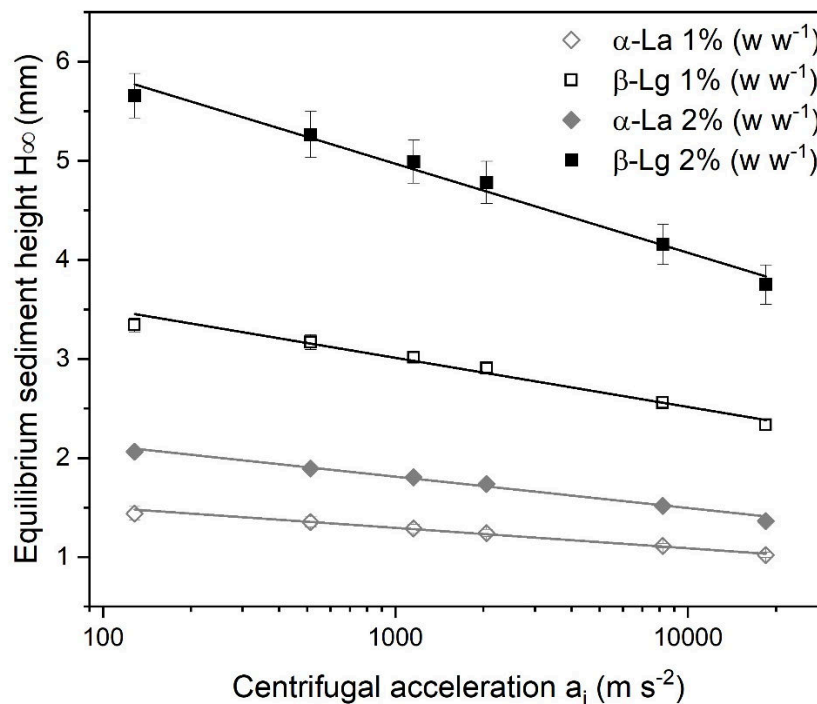
Fig. 3-8 Equilibrium sediment bed height as a function of centrifugal acceleration for samples with α-La and β-Lg aggregates containing 1% and 2% (w w^{-1}) solids mass.

With the following equation (3.12), a curve fit is performed to determine the constants c_0, c_1, c_2, c_3 with high accuracy.

$$\ln H_\infty = c_0 + c_1 \ln a + c_2 (\ln a)^2 + c_3 (\ln a)^3 \tag{3.12}$$

Thereof the quotient dH_∞/da can be calculated with (3.13) and used for further determination of ϕ_{base} and $P_y(\phi_{base})$ according to (3.7) and (3.8)

$$\frac{dH_\infty}{da} = \frac{H_\infty}{a}[c_1 + 2c_2 \ln a + 3c_3 (\ln a)^2] \tag{3.13}$$

The results for the theoretical volume fraction ϕ_{base} with respective compressive yield stress $P_y(\phi_{base})$ for the sediment layer in direct contact with the cuvette bottom are illustrated in Fig. 3-9. At low P_y, the volume fraction for β-Lg aggregates is just slightly higher than the initial concentration. Even at high stresses, the volume fraction stays in a low range. The interpretation of this data suggests that compression and therefore the deformation of particles seems to be highly limited. The broad β-Lg particle size distribution with irregularly shaped aggregates may lead to inhomogeneous cake structure. At low pressures, cavities may form, which enclose water. Dewatering occurs, when particles break down, resulting in a reduction of the distance between two aggregates and thus squeezing out intermediate water. The stabilization via disulfide bonds results in rigid complexes that are highly resistible to pressure. Therefore, the dewatering process in this sediment is restricted to high g-forces. Apart from that, humidity may be enclosed in intraparticular holes and can therefore not be removed by compression unless complete structural breakdown into primary aggregate units takes place. Compared to that, α-La aggregates showed a high compressibility, even at low stresses. The distance between particles is a function of the electrostatic repulsion, the van der Waals attraction, and the external pressure. As α-La aggregation was performed close to its isoelectric point, the electrostatic repulsion is supposed to be on a very low level, whereas the van der Waals attraction might be the dominating force. Probably, these attractive forces have impact on the flocculation and enable the high degree of consolidation of the sediment cake.
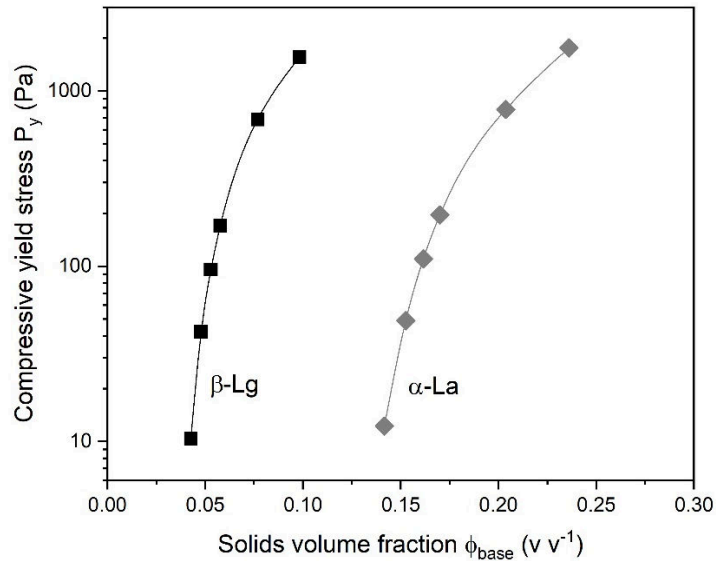
Fig. 3-9 Compressive yield stress plot for α-La and β-Lg aggregates in dependence of solids volume fraction.

3.3.4 Analysis of adhesiveness of the sediments

To investigate the tendency of the sediment to stick to parts of the centrifuge, texture analysis experiments were performed as described in chapter 3.2.4. In dependence of the solids weight fraction, the adhesiveness of both, α-La and β-Lg, sediments were investigated, because continuous solids discharge by the scroll of the decanter centrifuge might be impaired by high stickiness of sediment. As depicted in Fig. 3-10, the α-La sediment showed only little interaction with the measurement geometry at low solids concentrations, as the necessary dragging force was low. Above 20%, adhesiveness tremendously rose with increase in solids fraction, indicating a high stickiness for the α-La sediment at high dry matter concentrations. In contrast to this, the β-Lg sediment showed maximal adhesiveness at ca. 12% solids weight fraction. However, exceeding 24%, the sediment showed nearly no stickiness to the geometry surface. Transferring these results to the separation process in the decanter, it becomes obvious that a discharge of high dry matter β-Lg sediment will presumably be unproblematic, as the interactions between product contact surfaces and β-Lg sediment are low. Higher dry matters of the α-La sediment, however, seems to increasingly favor the adhesion to surfaces. As an accumulation of cake in the bowl can provoke imbalance or blockage, this may impair the sediment discharge out of the bowl. The conditions used in the performed experiments indeed deviate from real centrifugation trials, e.g., no centrifugal force is applied during the experiment, this implies that the sediment is not compressed at the timepoint of measurement, what may alter the porosity and the interactivity with materials. Thus, centrifugal experiments were performed to confirm the tendencies observed in this approach.
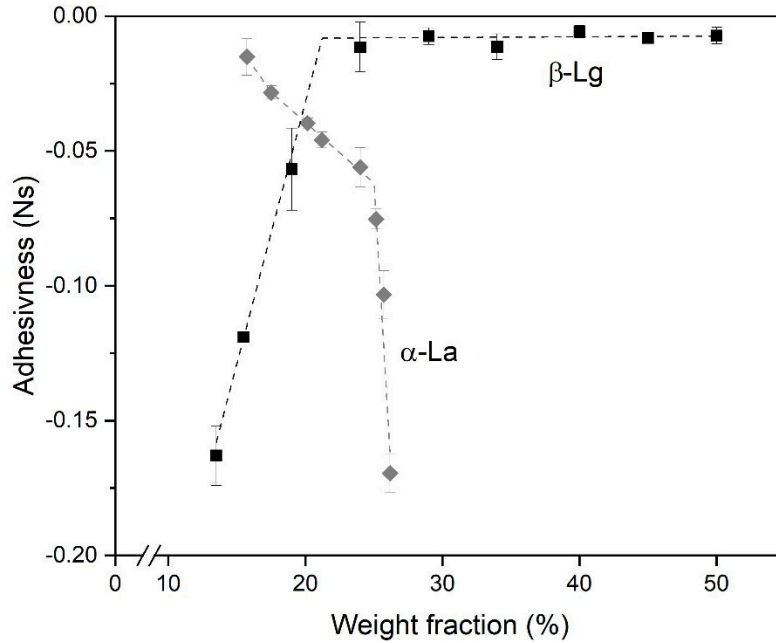
Fig. 3-10 Adhesiveness of α-La and β-Lg aggregate sediments in dependence of aggregate concentration.

3.3.5 Separation behavior in the decanter centrifuge

Based on previous results, the suspension inlet concentrations were chosen 2.5% (w v^{-1}), where sedimentation velocity was maximal for both types of suspensions. Separation of both aggregate systems was performed in lab-scale decanter at variable g-forces in a range of 1,000 to 4,000 g.

For separation of the α-La sediment, the first trials with a weir disc of medium height (h = 10 mm) ended up in an overload shut down of the decanter, with a sparely cleared supernatant and no discharged sediment. A constant operation of the centrifuge was neither possible by manual variation of scroll differential speed, nor by reduction of inlet flow rate. After disassembly of the machine, the sediment was found to stick to the backside of the scroll flights, which was presumably caused by pulling the scroll out of the bowl at its cylindrical end (Fig. 3-11c). The high accumulation of sediment in the bowl is presumably provoked by an unappropriated length of the drying zone, i.e., the conical part of the bowl that is not in contact with liquid is too long for this application. As the α-La sediment got to dry, its adhesiveness rose immensely as could be observed in previous experiments (chapter 3.3.4). Thus, the transportability got impaired and discharge of sediment was impeded. An arrangement to avoid this situation is the reduction of the drying zone to prevent excessive dewatering of the sediment. The length of the drying zone can be varied by the weir disc height, as the upper edge of this element determines the liquid gauge in the bowl. After setting the height of weir disc to maximum (h = 14 mm), continuous discharge of the sediment was observed. The obtained α-La sediment presented solids concentrations between 20 and 25% (w w^{-1}) dependent

on the applied centrifugal acceleration (Fig. 3-12a). In consent with rising sediment dry matter, the consistency changed from creamy and sludgy to a curd-like, pastose texture (Fig. 3-11a). The clearance of the respective supernatants presented an enhancement in dependency of applied g-force, too. The obtained clarification rates were between 62 to 71%, indicating that a distinct number of particles remained in the supernatant. A further enhancement of clarification could be achieved by extension of residence time or by raising the centrifugal acceleration. A further increase in centrifugal acceleration was not possible due to constructional restrictions of the centrifuge, and the chosen volume flow rate was already on the lower edge of manufacturers advice. The inlet flowrate was chosen such that the available residence time of the smallest particle was more than ten times longer than it theoretically needs for reaching the sediment cake. This suggests the occurrence of particle breakage, which can be induced through high shear stress. A reduced particle size consequently requires longer sedimentation durations. Thus, to overcome these obstacles, a change in separation plant might be advisable for this issue.
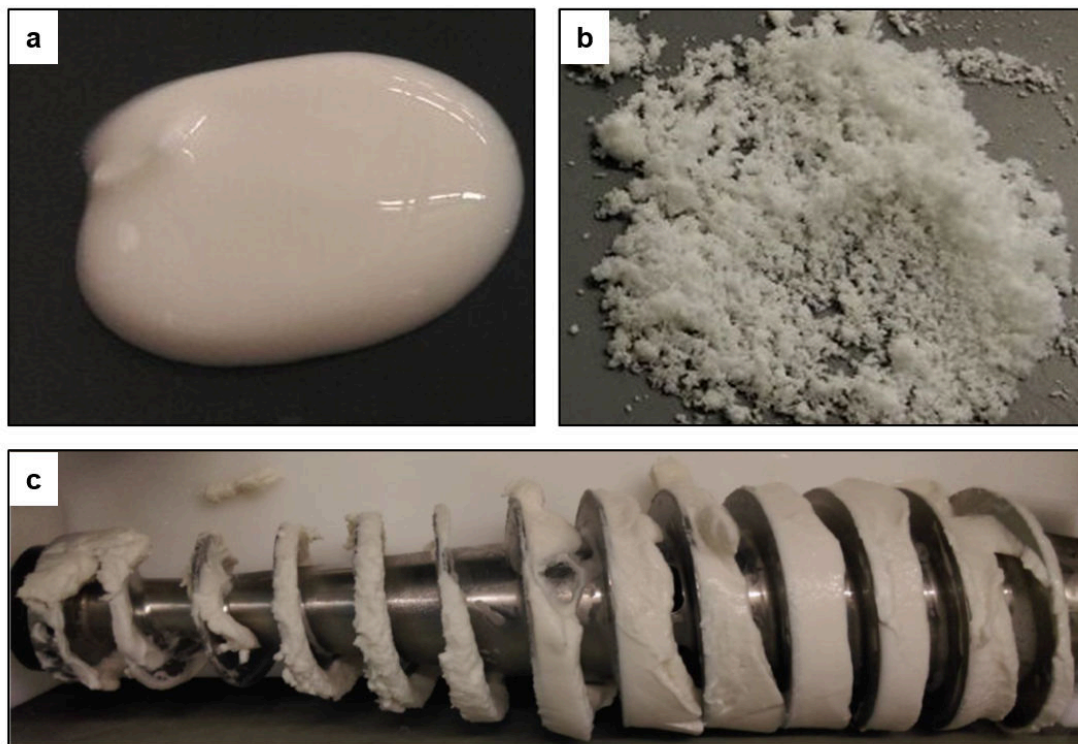
Fig. 3-11 Discharged α-La sediment from decanter with dry matter of 21% (a), β-Lg sediment with a dry matter of 34% (b) and scroll with adhering α-La sediment after overload shut down (c).

In contrast to the challenging α-La separation, sedimentation and discharging of β-Lg aggregates were unproblematic under all conditions. An elevation of applied g-force led to a nearly linear increase of sediment dry matter, as well as to a higher clearance of supernatant. The β-Lg sediment was discharged almost as free flowing powder at dry matters exceeding 25% (w w^{-1}). Below this dry matter, sticky clumps were obtained at the sediment outlet of the centrifuge. However, solid aggregate structures were clearly visible. Fig. 3-11b shows the macroscopic appearance of the β-Lg sediment with a dry matter of 34% (w w^{-1}). Regarding the supernatant, clarifications between 60 to 95% were obtained, depended on applied acceleration (Fig. 3-12b). Based on these results, one can expect a further improvement of separation efficiency by application of higher accelerations, and reduction of aggregate concentration.
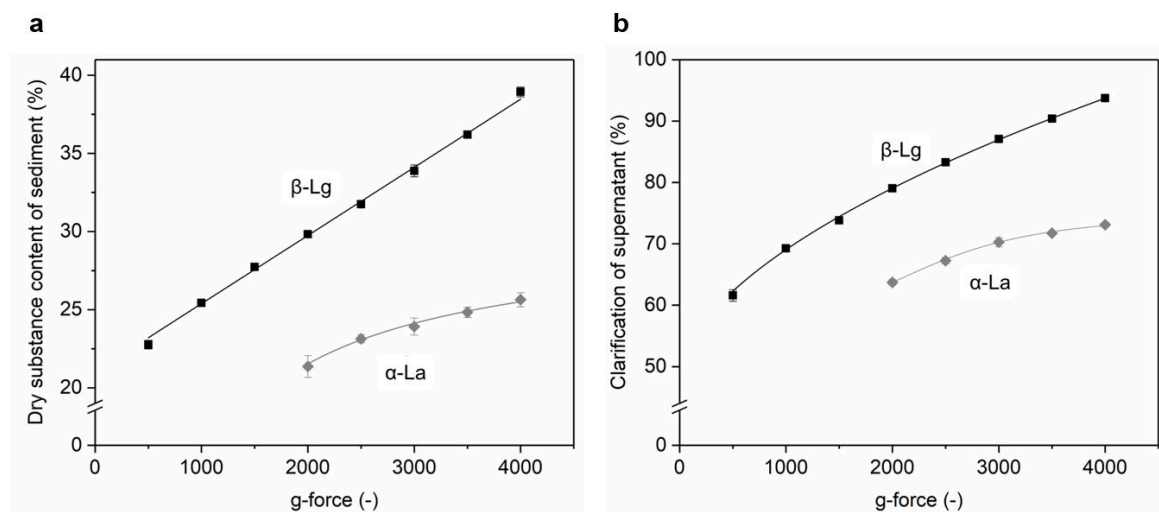
Fig. 3-12 Obtained sediment dry matter (a) and clarification rate of supernatant (b) for separation of α-La and β-Lg aggregate suspensions (2.5% (w v^{-1})) in dependence of g-force.

3.4   Conclusion

This study investigates the specific and intrinsic particle properties of two different types of selectively aggregated whey proteins and relates the results to their presented sedimentation and consolidation characteristics. The α-La precipitates, connected via hydrophobic interactions, presented beneficial flocculation effects in static sedimentation experiments, leading to 10-fold higher velocities than expected from calculations. In decanter centrifuge separation, however, the beneficial sedimentation effects were no more observable. Centrifugal acceleration forces exceeded the stabilizing forces of the α-La particles and led to their disruption. The disintegrated small particles were partly hard to segregate and remained in the centrate after centrifugation. Moreover, the α-La sediment cake was hard to handle at high solids concentrations. This, however, stands in conflict with the aim

of centrifugation, the maximization of dewatering. Nevertheless, as it was demonstrated that sedimentation of α-La aggregates is possible, a centrifuge with another discharge mechanism would be more appropriate for this purpose.

The β-Lg aggregates, stabilized by disulfide bridges, formed stable and solid particles, resulting in powder-like sediment that was simple to discharge and showed nearly no adhesiveness. The clarification of supernatant was satisfying and indicated that decanter centrifuges are the tool of choice for covalently stabilized particles. The obtained dryness of sediment was, however, surprisingly low. This might be related to intra-aggregate fluid, which got enclosed while aggregation.

This study might be an example for further applications in protein aggregate separation using continuous working centrifuges, not only in the field of food processing, but also in biopharmaceutical downstream processing.

4 Continuous centrifugal separation of selectively precipitated α-Lactalbumin

Summary and contribution of the doctoral candidate

The aim of this work was to evaluate the suitability of a co-current continuous centrifuge for the separation of selectively precipitated α-La at industrial-like scale. Tested process variables included different applied g-forces, separation temperatures of 20 °C and 50 °C, different concentrations of inlet dry matter, and the use of WPC80 and WPI as starting material. Separation efficiency reached a plateau at an applied g-force of 6,500 g and did not further improve with an increase of the centrifugal acceleration. The reduction of inlet dry matter led to improved separation efficiency as well as higher sediment dry matter contents. A significant improvement was also observed, when the separation was executed at a temperature of 50 °C, which was attributed to reduced viscosity of liquid phase and intensified particle stability. Generally, WPC80 and WPI showed similar behaviors, the results for separation efficiency and obtained sediment dry matter were only little superior when WPI was used.

As the sediment still contained residues of soluble β-Lg and buffer salts, the α-La-enriched sediment was resuspended in acidified water and two steps of reslurry washing were performed. Along the three centrifugation steps, a slight susceptibility to particle fragmentation was recognized by reduction of median particle size from 10.3 μm to 0.6 μm to 0.4 μm. This was also reflected in the visible texture of the discharged sediment, changing from irregularly shaped lumps to creamy long filaments. However, separation efficiency and dry matter content of sediment were rarely impaired by the fragmentation. The minor relevancy of the particle size as an influencing factor on the overall separation was additionally confirmed by a principal component analysis (PCA).

Finally, two high purity protein fractions were obtained, the supernatant of initial separation step contained 99.7% pure and native β-Lg, while the two-times washed α-La sediment fraction was 99.4% free of β-Lg. In conclusion, it was shown that this type of centrifuge has the ability to cope with the pseudoplastic flow behavior of the α-La precipitate, which is strongly dependent on dry matter. The achieved purities and yields are superior to most reported results in literature.

All experiments and analyses were designed and conducted under the responsibility of the doctoral candidate. She substantially contributed to the data evaluation, interpretation, and discussion. Moreover, the generated results were put into context with existing literature. The doctoral candidate concepted and wrote the majority of the manuscript. She was primary point of contact in the peer-review process and conducted the revision.

Continuous centrifugal separation of selectively precipitated α-Lactalbumin[2]

Nicole Haller[a], Ulrich Kulozik[a]

[a]Chair for Food and Bioprocess Engineering, Technical University of Munich, Weihenstephaner Berg 1, 85354 Freising, Germany

Abstract

The whey proteins α-La and β-Lg are valuable proteins for various food, nutraceutical, and medical applications. Their fractionation is, however, still a challenging task on industrial scale. This study describes a novel separation approach using selective thermal precipitation of α-La under acidic conditions, followed by high-throughput continuous centrifugation. The obtained α-La enriched sediment presented pseudoplastic flow behavior with strong dependency on dry matter. As the sediment still contained residues of soluble β-Lg and buffer salts, two steps of res-lurry washing were performed. Along the three centrifugation steps, a slight susceptibility to particle fragmentation was recognized, however, separation efficiency was rarely impaired by it. Finally, two high purity protein fractions were obtained, the supernatant contained 99.7% pure and native β-Lg, while the washed α-La sediment fraction was 99.4% free of β-Lg.

4.1   Introduction

The whey proteins α-La (14.2 kDa) and β-Lg) 18.0 kDa are small globular proteins of exceptional biological value and excellent functionality. Their specific properties and potential application areas are summarized in numerous reviews (Chatterton

---

et al., 2006; De Wit, 1990; Keri Marshall, 2004; Smithers, 2008) and are briefly outlined in the following.

On the one hand, formulae enriched with α-La were shown to be superior to classical infants' formula (Heine et al., 1996). This can be attributed, on the one hand, to the high similarity to the amino acid profile of mothers' milk, and on the other hand to the absence of β-Lg in human milk (Heine et al., 1991; Jost et al., 1999; Lien et al., 2004; Trabulsi et al., 2011). On the other hand, β-Lg comprises a high amount of branched chain amino acids (Etzel, 2004) and is appreciated for its technofunctional properties, i.e., gelation, emulsification, and foaming characteristics (Das and Kinsella, 1989; Dombrowski et al., 2017; Mulvihill and Kinsella, 1988). Moreover, studies have attested antimicrobial, antiviral, anti-tumour properties to these proteins (Håkansson et al., 2000; Ng et al., 2015; Pellegrini et al., 1999; Rammer et al., 2010).

In nature, α-La and β-Lg do not appear in an isolated form, but in a complex aqueous protein-carbohydrate system, generally known as whey. There is still a lack of an efficient process for fractionation of these two proteins that provides high yield, completely undenatured products, and is suitable for scale-up. Several approaches for isolation of the single protein fractions are described in literature and are briefly reviewed in the following.

Primarily, IEC generally achieves high purities for the isolated fractions; however, it presents major drawbacks regarding throughput and price efficiency (Santos et al., 2012). Another approach is two-phase partition, which often comprises one aqueous and one organic solvent phase. Thereby, the affinity of α-La to some organic solvents is exploited, while β-Lg mainly stays in the aqueous phase (Kalaivani and Regupathi, 2013). A recent publication presents an environmental friendly aqueous two-phase flotation approach using a PEG/trisodium citrate system with subsequent dialysis for isolation of α-La (Jiang et al., 2020). The achieved purities were promisingly high; however, this process requires a proof of concept at industrially relevant scale. In another study, the aqueous two-phase flotation was shown to be superior to aqueous two-phase extraction for the fractionation of antioxidant peptides from whey hydrolysate (Jiang et al., 2019). Alternatively, the recovery of β-Lg by NaCl salting-out at low pH values, followed by centrifugation and DF for salt removal was demonstrated by Maté and Krochta (1994). The purity of 95% was satisfactory, but the recovery rate was only 65%, and also the denaturation of the proteins might be severe with this procedure. Recent investigations show that casein exhibits chaperone like activities under high hydrostatic pressure and enhances the aggregation of β-Lg. This effect may be used to deliver α-La-enriched fractions (Marciniak et al., 2019).

Another emerging application in whey protein fractionation is high gradient magnetic separation (Chen et al., 2007; Meyer et al., 2007). Here, magnetic beads are loaded with the target protein, magnetically separated, and after a washing step,

target protein can be recovered from the particles. This method appears to have high selectivity and might be competitive to other chromatographic solutions. However, this application is limited to lactoferrin, which incorporates ferrous ions. Further to that, also the separation based on membrane filtration of the native proteins seems to be not appropriate as the molecular weights of α-La and β-Lg present too little difference (Heidebrecht and Kulozik, 2019). However, the separation of a fraction containing both proteins, α-La and β-Lg, from the other minor whey proteins comprising higher molecular weights can be successfully conducted by ultrafiltration (Bhattacharjee et al., 2006b).

In contrast to the above described separation methods, in this study a combination of selective aggregation of one candidate protein with a subsequent centrifugal separation is suggested. A reversible precipitation mechanism via hydrophobic interactions for α-La is known. Based on this knowledge, a process can be designed, that enables the reception of the α-La and β-Lg fraction in native state.

The basic research for the selective aggregation of α-La using acidic conditions close to its isoelectric point (i.e., pH 4.6) were conducted by Bramaud et al. (1995, 1997a), Maubois et al. (1987), Pearce (1983; 1987; Pierre and Fauquant) and Pierre and Fauquant (1986). The model derived describes the equilibrium between the calcium-bound holo- and the calcium-free apo-form of α-La as the central aspect of the selective precipitation reaction. This conversion into the apo-form under acidic conditions on the one hand reduces the heat stability of the protein (Hendrix et al., 2000), but on the other hand it increases its hydrophobicity. By the addition of a calcium sequestrant, a further improvement of this precipitation method was realised. Thus, shifting of the equilibrium towards the apo-α-La is promoted, as demonstrated by various authors (Alomirah and Alli, 2004; Bramaud et al., 1997b; Lucena et al., 2006; Tolkach and Kulozik, 2008; Toro-Sierra et al., 2013). Independent of the choice of α-La destabilisation strategies, the secondary structure stays widely intact and allows subsequent molecule dissociation and lat-er refolding under adequate conditions (Permyakov and Berliner, 2000; Toro-Sierra et al., 2013).

As the precipitation mechanism of α-La and its influencing factors are well understood, the need for an industrially adequate separation method for large scale applications arises. Studies describing the removal of the precipitated α-La fraction by membrane filtration, however, resulted in low permeability due to fouling issues (Gésan-Guiziou et al., 1999; Toro-Sierra et al., 2013). Centrifugal separation of the precipitates has been successfully conducted in discontinuous mode (Fernández et al., 2012; Lucena et al., 2006), and a promising approach was demonstrated by means of a continuously working laboratory scale decanter (Haller & Kulozik, 2019). The advantage of continuous centrifugation as separation method is its simplicity and speed, also enabling the removal of small precipitated aggregates under high acceleration forces.

The challenges related to centrifugal separation of α-La aggregates were demonstrated in our previous study (Haller and Kulozik, 2019). The α-La precipitates were characterised as fragile and small particles of low density. The sediment formed had a sludgy to pasty appearance and exhibited a high adhesion tendency. Moreover, it showed poor drainage capacity despite high compressibility.

In this study, we wanted to evaluate the suitability of a co-current decanter centrifuge for large-scale separation of precipitated α-La. Hence, one key question was whether a continuous sediment discharge could be achieved with this type of decanter, thus resulting in two high purity fractions, i.e., a high dry matter ala sediment and a well clarified β-Lg supernatant. The hypothesis was that a decanter characterised by a bowl construction without drying zone, i.e., with a fully submerged separation room, should allow for better sediment transportation characteristics. Furthermore, we expected higher sediment dewatering by consolidation as could be achieved by drainage on a drying zone in the lab-scale device. The second key question therefore arose as to whether the fragile precipitates would maintain their physical integrity along the separation process, despite high mechanical stress imposed by high g-forces, compressive yield stress and shearing through the scroll. Thus, it was critical to investigate the aggregate stability of the α-La precipitates during the washing process, which is important for the realisation of a high yield of the α-La fraction and a high purity of soluble native β-Lg in the supernatant.

4.2 Materials and methods

4.2.1 Preparation of α-La aggregate suspension

WPC (WPC80 Milei GmbH, Leutkirchen, Germany) with a protein content of 80.0% (Vario MAX cube, Elementar Analysesysteme, Langenselbold, Germany) and WPI (Davisco, Le Seur, Minnesota, USA) with a protein content of 94.2%, as related to the dry matter (CEM, Kamp-Lintfort, Germany), served as basis for the preparation of α-La aggregate suspensions. WPC80, made from fresh sweet whey, had a protein composition of 21% α-La, 34% β-Lg A, 32% β-Lg B, and 13% minor proteins, with 5% lactose and, on a WPC powder basis, 2.4 mg g^{-1} sodium and 1.3 mg g^{-1} calcium. The WPI had a protein composition of 18% α-La, 44% β-Lg A, 30% β-Lg B, and 8% minor proteins with 6.0 mg g^{-1} sodium, 1.2 mg g^{-1} calcium, and no lactose.

The different whey protein powders (WPC80 or WPI) were dissolved in DIW to a final protein concentration of 150 g L^{-1} using a powder mixer system (Fristam Pumpen KG, Hamburg, Germany). The end volume of WPC batch was 750 L, and 250 L for WPI. Gentle agitation for 12 h at 4 °C ensured complete hydration of the proteins. Prior to further processing, the whey protein solutions were tempered to 20 °C. Then, the pH value was adjusted to 3.4 using trisodium citrate dihydrate and

citric acid monohydrate (Bernd Kraft GmbH, Duisburg, Germany), whereby a final citrate content of 60 g L^{-1} was striven for (Toro-Sierra et al., 2013). Selective formation of α-La aggregates was achieved by subsequent heat treatment by indirect heating via the heating jacket of a 500 L tank. Thereby, a constant heating rate of 0.5 K min^{-1} was applied and strictly regulated. Steady stirring of the whey protein solutions at 150 rpm ensured even heating. Upon reaching of 50.0 °C ± 0.5 °C, a holding period of 120 min was followed by a fast cooling phase down to a temperature of 20.0 °C. For monitoring of the progress of α-La aggregation, whey protein solution samples were taken every 15 min and analysed using RP-HPLC (section 4.2.3).

4.2.2 Centrifugal separation

Separation of α-La aggregate suspensions was conducted with the industrial-scale decanter centrifuge Sedicanter® S3E-3 (Flottweg SE, Vilsbiburg, Germany), which is illustrated in Fig. 4-1. It is a horizontal bowl centrifuge with an integrated conveyor screw, wherefore continuous separation of solid and liquid phases is enabled. The basic working principle is as follows: the aggregate suspension is pumped through an inlaying pipe to the end of the double conical bowl, where it enters the separation zone via the feed port. The conveyor scroll transports the sediment cake towards the junction of the two cones, where the radius is maximal, resulting in high compressive forces on the solids. The sediment is pressed underneath the weir disc and is actively discharged by a second scroll at the steep cone. The liquid phase is collected by an impeller disc and is discharged under pressure as the so-called centrate.
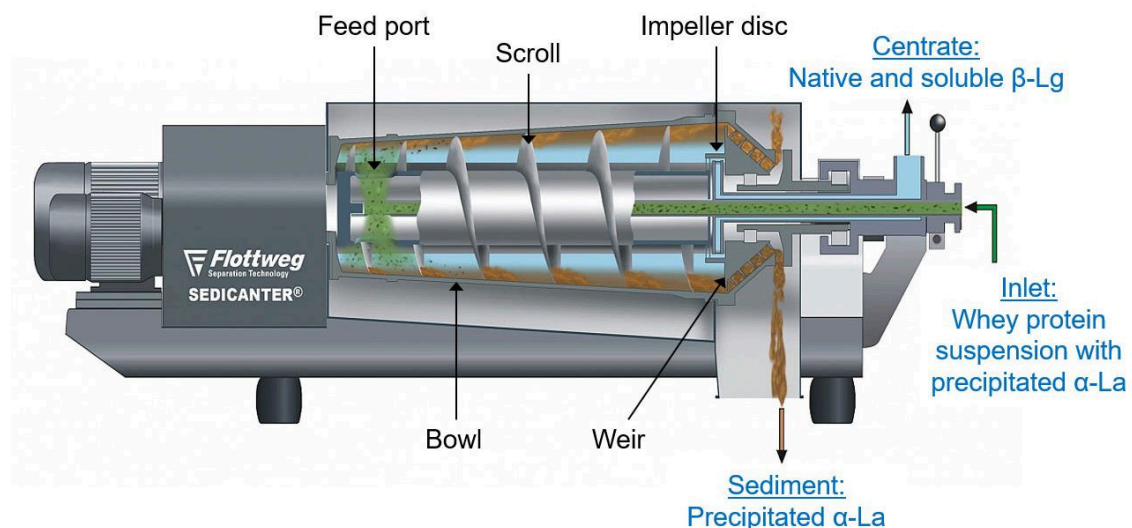
Fig. 4-1 Schematic drawing of the Sedicanter® (modified image, permission for usage is given by Flottweg, Vilsbiburg, Germany).

The precipitate suspension made from WPC80, which was produced as described in section 4.2.1, was diluted with DIW at 20 °C or 50 °C to 400 L with dry matter content of 20% (w w^{-1}), 800 L with 10% (w w^{-1}), and 400 L with 6% (w w^{-1}), respectively. The precipitate suspension from WPI was diluted to a volume of around 800 L with a dry matter content of 6% (w w^{-1}). Suspensions were kept under agitation at 100 rpm to ensure a uniform temperature and to avoid sedimentation of the aggregates in the jacketed feed tank. If needed, the centrifuge was pre-warmed with hot DIW to adapt the bowl temperature to the suspension. Specific constructional details and the used settings are listed in Tab. 4-1. Weir diameter and differential speed were regulated inline to obtain best separation results. The suspension was pumped from the jacketed vessel to the centrifuge using a NEMO® Progressing Cavity Pump (Netzsch Pumpen & Systeme GmbH, Waldkraiburg, Germany). Sampling was performed after reaching a steady state of separation performance, representing Hᵷ Ȧ bowl throughputs. After initial separation, the sediment still contained soluble β-Lg and citrate. To maximize the purity of the α-La fraction, reslurry washing was performed. This was done by suspending of the sediment in DIW at 50 °C, which was acidified with 3 N HCl to pH 3.4, corresponding to awash ratio of 4 (wash liquid is four times the volume of the residual humidity in the cake). Reslurried suspensions were separated again into sediment and liquid phase using an acceleration of 10,000 g. In total, two washing steps of sediment were performed. The inlet dry matter contents were 8.7% and 7.9% for the first and second wash, respectively. For each separation step, samples were taken simultaneously from the inlet, the centrate and the sediment.

Tab. 4-1 Machine conditions and decanter settings used in this study.

Bowl diameter, mm	300 (max.)
Clarification length, mm	560
Bowl speed, min^{-1}	5531-7735
Centrifugal acceleration, g	5,000-10,000
Differential speed, min^{-1}	5.4-6.4
Weir height, mm	126-132
Feed rate, L h^{-1}	150

4.2.3 Analysis of the precipitate suspension

To investigate the progress in aggregate formation during heat treatment, taken samples were immediately cooled down in an ice water bath to stop further reaction. Firstly, the sample preparation comprised a pre-dilution with DIW to a protein content around 20 mg mL^{-1}. From each sample, an aliquot of 200 mL was directly mixed with 800 mL guanidine buffer (6 N guanidine buffer containing 19.5 mM DTT) to determine the total protein content. The rest of the sample was centrifuged at 6,000 g for 15 min in a laboratory centrifuge (Multifuge 1S-R, Heraeus Holding GmbH, Hanau, Germany). The supernatant was then filtered through a 0.45 mm

syringe filter to remove remaining precipitates, and again an aliquot of 200 mL was diluted in the guanidine buffer and forwarded to RP-HPLC analysis. Incubation time for complete dissolution of proteins was at least 30 min. In Dumpler et al. (2017) a constant value for the whey protein content was proven for incubation times up to 72 h. In this study all samples were generally analyzed within 24 h (maximum 48 h) after preparation; samples were stored chilled until analysis started.

An Agilent 1100 Series chromatograph (Agilent Technologies, Waldbronn, Germany) was used, equipped with a C18 analytical silica-based column (Agilent Zorbax 300SB-C18, 4.6 x 150 mm, 5 mm) as described by Dumpler et al. (2017). Solvent A consisted of 0.1% TFA, 10% acetonitrile in HPLC grade water. Solvent B was 0.07% TFA, 90% acetonitrile in HPLC grade water. The injection volume was 20 mL, the flow rate was set to 1.2 mL min^{-1}, while the column temperature was constantly at 40 °C. Protein detection was done with a UV Detector at 226 nm. The yield of the precipitated fraction X_P for each protein x (x = α-La or β-Lg) was calculated according to (4.1). Hereby, the difference of total concentration $c_{x,total}$ of each protein x in the suspension to the concentration of this protein in the supernatant $c_{x,supernatant}$ is used.

$$X_P = \frac{c_{x,total} - c_{x,supernatant}}{c_{x,total}}$$
(4.1)

Furthermore, particle size distribution of the precipitates was measured by laser diffraction using the Malvern Mastersizer 2000 equipped with the Malvern Hydro 2000S sample dispersion unit (Malvern Instruments GmbH, Herrenberg, Germany). Refractive indexes for water (dispersant) and protein were set to 1.33 and 1.41, respectively, according to manufacturer's protocol.

The dry matter content of the suspensions was determined using differential weighing (CEM Smart Turbo CEM GmbH, Kamp-Lintfort, Germany).

4.2.4 Analysis of centrates

For evaluation of the separation success achieved by centrifugation, the separation efficiency η_{sep} was calculated, based on RP-HPLC data (section 4.2.3). η_{sep} of precipitated α-La from the centrate was then calculated using concentration of α-La in centrate $c_{α\text{-}La,\,centr,}$ total obtained volume of centrate V_{centr}, as well as α-La concentration $c_{α\text{-}La,\,inlet}$ and total volume V_{inlet} of inlet suspension.

$$\eta_{sep}\,(\alpha\text{-}la) = 1 - \frac{c_{\alpha\text{-}La,centr} \cdot V_{centr}}{c_{\alpha\text{-}La,inlet} \cdot V_{inlet}} \cdot 100\%$$
(4.2)

Furthermore, quantification of citrate content was done via HPLC as described by Schmitz-Schug (2014). Proteins in the samples were removed by the addition of 50 μL of 60% perchloric acid to 1 mL of sample and subsequent filtration through a 0.45 μm syringe filter. Samples were diluted with DIW to fit the calibration range.

4.2.5 Analysis of the sediments

Success in removal of soluble β-Lg and citrate from the sediment were calculated as given in (4.3) and (4.4), and expressed as η_{sep} *(β-Lg)* and η_{sep} *(citrate)*.

$$\eta_{sep}\ (\beta\text{-}lg) = \frac{c_{\beta-lg,centr} \cdot V_{centr}}{c_{\beta-lg,inlet} \cdot V_{inlet}} \cdot 100\% \tag{4.3}$$

With $c_{β-Lg,centr}$ and $c_{β-Lg,inlet}$ as concentration of soluble β-Lg in centrate and in the inlet suspension, respectively.

$$\eta_{sep}\ (citrate) = \frac{c_{citrate,centr} \cdot V_{centr}}{c_{citrate,inlet} \cdot V_{inlet}} \cdot 100\% \tag{4.4}$$

With $c_{citrate,centr}$ and $c_{citrate,\ inlet}$ as citrate content in the centrate and in the inlet suspension, respectively.

Furthermore, flow properties of the sediment in dependence of dry matter content (section 4.2.3) were investigated by rheological measurements. For this, a cone-plate geometry (diameter = 50 mm, angle = 2°, gap width = 0.213 mm) and the rheometer MCR302 (Anton Paar, Graz, Austria) equipped with the software RHE-OPLUS/32 V3.61 were used. Shear rate was linearly increased from 1 to 100 s^{-1} within 3 min, shear rate of 100 s^{-1} was held for another minute, followed by a 3 min lasting downwards ramp to 1 s^{-1} again. The experimental data of the descending ramp was fitted using the Herschel-Bulkley model (4.5) with τ as shear stress, τ_0 as yield shear stress, k as the consistency index, γ as the shear rate, and n as the flow index.

$$\tau = \tau_0 + k\gamma^n \tag{4.5}$$

If n <1 the fluid is shear-thinning, for n >1 the fluid is shear-thickening, and if n = 1 and τ_0 = 0 it presents Newtonian flow behaviour.

4.2.6 Overall process evaluation

For overall evaluation of process success after the washing steps, purity and yield of the protein fractions x (α-La or β-Lg) were determined based on concentrations determined by means of RP-HPLC analysis according to (4.6) and (4.7), respectively. The yield of α-La refers to recovered amount of this protein in the sediment after second washing step, whereas the yield of β-Lg refers to the sum of recovered amounts in all three supernatants.

$$Purity\ (x) = \frac{c_x}{c_{\alpha-la} + c_{\beta-lg}} \cdot 100\% \tag{4.6}$$

$$Yield\ (x) = \frac{c_{x,end} \cdot V_{end}}{c_{x,start} \cdot V_{start}} \cdot 100\% \tag{4.7}$$

The index *start* refers to the initial precipitate suspension, while the index *end* refers to last fraction obtained, i.e., the sediment after the second washing step for α-La, as well as the centrate of the initial separation step for or β-Lg.

4.2.7   Statistical analysis

In total, two batches of each sample condition were prepared, and each sample was analyzed in duplicate. Thus, a four-fold determination was carried out. Data points shown in figures and tables represent the mean values, while the error bars give the standard deviations (n = 4), which were calculated with Microsoft Excel (Microsoft Corporation, Redmond, USA). The 95% confidence intervals were calculated by use of Student's t-distribution. Data was evaluated and plotted using OriginPro 2018b (OriginLab Corporation, Northampton, USA).

Additionally, a principal component analysis (PCA)[3] was carried out to evaluate which variables convey the most variation in the dataset, i.e., which influencing factors contribute the most in the overall separation. Based on the correlation matrix and the scree diagram a reduction to three PC (with eigenvalue > 1) was conducted, which explained 89.1% of the variance in the data. The resulting PCA biplot is a combination of the loading plot (arrows) and the score plot (dots).

4.3   Results and discussion

In the following section, results are described for precipitation procedure, centrifugal separation, including initial separation and the consecutive washing steps, as well as analysis of rheological properties. The whole process was conducted using two different whey starting materials, WPC80 and WPI, respectively. The two systems were chosen in order to compare an "ideal" protein system (WPI) with a more realistic protein system (WPC80), which comprises traces of impurities like lactose, fat, and minerals. In industrial processing, most likely raw whey will be chosen as starting material. Depending on the intensity of pretreatment, including concentration and purification steps, this material may present comparable characteristics as the ones described here. In order to maintain comparability and to standardize the starting material, we used the above-mentioned whey powders.

4.3.1   Precipitation of α-Lactalbumin

For assessing the progress of aggregate formation during heat treatment and for determination of final precipitation yield, samples were regularly taken and analyzed by means of RP-HPLC. Fig. 4-2 depicts the precipitation progress for the fractions X_P of α-La and β-Lg, respectively. Investigation of precipitation was performed using WPI (a) and WPC80 (b) as starting material. The curves are presented in dependence of time and temperature, starting with the time point, where the desired environmental conditions were established. As the heating-up phase

---

[3] PCA was performed with OriginPro 2018b (OriginLab Corporation, Northampton, USA).

to reach the target temperature of 50 °C took one third of the total heating time, the aggregation progress in this phase is also depicted. It is marked with grey background.
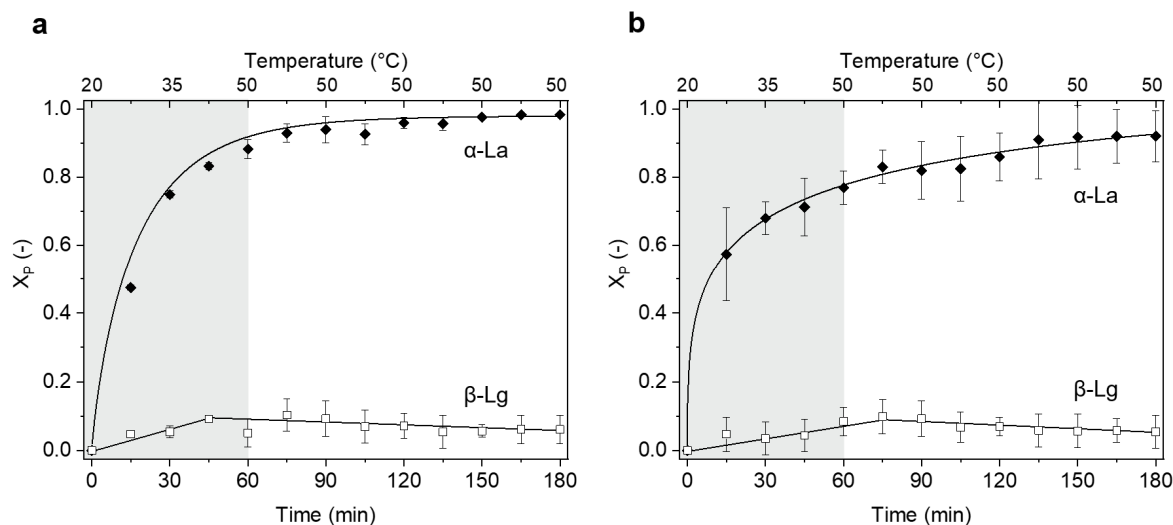
Fig. 4-2 Precipitation yield Xp for α-La (♦) and β-Lg (□) in dependence of time and temperature using WPI (a) or WPC80 (b) as starting material.

As can be seen in Fig. 4-2a, the main part of α-La precipitation occurred already during the heating-up phase, although temperatures were still far below the target temperature. According to Hendrix et al. (2000), the transition temperature of holo- to apo-α-La is between 22 and 34 °C, depending on the environmental conditions. This implies that unfolding of apo-α-La, which is followed by its precipitation, even starts at room temperature. During the heating-up phase, X_P already reached 0.88, at the end of the holding time a nearly complete precipitation yield of 0.98 was achieved. Regarding the precipitation kinetic of α-La, the obtained asymptotical shape of the curve was already described by Bramaud et al. (1995) in dependence of denaturation time under acidic conditions.

The free content of β-Lg initially decreased slightly due to entrapment in aggregates. In the course of the heating time, however, some enclosed β-Lg was depleted from the precipitates, which happens presumably through a rearrangement of the α-La precipitated due to stirring. At the end of the heating, an amount of 6% β-Lg stayed within the aqueous phase inside the α-La precipitates. A formation of stable α-La-β-Lg aggregates seems to be improbable, because the exposition of β-Lgs free thiol group usually starts at temperatures of 60 °C, upon unfolding (De Wit, 2009). Furthermore, in an acidic environment the reactivity of sulfhydryl groups is reduced (Guyomarc'h et al., 2015; Park and Lund, 1984), and overall denaturation temperature of β-Lg is higher (Dissanayake et al., 2013a).

The precipitation curve of WPC80 in Fig. 4-2b presented a similar parabolic shape, obtaining a final X_P 0.92, with 5% of β-Lg remaining in the aggregates after 180 min heating time. However, the curve suggests that the equilibrium is not necessarily reached after this time. The root cause is probably an deceleration of the

precipitation due to hindrance effects in the aggregate rearrangement by lactose and fat, which are present in WPC, but not in WPI.

4.3.2 Optimization of centrifugal conditions

After precipitation, suspensions obtained from WPC80 were diluted to dry matter contents of 20%, 11%, and 6% (w w^{-1}), using cold or pre-warmed DIW at 20 °C or 50 °C, respectively. In the following, the influences of inlet concentration, suspension temperature, and applied g-force were investigated in order to optimize centrifugal separation of α-La aggregates. The results of the obtained separation efficiencies of centrate are displayed in Fig. 4-3a, whereas the obtained sediment dry matters are presented in Fig. 4-3b, in dependence of applied centrifugal acceleration for all suspensions.
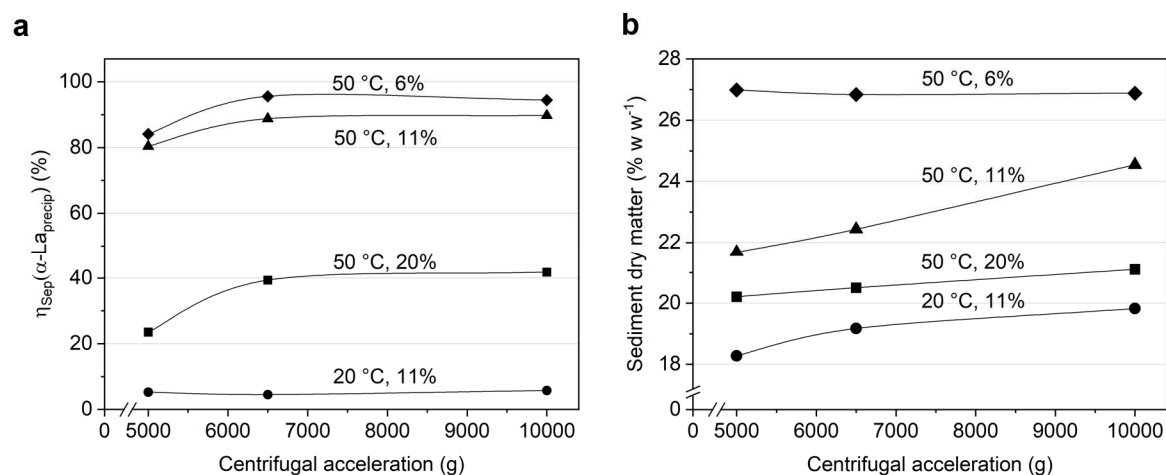
Fig. 4-3 Separation efficiency of α-La precipitates (a) and dry matter of obtained sediments (b) at different suspension temperatures and inlet dry matters between 6 and 20% (w w^{-1}).

Relating to Fig. 4-3a, it can be clearly seen that the separation efficiency increased upon reduction of the inlet dry matter for 50 °C. If a suspension contains less precipitates, the particle-particle interactions are reduced during sedimentation, thus enabling higher median settling velocities. Moreover, the residence time of particles settled on the cake is longer, as there is a lower number of particles coming after. This is accompanied by a longer phase for sediment consolidation, thus enabling a better dewatering of the sediment.

Referring to the impact of temperature, the increase in temperature from 20 °C to 50 °C had a tremendous effect on separation. On the one hand, this is due to the reduction of the viscosity of the continuous phase, which reduces the uplifting drag force for the particles while sedimentation. On the other hand, the higher temperature also might influence the aggregate stabilization. The apo-α-La form is characterized as the calcium-free variant of this protein, which presents a less dense conformation of the tertiary structure (Hirose, 1993). Moreover, it was demonstrated that the apo-form leads to partly unfolding, thus exposing inner patches of

the protein resulting in higher hydrophobicity (Stănciuc et al., 2012). As the system attempts to minimize thermodynamically unfavorable states, non-polar groups establish strong interactions, the hydrophobic interactions. Characteristic for hydrophobic interactions is their tendency to get stronger upon moderate temperature increase up to 60 °C (Bryant and McClements, 1998). The intensified interaction between the protein molecules might, thus, also lead to an intensified exclusion of the polar water molecules, which consequently increases the dewatering capability of the sediment.

Regarding the influence of the applied g-force, a nearly linear trend was observed as a function of sediment dry matter (Fig. 4-3b). A higher acceleration leads to better dewatering of the sludge-like sediments by compression. Thus, the sediment pores are compressed, resulting in drainage of the aqueous phased in direction to the top of the sediment layer. As can also be seen from Fig.4-3a, the maximum in separation efficiency η_{sep} was already achieved at 6,500 g, and not at the highest applied acceleration. Regarding Stokes's law, an enhancement of centrifugal acceleration results in a proportional increase in sedimentation velocity, correlating with the separation efficiency. This effect obviously applied up to 6,500 g. A further increase to 10,000 g, however, showed no enhancement in separation efficiency for all suspensions. As stated in Stahl (2004), disintegrative forces and shear stress on particles are highest when entering the bowl via the feed port. Transported under laminar flow conditions through the feed pipe, the particles are rapidly accelerated by the rotational forces generated by the bowl. Probably, the loosely bound molecules at the outer parts of the aggregates were mainly affected by the fragmentation, whereas the precipitate kernels were more resistant to destruction by shear (Byrne and Fitzpatrick, 2002). Some of these fragments were much smaller than the foregoing aggregates so that they were not able to sediment anymore in the applied centrifugal field, and consequently stayed in the supernatant. As the precipitate kernels were not destroyed by acceleration forces, they were able to settle independently form g-force at accelerations above 6,500 g.

4.3.3 Investigation of flow properties of the α-La sediment

The transportability of a sediment is distinctly affected by its flow behavior, which depends beside others on the total number of potentially interacting particles. Thus, rheological experiments were performed with α-La aggregate suspension containing dry matter contents between 5 and 28%, as described in section 4.2.5. Experimental results from WPI and WPC80 were fitted according to (4.5). The results for the received flow index n (Fig. 4-4a) and the consistency index k (Fig. 4-4b) are presented in dependency of dry matter concentration.

In Fig. 4-4a, for concentrations up to 10% (w w^{-1}), a Newtonian flow behavior was observed ($n = 1$). With increasing concentration, the suspension presented a ten-

dency to shear thinning behavior ($n < 1$), which got more prominent at concentrations higher than 25% dry matter. The change to a pseudoplastic flow behavior at high particle concentrations was additionally reflected by the consistency factor, which showed also a slope divided in three distinct parts.
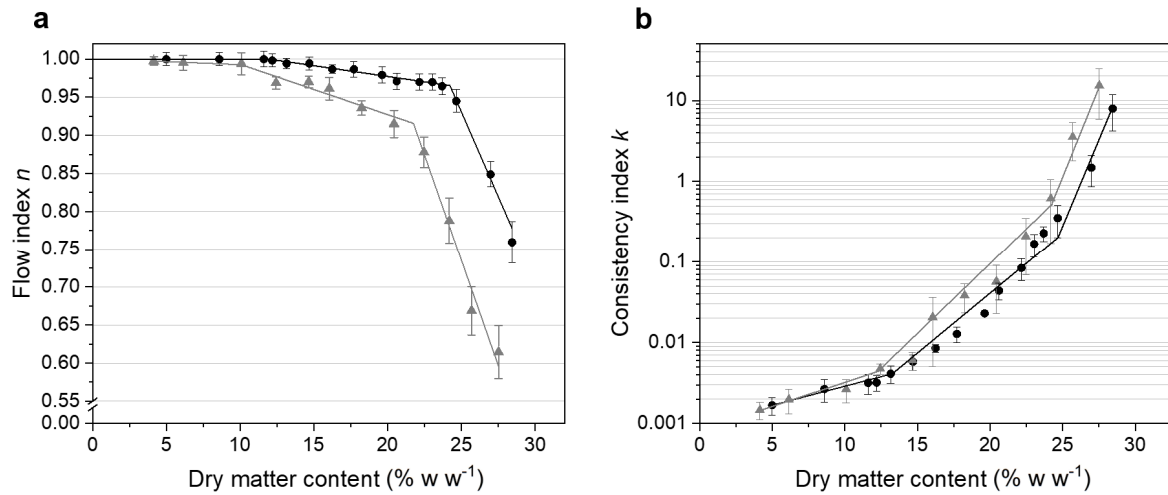
Fig. 4-4 Flow index n (a) and consistency factor k (b) of precipitated α-La in dependency of dry matter fraction of sediment for the two starting materials WPC80 (black dots) and WPI (grey triangles).

Many other workers investigated the flow properties of native WPC in dependence of protein concentration (Herceg and Lelas, 2005; Hermansson, 1975; Patocka et al., 2006; Tang et al., 1993). All agree on Newtonian behavior up to 10% (w w⁻¹), what matches the herein presented results. In the range between 10% < w < 20% the flow behavior was demonstrated to present pseudoplastic flow behavior at shear rates below 50 s⁻¹. In contrast to that, at higher shear rates (> 50 s⁻¹), the rheological behavior appears to be Newtonian (Tang et al., 1993). In this study, the applied shear rate was 100 s⁻¹, however, a pseudoplastic behavior is clearly visible in this concentration range. This observation is considered to be caused by the presence of the α-La aggregates, which provide structural elements in the suspension compared to native whey proteins. For concentrations over 20% a pseudoplastic rheological behavior is described in literature, which is also seen with the herein processed α-La aggregate suspension (Alizadehfard and Wiley, 1996). With an increase in the protein content, the respective volume fraction of particles rises as well. Consequently, the distance between α-La aggregates is diminished. Additionally, the net charge of α-La is supposed to be on a low level, as the environmental pH is close to its isoelectric point. Thus, the attractive Van der Waals forces may favor an entanglement of the apo-α-La molecules.

Comparing the curves from WPI and WPC80, the same trending of the curves can be observed. The values for WPI were comparable with the ones for WPC80 in the Newtonian flow region, but were slightly higher in pseudoplastic region. However, the distinction appears not to be significant. As stated before, the main difference of the two systems is the lactose content in WPC80. Thus, sediments of WPI and

WPC80 containing the same value of dry matter might differ in their relative protein concentration. However, lactose generally presents high solubility in water and preferentially remains in the liquid phase, i.e., the supernatant. As only low amounts of lactose stay in the sediment, the influence in diminishing the relative protein content is obviously minor. Furthermore, the non-Newtonian flow behavior is generally originated from large molecules, e.g., proteins. Thus, it is not surprising that the lactose does not affect the flow behavior, and the curves from both systems look similar (Morison and Mackay, 2001).

With this data, it was shown that the flow behavior of WPC80 and WPI have high similarity. Thus, the investigation of different centrifugal conditions using WPC80 appears to be appropriately and transferable to the WPI system. Moreover, a strong dependency on dry matter content was demonstrated. This development of flow behavior might on the one hand promote the sediment accumulation on the lowest point of the bowl, thus further improving dewatering. On the other hand, the intense particle entanglement might lead to particle disintegration, when shear forces perpendicular to flow direction are applied.

4.3.4 Separation performance and aggregate stability along the separation process

Based on the observations in section 4.3.2 and 4.3.3, the whole separation process of α-La including two washing steps was performed. Herein, the focus was on evaluating the separation efficiency of all three centrifugation steps and on the observation of aggregate stability. For the further experiments WPI was used as starting material, because this system provides a lower level of impurities (lactose, fat, ash) and allows to investigate the specific protein interactions and behavior, nearly without unpredictable cross-reactions from other components. The separation was conducted using the aggregate suspension at 50 °C with an inlet dry matter of 6% (w w^{-1}) at centrifugal acceleration of 6,500 g. A two-step reslurry washing procedure was chosen to remove other low molecular solutes and soluble proteins like β-Lg from the aqueous phase filling the sediment´s pores. Tab. 4-2 presents the results of the separation efficiencies as in (4.2), (4.3) and (4.4) for initial separation as well as the two subsequent washing steps and the final yields as in (4.6) and purities (4.7) for the respective protein fractions. In addition to that, the respective chromatograms for the WPI inlet (Fig. 4-5a), the centrate after the initial separation (Fig. 4-5b), and the twice washed sediment (Fig. 4-5c) are presented.

Tab. 4-2 Summary of achieved separation efficiencies along the separation and washing steps, with additional yield and purity of target protein fractions.

Parameter	Centrate	Sediment	
	Precipitated α-La (%)	Soluble β-Lg (%)	Citrate (%)
η_{sep} (Initial separation)	99.7 ± 0.1	86.7 ± 0.9	71.7 ± 2.4
η_{sep} (Wash 1)	95.0 ± 0.2	85.5 ± 5.4	20.1 ± 4.2
η_{sep} (Wash 2)	92.6 ± 1.0	68.3 ± 10.0	4.8 ± 3.4
Final yield	75.2	83.5	n.a.
Final purity	99.4*	99.7**	n.a.

* Fraction after resolubilization, pH adjustment to 5.1 and removal of denatured β-Lg ** Supernatant of initial separation step

After the initial separation step, the centrate consisted of over 99.7% β-Lg, mainly in the native state. This means that the α-La precipitates were (almost) completely removed from the supernatant, as can also be seen in Fig. 4-5b. For the first and second washing step, η_{sep} for α-La reached 95.0% and 92.6%, respectively. The reduction of η_{sep} presumably is an indication for the fragmentation of precipitated α-La, which led to an increased impurity of the supernatant. In total, 75% of α-La aggregates were recovered throughout the process.
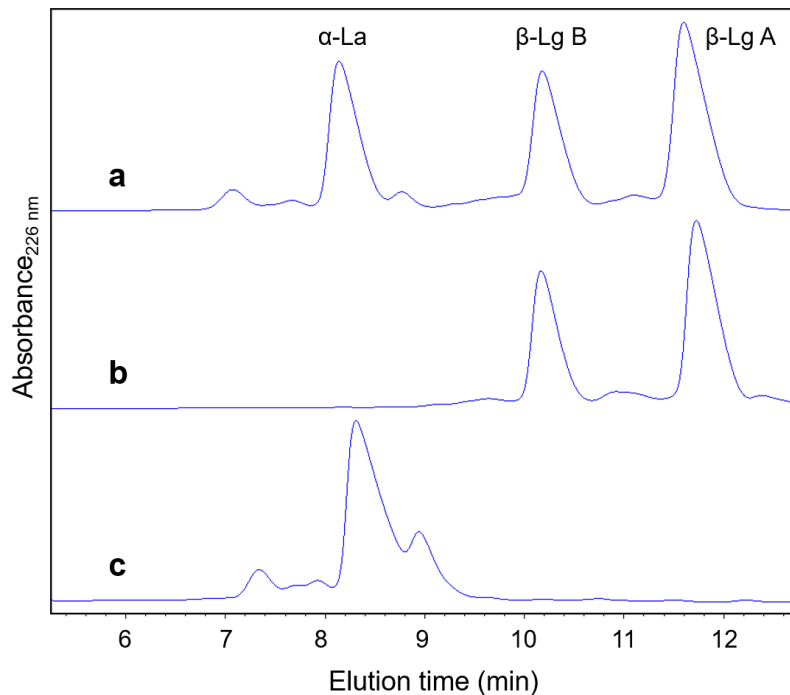
Fig. 4-5 Chromatograms from initial inlet (a), centrate after initial separation (b), and sediment after second washing step (c), using WPI as starting material.

Within the initial separation step, nearly 87% of soluble β-Lg migrated into the centrate. Vice versa, this means that around 13% of soluble β-Lg remained in the sediment fraction, which was enclosed in the aqueous phase of the particle's pores. After the second washing step, an almost complete absence of soluble β-Lg, with only 0.3% remaining in the sediment, was achieved. This refers to a purity of 99.7% of the α-La sediment fraction, which was calculated based on the chromatogram shown in Fig. 4-5c. Also, in laboratory scale, two washing steps using acidified water at 55 °C as washing medium were shown to be suitable for nearly complete depletion of β-Lg (Fernández et al., 2012; Lucena et al., 2006).

The removal of citrate, which was initially added in order to act as calcium sequestrant, was, however, not as successful as the washing out of β-Lg. After the initial separation, the sediment comprised 28.3% citrate, which could be reduced to 22.6% and 21.5% with the following washing steps. The reason is that the formed tricalcium citrate shows poor solubility (1 g L^{-1} at 25 °C) compared to trisodium citrate (425 g L^{-1} at 25 °C), and therefore, tends to be present in solid state. Due to its high density, it is likely that it is obtained in the sediment. The conclusion from this is that the calcium citrate should be removed by a subsequent ultrafiltration step after the resolubilization of the α-La molecules.
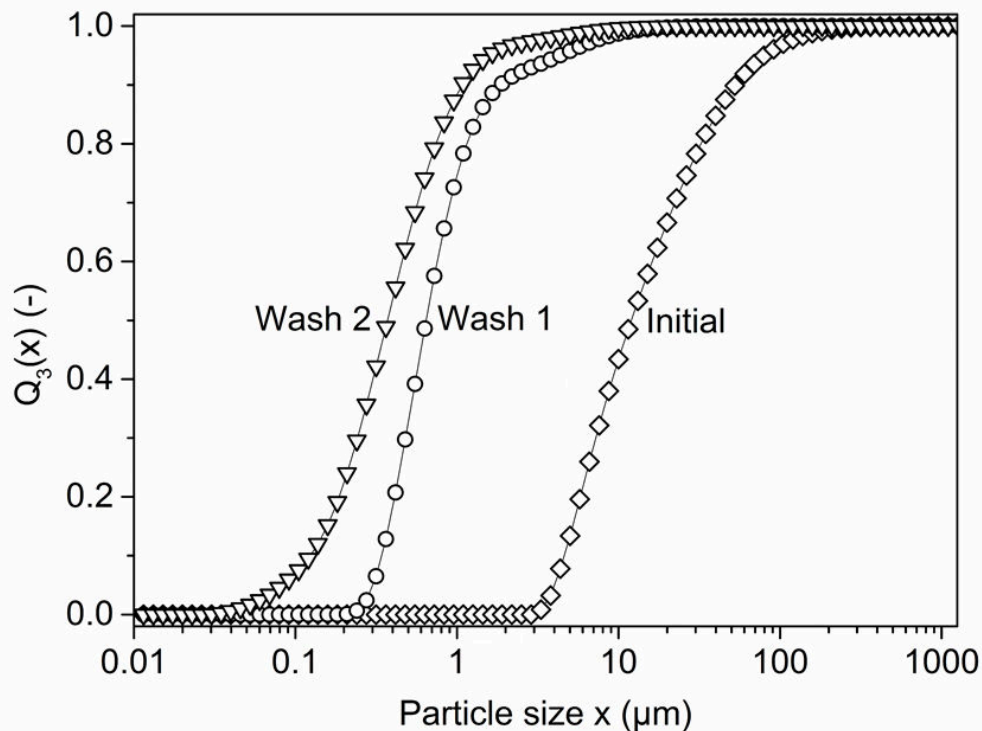
Fig. 4-6 Particle sizes of α-La precipitate suspension of initial separation (◊), first wash (○), and second wash (Δ) displayed as sum distribution, using WPI as starting material.

To prove the assumption of particle fragmentation, particle size measurements were conducted. Fig. 4-6 depicts the particle size sum distribution $Q_3(x)$ for the inlets of the initial separation as well as for both washing steps. As can be clearly

seen, aggregate sizes were reduced with each separation step. The median particle size of the initial suspension was 10.3 µm, the suspension entering the first washing step only had a median size of 0.6 µm, and for the second washing step the particles were smaller than 0.4 µm, respectively. The particle size reduction of the α-La aggregates by 94% in the initial separation step may therefore be explained by fragmentation into the primary aggregates or small fragments. According to the model of floc disintegration by Kleine and Stahl (1989), fragmentation generally occurs, when the applied the acceleration force F_C exceeds the individual linkage forces F_A. F_C is hereby proportional to the product of the density difference $\Delta\rho$, gravitational acceleration g, acceleration factor c, and the cubic of particle size x. In concrete, this means that especially big aggregates are subjected to fragmentation as the size is a cubic factor in (4.8).

$$F_C \propto \Delta\rho \, g \, c \, x^3 \tag{4.8}$$

The linkage force F_A of each particle within a floc arises from the charges on the surface of the particle. Here, F_A is proportional to a surface specific adhesion force f and the corresponding particle surface area.

$$F_A \propto f \, x^2 \tag{4.9}$$

However, also the interparticular shear forces may not be neglected, especially at high particle concentrations. Such high concentrations can be found towards the end of their settling way in the centrifuge (region of hindered settling), and of course in the sediment itself (Scales et al., 1998). Particularly, for soft particles, as the α-La aggregates, the compressive yield stress may be considered as an additional mechanism for particle disrupture (Haller and Kulozik, 2019). The particles experience compressive forces due to the pressure from the weight of the upper layers of the sediment, which is multiplied by the centrifugal acceleration number (Green et al., 1996). Moreover, the upward drag force of liquid, which is squeezed out of the particle pores generates a counterflow and induces shear forces. Additional shearing in decanter centrifuges is executed by the scroll in horizontal direction. Indeed, fragmentation can be observed in this approach due to various reasons. However, the high acceleration possibilities of this centrifuge still enable adequate separation efficiencies.

4.3.5   Sediment analysis along the separation steps

Within the three separation steps, the α-La sediment was purified from soluble β-Lg and citrate, simultaneously changing its composition and visible appearance. In the first separation step, irregularly shaped lumps of sedimented aggregates were observed falling out from the sediment discharge port (Fig. 4-7a). After the first wash of the sediment, the texture of the separated sediment got visibly smoother (Fig. 4-7b) until creamy long filaments were obtained after the second wash (Fig. 4-7c).
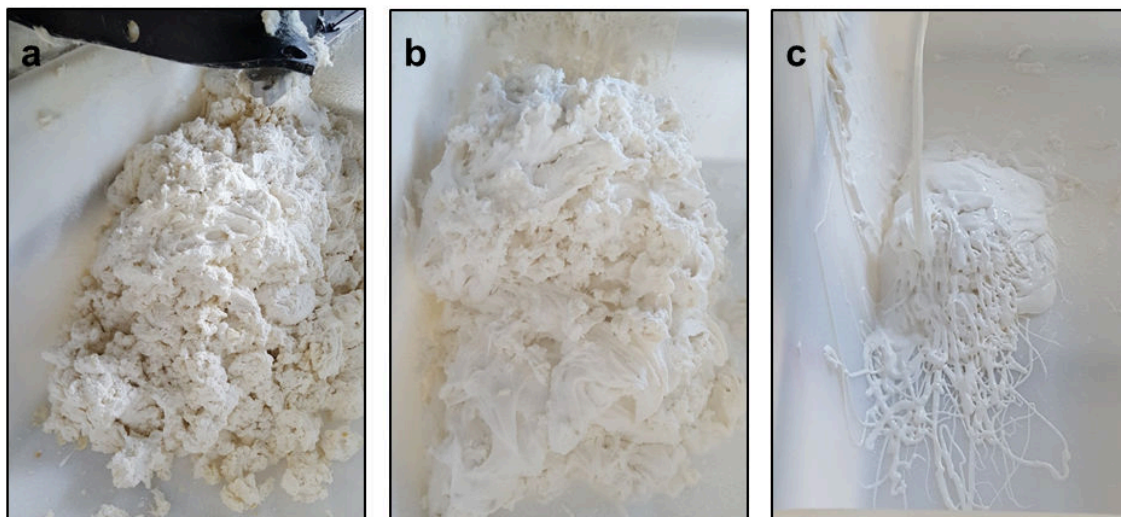
Fig. 4-7 Discharged α-La sediment after initial centrifugal separation (a), after the first washing step (b) and after the second washing step (c), using WPI as starting material.

As listed in Tab. 4-3, the total sediment dry matter decreased slightly from 30.5% in initial separation to 26.6% and 26.3% within the washing steps. Additionally, the protein to dry matter ratio increased from 84.8% up to 88.5% and finally to 90.0%, respectively. The remaining 10% of dry matter within the α-La sediment can presumably be ascribed to the residues of enclosed solid calcium citrate, as described previously.

Tab. 4-3 Obtained results for respective sediments along the three separation steps, presented in values of dry matter and protein to dry matter ratio

Separation step	Dry matter content (% w w⁻¹)	Protein to dry matter ratio (% w w⁻¹)
Initial separation	30.5 ± 0.7	84.8 ± 0.1
Wash 1	26.6 ± 0.1	88.5 ± 1.5
Wash 2	26.3 ± 0.4	90.0 ± 2.5

The reduction of overall achievable dry matter along the washing steps is probably related to the particle breakage. During the production of the precipitate suspension, the apo-α-La molecules formed oligomers due to attractive forces of their hydrophobic regions. Through the long heating duration and the gentle stirring, strong and particulate aggregates arranged (Byrne and Fitzpatrick, 2002). These aggregates were thermodynamically stable as the non-polar amino acid residues conglomerated, thus excluding the polar water molecules (Bryant and McClements, 1998). From a superior view, this equals a system that has a low amount of interior bound water. Upon breakage of the precipitates, an increase of the surface to volume ratio of the aggregates occurs. Thus, a larger surface area is available for hydration, as proteins generally have a high solubility in water.

The observed change of the sediment texture from clumpy to filamentous shall be discussed in the following. The arrangement of single protein molecules to particulate aggregates is a highly complex process, subjected to collision mechanisms, e.g., as described in Smoluchowski (1918). In regard to this, it appears to be improbable that particle fragments rearrange into globular aggregates during the reslurry washing steps. As the interior hydrophobic regions of the apo-α-La are still exposed and "reactive", it is likely that they will resume the attractive interactions with hydrophobic patches from other apo-α-La molecules. There is a high probability that the molecules will adopt new structures, which are easier to achieve than particulates, e.g., filaments (Pelegrine and Gasparetto, 2005). As the environmental conditions are close to α-La's IEP, the low level of electrostatic repulsion, on the on hand, and the increased importance of the van-der-Waals forces, on the other hand, might also act in a supportive manner in this case.

4.3.6 Overall evaluation

For overall evaluation of the data, a PCA was performed that aims at emphasizing the main influencing factors and also at discovering correlations of the separation variables. The PCA is a statistical tool which reduces the number of dimensionalities, thus transforming a large set of variables into a smaller one that still contains most of the information. The received biplot comprises a loading diagram (blue arrows) and a score plot (black dots), and is given in Fig. 4-8.

The PC1 is given on the x-axis, the PC 2 on the y-axis, with percentages of 42.0% and 29.4% of the data variance, respectively. In this standardized diagram, the length of the loading vectors, the arrows, is a direct measurement on how big theirs influence on the PCs is (-1 = maximal negative influence, 0 = no influence, 1 = maximal influence). Here, it is obvious that nearly all characteristics have a severe influence on the PCs, except the $d_{50,3}$, which is the median particle size in suspension, has only little influence, followed by the applied g-force, which is the second shortest vector.

Moreover, the angle between a loading vector and the x- or y-axis also represent the degree to which PC1 or PC2 are influenced by this vector. This relationship additionally provokes that the correlation of one variable with another is described by the angle between them (0° < 90° positive correlation, 90° independent, 90° > 180° negative correlation). Looking on the given vectors, a negative correlation with an angle close to 180° can be seen for particle size and g-force. Basically, this means that a higher g-force is able to compensate a reduction in particle size in order to keep the acceleration force (or separation result) constant, i.e., particle size and g-force are indirectly proportional. This relationship was already given in (4.8), which described the proportionality of the acceleration forces. Thus, the loading diagram emphasizes which factors correlate either positively or negatively with the separation efficiency.
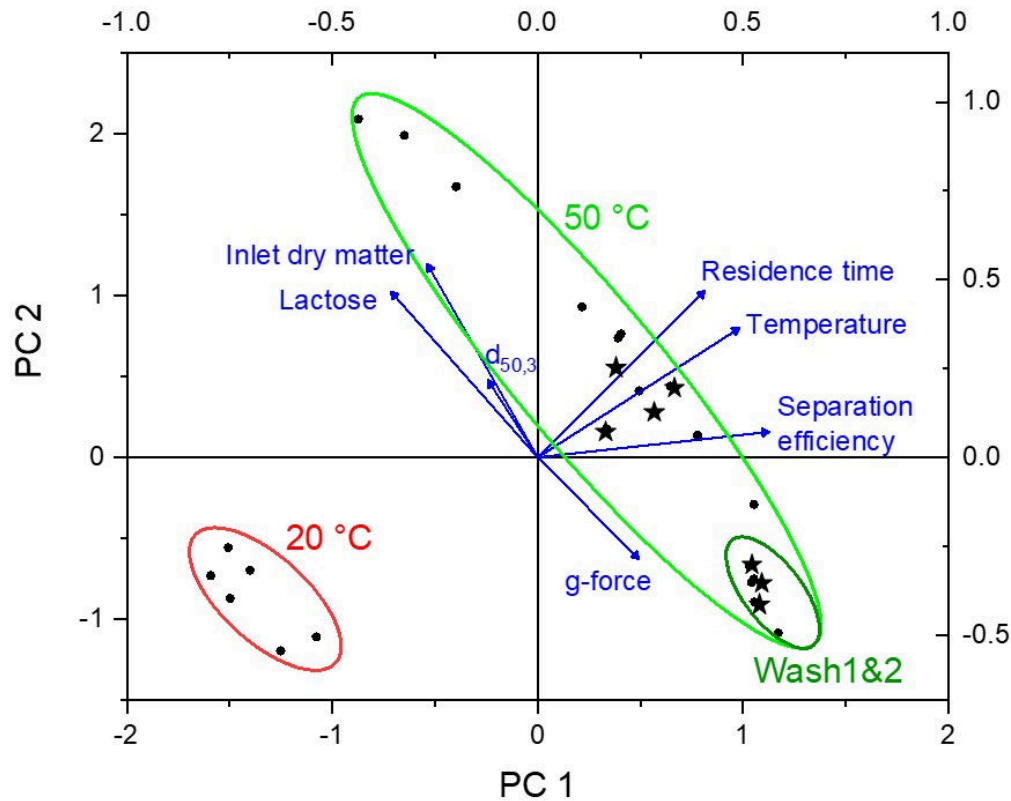
Fig. 4-8 PCA biplot presenting the loading plot of all analyzed variables (blue arrows) and the score plot (black dots for WPC80, black stars for WPI), which reflect the measured data points.

A strong positive correlation with the separation efficiency is seen for the influencing factor temperature, but also for residence time and g-force. Basically, one could classify these variables as process-related influencing factors. A negative correlation for separation efficiency is seen for the arrows for particle size described as $d_{50,3}$, lactose, and dry matter content, as the intermediate angle is over 90°. These three variables can be generalized as suspension-related influencing factors. These relationships suggest that process-related variables, i.e., higher temperature, extended residence time, beneficially influence the separation efficiency. While suspension-related variables, i.e., higher lactose content, more inlet dry matter, impede the separation efficiency. It seems astonishing that the $d_{50,3}$ is assigned to negatively correlate to the separation efficiency. However, as stated already above, due to the short absolute length of this arrow, its influence is minor. Apart from that, bigger particles in the inlet suspension are more prone to disintegration during centrifugation than already fragmented particles, as discussed in chapter 4.3.4. A higher occurrence of fragmentation during a centrifugation step might thereby impair the overall separation efficiency of this step.

Regarding the data points, two distinct clusters are visible, one comprising all values from separations performed at 20°C, and one with the data points from 50°C.

Within the 50°C separation temperature cluster, a smaller one is highlighted that comprises the data points from all the washing steps. Interestingly, no different behavior of WPI (stars) and WPC80 (dots) are observed as the data points lie close to each other and are not separated. This means, that the aggregates of both starting material follow the same dependencies in separation. And the differences due to lactose content are neglectable. From this diagram, one can conclude that the temperature is one of the main influencing factors.

4.4 Conclusion

In this study a successful process for the separation of the two major whey proteins, α-La and β-Lg, was demonstrated that has high suitability for industrial utilization. A lean process design is described that comprises high throughput unit operations, where further scale-up appears to be simple. Moreover, we achieved two high purity fractions, with both proteins in native state, with respectable yields. Further to that, for this approach only components with the GRAS (generally regarded as safe) state were used. Due to these advantages, we consider this process to be superior to many others suggested in literature.

Nonetheless, the major challenges of this fractionation method shall be outlined, which needed special attention in this study. The selective thermal precipitation of α-La under acidic conditions is a well described, state-of-the-art pre-treatment for whey proteins. However, the generated α-La precipitates are small, fragile particles that are prone to shear forces. Indeed, analysis presented a significant particle size reduction from initially 10 µm to 0.4 µm after three consecutive centrifugation steps. Nonetheless, separation efficiencies just declined from 99.7% to 92.6% over the whole process. Moreover, a pseudoplastic flow behavior of the α-La sediment was demonstrated being strongly dependent on dry matter. Generally, such characteristics might cause discharge issues due to sediment backflow to the lowest point of the bowl or adhesion to the scroll flights. However, in this study a constant discharge with highly dewatered sediment was observed. In summary, the suitability of the herein used decanter centrifuge for this application was proven, achieving purities for α-La and β-Lg fraction over 99%.

However, the authors see further potential for improvement of this process, thus making it even more time- and cost effective. On the one hand, the time span for powder hydration was chosen generously long. Re-hydration of proteins might be completed after several minutes, depending on the powder used. Alternatively, also liquid raw whey can be considered as starting material, thus skipping the whole re-hydration step. On the other hand, the heating process has potential for improvement by using steeper heating rates in a tubular counter-current heat exchanger. Potentially, also the heat holding phase can be reduced by applying

higher temperatures. However, the thermal stabilities of the other proteins need to be respected, though.

In the study, two different starting materials, WPI and WPC80 were used. Generally, both systems showed promising results and had comparable values in rheological analysis. However, separation efficiencies were higher using the purer WPI system. Presumably the α-La precipitates originated from WPC80 have lower stability while centrifugation, resulting in hardly separable particle fragments. As the main difference of the composition of the two whey powders is the content of lactose and fat, we assume that these components are responsible for impairing the aggregate strength in WPC80 batches.

5 Separation of aggregated β-Lactoglobulin with optimized yield in a decanter centrifuge

<u>Summary and contribution of the doctoral candidate</u>

The β-Lg aggregates obtained from selective thermal denaturation processes can reach sizes up to 700 µm. They consist of multiple interconnected primary aggregate, which are spherically shaped with sizes around 1 µm. During general suspension processing mechanical and shear forces affect the integrity of the aggregates, which can lead to fragmentation and breakage. These fragments, however, are often too small for sedimentation in centrifuges and impair the overall separation efficiency. This study investigates the possibility of a pH-induced flocculation of the β-Lg aggregate fragments with the aim to optimize the separation results in a decanter centrifuge.

Firstly, the fragments and particles smaller than 20 µm were isolated from a β-Lg aggregate suspension for further analysis. Particle size measurement under controlled environmental conditions showed size enlargement of the fragments in a pH range between 4.0 to 5.0, which was ascribed to flocculation. The clarification velocity was determined based on data from a time- and space resolved analytical centrifuge. Only in the pH range between 4.0 to 5.0 a clarification of the supernatant was observed. At the other pH values, a two-step sedimentation was seen, with the largest fragments settling in the first minutes and nearly no further clarification afterwards. The highest clarification velocity was measured at pH 4.4.

Finally, the analytical results were transferred to a decanter separation of aggregated β-Lg from soluble α-La. All results at pH 7.0 were inferior to the separation outcomes at pH 4.4. The best obtained results were a separation efficiency of 99.8% and a sediment dry matter close to 50%, when using a 0.5% inlet dry matter and suspension pH was adjusted to 4.4. Generally, the discharged β-Lg aggregates are a highly valuable source for food applications. Upon further break down in the primary aggregates, e.g., by homogenisation, they would comprise the ideal size to use them as fat replacers. The high degree of absence of particles in the centrate makes it a suitable stream for further chromatographic polishing or capture of the remaining individual whey proteins.

Most significant contribution to this manuscript was made by the doctoral candidate. This comprises the conception, design and execution of experiments based on preceded critical literature review as well as major conduction of data analysis and data interpretation. In addition, writing and revising of the manuscript was done by the doctoral candidate.

Separation of aggregated β-Lactoglobulin with optimized yield in a decanter centrifuge[4]

Nicole Haller[a], Andreas Stefan Greßlinger[a] and Ulrich Kulozik[a]

[a]Chair for Food and Bioprocess Engineering, Technical University of Munich, Weihenstephaner Berg 1, 85354 Freising, Germany

Abstract

The interest in individual whey protein fractions, especially the main proteins α-La and β-Lg, has been growing due to their unique nutritional value and their exceptional technofunctional properties. Various fractionation and purification methods have been published. However, none of them realized highest purity, maximal recovery, and transferability to industrial scale. This study used thermal treatment for selective aggregation of β-Lg, which was subsequently separated in a pilot-scale decanter centrifuge from the α-La-enriched centrate. The aim was to investigate if the centrifugal separation can be improved by pH-induced flocculation of the aggregates compared to non-flocculated suspension at pH 7.0. With various analytical methods, it was demonstrated that the strongest flocculation occurred at pH 4.4 and facilitated separation of aggregate fragments sized below 20 µm. Finally, separation efficiencies of more than 99% were achieved by aggregate flocculation in the pilot-scale decanter even at low centrifugal forces.

5.1 Introduction

Whey is a mixture of different proteins, the carbohydrate lactose, salts, minerals and vitamins. The most abundant proteins in whey comprise α-La, β-Lg, BSA, LF, and IgG. Each protein has a unique amino acid profile and molecular conformation, created by nature with a certain specific biological function. In case of the whey protein, their unique properties, however, make them an irreplaceable starting material for diverse applications in food technology and other sectors by either using

---

[4] Adapted original manuscript. Adaptions of the manuscript refer to numbering of sections, figures, tables and equations, abbreviations, units, spelling, format, and style of citation. All references have been merged into a joint list of publications to avoid redundancies.

all whey proteins as a whole or as individual fractions of the major single whey proteins, mainly β-Lg and α-La.

As one of the major proteins in whey, α-La (14.2 kDa), is present in nearly all mammalian milks. It naturally plays a central role in the regulation of lactose production, is a source of bioactive peptides, and contains various amino acids that are crucial for infant's development, e.g., Try, Lys, Cys (Layman et al., 2018). The enrichment of infant formulas with α-La has been demonstrated to increase emulsion stability (Buggy et al., 2017), and allows for the reduction of total protein content, thus further approaching the composition of humans' breast milk (Lönnerdal, 2014; Rozé et al., 2012). Nonetheless, α-La is also a valuable protein in adult nutrition. Studies describe effects of α-La on enhanced immune response, general mood improvement (Kroes et al., 2014; Silber and Schmitt, 2010), sleep quality enhancement (Lieberman et al., 2016), and promotion of gastrointestinal health (Brück et al., 2003).

On the other hand, β-Lg (18.0 kDa), is absent from human milk, but the most prevalent protein in bovine whey. Therefore, it is suspected to be one of the candidates for inducing bovine milk allergies (Martorell-Aragonés et al., 2015), although generally any protein can provoke allergenic reactions, depending on individuals´ sensitivity. In bovine milk β-Lg presumably fulfills transport functions for fatty acids as it can be assigned to the class of lipocalins. This protein comprises a large amount of branched chain amino acids, making it a perfect source for sports nutrition aiming at muscle mass increase (Hulmi et al., 2010). In its microparticulated form, it shows excellent characteristics for the use in dietary or other milk products, such as low-fat yoghurts (Torres et al., 2018), Caciotta and other cheeses (Hinrichs, 2001; Perreault et al., 2017; Sturaro et al., 2015), ice cream (Daw and Hartel, 2015; Koxholt et al., 2000; Olivares et al., 2019) and others (Ipsen, 2017).

To exploit the full potential of each single component, fractionation of the single whey proteins has been reported to offer additional options. Many approaches have been published in recent times that address the goal of whey protein fractionation. Beyond other methods, IEC, two-phase flotation, membrane separation, salt treatments, complexations, magnetic separation are investigated for their capability. Detailed analysis of the respective benefits and disadvantages of each approach have been extensively reviewed or reported in several articles (Ganju and Gogate, 2017; Smithers, 2015; Yada, 2018).

Previous works in the field of selective thermal aggregation of the major whey proteins and separation of the aggregates from the suspension, including those from our own group, relied on separation of aggregated and native molecules by MF (Toro-Sierra et al., 2013). However, MF requires a time-consuming multistep DF process if a high yield of both the aggregated and native fractions is targeted. In order to address this issue, we were able to show that the separation of aggregates in a continuous centrifuge is a feasible one-step alternative, also for the separation

of aggregated β-Lg from the native α-La fraction (Haller and Kulozik, 2019). The yield at that stage of our investigations, however, was not optimal due to losses of small aggregates and fragments.

In other approaches, continuous scroll centrifuges were applied for separation of precipitate α_s- and β-casein (Schubert et al., 2018), isoelectric precipitated soy protein (Bell and Dunnill, 1982), or precipitated α-La from soluble β-Lg (Haller and Kulozik, 2020). According to Haller and Kulozik (2020), the aggregation target component α-La formed highly hydrated, fragile aggregates, sized around 10 µm. A procedure for resolubilization of the α-La aggregates by adjustment of pH and ionic environment causing dissociation and induction of refolding to a native state was described. Finally, both α-La and β-Lg were obtained in their soluble, native forms with fraction purities of more than 99%. Refolding of denatured α-La was shown to be possible, because the aggregation of α-La relies on reversible binding mechanisms, in contrast to β-Lg, which is covalently cross-linked when aggregated (Toro-Sierra et al., 2013).

Taking this approach as a role model, the question was whether and how the process described by Haller and Kulozik (2020) could be adapted such that β-Lg is the target molecule for selective thermal aggregation. As a base, the thermal denaturation kinetics of β-Lg are well described in literature and allows targeted aggregation of β-Lg in a well controllable process (Tolkach et al., 2005; Toro-Sierra et al., 2013). The first reversible structural changes of β-Lg's conformation are measurable starting at temperatures as low as 40 to 55 °C, known as the Tanford transition (Euston, 2013; Loveday, 2016). Starting at temperatures above 60°C, the thiol group of Cys121 located in the inner core of the globular β-Lg structure is exposed, which shows increasing reactivity upon further heating and higher temperatures (Mulvihill and Donovan, 1987; Verheul et al., 1998). At 80 to 85 °C, the process changes from an unfolding-limited to an aggregation-limited process resulting in a steeper increase of reaction rate leading to the formation of aggregates cross-linked by disulfide bonds (Dannenberg and Kessler, 1988; Khaldi et al., 2018; Petit et al., 2016).

Beside the heating temperature, there are other well-known influencing factors, which comprise pH, protein concentration, ionic strength, salt type and concentration, chelating agents, presence of other proteins and their concentration, e.g., caseins. An optimization approach of environmental conditions aiming at maximal aggregation of β-Lg with simultaneous minimal loss of nativity of the other proteins in whey protein isolate solutions was investigated by Tolkach et al. (2005a). In this study, the optimized conditions were stated as follows: protein content 5 g L^{-1}, lactose content 0.5 g L^{-1}, calcium content 0.55 g L^{-1}, and pH 7.5. Thus, heat treatment at 97 °C for 30 s resulted in 99.6% β-Lg denaturation, with a 24.4% loss of native α-La. These environmental conditions were chosen as a starting point for the settings used in this study.

The β-Lg aggregates generated by these type of heat treatments are characterized as solid, elongated and stable particles with low density (Haller and Kulozik, 2019). β-Lg aggregates can reach high sizes, which facilitates their sedimentation. However, fragmentation of the aggregates appears to be a common issue in aggregate suspension handling. Due to exposure to shear during pumping, stirring and also during centrifugation, single primary aggregates or smaller fragments comprising several primary units are separated from the main particle (Byrne et al., 2002; Zumaeta et al., 2005).

Primary aggregates are described to have sizes of approximately 50 nm to 1 μm and are thus not very sedimentable (Guyomarc'h et al., 2015; Nicolai et al., 2011). Particles below 0.1 μm continuously remain in a randomly oriented motion as a consequence of their thermal energy, also known as Brownian motion, which prevents their sedimentation (Ghernaout et al., 2015). From a process efficiency standpoint, however, these small β-Lg aggregates that do not sediment, even at applied accelerated gravitational forces, reduce yield and purity of the supernatant. In order to assess the impact of processing conditions on the separation of β-Lg aggregates with optimal separation efficiency, we investigated sedimentation enhancement strategies, especially for promoting the sedimentation of smaller particles and of particle fragments to increase yield and to avoid reduction of purity of the fraction of unaggregated proteins.

The hypothesis was, that by variation of pH, electrostatic interactions can be reduced, thus enabling the formation of flocs by van-der-Waals forces comprising numerous fine particles. This effect can be achieved either by using active ingredients, so-called flocculants, e.g., multivalent cations or long-chain polymer flocculants, such as modified polyacrylamides, or, in the case of pure protein suspensions, pH adjustment can be used to alter the surface potential of charged protein particles.

The aim of this study was to induce an enlargement of aggregate fragments, which would otherwise not be separated in a decanter, thus enhancing the clarification of supernatant, consisting of soluble and native α-La. The approach of this study focused on investigating the flocculation possibilities for β-Lg aggregates and to prove that the stability of the formed flocs is sufficient for centrifugal separation. Moreover, it was critical to investigate any side effects of the flocculation, e.g., change in sediment dewaterability, or increased loss of α-La due to pH-induced precipitation.

5.2   Materials and methods

5.2.1   Preparation of β-Lg aggregate suspension

WPI (Davisco, Le Seur, Minnesota, US) with a protein content of 94.2% (18% α-La, 44% β-Lg A, 30% β-Lg B, and 8% minor proteins) was used for preparation of β-Lg aggregate suspension. WPI powder was dissolved in DIW to a protein concentration of 2.5% (w w^{-1}). All batches of 30 L each were homogenously stirred at 350 rpm for 12 h at 4°C using a three-blade stirrer (Heidolph Instruments GmbH & Co. KG, Schwabach, Germany). Prior to further heat treatment, the whey protein solutions were tempered to 20 °C. The ionic calcium concentration (CaCl$_2$ 2 H$_2$O, Sigma Aldrich, St. Louis, United States) was set at 0.55 g L^{-1}, as measured by flame photometry (Elex 6361, Eppendorf, Hamburg, Germany). Lactose content of the WPI powder was known and a respective amount of lactose was added to get a final concentration of 0.5 g L^{-1}. The pH was set at 7.0 by adding 1 M HCl, because at this pH value the α-La fraction is in its most stable configuration and least sensitive to heat treatment.

Aggregation of β-Lg was induced by heat treatment. Therefore, a pilot-scale indirect tubular pilot-plant heat-exchanger was used (GEA TDS GmbH Ahaus, Germany). The plant consisted of heating (27.1 m), temperature holding (15.6 m), and cooling (30.0 m) sections. The protein solution was heated from the inlet temperature of 20 °C to 92 °C (heating rate = 2 K s^{-1}), and this temperature was held for 23 s (inner pipe diameter of holding section = 8.0 mm), followed by rapid cooling to 4 °C. Thereby, the flow rate was set to 120 L h^{-1}.

5.2.2   Protein quantification

Whey protein quantification was performed by RP-HPLC based on the method described by Haller and Kulozik (2020). In short, 200 µL of homogenized samples were dissolved in 800 µL of a buffer containing 6 N guanidine hydrochloride and DTT for complete unfolding of proteins within an incubation time of at least 30 min. Each sample (suspension, centrate or sediment) was divided in two aliquots for HPLC analysis, one was the untreated sample containing denatured and native proteins (c_{total}), the other one was rendered free of denatured proteins by pH adjustment to 4.6 (c_{native}).

The DD for each protein, α-La or β-Lg, respectively, was calculated with (5.1)

$$DD = \frac{c_{total} - c_{native}}{c_{total}} \cdot 100\%$$
(5.1)

The respective DD for both main proteins were determined subsequently to heat treatment. For each batch (n = 26) the DD for β-Lg was 94.5% ± 0.4%, and for α-La 16.2% ± 3.6%.

5.2.3 Isolation of aggregate fragments fraction

For investigation of aggregate flocculation effects induced by pH adjustment, it was necessary to isolate the respective aggregate fraction with a size below 20 µm. For isolation of the target aggregate fraction, the whole aggregate suspension was thoroughly filtered through a sieve with a cut-off size of 20 µm (Retsch GmbH, Haan, Germany). The filter cake was washed with DIW twice to maximize yield. The received fraction of small aggregates was concentrated by bench-top centrifugation (30 min, 6,000 g; Multifige 1 S-R, Heraeus Holding GmbH, Hanau, Germany). For removal of salt and lactose residues, the fragments were washed in DIW twice.

5.2.4 Particle size distribution

The particle size distribution of formed aggregates was measured based on the principle of laser diffraction using a Malvern Mastersizer 2000. The equipment comprised a sample dispersion unit (Malvern Hydro 2000S) and a small volume dispersion unit (Malvern Instruments GmbH, Herrenberg, Germany). The Hydro 2000S unit was used for particle size measurement of aggregates obtained after heat treatment in water (refractive index of dispersant 1.33, refractive index of protein 1.44).

The small volume dispersion unit was used for particle size measurements at defined media in order to investigate particle growth of aggregate fragments due to pH-induced flocculation. Thereby, defined media (DIW containing calcium and lactose concentrations as used for preparation of WPI solution) was used and pH values between pH 3.0 and 8.0 were adjusted using NaOH or HCl. The small aggregate and fragment fractions isolated as described in chapter 5.2.3 were gently re-suspended in the defined media, and transferred into the measurement chamber. From the obtained data, cumulative number distribution Q_0 and volume distribution Q_3 were calculated. By division through adequate class widths, dx, the respective density distributions q_0 and q_3 were obtained (5.2).

$$q_i = \frac{Q_i(x)}{dx} \tag{5.2}$$

Furthermore, $d_{10,3}$, $d_{50,3}$, and $d_{90,3}$ were determined to provide information on the size of 10%, 50%, and 90% of the smallest particles in a volume-based distribution, respectively.

5.2.5 Analytical centrifuge

A temperature-controlled analytical centrifuge (Lumifuge, LUM GmbH, Berlin, Germany) was used for characterization of the particles´ sedimentation behavior in a centrifugal field. The working principle of the analytical centrifuge is explained in detail in Sobisch und Lerche (2000). The measurements contain data on time- and

space-resolved transmission, which allows to analyze the sedimentation kinetics. A change in the transmission profile is representative for a change in the local particle concentration. The isolated and pH-adjusted small particle fractions were given in 3 mL polycarbonate cuvettes. The samples were properly resuspended before insertion in the analytical centrifuge. The temperature was kept constant at 20 °C, and samples were centrifuged for 50 min at 4,000 rpm, which equals 2,300 g at the bottom of the cuvette. Every 20 s, one transmission profile was recorded. The variable of time is visualized by a color change from red to green of the transmission profiles (Fig. 5-1 left side). In an ideal monodisperse system, a clearly visible sedimentation front would move towards the cuvette bottom. However, due to the high content of fines, it is more likely that class segregation takes place, which is represented as a gradual progress in clarification of the whole liquid phase. Therefore, the area under each single transmission profile was integrated starting from the air-liquid interface up to sediment-cuvette interface at the bottom. Displaying the values in a diagram with time plotted against integrated transmission results in a hyperbolic curve asymptotically approaching the maximal integrated transmission value. The linear part of the slope of the hyperbolic curve yield a measure for the clarification velocity given in % s^{-1}, describing the progress of the clarified supernatant and the sedimenting particles (Giraud et al., 2013).
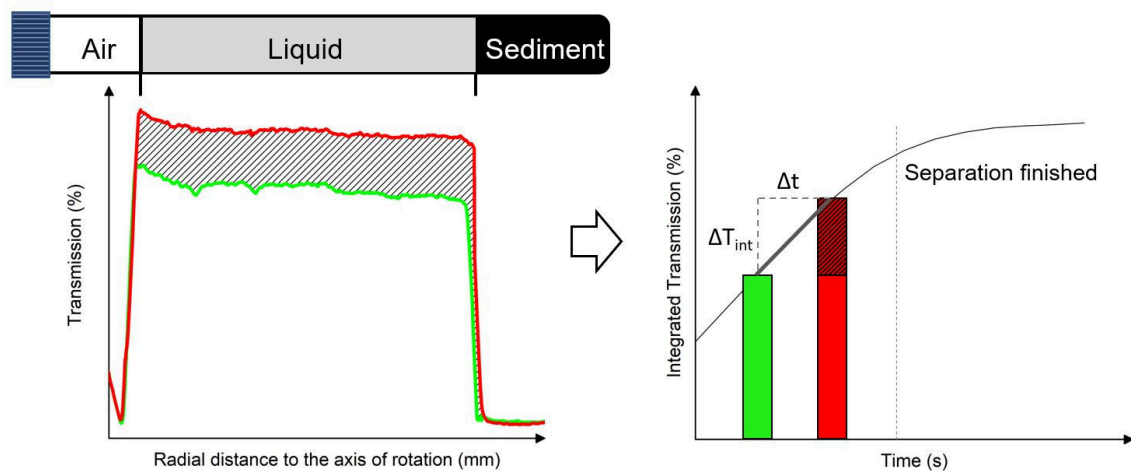
Fig. 5-1 Graphical illustration of the determination of clarification velocity, which comprises space- and time resolved transmission profiles (indicated by x-position and color change, respectively) on the left side, and derivation of clarification velocity as slope of a resulting time vs. integrated transmission plot on the right side.

5.2.6   Measurement of particle surface charge

The surface charge of β-Lg aggregates at various pH values from pH 3.0 to 8.0 was determined by the Zetasizer Nano ZS device, equipped with the Zetasizer Software 7.03 (Malvern Instruments GmbH, Herrenberg, Germany). Only the isolated aggregate fragments (< 20 μm) were characterized for their zeta-potential, as bigger aggregates would sediment within the measurement cell and would distort the results for electrophoretic mobility. For each data point, three replicate measurements were performed, each one consisting of 10 subsequent individual runs.

5.2.7   Scanning electron microscopy

Samples of the aggregates directly after heat treatment and of the sediment after discharge of decanter were prepared for scanning electron microscopy (SEM, JEOL JSM 5900 LV JEOL GmbH, Eching, Germany) analysis. Both types of samples were washed twice with DIW using gentle centrifugation (2,000 g, 6 min) for separation of washing supernatant. Subsequently, settled aggregates of both sample types were diluted with DIW to a final concentration of approximately 10% total solids. A drop of 20 μL was spread on a microscope cover glass (VWR International GmbH, Darmstadt, Germany) and dried under a gentle flow of filtered air within 5 min. The dried samples were sputtered with gold under vacuum for 70 s (BAL-TEC SCD 005, Bal-Tec AG, Liechtenstein). Scanning electron microscopy was performed using a voltage of 15 kV.

5.2.8   Decanter separation

The separation of β-Lg aggregates from the soluble proteins was performed in a laboratory decanter centrifuge (Lemitec MD 80, Berlin, Germany), which had a bowl diameter of 80 mm, a clarification length of 153 mm, and a weir height of 6 mm.

In brief, the heat-treated protein suspension, containing mostly β-Lg aggregates and native α-La, was pumped with a feed rate of 13 L h^{-1} from a stirred feed vessel (three-blade stirrer, 200 rpm) by a peristaltic pump (Verderlab VL1000, Verder Deutschland GmbH, Haan, Germany) into the feed tube of the decanter. Through holes located in the feed pipe reaching into the decanter the suspension enters the rotating bowl. Centrifugal forces from 2,000 to 4,000 g (equal to bowl speed 6,687 to 9,458 min^{-1}) were applied to accelerate particles to sediment at the inner wall of the bowl, building up a sediment cake. A conveyor scroll, rotating with a slightly higher differential speed (Δn = 1 to 10 rpm) faster than the bowl, transports the sedimented aggregates towards the conical part of the bowl, where it is dewatered and finally discharged at its upper end. The supernatant leaves the bowl at the opposite end of the bowl with a weir as barrier defining the aqueous phase height

in the bowl and, thus, apart from the volume throughput, its residence time in the centrifuge. The liquid phase is discharged as the so-called centrate.

Sampling was conducted after reaching a steady state of separation performance, representing 3 to 4 bowl volume throughputs. Samples were taken simultaneously from inlet, centrate and sediment in order to determine separation efficiency η_{sep} and sediment dry matter. All runs were performed at least in triplicate. Investigated were the effects of varying suspension inlet dry matter, pH values, and centrifuge settings, such as g-force and weir height.

Separation efficiency η_{sep} was calculated for each centrifugation setting according to (5.3), based on RP-HPLC data using concentration of denatured β-Lg $c_{β\text{-}Lg,denat,centr}$ in the centrate and in respective inlet $c_{β\text{-}Lg,denat,inlet}$.

$$\eta_{sep} = 1 - \frac{c_{β-\text{Lg},denat,centr}}{c_{β-Lg,denat,inlet}} \tag{5.3}$$

Dry matter content of discharged sediments was determined using a microwave dryer with integrated weighing machine (CEM Smart Turbo 5, CEM, Kamp-Lintfort, Germany).

5.2.9 Statistical analysis

For the investigation of the aggregate suspension and the flocculation, three independent repetitions were performed, each comprising at least a duplicate measurement of each sample, if not otherwise stated. The presented data of separation experiments in the decanter centrifuge consists of at least two independent runs for each condition, with each sample being analyzed in duplicate. Thus, a four-fold determination was carried out. Data points shown in figures represent the mean values, while the error bars give the standard deviations. This calculation was done with Microsoft Excel (Microsoft Corporation, Redmond, USA). The 95% confidence intervals were calculated by use of Student's t-distribution. Data were evaluated and plotted using OriginPro 2020 (OriginLab Corporation, Northampton, USA).

5.3 Results and discussion

5.3.1 Initial β-Lg aggregate formation and suspension

Subsequent to the heat treatment of the whey protein solution, particle size distribution of particles formed was measured. Fig. 5-2 presents the median particle size distribution of β-Lg aggregates based on number $q_0(x)$ and volume fraction $q_3(x)$ of n = 36 aggregate suspensions. Regarding the q_3 distribution, the main volume of particles clearly lies between 20 and 700 μm. The respective percentiles of the 10, 50 and 90% of smallest particles in a volume-based distribution were $d_{10.3}$ = 49.4 μm ± 3.6 μm, $d_{50.3}$ = 114.4 μm ± 8.7 μm, and $d_{90.3}$ = 320.5 μm ± 37.9 μm.
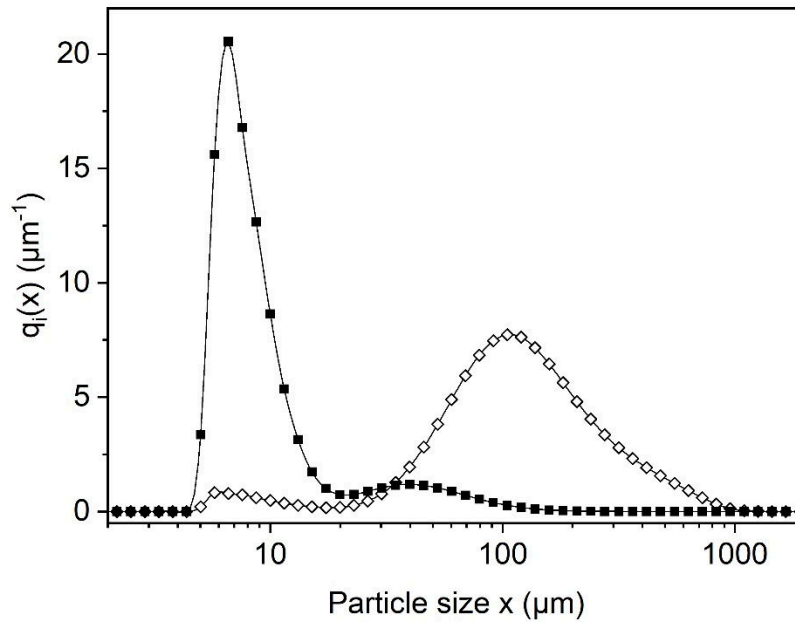
Fig. 5-2 Particle size distribution of heat-treated whey protein solution, with number-based $q_0(x)$ distribution marked with (■), and volume-based $q_3(x)$ distribution presented as (◊) of β-Lg aggregates.

Only a small pre-peak between 3 and 20 µm was visible in q_3 distribution. As larger aggregates take a higher volume, the small particles are inadequately represented in this volume-based distribution. The picture changes tremendously when looking at the number-based distribution $q_0(x)$. Only a small portion of particles is bigger than 100 µm, the vast majority is sized 3 to 10 µm. Exactly this size class, i.e., the particles below 20 µm, will be the target for pH-induced flocculation in this study. This type of bimodal particle population is well known for protein aggregate suspensions (Byrne and Fitzpatrick, 2002). However, the particle size distribution data does not give insights in particle form, construction and structure, such as an imaging method.

The analysis with SEM provided high resolution photographs of the β-Lg aggregates. Fig. 5-3 correspondingly shows pictures from this analysis with 1,000- (a), 4,000- (b), and 12,000-fold (c) magnification. Small primary aggregate units can be seen, which agglomerate in high numbers to finally build up one large aggregate. The primary aggregate units have a rounded, some of them even spherical appearance with sizes of up to 1 µm. The main portion of the aggregate units may connect to create a huge particle, forming the aggregate main body, as can be seen in Fig. 5-3b. These main aggregates may reach sizes of several hundred microns. At a closer look, also filigree particle chains are observed that branch from the main body (Fig. 5-3c). The branches appear to be the weak spot that may be subject to breakage at even low forces. In Fig. 5-3a, some fragments can be seen that have already went through disintegration. The results from size distributional

91

and SEM analysis show that most aggregates present sizes below 10 µm that comprise only low numbers of primary aggregates, such as 5 to 50 units.
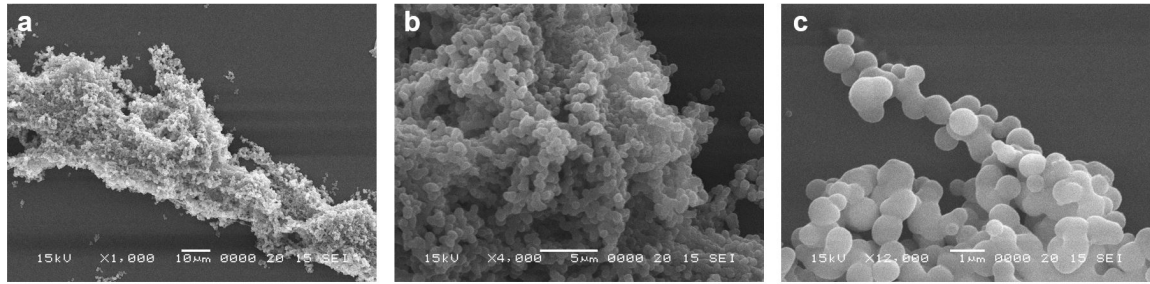
Fig. 5-3 SEM pictures of β-Lg aggregates with magnifications of factor (a) 1,000, (b) 4,000, and (c) 12,000. Included scale bars present the sizes of 10, 5, and 1 µm in the pictures, respectively.

Two main sources of these small-sized particle fractions can be identified. On the one hand, numerous primary aggregates did not have the chance to attach to one of the kernels that became an main aggregate during heat treatment. As there is no more particle forming activity via disulfide bonding as soon as the temperature drops below 60 °C, it can be concluded that this process does not influence the particle size distribution any further in the subsequent process. On the other hand, previously attached aggregate units, are forced to dissociate from an adult aggregate due to applied shear stresses such as stirring, pumping, and other fluid handling operations (Heffernan et al., 2005). This progression of aggregate disintegration is inevitable with every handling step and leads to a continuous change in the particle size distribution (Péron et al., 2007). Coming back to the distribution present in Fig. 5-2, it appears to be only a snapshot at a distinct point of time. The overall distribution, however, will trend towards a further increase of particles below 20 µm upon processing.

5.3.2 pH-induced flocculation of aggregate fragments below 20 µm in size

The small aggregate fraction was isolated as described in section 5.2.3, properly resuspended in various pH values, and then investigated for particle size, particle surface charge, and settling velocity in an analytical centrifuge.

The results for the volume-based factor $d_{90,3}$ at pH values ranging from 3.0 to 9.0 are presented in Fig. 5-4. In the pH 4.0 to 5.0 range, the values for $d_{90,3}$ are distinctly higher than those at pH 3.0, as well as those at pH values higher than pH 6.0. In the latter two ranges, nearly similar particle sizes around 1 µm were measured. The size of around 1 µm corresponds with the results from the SEM analysis to be single primary aggregates. The main peak in the $q_0(x)$ distribution that was found in particle size measurement straight after heat treatment, indeed showed

higher particle sizes of 3 to 20 μm. This means that the fragments further dissociated into their primary units during the isolation procedure. In contrast, the primary aggregates were found to be highly resistant to shear stress.
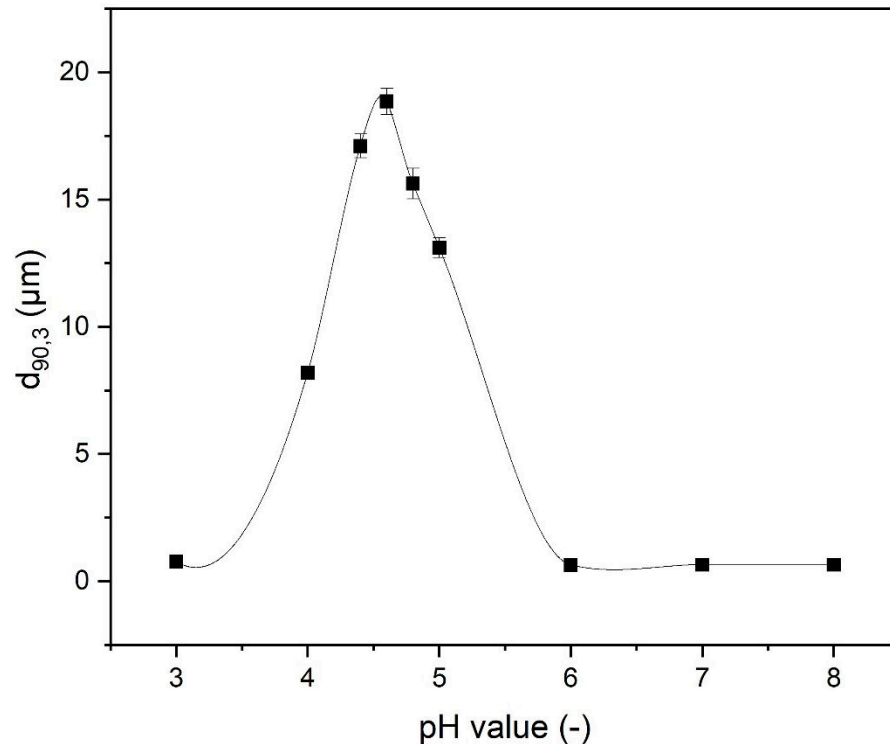
Fig. 5-4 $d_{90,3}$ values at different pH values in the range of pH 3.0 to 9.0 for the isolated small particles fraction.

In the pH range between 4.0 to 5.0, however, the particle size measures $d_{90,3}$ were determined to be significantly higher. Maximal sizes were reached at a pH value of 4.6, with a $d_{90,3}$ of 18.8 μm. As the pre-treatment for isolation was the same for all pH values, these particles are not assumed to be remaining particle fragments from heat treatment. They are supposed to be newly formed precipitates made of several primary aggregates that originated from the specific environmental conditions set.

Fig. 5-5 depicts the results of particle surface charge measurements at pH values from 3.0 to 8.0 of the isolated small particle size fractions. The IEP of the small β-Lg particles was determined at pH 4.5. At the IEP, the net surface charge is zero, which means that electrostatic repulsion of particles is at a minimum level. In turn, the attractive van-der-Waals forces dominate and result in association of particles. At pH values lower than the IEP, the functional groups of the amino acid side chains become protonated, resulting in positive particle surface charge. A respective deprotonation of the functional groups appears at pH values higher than the IEP, leading to a negative surface charge. The dispersions generally show higher stability with increasing absolute surface charge, and show a flocculation tendency at charges close to zero. In all cases, particle-particle interactions based on pH shifts, such as floc formation, are reversible processes.
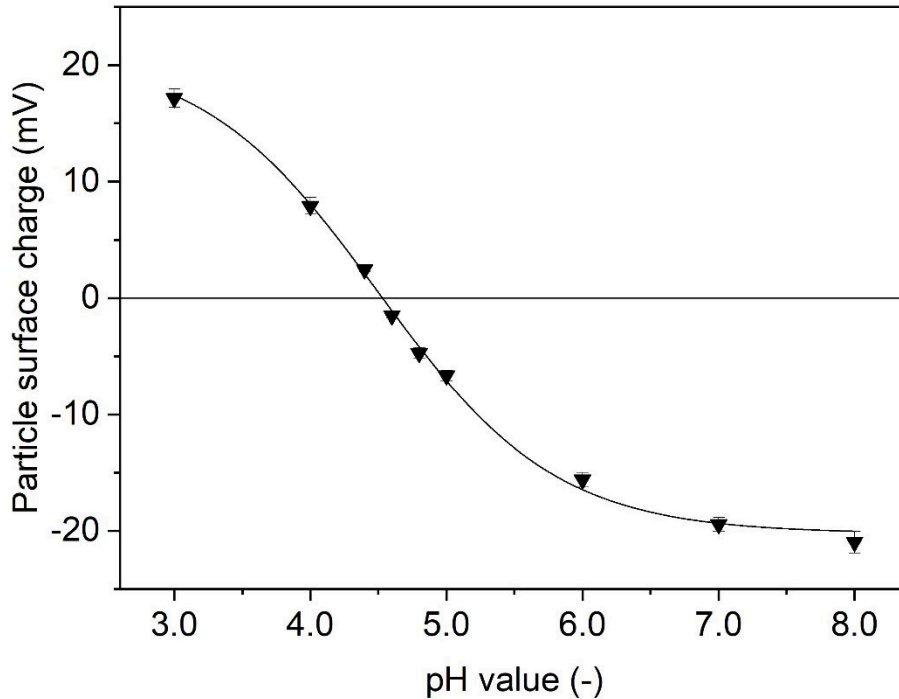
Fig. 5-5 Particle surface charge of the isolated small particles fraction in the range of pH 3.0 to 8.0.

Values for IEP of native β-Lg reported in literature are not consistent, ranging from pH values between 4.6 and 5.2, depending on type of salts, ionic strength, and also traces of other proteins (Barnett and Bull, 1960). However, most works report an IEP at pH 5.1. The β-Lg aggregates herein measured have been exposed to heat treatment, which provokes conformational changes. Thereby, inner domains get exposed, which are not accessible in surface charge measurement on the native protein. Furthermore, the herein investigated aggregates consist of at least 12% α-La, which used to have a lower IEP of approximately pH 4.2 (Lam and Nickerson, 2015), what also contributes to the lower IEP of the aggregates compared to native β-Lg.

The study of Majhi et al. (2006) demonstrated that, however, a zero net charge of β-Lg is not the most important factor which leads to an electrostatically driven aggregation of β-Lg. Instead, it is a high degree of asymmetry in electrostatic potential distribution. This means that the aggregation rate is highly increased in case differently charged domains are randomly distributed on the outer shell. In concrete, Majhi et al. (2006) reported the highest aggregation rate at pH 4.6, below the IEP, where positive and negative potential domains were not of equal magnitude. As precipitation occurred with maximum intensity at the IEP, one may call this isoelectric precipitation, which follows the rules of dominance of the attractive Van der Wales forces, described above.
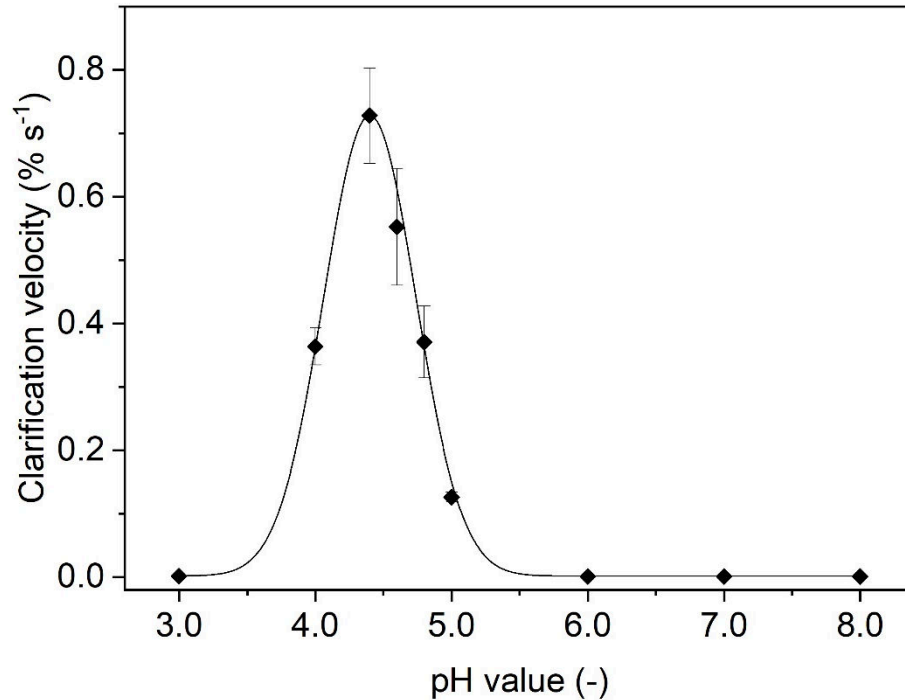
Fig. 5-6 Clarification velocity of the small particles fraction in the range of pH 3.0 to 8.0, as determined by analytical centrifugation.

By analytical centrifugation, the clarification velocity of the isolated small aggregate fraction was determined within the pH range of 3.0 to 8.0 (Fig. 5-6). These results indicate that only in the pH 4.0 to 5.0 range the transmission increase over time, which is equivalent to an increase in clarification of the supernatant. At a pH value of 3.0 and higher than 5.0, almost no increase in measured transmission was detected after 50 min of centrifugation. Highest clarification velocity was seen at a pH value of 4.4, which is however not fully congruent with the maximum measured particle size of pH-induced flocs, which was found at pH 4.6. The slight discrepancy can be explained by the high complexity of the sedimentation process itself, which is not only related to particle size, but also to various other influencing factors, such as particle stability and particle shape.

Fig. 5-7 depicts two transmission profiles of the small particle fraction measured at pH 4.4 and pH 7.0 to provide an impression of the primary analytical result regarding sedimentation behavior as a function of pH. In the profiles at pH 4.4, a slow but steady increase of transmission along the sample length is visible. In the final profile (green line at the top), a nearly complete clarification of the whole supernatant was achieved. The maximum clarity with a transmission of 86% was only detected on the top of the supernatant. This specific profile can be assigned to a polydisperse suspension, where distinct particle classes sediment one after another (Lerche and Sobisch, 2014). This indicates that there are weak attractive forces between the particles, which would enable a separation of all particles.
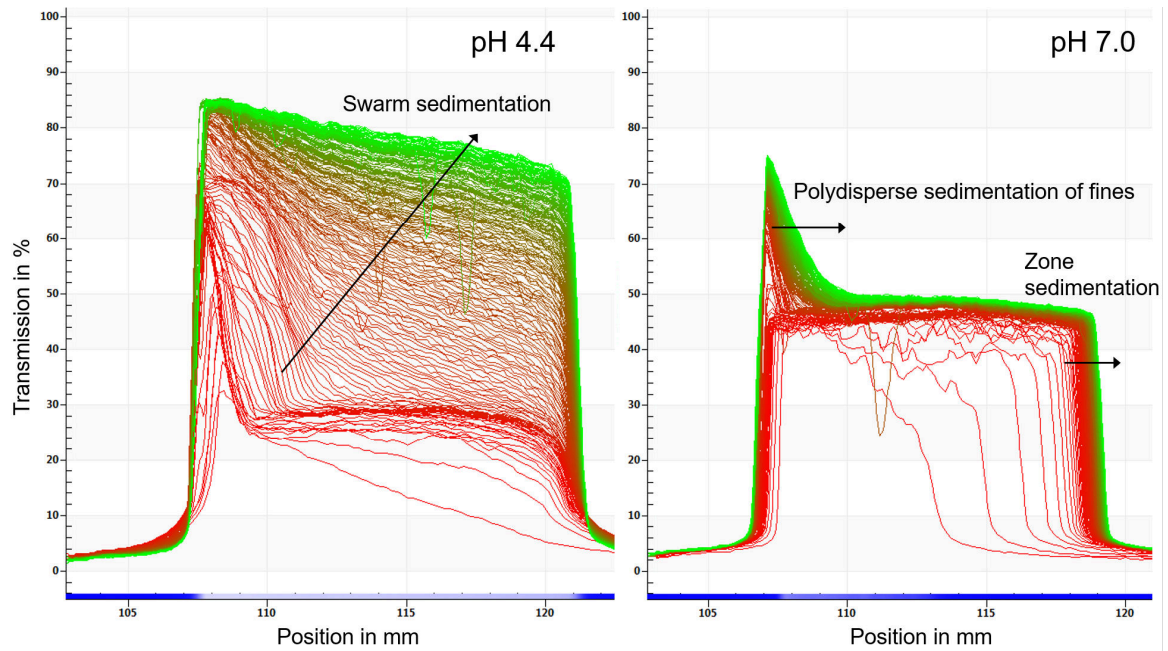
Fig. 5-7 Transmission profiles of small particle fraction at pH 4.4 (left) and pH 7.0 (right). Both suspensions contain a dry matter content 2.5%.

The profile plot of the small particle fraction at pH 7.0 clearly demonstrates a two-step sedimentation. Within the first three minutes, a clear and fast-moving sedimentation front can be observed, which are related to the largest particles present in the suspension, whereas, thereafter, almost no further progress in sedimentation occurs. This very slow progress in particle settling is characteristic for zone sedimentation, with sedimentation velocity of the whole zone being lower than Stokes velocity would facilitate (Lerche and Sobisch, 2014). Usually, zone sedimentation occurs at high particle volume fractions and conditions favoring sedimentation hindrance effects. The measured particle charge at pH 7.0 was indeed shown to be repulsive, and keeps the fraction of fines away from settling.

In summary, the investigation of pH-induced flocculation of aggregate fragments below 20 μm in size, showed the largest particle size at pH 4.6, a zero net charge at pH 4.5, and highest clarification velocity at pH 4.4. In the next section, these findings are transferred to a continuous decanter centrifuge system using pH 4.4 to represent the flocculated suspension. The pH 4.4 had the best results in the analytical centrifuge, which as an analysis technique has better comparability to decanter centrifugation than the other characterization methods used in this study.

5.3.3 Separation of flocculated and original β-Lg aggregate suspension in a decanter centrifuge

After determination of optimal conditions for pH-induced flocculation of the isolated small aggregate fraction, the question was whether the benefits of this sedimentation enhancing effect are also applicable in decanter separation of the original β-Lg aggregate suspension. The aim was to prove that pH-induced flocculation leads to better separation results compared with non-treated suspension. The separation of aggregate suspension was performed at pH 4.4 and at the original pH of 7.0. Additionally, two different inlet dry matter levels of 0.5% and 2.0% were investigated with the two pH values, respectively. For evaluation of the separation process, the separation efficiency of the centrates and the dry substance of the sediments were determined.

The separation efficiency was determined by quantification of remaining denatured β-Lg in the collected centrates. For all inlet suspensions investigated, the separation efficiencies were enhanced with increasing centrifugal acceleration (Fig. 5-8). The highest separation efficiencies were obtained for the inlet suspension adjusted to a pH of 4.4, reaching more than 99.8% of complete aggregate removal. The pH-induced particle size growth of the small aggregate fraction enabled the separation of particles, which would otherwise had been too small for sedimentation under given conditions. Slightly better results were obtained at the lower inlet dry substance concentration, which can be ascribed to lower particle hindrance effects during sedimentation. Separation results of the inlets at pH 7.0 were generally below the separation result of the respective pH-induced flocculated suspension. Also, standard deviations of the inlets at pH 7.0 presented higher values, which is an indication of varying quantities of the small aggregate fraction. However, it is noticeable that the suspension at pH 7.0 and 0.5% dry matter shows a steep improvement in separation efficiency, when increasing the centrifugal acceleration. Thus, industrial-scale decanter centrifuges capable of delivering higher g-levels could possibly reach sedimentation efficiencies close to the maximum even without pH adjustment. HPLC analysis furthermore revealed that there was a slightly increased loss of native α-La in the centrate with pH adjustment to 4.4, which reduced total recovery of α-La by 2 to 5%. This is most likely attributed to higher destabilization of α-La at lower pH values (Pedersen et al., 2006).
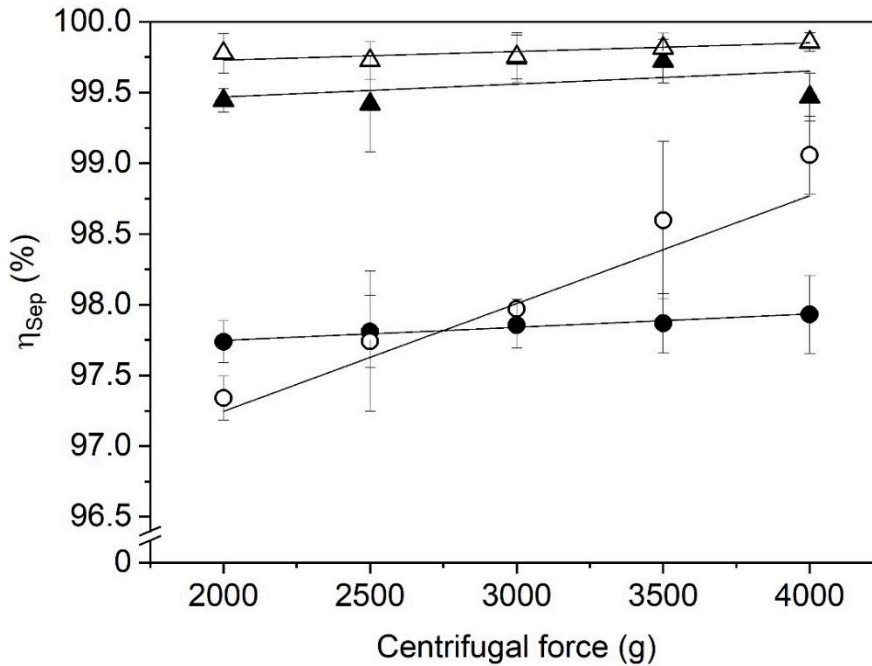
Fig. 5-8 Separation efficiencies of centrates received from decanter separation of β-Lg aggregate suspension at pH 4.4 and pH 7.0 with suspension dry matter levels of 0.5% and 2.5% as a function of centrifugal force. (●) represents suspension with pH 7.0 and 2.5% dry matter content, (▲) suspension with pH 4.4 with 2.5% dry matter content, (○) suspension with pH 7.0 and dry matter content 0.5%, (Δ) suspension with pH 4.4 and dry matter content 0.5%.

Simultaneously to sampling of the centrate, specimens of the sediment were taken and analyzed. Fig. 5-9 shows the values for dry substance content of received sediments under given settings. With higher centrifugal accelerations, the dry substance content in the discharged sediments also increased. Generally, it is recommended to strive for high dry matter contents in the sediment, because the remaining liquid portion filling the void volume of the sediment contain soluble proteins, and their loss will minimize the total recovery of native α-La fraction in the centrate. For β-Lg aggregates, the highest content of dry substance achieved was 60%, which is a comparably high value. Especially for biological sediments, a non-neglectable amount of humidity is bound water, which can be categorized as interstitial water, vicinal water, and hydrational water (Christensen et al., 2015).
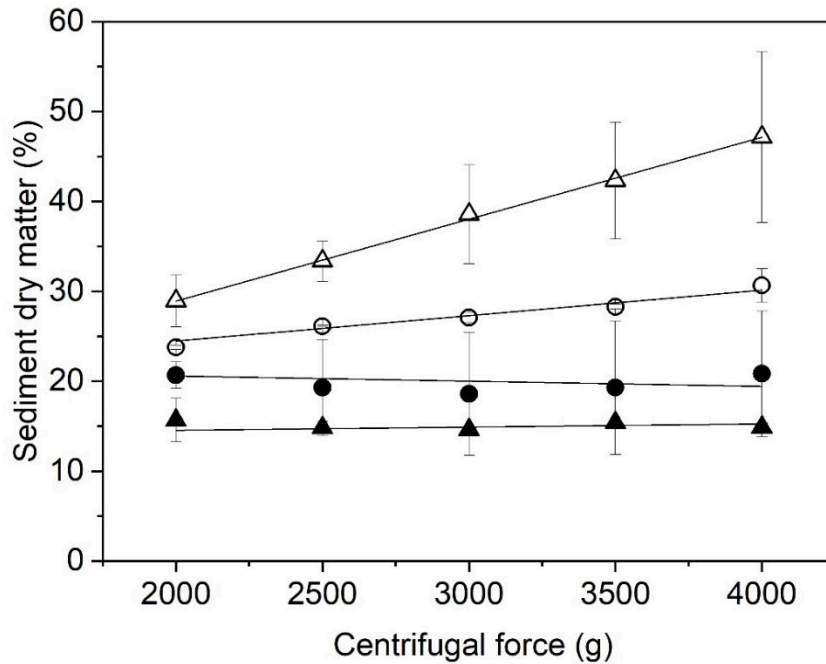
Fig. 5-9 Sediment dry matter received from decanter separation of β-Lg aggregate suspension at pH 4.4 and pH 7.0, as well as with suspension dry matter levels of 0.5% and 2.5% as a function of centrifugal force. (●) represents suspension with pH 7.0 and 2.5% dry matter content, (▲) suspension with pH 4.4 with 2.5% dry matter content, (○) suspension with pH 7.0 and dry matter content 0.5%, (Δ) suspension with pH 4.4 and dry matter content 0.5%.

A high dry substance content requires a proper dewatering of the sediment. The two main principles of sediment dewatering comprise compression of the sediment due to its self-weight, and the drainage of liquid, which occurs when the sediment is transported along the conical part of the bowl (Wakeman, 2007). Pictures from SEM analysis of the β-Lg aggregates that were discharged as sediment are presented in Fig. 5-10. The interstitial water may be located in formed voids inside or at the outer shell of the aggregate itself. Looking at the shape of the aggregates, a clear flattening through compression of initially spherical shaped primary aggregate units is visible. Additionally, no more filigree structures, such as thin branches were found, as they most likely were broken by shear forces. Besides the optical deformation of the aggregates, their suitability for applications as microparticulate to fortify functional food is not impaired.
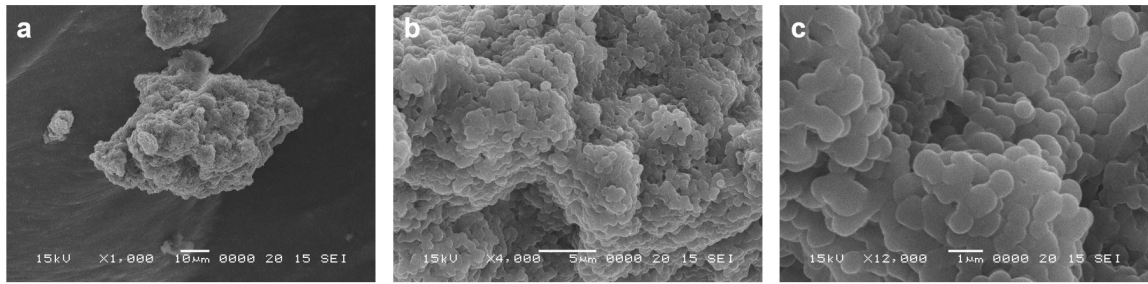
Fig. 5-10 SEM pictures of β-Lg aggregates from discharged sediment with magnifications factor of (a) 1,000, (b) 4,000, and (c) 12,000. Scale bars indicate sizes of 10, 5, and 1 μm, respectively.

5.4   Conclusion

The presented approach results in a microparticulated β-Lg fraction obtained as sediment from centrifugal separation with high dry substance content, and a high purity liquid phase containing native α-La and traces of other minor whey proteins. It was shown that yield and purity of fractions can be optimized by adjusting the pH of the particle suspension produced by thermal aggregation of native β-Lg.

This study demonstrated that a pH adjustment step could increase the separation efficiency by up to 2.5%, reaching a value of 99.8% separation efficiency in total. The pH-induced flocculation especially affected small particle fragments, which otherwise would have been lost in the supernatant thus reducing purity of the soluble fractions contained in the aqueous phase. At industrial scale, where the suspension might be subjected to even harsher processing with higher shear load and thus increased particle fragmentation, the flocculation might show even higher separation improvements. Regarding the sediment fraction obtained, the influence of used suspension inlet dry matter was significantly higher than any effect of pH-adjustment on sediment dry matter.

In industrial production, these two phases may require further processing steps for preparing potential applications. For the sedimented β-Lg fraction, a subsequent milling or high-pressure homogenization step can be used to adjust the particle size to a narrow mono-modal distribution between 0.1 and 2.0 μm, which is determined to best mimic the sensory impression of creaminess (Desai and Nolting, 1995; Singer and Dunn, 1990). The particles are then sufficiently small to be used as microparticulated whey proteins with functional benefits, e.g., increased water-binding capacity and slowing down of melting of ice cream outside the freezer (Spiegel, 1999b).

The liquid phase could subsequently be spray-dried. This would yield a high purity α-La powder, which could be an interesting source to increase the content of this protein in infant food formula as part of concepts of amending bovine-derived products to the golden standard of human mothers' milk. If a complete absence of β-Lg

is required, e.g., for hypoallergenic food products, the obtained centrate from decanter may be additionally purified by IEC to remove the low content of unaggregated β-Lg. So far, the limiting factor using exclusively IEC for removal of β-Lg, is the high concentration of β-Lg of nearly 60% in the native whey. Thus, the process herein presented for elimination of at least 94% of β-Lg in a whey protein solution might be a reasonable pre-treatment step for removing β-Lg prior to IEC to avoid overcharging of the limited binding capacity of the IEC columns.

6 Molecular analytical assessment of thermally precipitated α-Lactalbumin after resolubilization

<u>Summary and contribution of the doctoral candidate</u>

This study reports on the analytical characterization of resolubilized α-La received from selective thermal precipitation and centrifugal separation. The aim was to compare the processed and resolubilized α-La to its native counterpart as a reference in order to assess whether the resolubilized α-La can be considered close to `native´. Refolding pH values ranging from 6.0 to 10.0 were investigated and assessed for significance of the result. Turbidity measurement and quantification by RP-HPLC of the resolubilized α-La solutions were used as a measure of solubility in aqueous environment. Best results were seen at pH values from 8.0 to 10.0, with a resolubilization degree higher than 91%. Differential scanning calorimetry (DSC) measurement was performed to determine the denaturation peak temperature of resolubilized α-La. The best match was achieved at a refolding pH of 8.0. However, the difference in the peak denaturation temperature of all refolded batches compared to the native reference was proven to be significant. RP-HPLC was also applied to determine the elution time as a measure for protein´s hydrophobicity. All refolded samples represented a higher hydrophobicity compared to native state. A Fourier-transform infrared (FTIR) spectroscopy provided further insights in the secondary structure. For none of the refolded samples, the identical conformation from the native state was entirely restored. All refolded batches comprised a lower amount of β-turns and unordered structure, whereas the relative amount of α-helices and β-sheets increased. These changes could originate from intensified intermolecular interactions due to increased hydrophobicity upon unfolding, which might have resulted in intermolecular β-sheets, and potentially in the formation of α-La dimers.

Among the different investigated refolding batches, the use of pH 8.0 and a three-fold stoichiometric amount of calcium showed the highest resemblance to the native reference. The results indicate that the mechanism of precipitation induced by thermal treatment under acidic conditions with subsequent mechanical separation is reversible to a certain extent, however, the exact native conformation was not restored. With this fractionation approach, the high yield and good separation efficiency is achieved at the expense of a minor restructuring of α-La. Nevertheless, both main fractions, α-La and β-Lg, can be received in a soluble state and are obtained in a still functional state from nutritional and technological perspective.

The substantial contributions of the doctoral candidate include conception and design of the experiments based on preceding critical literature review, as well as the writing and the revision of the majority of the manuscript. The doctoral candidate carried out major parts of the data analysis, interpreted the data set, and discussed it.

Molecular analytical assessment of thermally precipitated α-Lactalbumin after resolubilization[5]

Nicole Haller[a], Isabel Maier[a] and Ulrich Kulozik[a]

[a]Chair for Food and Bioprocess Engineering, TUM School of Life Sciences, Technical University of Munich, Weihenstephaner Berg 1, 85354 Freising, Germany

Abstract

Selective thermal precipitation followed by a mechanical separation step is a well described method for fractionation of the main whey proteins, α-La and β-Lg. By choosing appropriate environmental conditions the thermal precipitation of either α-La or β-Lg can be induced. Whereas β-Lg irreversibly aggregates, the precipitated α-La can be resolubilized by a subsequent adjustment of the solution's pH and the ionic composition. This study reports on the analytical characterization of resolubilized α-La compared to its native counterpart as a reference in order to assess whether the resolubilized α-La can be considered close to `native´. Turbidity and quantification by RP-HPLC of the resolubilized α-La solutions were used as a measure of solubility in aqueous environment. RP-HPLC was also applied to determine the elution time as a measure for protein´s hydrophobicity. DSC measurement was performed to determine the denaturation peak temperature of resolubilized α-La. FTIR spectroscopy provided insights in the secondary structure. The refolding of α-La achieved best results using pH 8.0 and a 3-fold stoichiometric amount of Ca^{2+} per α-La molecule. The results showed that the mechanism of aggregation induced by gentle thermal treatment under acidic conditions with subsequent mechanical separation is reversible to a certain extent, however, the exact native conformation was not restored.

Keywords: α-Lactalbumin, refolding, resolubilization, whey protein, thermal denaturation, native, FTIR, DSC

6.1 Introduction

Whey is a source of protein with excellent techno-functional properties and bioactive peptides. The key components, β-Lg and α-La, make up for approximately 50% and 20% of the whey protein content, respectively. Due to their individual functional or physiological properties, the isolation in pure fraction is of increasing interest. Since several years, the development of cost-efficient separation methods of the individual whey protein fractions has evolved as an important driver for innovation in dairy industry and food research. A common concomitant of traditional dairy processing is the partial loss of native conformation caused by thermal, mechanical or chemical stresses on the protein (Muuronen et al., 2021).

α-La incorporates specific physiological and medical functionalities and a nutritional value that makes it an interesting candidate for the use as food additive or as a part of therapeutic concepts. Bovine α-La's richness in tryptophan and its similarity to the human α-La makes it an ideal source for infant food formulations, allowing further adaption to the golden standard, mother's milk (Lien et al., 2004; Chatterton et al., 2006). Of special interest is its property to carry different minerals, such as Mg^{2+}, Mn^{2+}, Na^+, K^+, and of course Ca^{2+}, which is natively bound in the holo-state (Permyakov, 2020). α-La is reported to enhance the regeneration of cells (Heine et al., 1991), to possess antimicrobial properties against a broad spectrum of bacteria, including anti-biotic resistant strains (Expósito and Recio, 2006; Stănciuc and Râpeanu, 2010), and to have antitumor properties in a complex with oleic acid (Delgado et al., 2015b; Hoque et al., 2015).

Generally, there are two ways for the separation of the whey protein main components that are based on selective aggregation of one of the fractions. An aggregation of β-Lg can be initiated by a short heat treatment at high temperatures, which is irreversible due to the covalent disulfide bridge formation. The alternative is to selectively precipitate α-La under acidic conditions, which are not affecting β-Lg. In both cases the aggregated fraction can easily be separated either by MF or by centrifugation in order to obtain the native other fractions in the supernatant or permeate, respectively. The difference between these concepts is that in the second route, the aggregated α-La can be resolubilized, as shown by Toro-Sierra et al. (2013), and both fractions were finally be assumed to be obtained in their native soluble states.

In any case, it should be priority to keep the nativity of the proteins at a maximum throughout the processing. Primarily, the bioactivity and anti-inflammatory or immunomodulating properties are substantially dependent on the native state of the whey proteins (Patel, 2015; Pérez-Cano et al., 2007; Prussick et al., 2013). From a nutritional perspective, it is reported that whey proteins in their native states promote gastro-intestinal tolerance and maturation of infants (Navis et al., 2020a; Navis et al., 2020b). Furthermore, Abbring et al. (2019a; 2019b) showed that native

whey protein has a lower allergenicity than the processed, i.e., heat-treated, equivalent. Additionally, any further processing will benefit from using standardized raw material with defined properties rather than a coincidental product with fluctuating characteristics.

In this study, the method of acidic precipitation of α-La with gentle heat treatment and subsequent separation from soluble and native β-Lg was used. A previous study demonstrated that this process in combination with a separation by a decanter centrifuge provides high yields, easy scalability, and high purities of the obtained fractions (Haller and Kulozik, 2020). With a comparably low heat load and a good stability at acidic pH values, the nativity of β-Lg remains virtually unaffected by this method as demonstrated by Kella and Kinsella (1988).

Back in 1964, Kronman et al. reported on the release of the bound Ca^{2+}-ion from α-La at an acidic pH, followed by its thermally induced aggregation. An additional calcium-complexing agent, such as EDTA (Bernal and Jelen, 1984), sodium hexametaphosphate (Alomirah and Alli, 2004), lactic acid (Lucena et al., 2007), or citrate (Bramaud et al., 1997b) prevents the re-transition to holo-state. In the calcium-free apo-form, the hydrophobic parts of the α-La protein are easier accessible, which is further promoted by gentle heating up to 60 °C (Bonnaillie and Tomasula, 2012). Under these conditions, α-La forms precipitates, most likely caused by a combination of hydrophobic and electrostatic interactions (Pedersen et al., 2006). The formed precipitates enable a size-based separation either by MF (Gésan-Guiziou et al., 1999; Toro-Sierra et al., 2013) or centrifugation (Fernández et al., 2012; Lucena et al., 2006; Haller and Kulozik, 2020).

Already in the early stages of research in this field, the possibility to resolubilize the α-La precipitate by increasing the pH plus the addition of calcium was reported (Bramaud et al., 1997a; Kronman et al., 1981). In fact, several studies proved that α-La is able to refold from a thermally unfolded apo-state to a native holo-conformation (Bernal and Jelen, 1984; Permyakov, 2020; Stănciuc and Râpeanu, 2010). However, all of these studies have been performed under ideal and protected laboratory conditions, excluding any additional mechanical stress. It is highly questionable if the results of these isolated folding studies are transferable to industrial-like whey protein processing.

A definite proof is still lacking, whether α-La returns to the same globular folded state after the acidic precipitation and mechanical separation compared to the native holo-state. Therefore, the aim of this study was to characterize the molecular state of α-La after selective precipitation, separation and subsequent resolubilization. Turbidity by means of optical density and quantification by RP-HPLC were used as a measure for dissociation of precipitates upon basification. DSC was used to determine the denaturation peak temperature of refolded α-La and to compare its thermal stability with its native reference. The Amid I band was analyzed by FTIR, which allows quantification of certain secondary structure motifs such as

α-helix, β-sheet, and β-turns (Kong and Yu, 2007). The aim was to answer the question whether or to which extent the original 'nativity' of α-La – after having been exposed to thermal, chemical and mechanical stress – can be re-established.

6.2 Materials and methods

6.2.1 Materials

WPI from Davisco (Le Seur, MN, USA) was used as raw material to produce the α-La precipitate suspension. This WPI has a protein content of 94.2% per dry matter. Trisodium citrate dihydrate and citric acid monohydrate were purchased from Bernd Kraft GmbH (Duisburg, Germany). HCl, NaOH, $CaCl_2$ and EtOH were purchased from Sigma Aldrich (Steinheim, Germany). Analytical grade TFA and acetonitrile for HPLC analysis were purchased from Sigma Aldrich (Steinheim, Germany). DIW was used for solution preparation and analytical methods. For the HPLC methods Milli-Q (Merck KGaA, Darmstadt, Germany) purified water was used.

6.2.2 α-La precipitation, separation, and refolding procedure

WPI powder was dissolved in DIW to a final protein concentration of 150 g L^{-1} and was gently stirred using a three-blade agitator at 350 rpm (Heidolph Elektro GmbH & Co. KG, Schwabach, Germany). Total mixing time was 12 h at a temperature of 4 °C. The pH value of the protein solution was adjusted to pH 3.4 using trisodium citrate and citric acid. A final citrate content of 60 g L^{-1} was achieved. The beaker glass with the protein solution was placed in a water bath, while it was gently mixed by a magnetic stirrer. Upon reaching the solution target temperature of 50 °C, the temperature was kept at 50 ± 1 °C for 120 min, followed by a fast cooling phase in ice water to stop precipitation process. The suspension was transferred to 50 mL tubes and centrifuged at 6,000 g for 30 min (Multifuge 1 S-R, Heraeus Holding GmbH, Hanau, Germany) to separate precipitates from β-Lg enriched supernatant. In a previous study, it was shown that a considerable amount of native β-Lg remains in the sediment phase (Haller and Kulozik, 2020). Two washing steps of the sediment using DIW with adjusted pH to 3.4 using 0.1 M HCl were performed to remove β-Lg residues from the sediment. The washing procedure resulted in a sediment consisting of more than 99% α-La, based on RP-HPLC analysis. For the refolding, the sediment was diluted in a ratio of 1:5 in DIW and mixed for 30 min on a magnetic stirrer at 150 rpm. The pH was increased with 0.5 M and 0.1 M NaOH to adjust the pH value to the respective target value between pH 6.0 and 10.0. Subsequently, $CaCl_2$ was added to a final stochiometric ratio of three ionic calcium

ions per α-La molecule. The solution was stirred for another 30 min at room temperature and target pH was confirmed once more, before HPLC, FTIR and DSC measurements were performed.

6.2.3 Determination of resolubilization degree

After refolding of the α-La samples at different pH values and CaCl$_2$ addition, the optical density at 550 nm (OD$_{550}$) as a measure of turbidity was determined by a spectrophotometer (Ultrospec III, Pharmacia AG, Uppsala, Sweden) as described in (O'Loughlin et al., 2015). Cuvettes with a path length of 1 cm were used. DIW served as reference.

The quantification as well as determination of the degree of resolubilization of α-La was performed by RP-HPLC analysis as described by in (Haller and Kulozik, 2020). For calculation of resolubilization degree (RD) (6.1), it was required to prepare one sample that was clarified from insoluble protein by a pH 4.6 isoelectric precipitation and centrifugation ($c_{\alpha-La,soluble}$), and another one that was left untreated and in original composition ($c_{\alpha-La,total}$). Both samples were pre-diluted with DIW, followed by dissolving 200 µL of properly homogenized sample in 800 µL of a 6 N guanidine buffer. The incubation time was at least 30 min. Afterwards samples were transferred to screw-capped glass vials and measured by RP-HPLC (Agilent 1100 Series chromatograph, Agilent Technologies, Waldbronn, Germany, equipped with Agilent Zorbax 300SB-C18, 4.6 × 150 mm, 5 µm).

$$RD = \frac{c_{\alpha-La,soluble}}{c_{\alpha-La,total}} \cdot 100\% \tag{6.1}$$

6.2.4 Production of native α-La as analytical standard

The reference standard for native α-La was manufactured in-house using the same starting material as for the precipitate production. The method of selective thermal aggregation of β-Lg was used as described in (Haller et al., 2021). In brief, a WPI solution with 2.5% protein content, pH of 7.5 and 0.5 g L^{-1} CaCl$_2$ was heated at 97 °C for 9 s. Upon β-Lg aggregation, pH was adjusted to 4.6 for isoelectric precipitation of denatured proteins and higher separation efficiency in centrifugal separation. The α-La-enriched supernatant was separated from the sediment containing denatured protein by a decanter centrifuge (MD 80, Lemitec, Berlin, Germany) at 4,000 g and a throughput of 10 L h^{-1}. Subsequently, the pH was adjusted to 8.0 in order to increase α-La stability. A 10 kDa cassette membrane filter cut-off was used for a 5-fold concentration of the solution and subsequent DF steps using DIW to remove lactose and salts. The α-La standard was determined to have a nativity of 97%, containing 89% α-La, based on RP-HPLC analysis.

6.2.5 Characterization of elution time by RP-HPLC analysis

Using a standardized and highly reproducible RP-HPLC analysis method for one specific protein allows to use the retention time as a measure for the proteins' relative hydrophobicity.

The resolubilized α-La samples were diluted to a protein concentration of approximately 1%. The pH value was adjusted to 4.6 and the samples were filtered through a 0.45 µm syringe filter into a glass vial, before being analyzed be RP-HPLC. An Agilent 1100 chromatograph with a PLRP-S 8 µ 300 Å 150 × 4.6 mm column (Latek, Eppelheim, Germany) was used. Eluent A (1% TFA in water) and a gradient of eluent B (80% acetonitrile and 0.055% TFA in water) were used at a flow rate of 1 mL min^{-1} at 40 °C. The eluent was detected using an UV detector at 226 nm.

In the resulting chromatograms, the time point when the peak maximum of each α-La sample was reached was defined as the elution time. The elution times of the different α-La batches, which were resolubilized at different pH values between 6.5 and 9.5, were compared.

6.2.6 Determination of denaturation temperature by DSC

Unfolding temperature of the α-La samples was determined by DSC including the Refrigerated Cooling System (Q1000, TA Instruments, Alzenau, Germany). An amount of 20 µg of the refolded α-La solutions with an approximate protein content of 5% (w w^{-1}) were used as sample, while DIW was used as reference. For each measurement, one sample and a reference were given in aluminum pans and crimped with a lid, respectively. They were placed on the respective platforms in the measurement cell, which are equipped with heat flow sensors. The cell was closed, evacuated and the temperature was controlled as defined in the recipe. The first step was an equilibration at 10 °C for 5 min, followed by heating rate of 3 °C min^{-1} to 85 °C, which was held for 1 min. The final step was to ramp down to 10 °C with 10 °C min^{-1}. Conformational changes such as unfolding of the protein result in a deviating heat flow of the sample compared to the reference. Obtained data were evaluated by OriginPro 2020 to determine the heat flow peak maximum, which was defined as denaturation temperature of the sample.

6.2.7 Analysis of the secondary structure by FTIR

α-La secondary structure and success of refolding were analyzed by FTIR spectroscopy (Tensor 27, Bruker Optik GmbH, Ettlingen, Germany) equipped with an attenuated total reflectance (ATR) crystal. Before each measurement, the crystal was cleaned with DIW and 70% EtOH, and a background measurement with air was performed. Then, 5 µL of the sample was applied on the crystal and dried under regulated conditions (gaseous N_2 overflow at flow rate of 100 mL min^{-1} for

10 min). Each measurement comprised 60 scans and each sample was applied and measured 5 times. The scans recorded the spectrum between 400 and 4,000 cm^{-1} with a nominal instrument resolution of 2 cm^{-1}.

Data evaluation was performed with the software OPUS 7.2.139.1294 (Bruker Optik GmbH, Ettlingen, Germany). Data preparation covered the following steps: The spectra were cut between 1,600 and 1,700 cm^{-1}, which represents the so-called Amid I band that reflects protein secondary structures. Elastic baseline correction using 64 points was applied. Spectra were normalized by Min.-/Max.-method and afterwards second derivation of spectra were calculated. All obtained minima in second-derivative spectra indicate an inflection point in the original absorbance spectra, meaning each minimum represents a peak position at a certain wavenumber. A median spectrum was calculated from all appropriate spectra. Finally, Lorenz-deconvolution with noise reduction of 0.55 and band shape 2 was applied. The Levenberg-Marquardt-Algorithm was used to calculate peak areas at the positions, previously determined by the second derivative. The integrated areas of each peak were related to secondary structural motives as described in (Carbonaro and Nucara, 2010).

6.2.8 Data evaluation and statistics

Presented data points are the mean values with standard deviations. The number of replications n is given in the respective figure description. Data were evaluated and plotted using OriginPro 2020 (OriginLab Corporation, Northampton, MA, USA). The t-test was applied to compare significance of difference between the reference and the refolded α-La samples at a confidence level of 95%. The Student's t-test was used when the assumptions of normality and homogeneity of variances was fulfilled. In case of violation of the assumption of normality, Welch's t-test was used. Statistical significance was declared at $p < 0.05$. Pairwise comparison between different refolding pH values was performed using one-way ANOVA and Tukey's test as post-hoc test.

6.3   Results and discussion

6.3.1 Solubilization of α-La precipitates

As a scale of precipitate dissociation of the α-La refolding batches, the OD_{550} and the RD determined by RP-HPLC quantification were measured after pH adjustment and $CaCl_2$ addition. Resolubilized α-La samples in the pH range of 6.0 to 10.0 in steps of 0.5 pH-units were investigated. The results of OD_{550} are shown in Fig. 6-1a, the results of RD determination are presented in Fig. 6-1b.
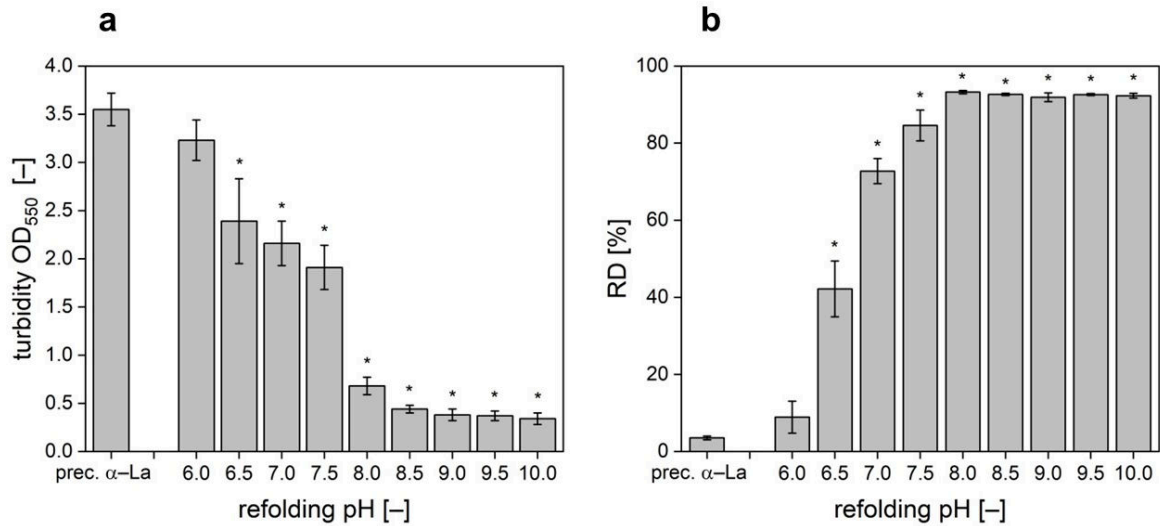
Fig. 6-1 (a) OD_{550} as measure for turbidity of the precipitated and washed α-La and of resolubilized α-La samples after pH adjustment and $CaCl_2$ addition. Data are given as mean ± SD, n = 3. * Significantly different than precipitated α-La (p < 0.05). (b) RD of the precipitated and washed α-La and of resolubilized α-La samples after pH adjustment and $CaCl_2$ addition. Data are given as mean ± SD, n = 2. * Significantly different than precipitated α-La (p < 0.05).

All samples with pH values in the acidic range showed high turbidity, which indicates a predominance of precipitates instead of single protein molecules. A remarkable jump in turbidity decrease was observed between pH 7.5 and pH of 8.0. With a further increase of the pH value the nominal OD_{550} was reduced slightly further. Based on pairwise statistical comparison, the refolding pH values 8.5 to 10.0 did not significantly differ from each other. However, the turbidity is only an indicator, but not a direct measurement of the extent nor of the quality of α-La's refolding. Additionally, the RD was determined based on RP-HPLC quantification of insoluble and soluble α-La (Fig. 6-1b). In the precipitated and washed α-La only 3.5% of the α-La was soluble. With a pH increase to pH 6.0 only a slight improvement of solubility to 8.9% was observed, though not being significantly different from the precipitated references. The biggest step in resolubilization was obtained between pH 6.5 and pH 7.0. The RD of the samples refolded at pH 8.0 to 10.0 lay between 91.9 to 93.2% and were not significantly different from each other.

Generally, the RD results support the OD_{550} measurements from a qualitative perspective. The RD results may suggest a more extensive resolubilization at a lower pH value. However, this shift may also be related to the sample preparation method that includes dilution. Both methods are in good accordance with results from literature. For example, Bramaud et al. (1997b) also reported an effective resolubilization of α-La starts at pH 8.0.

As described in the introduction, the α-La precipitates are mainly stabilized by hydrophobic interactions. The alkaline pH decreases the hydrophobic interactions, while the importance of the electrostatic forces increases and lead to repulsion of

the molecules (Lam and Nickerson, 2015; Wang et al., 2020). It is required to singularize the α-La molecules to make the calcium-binding site accessible for the subsequently added calcium.

In other experiments, the amount of added calcium was varied between 1 to 10-fold stoichiometric amount in respect to the number of α-La molecules. However, results indicated that the calcium concentration was not the main influencing factor in resolubilization. The results with 1 to 2 times calcium showed slightly inferior resolubilization results compared to the higher concentrations. The results with 3 to 10-fold calcium concentration were equal within a 95% confidential interval. The results are in agreement with literature, stating that addition of excess $CaCl_2$ only affects the transition temperature but does not change the protein substructures involved in the refolding (Zhong et al., 1999).

6.3.2 Investigation of thermal stability

The denaturation temperature was determined by DSC and provides information about the proteins' thermal stability, which strongly correlates with the tertiary structure of the protein. An identical or similar denaturation temperature suggests that two proteins follow a similar road map in unfolding and that the same binding types, such as thiol bridges and hydrogen bonds, are accessible and dissociate at the same threshold temperature. The peak denaturation temperature of native calcium-bound α-La was determined at 64.2 °C, which is indicated by the dashed line across the diagram in Fig. 6-2. The peak denaturation temperature of the native standard is in good accordance with values from literature (Boye and Alli, 2000; McGuffey et al., 2005).
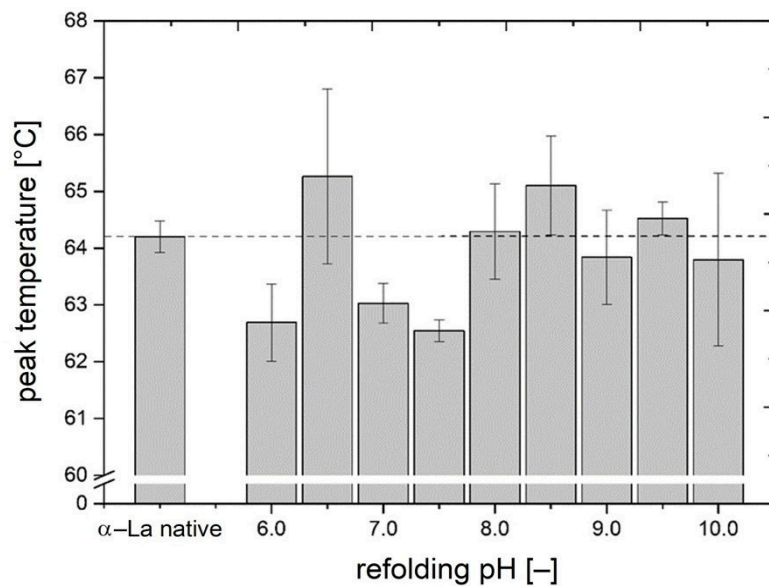
Fig. 6-2 Peak denaturation temperatures of α-La samples that were refolded at pH values between 6.0 and 10.0 in comparison with untreated native reference α-La (left), determined by DSC analysis. Data are given as mean ± SD, n = 2. All refolded batches were significantly different from native α-La (p < 0.05).

The refolded α-La samples showed peak denaturation temperatures between 62.5 and 65.3 °C. The samples being refolded at pH 6.0, 7.0, and 7.5 showed a denaturation temperature of more than 1 °C below the one of the native reference. Other refolded batches, such as pH 6.5, 8.5, and 9.5, demonstrated higher denaturation peak temperatures than the reference. The best match in denaturation peak temperature was achieved at a re-folding pH of 8.0 with a peak temperature of 64.3 °C. However, the difference in peak temperature of all refolded batches compared to the native reference was proven to be significant ($p < 0.05$). This is a first indication that the structural conformation of the refolded batches differs from the native state.

The samples with pH values from 8.5 to 10.0 had relatively high standard deviations. One possible explanation is the presence of partially irreversibly denatured α-La or of protein fragments that might occur as a consequence of mechanical separation forces. Another reason could be that the refolded α-La samples may contain several different conformations in one sample. Time-resolved IR studies suggest that the thermally unfolded apo-α-La likely initially transitions to a molten globule state, followed by either parallel or sequential folding pathways to resume the native holo-α-La state (Hsu et al., 2021). Though, a correct refolding to native state remains a challenging task, especially, when the protein was kept in a thermally unfolded state for a longer time and was further exposed to mechanical stress through stirring and centrifugation. Literature data indicate that the binding of Ca^{2+} to the calcium-binding site of α-La initiates a folding nucleus at the interface between the α- and β-domain, which appears to be a crucial step to trigger the correct re-organization of the native structure (Bushmarina et al., 2006). The two domains are held together by the disulfide bridges between Cys73 and Cys91 and between Cys61 and Cys77. The total of four disulfide bonds are considered crucial for the stability of α-La, even when transitioned to apo-form. The disulfide bridges in α-La can resist temperatures higher than 90 °C, when α-La is heated alone or no reactive sulfhydryl groups are present, such as β-Lg exposes at temperature above 60 °C (Calvo et al., 1993; Chang and Li, 2002). Therefore, it is very likely that the four disulfide bonds remained intact throughout the processing.

With the peak denaturation temperature all being higher than 62 °C, it is expected that the refolded α-La samples have a Ca^+ bound. The apo-form is described to unfold already at temperatures as low as low as 10 to 30 °C (Permyakov, 2020). Though, the results fail to clearly indicate whether the native calcium-binding site is restored or not.

6.3.3 Investigation of hydrophobicity

The RP-HPLC separates proteins according to their surface hydrophobicity, i.e., the hydrophobic stationary phase has a stronger affinity for hydrophobic compounds, which is the reason why more hydrophilic molecules are eluted first. With the increasing acetonitrile gradient, the hydrophobic interactions between the stationary phase and the molecule are gradually reduced, and thus hydrophobic molecules elute at a later point of time. This separation principle was used to investigate if the refolded α-La samples show differences in hydrophobicity, which would relate to a deviation in the tertiary structure. Fig. 6-3 shows that the elution time of the native reference α-La was 8.37 min. The α-La samples being refolded at a pH of 6.5 and 7.0 had a distinct later elution time, which means that these refolded samples have a higher hydrophobicity compared to the native reference. The closest match in elution time compared to the native reference is achieved with the sample that was refolded at pH 8.0 with a time of 8.38 min.

Statistical analysis resulted in a significant difference in elution time of all refolded samples compared to the native reference.
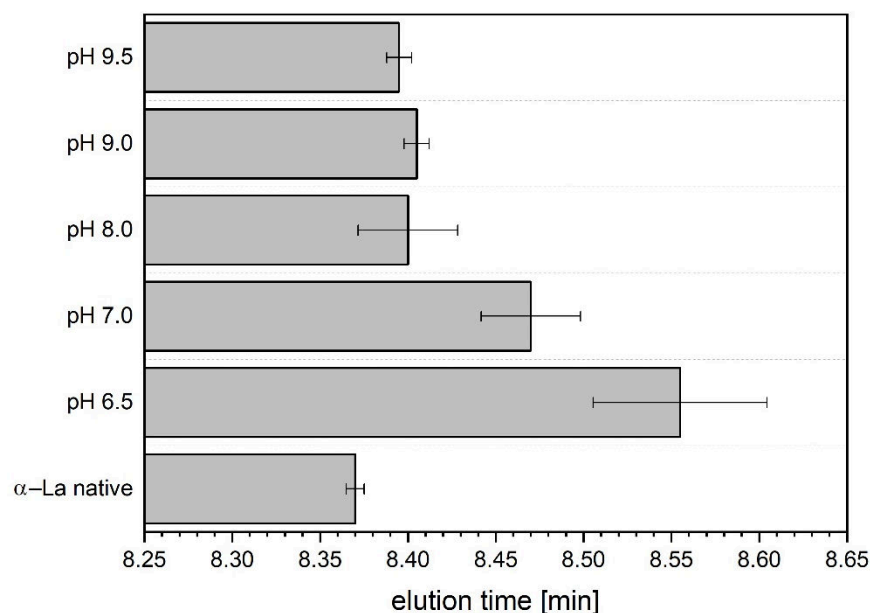
Fig. 6-3 Elution times in RP-HPLC analysis of native reference and refolded α-La samples at different pH values. Data are given as mean ± SD, n = 2. All refolded batches were significantly different from native α-La (p < 0.05).

Globular proteins locate most of their hydrophobic amino acid residues in the inner core (Rose et al., 1985), and so does α-La (Vanhooren et al., 2005). With the precipitation procedure used in this study, the α-La releases its calcium ion and unfolds to a certain extent, thus exposing the inner hydrophobic parts (Stănciuc et al., 2013). All refolded batches of α-La had a later elution time, implying a higher surface hydrophobicity. These results indicate that there are still inner hydrophobic residues exposed that are usually not accessible.

6.3.4 Analysis of secondary structure

FTIR spectrometry is an established method to determine a structural 'fingerprint' of a protein by providing insights in its secondary structure. The second-derivative spectra of native α-La sample was used to determine the approximate position and number of peaks in the Amid I band. Each of these peaks can be assigned to certain secondary structure motive of proteins. The assignment of structural motifs was performed based on results of Carbonaro and Nucara (2010) and is listed in Tab. 6-1.

Tab. 6-1 Assignment of secondary structural motifs to the peak positions obtained from FTIR spectrum analysis.

Peak position [cm^{-1}]	Secondary structure
1693	β-sheet
1680	β-turn
1666	α-helix
1658	α-helix
1650	α-helix
1643	unordered
1632	α-helix
1620	β-sheet
1612	β-sheet

In Fig. 6-4, the Amid I band spectrum of native α-La is compared to the spectra of the samples that were refolded at different pH values. The spectrum of the pH 7.0 refolded batch shows distinct differences, especially in the region of 1,700 to 1,680 cm^{-1}, as well as 1,620 to 1,600 cm^{-1}, which are assigned to β-sheet and β-turn structures (Tab. 6-1). Such an extensive formation of β-structures is characteristic for protein aggregation (Goers et al., 2002). This supports the assumption that a resolubilization pH of 7.0 is not sufficient to induce a proper dissociation of the α-La molecules from precipitated state, which is supported by the results from Fig. 6-1. The spectra of samples refolded at pH 8.0 to 10.0 show a certain resemblance to the spectrum of the native α-La, at least from a qualitatively perspective. Nevertheless, the peak heights still show discrepancies to the native reference.
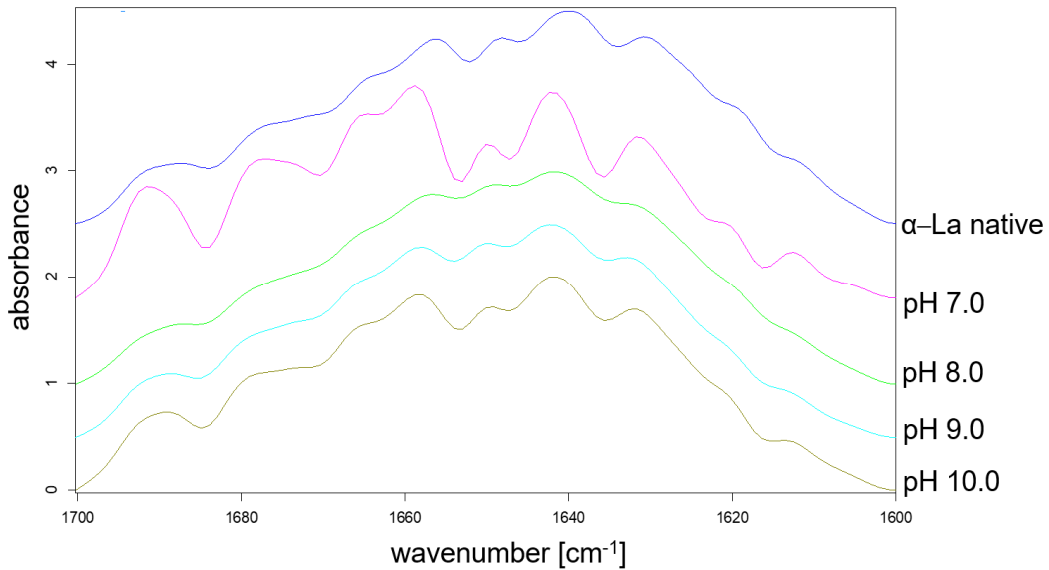
Fig. 6-4 FTIR spectrum of the Amid I band of native α-La is compared to the batches that were resolubilized at pH values between 7.0 and 10.0.

A Gaussian fitting was performed with the spectra from Fig. 6-4 considering that nine peaks were determined previously. The relative area under each of the Gaussian curves was calculated and assigned to a respective secondary structural motive, as listed in Tab. 6-1. Fig. 6-5 shows the relative amounts of β-turns, α-helices, β-sheets, and unordered structure for the refolded batches as well as for the native reference.
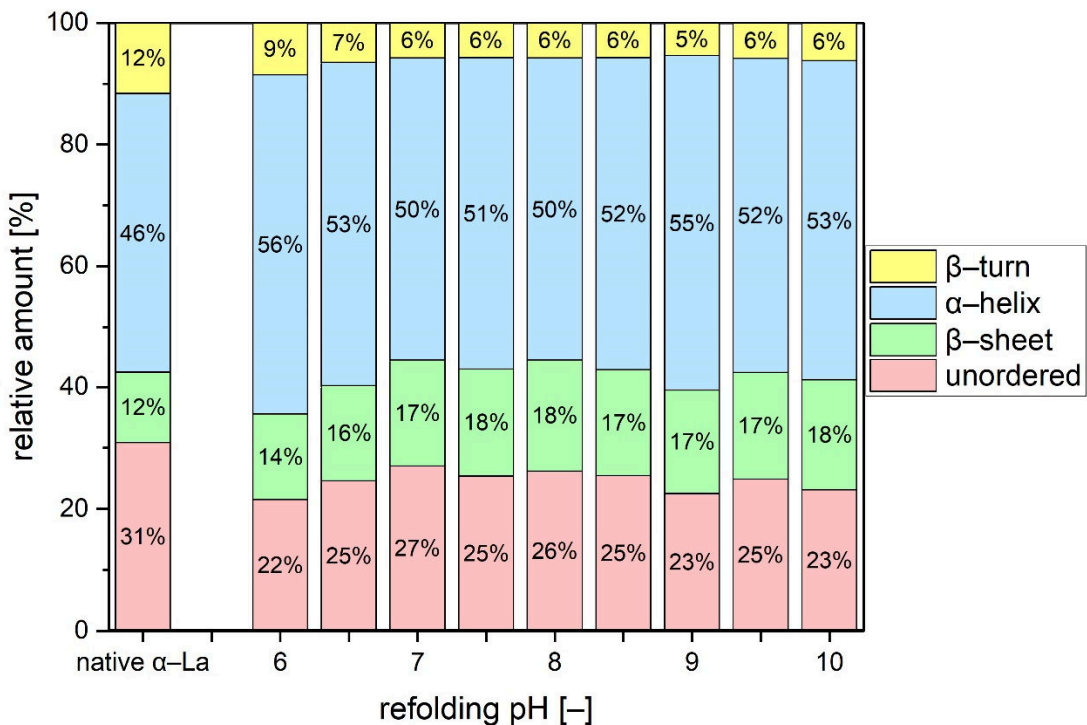
Fig. 6-5 The relative amounts of secondary structural motives calculated based on FTIR curve areas displayed for the refolded batches and the native α-La sample. Data are given as mean, n = 2. All refolded batches were significantly different from native α-La (p < 0.05).

The distribution of the structural elements clearly shows that for none of the re-folded samples, the identical conformation from the native state was entirely restored. Statistical analysis proved that the difference to the native reference was significant. All refolded batches comprise a lower amount of β-turns and unordered structure, whereas the relative amount of α-helices and β-sheets had increased.

Boye et al. (1997) investigated FTIR spectra of α-La samples at different pH values that were heated and subsequently cooled. At both, acid and alkaline pH, the cooled samples showed a loss of β-turns compared to native reference. Furthermore, they reported on an increased β-sheet formation in the samples heated and cooled under acidic conditions. This was attributed to intensified intermolecular interactions due to increased hydrophobicity upon unfolding, which finally resulted in the formation of intermolecular β-sheets. It was suggested that this formation of intermolecular β-sheets may indicate a (irreversible) denaturation of the protein or the formation of α-La dimers. Other studies suggest that non-native β-sheet formation may transiently appear, especially, when the refolding is slow (Troullier et al., 2000). In fact, the refolding to the native apo-structure in absence of calcium was reported to be slower than when calcium is present (Veprintsev et al., 1997). As described in the materials section, the calcium was added after the pH adjustment, which might affect the ability to refold properly.

Intermolecular interactions are likely the reason why a complete restoration of the native state was not achieved. Kuhlman et al. (1997) demonstrated that the native C-helix is crucial for formation of the calcium-binding site and promotes a proper connection of the two domains of α-La. In case the C-helix is sterically hindered, e.g., by intermolecular crosslinks, the normal connection of the α- and β-domain would be impaired. The resulting cleft would result in inner hydrophobic amino acids still being exposed to some extent, which is supported by the previously presented elution time results.

Generally, refolding to the native conformation from a thermally unfolded state requires a correct formation of the β-sheets domain, the calcium binding site and the numerous loop and turn structures, as well as the restoration of a stable tertiary structure. Major changes in the environment, however, which could be caused by different pH values, temperature or solvent conditions, can affect the folding of the β-sheet domain and the structure of the loops in the molten globule (Dobson et al., 1998). Furthermore, apo-α-La is not only more susceptible to thermal treatment, but also to hydrostatic and mechanic stress compared to its holo-form (Haller and Kulozik, 2020; Hosseini-Nia et al., 2002). It is likely that the applied conditions, such as heating to 50 °C for several hours and the mechanical stress through stirring and centrifugation are the root cause for the deviating conformation after refolding.

6.4   Conclusion

The aim of this study was to determine to which extent the original and native structure of α-La — after having been exposed to chemical, thermal, and mechanical stress — can be re-established at alkaline pH and calcium addition. The overall outcome was that under none of the investigated refolding conditions, the exact native structure was fully restored. Among the different investigated refolding batches, the use of pH of 8.0 and a three-fold stoichiometric amount of calcium showed the highest resemblance to the native reference. Under these resolubilization conditions, the denaturation temperature was only 0.1 °C higher compared to the native α-La, although the resemblance was not statistically significant. In the analysis of RP-HPLC elution time, the pH 8.0-refolded α-La was also closest to the native α-La by a difference of less than 1 s. Even though the absolute shift in elution time seems to be comparably low, the difference was significant different from the native reference. A comparison of the full Amid I band spectra of native and resolubilized samples suggests an overall resemblance of the peak profile, but some respective secondary motifs have distinctly changed by the precipitation and resolubilization procedures. In conclusion, all analytical methods confirmed that, within a confidence interval of 95%, the native structure of α-La was not completely re-established by the presented resolubilization method. However, the degree of deviation across all analytical methods applied was not very large.

Generally, a refolding of thermally unfolded apo-α-La to a native holo-state appears to be possible, as it was demonstrated by various studies previously. However, these studies investigated the refolding process under isolated lab conditions, without any further stress on the proteins. In contrast to those works, this study examined the applicability of the refolding potential under real life conditions, i.e., in a technologically relevant environment. Although the four disulfide bridges seem to stay intact and although it appears as if the structurally decisive calcium ion between two domains of the native α-La was in fact re-integrated, the precipitation method obviously has remaining effects on the conformation of the refolded α-La samples. Overall, our results demonstrate that characteristic structural motifs were reorganized sustainably as a result of chemical, thermal and mechanical treatment of the protein. Therefore, the resolubilization results could be termed 'restructuring' rather than renaturation.

We see the main application field of the restructured α-La in functional and/or fortified foods, such as α-La-enriched infant formula. For this type of application, the key property is the amino acid composition, which is generally not affected by the procedure used in this study. If and to which extent the ability of cation binding was impaired should be verified in further experiments. The results of the denaturation temperature determined by DSC is, however, a strong indicator that the re-integration of the calcium into the protein´s structure has taken place.

The applied precipitation conditions were chosen based on previous studies, ascribing highest precipitation yield and best separation results to this method. In this case, the high yield and good separation efficiency is achieved at the expense of a minor restructuring of α-La. Given that this separation concept does not only yield β-Lg unaffected by the processing conditions applied, but also α-La in a soluble state, there is no loss in the whey protein main components, i.e., no low value side stream is produced. This way, the main whey proteins α-La and β-Lg can both be obtained in a still functional state both from a nutritional and technological perspective.

7 Overall Discussion and Conclusion

The constantly rising demand for pure and native fractions of the major whey proteins α-La and β-Lg necessitates an efficient, commercial production process. In this thesis, an innovative two-step separation process for whey protein fractionation was described. The first step comprises a selective thermal aggregation of either α-La or β-Lg, while the other fractions' nativity and solubility are not affected by the applied conditions. In the second step, the generated protein particles are separated by continuous centrifugal separation using a decanter type centrifuge.

As each of the four published articles comprised in this thesis elucidates a certain topic, this chapter aims to critically review all key findings, explain the overall connections, and discuss the results on a higher level. Firstly, the assessment of the particle characteristics is related to the underlying intermolecular binding mechanisms, and it is explained how these structural properties of the protein particles influence the behavior during settling, compression, and discharge of the sediment. With that information, a suitable decanter type for the respective sediments, consisting of α-La precipitates or β-Lg aggregates, was determined. In the next step, the herein achieved separation results are related to other established separation processes, and further possibilities for process optimization and scale-up are discussed. Lastly, recommendations are provided when to apply the α-La precipitation route and on what occasion the β-Lg aggregation route should be preferred.

7.1 Assessment of precipitation and aggregation results

The assessment of the protein particle properties played a central role in this thesis. While the α-La precipitates were found to be soft and irregularly shaped particle agglomerates, the β-Lg aggregates appeared to be rigid, stable, and elongated. In the following, it shall be further elucidated why the α-La precipitates and β-Lg aggregates had these specific properties, and how these characteristics affected the centrifugal separation.

The α-La precipitates
Generally, it is assumed that the underlying intermolecular binding mechanism predetermines the structure and shape of protein particles. Taking a closer look at the α-La precipitates, their connection seemed to be unstable and was shown to rely on attractive forces without any covalent interactions. The precipitate instability was also described by Bonnaillie and Tomasula (2012), reporting on a dramatic drop in particle size, when changing from a static size measurement under a microscope to a dynamic measurement in an AccuSizer. Furthermore, their results are congruent regarding the high amount of bound water (around 80% w w^{-1}) in the α-La precipitate fraction. This indicates that the particles are swollen and just loosely

119

packed. Indeed, α-La is reported to have a high water-sorption capacity, especially in the apo-state, as it was the case in this study (Rantamäki et al., 2000). Actually, the liquid content held in the precipitates was even high enough to allow for entrapment of native β-Lg. Along the heating time, however, a reduction of the enclosed β-Lg was observed (Fig. 4-2). Also, several other authors described the precipitation of α-La as a lasting process of rearrangement within the particles, often referred to as maturation or ageing (Bonnaillie and Tomasula, 2012; Heffernan et al., 2005; Toro-Sierra et al., 2013). It is known that the precipitation of proteins is controlled to a large extent by the charge on the particles: high charge will result in regular aggregation, whereas low charge – such as being close to the IEP of a protein – give rise to more disordered aggregation (Lin et al., 1989). Thus, the low surface charge of apo-α-La at an acidic pH, is supposed to stimulate an irregular agglomeration of the α-La molecules. The underlying binding mechanism under the acidic conditions with sequestered calcium, is a combination of hydrophobic and electrostatic interactions, which are both easily reversible and allow for rearrangement of intermolecular bonds. During maturation, the precipitates are continuously striving for a more stable state through rearrangement and are thus displacing water molecules and native proteins such as β-Lg having low surface hydrophobicity.

Even if the precipitation is predominantly regulated by the balance between electrostatic repulsive and van der Waals attractive forces, the possibility of involvements of other intermolecular forces cannot be excluded. At high α-La precipitate contents, it was suggested that the pseudoplastic flow behavior could result from a steric entanglement of the α-helices of the apo-α-La molecules. Studies demonstrate that such interactions are possible, when the protein is partially unfolded, as it is the case in the apo-form (Dissanayake et al., 2013b; Hu et al., 2013). However, suspensions of such randomly coiled molecules are prone to irreversible damage of the native protein structure induced by shear. This could be one of the root causes why a complete restoration of α-La's native state upon resolubilization was not achieved.

The β-Lg aggregates

In this work, the β-Lg aggregates were analyzed by SEM providing high resolution pictures of the microstructure. It can be clearly seen that the aggregate itself consists of interconnected ellipsoidal or sometimes even spherical primary aggregates as subunits (Fig. 5-3). Schmitt et al. (2007) and Zuniga et al. (2010) reported the primary aggregate structure to be worm-like to ellipsoidal with sizes in the nm-range when heating WPI or pure β-Lg, respectively, at a neutral pH. Other studies suggested that the primary particles are rather globular in shape and that the size of these spheres is insensitive to environmental conditions while heating (Aymard et al., 1996; Gimel et al., 1994). Tanger et al. (2021) suspect the shear stress to

be the decisive factor of the aggregate shape. However, as the shapes of the herein received primary aggregate units is quite heterogeneous, it is not possible to draw a conclusion on the main influencing factors on the final form. Disregarding shape, it is widely accepted that heat-induced aggregation of β-Lg at neutral pH is a two-step process, consisting of the formation of these primary globular aggregates, and the subsequent connection of the globules forming aggregate strands (Ikeda, 2003). Recent studies provide deeper insights in the formation of these primary subunits. It was shown that upon heating, β-Lg is able to build cross-β-sheets, i.e., intermolecular β-sheet assemblies, assembling to fibril-like structures (Carrotta et al., 2001; Krebs et al., 2007). Cross-β-sheets are typically found when proteins with high β-sheet content are heated away from their IEP. In the case of β-Lg, fibril formation used the be mainly reported in the context of fine-stranded gels, produced through extensive heating at low ionic strength and well below its IEP (Lefevre and Subirade, 2000). However, further analyses proved that β-Lg builds amyloid-like β-sheet stretches that arrange in densely packed spherical particles even at neutral pH (Krebs et al., 2009). These spheres are connected to each other and result in the pearl necklace-like microstructure, which was also observed in this thesis. The fibrils formed at neutral pH are reported to be a bit thicker, longer and more flexible than at other pH values (Langton and Hermansson, 1992). The results of Hamada et al. (2009) indicate that fibrils formed by the A, G, H and I β-strands are able to promote amyloid formation, with the A strand having a specifically high amyloidogenicity. This is explained by its natural hydrophobic character and its flexibility. The G, H and I strands are initially hindered by the presence of stabilizing disulfide bridges. However, as soon as the thiol-disulfide exchange reaction starts, they become accessible and promote amyloid formation. The provocative statement of Hamada et al. (2009) that their "results indicate that the presence of disulfide bonds represents a design principle that is […] promoting folding rather than aggregation" still requires further investigation. At any case, dozens of studies proved that intermolecular disulfide bridges are formed above 70 °C (Hoffmann and van Mil, 1997; McSwiney et al., 1994b). Additionally, it is known that the gel hardness is significantly improved, when β-Lg is heated together with α-La, which is transferrable to an improved aggregate stability as well (Matsudomi et al., 1992). In conclusion, the cross-β-sheets are likely the main driver for the fibrils that assemble to densely packed globular shaped primary aggregates. The final strength and stability of the interconnected globules is further enhanced by the intermolecular disulfide bridges, which are known to be one of the strongest bonding types.

Taking a more macroscopic look at the herein produced aggregates, it rather seems to be an agglomerate of numerous of these globule chains, which finally result in streamline formed, elongated particle with a few branches. The elongated overall form of the β-Lg aggregates presumably originates from the tubular heat exchanger at high flow rates. At heating in static set-ups, the aggregates do not

show such an elongation (Ikeda and Morris, 2002; Langton and Hermansson, 1992). It is, however, remarkable that the β-Lg aggregates are extremely large having a $d_{50,3}$ above 100 µm. Other studies reported particle sizes of 20 to 300 nm (Hussain et al., 2012; Nicorescu et al., 2008; Ryan et al., 2012;). In addition to the basic influencing factors, like temperature, heat holding time, protein and $CaCl_2$ concentration, the substantial effect of the presence of shear during aggregation should not be neglected. Erabit et al. (2014) provided evidence that the collision rate between aggregates bigger than 1 µm is significantly increased, when shear stress comparable to a heat exchanger is applied, resulting in larger median aggregate sizes compared to static heating conditions. That said, the choice of a tubular heat exchanger for pilot to industrial scale is actually superior to static heating approaches, which are often the tool of choice at lab-scale process development.

7.2 Evaluation of separation results

Subsequent to the selective precipitation of either α-La or β-Lg, the separability by decanter centrifuges was investigated. In general, the sedimentation and discharge of the α-La-enriched sediment with the counter-current decanter was far more challenging than of the β-Lg aggregates.

The α-La precipitates

For α-La precipitate separation in the decanter, it was required to use the highest available weir plate to avoid sediment drying during the discharge, which was shown to be associated with a tremendous increase in adhesiveness. The overall separation results for the α-La precipitates, however, were poor (3.3.5). The maximum dry matter content that was reached did not exceed 25% (w w^{-1}) under best found conditions. In comparison, with the co-currently working decanter, a dry matter content of more than 30% (w w^{-1}) was reached.

Not only the sediment recovery was enhanced, also the clarification of the supernatant was highly improved. While the counter-current decanter could achieve a maximum clarification of 71%, the co-current model was able to achieve a separation efficiency of 99.7% in the initial separation step. Unfortunately, different determination methods for the quantification of the centrate purity were used, which does not allow a quantitative comparison. Nevertheless, as the centrate from the co-current decanter was shown to be practically free of α-La and was visually fully transparent, it can be concluded that the separation in this decanter type was clearly superior to the counter-current model.

In the PCA (Fig. 4-8), the temperature was shown to be one of the main influencing factors on the separation efficiency. On the one hand, the elevated temperature led to an improved clarification of the centrate by reducing the viscosity of the liquid

phase during settling. On the other hand, the discharged sediment showed a significantly higher dry matter content, which is presumably related to intensified hydrophobic interactions within the α-La precipitates resulting in a higher level of water displacement combined with stronger intermolecular connection. It is assumed that an elevated process temperature could also positively influence the separation of α-La precipitates using a decanter centrifuge instead.

The level of g-force is the driving force for particle settling, however, it also plays a dominant role in the sediment compression, which is crucial for dewatering of the sediment. As demonstrated, the liquid phase enclosed in the sediment does still include soluble proteins. Therefore, the purity of the sediment fraction rises with an increasing sediment dryness. Bonnaillie and Tomasula (2012) used a benchtop centrifuge at 2,000 g acceleration, which was able to settle 99% of the α-La precipitates. However, it was reported that the sediment fraction still contained 42% of other soluble proteins, which is a clear sign of insufficient dewatering. In comparison, only 13% other soluble proteins were measured in the sediment at 6,500 g using the co-current decanter. Using an acceleration of 10,000 g increased the sediment dry matter content even further. However, as the higher g-force level did not improve the centrate clarity any further, it was decided from an economical point of view to keep the lower acceleration for the subsequent experiments. Therefore, it can be expected that the results for purity and yield for the α-La sediment fraction still have capability for improvement at higher g-forces.

Based on the findings and correlations described above, a schematic illustration of the α-La precipitates is shown in Fig. 7-1. Under static conditions and during (gentle) sedimentation, the swollen apo-α-La accumulate because of hydrophobic interactions and incorporate numerous water molecules into the precipitates. During compression, i.e., when settling is completed and the applied centrifugal force leads to compaction of the sediment, the α-La molecules are merged, leading to intermolecular entanglement. Thus, a portion of the water molecules are displaced, allowing for an increase of sediment dry matter. However, a significant amount of water remains in the precipitates, which is attributed to the slightly unfolded conformation that provides a large surface area for hydrational water. Occasionally, breakages and irreversible deformations of molecules may appear through high shear forces, such as the sediment transportation by the scroll.
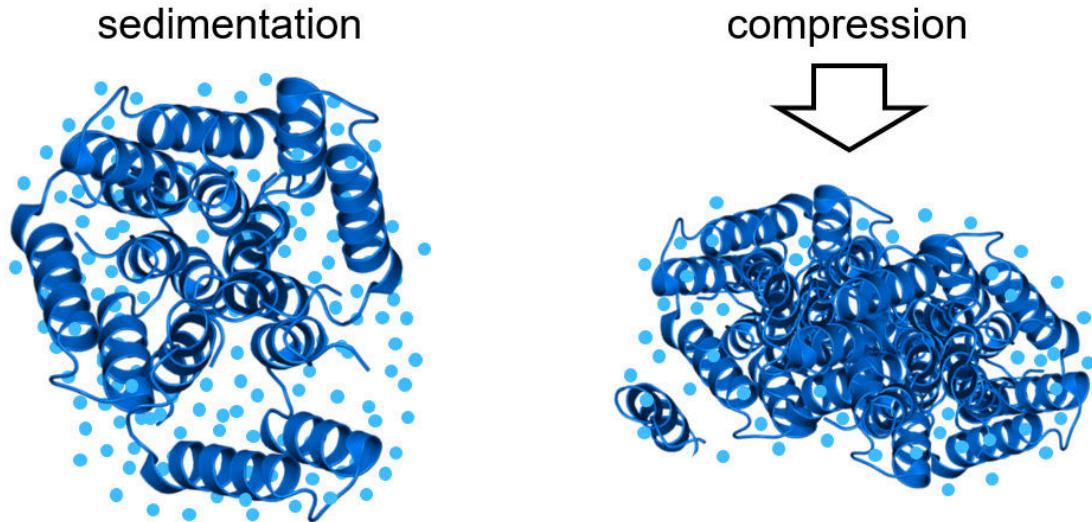
Fig. 7-1 Schematic illustration of α-La precipitates during sedimentation (left) and while compressive forces apply (right). The small light blue spheres represent water molecules.

Nevertheless, the separation process using the co-current decanter showed high stability and reliability, whereas the runs with the counter-current decanter were inconsistent and associated with unexpected discharge irregularities. Consequently, the co-current decanter can be termed the better choice for α-La precipitates separation.

When comparing the separation results of the co-current decanter to results achieved with TFF reported by Toro-Sierra et al. (2013), the centrifugal approach is superior in terms of final purities of the individual protein fractions. The centrifugal separation resulted in a 99.4% α-La and 99.7% β-Lg purity, while TFF yielded purities of 91.3% and 97.2%, respectively. In terms of overall process yield, both approaches lie in a similar range. The co-current decanter recovered 75.2% α-La and 83.5% β-Lg, whereas TFF yielded 60.7% to 80.4% of α-La and 80.2% to 97.3% of β-Lg.

The β-Lg aggregates

The decanter separation of the aggregates was unproblematic, even at low g-forces. This is mainly attributed to the extraordinary size of the vast majority of the produced β-Lg aggregates. However, it was shown that also the β-Lg aggregates are prone to fragmentation due to mechanical stress. Because of the low size of the fragments, the clarification of the centrate in the decanter centrifuge was impaired. Adjusting the pH to pH 4.4 prior to the sedimentation, induced a flocculation of the fines, such as dissociated particle fragments, thus improving the clarification of the centrate. With that strategy a separation efficiency of more than 99% was realized. However, as mentioned before, only denatured β-Lg can be separated, the native and soluble portion will remain in the α-La enriched centrate.

Another positive side effect of the pH adjustment to 4.4 at low inlet dry matter, was a distinct increase in the dry matter content in the discharged sediment compared to a separation performed at pH 7.0. A potential explanation for this is that the intermolecular association, i.e., the flocculation, via ionic mechanisms acts strongly dehydrating and was thus reducing the bound water in the sediment (Kuntz and Kauzmann, 1974). However, the predominant influencing factor on improving the sediment dry matter is the reduction of the inlet dry matter content. The reason is that a lower inlet dry matter content enables a faster completion of the settling, because of minimized hindrance effects. Furthermore, the overall residence time in the centrifuge is prolonged because the sediment build-up is slower compared to suspensions with higher inlet dry matter. With that, the particles spend more time in the compression phase and a higher dewatering through steadily progressing compaction is achieved.

Summarizing the findings in Fig. 7-2, the β-Lg aggregates consist of interconnected primary globules, which build a streamline shaped aggregate. The primary globules are densely packed, likely through cross-β-sheets. This is not only the reason for the high aggregate stability, but also for the generally low water content in the separated aggregates. The highest achieved sediment dry matter content was 60%, which is an indication that a distinct portion of water in the aggregates is not removable by centrifugation. It is assumed that some interstitial water is enclosed inside the particle during aggregation, which cannot be removed by compression. Additionally, some hydrational and vicinal water on the aggregate surface will likely remain.
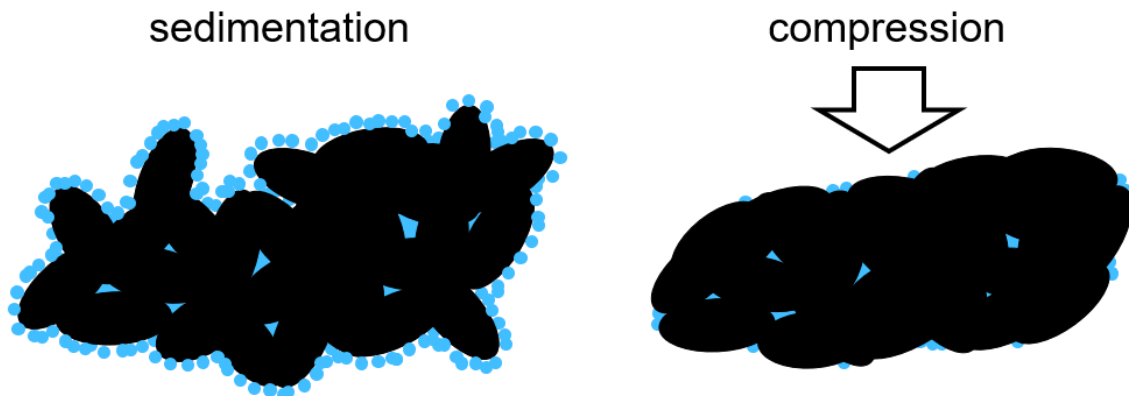
Fig. 7-2 Schematic illustration of β-Lg aggregates during sedimentation (left) and while compressive forces apply (right). The small light blue spheres represent water molecules.

Generally, the heat-induced selective aggregation of β-Lg already predetermines the maximum achievable purity of the α-La enriched supernatant. A longer heating time, or respectively a higher temperature, will allow for a higher degree of β-Lg aggregation, which in turn reduces the amount of remaining soluble β-Lg in the supernatant. However, the increased purity of the α-La fraction will always be on the expense of the final α-La yield. This is because under the applied conditions

125

α-La is not resistant to denaturation, its reaction rate is just slower than the one of β-Lg. Tolkach (2008) performed a similar thermal selective denaturation of β-Lg with subsequent separation of the aggregates by TFF. He used harsher heating conditions and achieved a nearly complete denaturation of β-Lg. This was, however, on the expense of more than 26% of native α-La. In this thesis (chapter 5), only 95% of β-Lg was denatured, along with only 16% α-La loss. Focusing on the aggregate separation, a total of 8 DF steps were used to have a satisfactory yield of native α-La in the permeate (Tolkach, 2008). In comparison to that, it required only one single pass through the decanter to obtain a similar separation effect. Therefore, the decanter centrifuge appears to be clearly superior in terms of economics and efficiency.

7.3 Critical assessment of the overall process design

This chapter focuses on a high-level assessment of the process described in this thesis. The future relevance of this study shall be discussed in the context of another recently published innovative approach. Furthermore, consideration on potential influences on the process are made regarding the choice of starting material. Lastly, recommendations are given when to choose which of the two routes, and an outlook on scalability is provided.

Future relevance of this work

One of the main drivers for this thesis was the idea to establish a process that yields β-Lg-free dairy products. The reason is that β-Lg is considered one of the main initiators of cow's milk allergy (Järvinen et al., 2001; Selo et al., 1999). Commonly, the removal of β-Lg from whey and milk is accomplished by means of separation technology. However, recently an interesting new approach was published, that takes a completely different path to pursue the goal of β-Lg-free milk. That approach is based on the genetic modification of cow's DNA to produce β-Lg-free milk. This can be realized by knockdown of the alleles, which are coding for β-Lg production. Jabed et al. (2012) used microRNA for the knockdown and proved for the first time that β-Lg can be reduced from milk by transgenic methods. Shortly after, Sun et al. (2018) generated a β-Lg bi-allelic knockout cow by zinc-finger nuclease mRNA and produced a completely β-Lg-free milk. According to the authors there were no mutations at off-target sites and the β-Lg allele knockdown was transmitted through the germline. However, as promising as this technology may sound in the first moment, a bunch of drawbacks and concerns persists. The studies reported on increased rates of abortion, as well as health problems and abnormalities of the transgenic calves, which is a major ethical concern. Additionally, mutated farm animals will likely be considered genetically modified organisms

(GMOs) by regulatory authorities in many countries, which would inhibit the potential spread of this technology. Even if the regulatory authorities give permission, the customer's acceptance is highly questionable. Consumers do have concerns regarding biological safety with "lab-derived" foods, as can be seen for example with the low acceptance of cultured meat (Bryant and Barnett, 2020). That said, it appears improbable that β-Lg-free milk of genetically modified cows is an appropriate alternative to established separation methods of traditional milk.

Choice of starting material

Starting from milk, a row of purification steps delivers whey protein in different levels of purities. In this study, WPI was chosen, which is the purest source of whey protein available on the market. Certainly, the high purity protein solutions are the best-case scenario because any interferences with impurities during the aggregation are minimized that way.

Chapter 4.3 compared the separation of α-La precipitates using WPC80 and WPI as starting material side by side. The precipitation progress was observed to be slower in the WPC80, and it appeared that the equilibrium was not necessarily reached after 180 min. The root cause is probably a deceleration of the precipitation rate because of interference with lactose and fat from the WPC. The slightly inferior precipitation results are transferrable to the centrifugation results as well. When applying the same conditions (6% inlet dry matter, 6,500 g centrifugal acceleration, 50 °C suspension temperature), the suspension made of WPI reached a separation efficiency of the centrate of more than 99%, while the WPC80 suspension was at 95%. The discharged sediment dry matter was 30% for WPI compared to 27% for WPC80.

These slightly inferior results through the use of WPC instead of WPI, are likely relevant for the β-Lg aggregation route as well. For example, other authors reported on a significantly lower gel strength, when using WPC80 instead of WPI under similar heat treatment conditions as used in this study (Jiang et al., 2018). In addition, gels with WPI were clearly more elastic than WPC gels, which could provide a higher stability during the centrifugal separation and the discharge process (Lorenzen and Schrader, 2006). The superior gelation and aggregation properties of WPI relative to WPC are mainly due to the low amount of lipids and lactose, as well as the high initial protein nativity, and the higher β-Lg/α-La ratio (Ramos et al., 2012). Therefore, the choice of starting material appears to be critical, as the particle properties are the crucial factors of the centrifugal separation. However, the "upcycling" from WPC to WPI is a common process in dairy industry and can easily achieved by UFDF.

Scale-up possibilities

Last but not least, an important criterion in the development of the herein proposed separation process, was a good scalability to facilitate commercial production. Regarding scale-up of decanter processes, Ambler's Σ-theory is widely used. The Σ-value is an index of centrifuge size, which represents the calculated equivalent area of a settling tank with the same separation capacity. When scaling from a smaller to a larger decanter, the throughput is amended proportionally to the Σ-value. However, the higher throughput, i.e., the higher flow rate that transfers the suspension into the decanter, could negatively affect the integrity of particles, specifically in flocculated suspensions. A shear induced break-up of particles may occur in large scale separations, caused by harsher shear conditions in the feed zone and/or turbulence in the settling zone, which were not present in the small-scale decanter. This requires a previous determination of the shear sensitivity of the particles (Rumpus, 1997). Generally, the Σ-theory allows the comparison of centrifuges which are geometrically similar, with that limiting the scale-up considerations solely to sedimentation performance. However, for a successful separation process in a decanter, also other factors need to be taken into account. One of the most important is the conveying and discharge of the solids once they are sedimented, which is specifically important for compressible sediments, like the α-La precipitates. Therefore, a profound characterization of the sediment's compressibility, flowabilty, and conveyabilty appears to be an obligatory additional task. In this case, CFD and DEM usually show a better predictability, because their algorithm also implies information on particle properties from experimental characterizations.

Concerning the separation of α-La precipitate, a larger co-current decanter might potentially not even be required, when treating a larger volume of suspension. A comparably slower throughput relative to the total treated volume in the centrifuge, would extend the stay of the suspension in a heated tank. As described above, the α-La precipitates mature with longer heating time, which is beneficial for the particle properties. Therefore, a linear increase of throughput appears not to be mandatory with larger processed α-La precipitates volumes.

Comparison of the two process routes

Comparing the two proposed processing routes in this thesis, the precipitation of α-La on the one hand, and the selective aggregation of β-Lg on the other hand, both have their strengths and potential fields of application.

Looking at the β-Lg aggregation route, the majority of β-Lg is aggregated and can be separated with centrifugation. However, depending on the applied heating conditions, a portion of soluble and native β-Lg remains in the α-La-enriched supernatant. Depending on the targeted purity of the α-La fraction, an additional polishing step with, e.g., chromatography, would be required. With that, α-La can be received

in a pure and native form. The β-Lg aggregates, however, are irreversibly denatured with no possibility to bring them back to a native state. Nevertheless, in food industry, there are multiple fields of application, where whey protein microparticulate is used. In case a reduction of the aggregate size is required, e.g., to mimic fat globules sized about 1 μm, a high-pressure homogenization could be used.

Taking a closer look on the α-La precipitation route, it was possible to isolate a native β-Lg fraction with extraordinary high purity. A subsequent concentration and desalting may be required before spray drying. The α-La sediment possessed a high purity after the two washing steps. Unfortunately, it was not possible to reestablish the exact native configuration upon resolubilization. However, it was shown that resolubilized α-La is still able to bind Ca^{2+}, which is a crucial attribute, when it comes to calcium fortification of formulated dairy-based nutritional products, such as infant formula. Barone et al. (2020) showed that α-La isolated by means of selective precipitation can actually present a stronger ability to bind Ca^{2+} than α-La, which derives from other fractionation methods. It was, however, not investigated, if this observation also applies to the selectively precipitated α-La in this study. Another important attribute of α-La enriched infant formula is the delivery of higher Trp content compared to regular formula. The primary structure, i.e., the sequence of amino acids in α-La, remains untouched with the proposed processing process. This means that the α-La yielded with selective precipitation, does fulfil the targeted nutritive purpose. Solely, in cases where the exact native configuration is required, it is advisable to use α-La that is isolated via a different route.

8 Summary & Zusammenfassung

8.1 Summary

The global demand for whey protein and especially for their individual pure fractions is constantly rising. Beside other reasons, the main drivers are an increasing health consciousness accompanied with higher consumption of performance and sports nutrition, as well as the exploration of new application fields, such as nutraceuticals, and medical usages. Over the last decades, several different separation processes have been proposed aiming at an efficient isolation of the individual whey protein fractions. However, all of them are showing distinct deficiencies, either in terms of the final product purity, the overall yield or production costs, which is often related to a missing scalability of the process.

An innovative process for separation of the major whey proteins, α-La and β-Lg, was developed, realizing good economics, as well as optimized yield and purities. The process basically consists of two production steps. The first one is a selective thermal aggregation of one of the major whey protein fractions, while the counterpart remains native and soluble in the liquid phase. The second step is the separation of the aggregated fraction from the liquid phase using a continuously working decanter centrifuge. For this separation process, two routes were explored. On the one hand the selective precipitation of α-La, on the other hand the selective thermal aggregation of β-Lg, both with subsequent separation by continuous centrifugation, respectively.

For the precipitation of α-La, a calcium sequestrant at pH 3.4 was added to enable its transition into the apo-form, which is characterized by a distinctly lower unfolding temperature compared to its holo-state. A heat treatment at 50 °C was sufficient to induce a precipitation of the α-La molecules via hydrophobic interactions. The α-La precipitates were characterized as irregularly shaped, loosely bound particle agglomerates with sizes around 12 µm. In settling experiments, it was demonstrated that α-La precipitates can benefit from sedimentation enhancing effects and exceed calculated Stokes velocity. Unfortunately, this phenomenon could not be reproduced during centrifugation, because of the higher turbulences that affected the integrity of the precipitates. The separation in a classical counter-current decanter centrifuge worked unstably presenting some complications during sediment discharge. The change to a co-current decanter model improved the separation results and the process stability significantly. Further improvement was achieved by increasing the process temperature to 50 °C. The clarification of the centrate was enhanced by reducing the viscosity of the liquid phase, and the discharged sediment showed a significantly higher dry matter content, which is presumably related to intensified hydrophobic interactions within the α-La precipitates. Sediment dry matter contents of more than 30% were achieved, while the centrate contained

99.7% pure and native β-Lg. As the α-La enriched sediment still contained residues of β-Lg, two steps of reslurry washing were performed. This resulted in a final α-La fraction with 99.4% purity.

Following the centrifugal separation, the possibility to resolubilize α-La was investigated. Best folding results were found using pH 8.0 and a 3-fold stoichiometric amount of calcium per α-La molecule. The results showed that the mechanism of precipitation induced by gentle thermal treatment under acidic condition with subsequent mechanical separation is reversible to a certain extent. However, the exact native conformation of α-La could not be re-established.

The selective aggregation of β-Lg was performed at neutral pH with supplemented calcium in order to stabilize α-La during the heat treatment at 92 °C. This procedure led to a denaturation of 94% β-Lg, accompanied by a loss of 12% α-La. The obtained β-Lg aggregates were rigid, had an elongated shape with few branches, and had a median size of 109 µm. SEM revealed that they consist out of multiple interconnected primary aggregate, which are roundly shaped with sizes around 1 µm.

The decanter separation of the β-Lg aggregates was unproblematic at all times and even at low g-forces. The β-Lg aggregates were highly resistant to compressive forces, which is attributed to the stabilization via disulfide bonds, and were discharged as a free-flowing powder with sediment dry matters up to 60%. However, the β-Lg aggregates were prone to fragmentation due to mechanical stress, which impaired the clarification of the centrate in the decanter centrifuge. Adjusting to pH 4.4 prior to the centrifugation, reduced the electrostatic repulsion, which led to a flocculation of these fragments by van-der-Waals forces. With this strategy a separation efficiency of more than 99% was realized.

Both routes were proven to meet the requirement of being an industrial suitable process with remarkable purities and yields, and are thus, superior to most of the formerly proposed separation processes. The two established routes have their individual strengths and potential fields of application, respectively. The α-La precipitation route allowed an isolation of a native β-Lg fraction with extraordinary purity. Even if the α-La fraction was not received in native conformation, the resolubilized α-La can still be used for calcium fortification and Try enrichment of formulated dairy-based nutritional products. Looking at the β-Lg aggregation route, depending on the applied heating conditions, a portion of soluble and native β-Lg can remain in the α-La-enriched supernatant. Depending on the targeted purity of the α-La fraction, an additional polishing step with, e.g., chromatography, would be required. With that, α-La can be received in a pure and native form. The β-Lg aggregates are a highly valuable source for food applications. Upon further break down in the primary aggregates, e.g., by homogenisation, they would comprise the ideal size to use them as fat replacers.

8.2   Zusammenfassung

Die weltweite Nachfrage an Molkenproteinen und insbesondere an deren reinen Fraktionen steigt stetig an. Haupttreiber sind neben anderen Gründen ein steigendes Gesundheitsbewusstsein bei gleichzeitigem höherem Konsum von Leistungs- und Sportnahrung sowie die Erforschung neuer Anwendungsfelder wie Nutraceuticals und medizinischer Anwendungen. In den letzten Jahrzehnten wurden verschiedene Trennverfahren vorgeschlagen, die auf eine effiziente Isolierung der einzelnen Molkenproteinfraktionen abzielen. Sie alle weisen jedoch deutliche Defizite auf, entweder in Bezug auf die finale Produktreinheit, die Gesamtausbeute oder die Produktionskosten, die oft mit einer fehlenden Skalierbarkeit des Prozesses zusammenhängen.

Ein innovatives Verfahren zur Trennung der Hauptmolkenproteine α-La und β-Lg wurde entwickelt, das eine gute Wirtschaftlichkeit sowie eine optimierte Ausbeute und Reinheit ermöglicht. Der Prozess besteht im Wesentlichen aus zwei Produktionsschritten. Der Erste ist eine selektive thermische Aggregation einer der Hauptmolkenproteinfraktionen, während die Andere in der flüssigen Phase nativ und löslich bleibt. Der zweite Schritt ist die Trennung der aggregierten Fraktion von der flüssigen Phase mittels einer kontinuierlich arbeitenden Dekanterzentrifuge. Für diesen Trennprozess wurden zwei Prozesswege untersucht. Zum einen die selektive Fällung von α-La, zum anderen die selektive thermische Aggregation von β-Lg, beide mit anschließender Separation durch kontinuierliche Zentrifugation.

Für die Präzipitation von α-La wurde ein Kalziumkomplexbildner bei pH 3,4 zugegeben, um den Übergang in die Apo-Form zu ermöglichen, die sich durch eine deutlich niedrigere Auffaltungstemperatur im Vergleich zum Holo-Zustand auszeichnet. Eine Wärmebehandlung bei 50 °C reichte aus, um eine Fällung der α-La-Moleküle durch hydrophobe Wechselwirkungen zu induzieren. Die α-La-Präzipitate wurden als unregelmäßig geformte, lose miteinander verbundene Agglomerate von Partikeln mit Größen um 12 μm charakterisiert.

In Absetzversuchen wurde gezeigt, dass α-La-Präzipitate von sedimentationsverstärkenden Effekten profitieren und dadurch die berechnete Stokes-Geschwindigkeit überschreiten können. Leider konnte dieses Phänomen während der Zentrifugation nicht reproduziert werden, da die höheren Turbulenzen die Integrität der Präzipitate beeinträchtigten. Der Trennvorgang in einer klassischen Gegenstrom-Dekanterzentrifuge lief instabil mit einigen Schwierigkeiten beim Sedimentaustrag. Der Wechsel zu einem Gleichstrom-Dekanter-Modell verbesserte die Trennergebnisse und die Prozessstabilität deutlich. Eine weitere Verbesserung wurde durch die Erhöhung der Prozesstemperatur auf 50 °C erzielt. Die Klärung des Zentrats wurde durch die Verringerung der Viskosität der flüssigen Phase erhöht, und das ausgetragene Sediment zeigte einen signifikant höheren Trockenmassegehalt, was vermutlich mit verstärkten hydrophoben Wechselwirkungen innerhalb der α-La-Präzipitate zusammenhängt. Es wurden Sedimenttrockenmassen von mehr

als 30% erreicht, während das Zentrat 99,7% reines und natives β-Lg enthielt. Da das mit α-La angereicherte Sediment immer noch Rückstände von β-Lg aufwies, wurden zwei Waschschritte durchgeführt. Dies führte letztendlich zu einer α-La-Fraktion mit 99,4% Reinheit.

Nach der zentrifugalen Trennung wurde die Möglichkeit der Resolubilisierung von α-La untersucht. Die besten Rückfaltungsergebnisse wurden bei pH 8,0 und einer 3-fachen stöchiometrischen Menge an Kalzium pro α-La-Molekül gefunden. Die Ergebnisse zeigten, dass der durch schonende thermische Behandlung unter sauren Bedingungen induzierte Fällungsmechanismus mit anschließender mechanischer Trennung bis zu einem gewissen Grad reversibel ist. Die exakte native Konformation von α-La konnte jedoch nicht wiederhergestellt werden.

Die selektive Aggregation von β-Lg wurde bei neutralem pH-Wert mit zugesetztem Calcium durchgeführt, um α-La während der Wärmebehandlung bei 92 °C zu stabilisieren. Dieser Prozess führte zu einer Denaturierung von 94% des β-Lg, begleitet von einem Verlust von 12% des α-La. Die erhaltenen β-Lg-Aggregate waren starr, hatten eine längliche Form mit einigen Verzweigungen und eine mittlere Größe von 109 µm. Eine Analyse mittels SEM ergab, dass sie aus mehreren miteinander verbundenen Primäraggregaten bestehen, die rundlich geformt sind und Größen um 1 µm haben.

Die Trennung der β-Lg-Aggregate mit dem Dekanter war zu jeder Zeit und auch bei niedrigen g-Kräften unproblematisch. Die β-Lg- Aggregate waren sehr beständig gegen Kompressionskräfte, was auf die Stabilisierung über Disulfidbindungen zurückzuführen ist, und wurden als rieselfähiges Pulver mit Sedimenttrockenmassen bis zu 60% ausgetragen. Die β-Lg-Aggregate waren aufgrund mechanischer Beanspruchung anfällig für Fragmentierung, was die Klärung des Zentrats in der Dekanterzentrifuge beeinträchtigte. Die Einstellung auf pH 4,4 vor der Zentrifugation reduzierte die elektrostatische Abstoßung, was zu einer Flockung dieser Fragmente durch Van-der-Waals-Kräfte führte. Mit dieser Strategie wurde eine Separationseffizienz von mehr als 99% realisiert.

Beide Prozesswege erfüllen nachweislich die Anforderung, ein industrietaugliches Verfahren mit bemerkenswerten Reinheiten und Ausbeuten zu sein, und sind daher den meisten der zuvor vorgeschlagenen Trennverfahren überlegen. Die beiden etablierten Prozesswege haben ihre individuellen Stärken bzw. potenziellen Anwendungsfelder. Die α-La-Präzipitation ermöglichte eine Isolierung einer nativen β-Lg-Fraktion mit außergewöhnlicher Reinheit. Auch wenn die α-La-Fraktion nicht in nativer Konformation erhalten wurde, kann das resolubilisierte α-La immer noch zur Anreicherung von gebundenem Calcium und als Trp-Lieferant in formulierten Milchprodukten verwendet werden. Betrachtet man die β-Lg-Aggregationsroute, so kann je nach den angewandten Erhitzungsbedingungen ein Teil des löslichen und nativen β-Lg im α-La-angereicherten Überstand verbleiben. Abhängig von der angestrebten Reinheit der α-La-Fraktion wäre ein zusätzlicher Reinigungsschritt

mit z.B. Chromatographie erforderlich. Damit kann α-La in reiner und nativer Form gewonnen werden. Die β-Lg-Aggregate sind eine sehr wertvolle Ressource für Lebensmittelanwendungen. Bei weiterer Zerkleinerung in die Primäraggregate, z.B. durch Homogenisierung, würden sie die ideale Größe haben, um sie als Fettersatz zu verwenden.

9 List of publications and presentations

The following articles and presentations were published with major contribution from this work. They are listed in chronological order.

9.1 Peer reviewed publications

Leeb, E., **Haller, N.**, & Kulozik, U. (2018). Effect of pH on the reaction mechanism of thermal denaturation and aggregation of bovine β-lactoglobulin. *International Dairy Journal*, *78*, 103-111.

Haller, N., & Kulozik, U. (2019). Separation of whey protein aggregates by means of continuous centrifugation. *Food and Bioprocess Technology*, *12*(6), 1052-1067.

Haller, N., & Kulozik, U. (2020). Continuous centrifugal separation of selectively precipitated α-Lactalbumin. *International Dairy Journal*, *101*, 104566.

Haller, N., Greßlinger, A. S., & Kulozik, U. (2021). Separation of aggregated β-lactoglobulin with optimised yield in a decanter centrifuge. *International Dairy Journal*, *114*, 104918.

Haller, N., Maier, I., & Kulozik, U. (2021). Molecular Analytical Assessment of Thermally Precipitated α-Lactalbumin after Resolubilization. *Foods*, *10*(9), 2231.

Rafe, A., Glikmab, D., Rey, N. G., **Haller, N.**, Kulozik, U., & Braunschweig, B. (2022). Structure-property relations of β-lactoglobulin/κ-carrageenan mixtures in aqueous foam. *Colloids and Surfaces A: Physicochemical and Engineering Aspects*, 128267.

9.2 Non reviewed publications

Haller, N.; Kulozik, U. (2015): Selektive Abreicherung von β-Lactoglobulin aus Molkenproteinisolat: Einfluss der Erhitzungstemperatur auf die strukturellen Eigenschaften der gebildeten Aggregate. Jahresbericht zur Milchwissenschaftlichen Forschung am Zentralinstitut für Ernährungs- und Lebensmittelforschung (ZIEL). ISBN 978-3-939182-63-4. 105-107

Haller, N.; Kulozik, U. (2016): Separation von β-Lactoglobulin-Aggregaten in einem Labor-Dekanter. Jahresbericht zur Milchwissenschaftlichen Forschung am Zentralinstitut für Ernährungs- und Lebensmittelforschung (ZIEL). ISBN 978-3-939182-75-7. 81-83

Haller, N.; Kulozik, U. (2017): Kontinuierliche zentrifugale Separation von aggregiertem α-Lactalbumin. Jahresbericht zur Milchwissenschaftlichen Forschung am Zentralinstitut für Ernährungs- und Lebensmittelforschung (ZIEL). ISBN 978-3-939182-89-4. 83-84

9.3 Oral presentations

Haller, N. & Kulozik, U.: An innovative process for selective removal of β-lactoglobulin from whey. 12th International Congress on Engineering and Food (ICEF12), 14.-18.06.2015, Quebéc City, Canada

Haller, N. & Kulozik, U.: Whey protein fractionation for infant food manufacture by means of selective thermal aggregation and enzymatic hydrolysis. Seminar on Emerging Dairy Technologies, 16.-18.09.2015, Freising, Germany

Haller, N. & Kulozik, U.: Vorstellung eines innovativen Verfahrens zur selektiven Entfernung von β-Lactoglobulin aus Molkenproteinisolat. Weihenstephaner Milchwirtschaftliche Herbsttagung 2015, 08.-09.10.2015, Freising, Germany

Haller, N. & Kulozik, U.: Innovative fractionation process for whey proteins aiming for preservation of maximal nativity of all components. 18th World Congress on Food Science and Technology (IUFoST), 21.-25.08.2016, Dublin, Ireland

Haller, N. & Kulozik, U.: Selective thermal aggregation of the major whey protein fractions – Comparison of heating strategies and subsequent separation techniques. Seminar on Emerging Dairy Technologies, 14.-16.09.2016, Freising, Germany

Haller, N. & Kulozik, U.: High throughput chromatographic applications for the isolation of minor components in whey. Seminar on Emerging Dairy Technologies, 14.-16.09.2016, Freising, Germany

Haller, N., Kulozik, U.: Kann man aus Kuhmilch Muttermilch machen? Prozesstechnische Methoden zur Annäherung an den goldenen Standard der Säuglingsnahrung, Studienfakultätstag der Studienfakultät Brau- und Lebensmitteltechnologie, 30.06.2017, Freising, Germany

Haller, N., Kulozik, U.: Innovative process platform for fractionation of whey proteins by means of continuous centrifugal separation, 8th International Whey Conference, 17.-21.09.2017, Chicago, Illinois, USA

Haller, N., Kulozik, U.: How to draw maximal benefit from the single whey proteins? On the fractionation and further treatment for creation of functional nutrition, 7th International Symposium on "Delivery of Functionality in Complex Food Systems", 05.-08.11.2017, Auckland, New Zealand

9.4 Poster presentations

Haller, N. & Kulozik, U.: Innovative fractionation process for whey proteins by means of reversible thermal aggregation and centrifugal separation. 1st International Conference on Innovations in Food Science & Technology (IFST 2017) 10.-12.05.2017, Erding, Germany

10 References

Abbring, S., Hols, G., Garssen, J., van Esch, B. C., 2019a. Raw cow's milk consumption and allergic diseases–the potential role of bioactive whey proteins. *European Journal of Pharmacology* 843, 55–65.

Abbring, S., Kusche, D., Roos, T. C., Diks, M. A. P., Hols, G., Garssen, J., Baars, T., van Esch, B. C., 2019b. Milk processing increases the allergenicity of cow's milk—Preclinical evidence supported by a human proof-of-concept provocation pilot. *Clinical and experimental allergy: Journal of the British Society for Allergy and Clinical Immunology* 49, 1013–1025.

Abd El-Salam, M. H., El-Shibiny, S., Salem, A., 2009. Factors affecting the functional properties of whey protein products: A review. *Food Reviews International* 25, 251–270.

Adisaputro, I. A., Wu, Y.-J., Etzel, M. R., 1996. Strong cation and anion exchange membranes and beads for protein isolation from whey. *Journal of liquid chromatography & related technologies* 19, 1437–1450.

Alexandrescu, A. T., Evans, P. A., Pitkeathly, M., Baum, J., Dobson, C. M., 1993. Structure and dynamics of the acid-denatured molten globule state of alpha-lactalbumin: a two-dimensional NMR study. *Biochemistry* 32, 1707–1718.

Alizadehfard, M. R., Wiley, D. E., 1996. Non-Newtonian behaviour of whey protein solutions. *Journal of Dairy Research* 63, 315–320.

Almécija, M. C., Ibáñez, R., Guadix, A., Guadix, E. M., 2007. Effect of pH on the fractionation of whey proteins with a ceramic ultrafiltration membrane. *Journal of Membrane Science* 288, 28–35.

Alomirah, H. F., Alli, I., 2004. Separation and characterization of β-lactoglobulin and α-lactalbumin from whey and whey protein preparations. *International Dairy Journal* 14, 411–419.

Altieri, G., Di Renzo, G. C., Genovese, F., 2013. Horizontal centrifuge with screw conveyor (decanter): optimization of oil/water levels and differential speed during olive oil extraction. *Journal of Food Engineering* 119, 561–572.

Ambler, C. M., 1959. The theory of scaling up laboratory data for the sedimentation type centrifuge. *Journal of Biochemical and Microbiological Technology and Engineering* 1, 185–205.

Anema, S. G., 2000. Effect of milk concentration on the irreversible thermal denaturation and disulfide aggregation of β-lactoglobulin. *Journal of Agricultural and Food Chemistry* 48, 4168–4175.

Angle, C. W., Clarke, B., Dabros, T., 2017. Dewatering kinetics and viscoelastic properties of kaolin as tailings model under compressive pressures. *Chemical Engineering Research and Design* 118, 286–293.

Aparicio, S., Garau, C., Esteban, S., Nicolau, M. C., Rivero, M., Rial, R. V., 2007. Chrononutrition: use of dissociated day/night infant milk formulas to improve the development of the wake-sleep rhythms. Effects of tryptophan. *Nutritional neuroscience* 10, 137–143.

Arai, M., Ito, K., Inobe, T., Nakao, M., Maki, K., Kamagata, K., Kihara, H., Amemiya, Y., Kuwajima, K., 2002. Fast compaction of α-lactalbumin during folding studied by stopped-flow X-ray scattering. *Journal of Molecular Biology* 321, 121–132.

Aramini, J. M., Hiraoki, T., Grace, M. R., Swaddle, T. W., Chiancone, E., 1996. NMR and stopped-flow studies of metal ion binding to α-lactalbumins. *Biochimica et Biophysica Acta (BBA)-Protein Structure and Molecular Enzymology* 1293, 72–82.

Arslan Kulcan, A., Karhan, M., 2021. Effect of process parameters on stevioside and rebaudioside A content of stevia extract obtained by decanter centrifuge. *Journal of Food Processing and Preservation* 45, e15168.

Arunkumar, A., Etzel, M. R., 2013. Fractionation of α-lactalbumin from β-lactoglobulin using positively charged tangential flow ultrafiltration membranes. *ECFS 2006 2nd European Conference on Filtration and Separation* 105, 121–128.

Aymard, P., Gimel, J.-C., Nicolai, T., Durand, D., 1996. Experimental evidence for a two-step process in the aggregation of β-lactoglobulin at pH 7. *Journal de Chimie Physique et de Physico-Chimie Biologique* 93, 987–997.

Bargieł, M., Tory, E. M., 2013. Extension of the Richardson–Zaki equation to suspensions of multisized irregular particles. *International Journal of Mineral Processing* 120, 22–25.

Barnett, L. B., Bull, H. B., 1960. Electrophoresis of ribonuclease and of β-lactoglobulin: Isoelectric points of proteins. *Archives of Biochemistry and Biophysics* 89, 167–172.

Barone, G., Moloney, C., O'Regan, J., Kelly, A. L., O'Mahony, J. A., 2020. Chemical composition, protein profile and physicochemical properties of whey protein concentrate ingredients enriched in α-lactalbumin. *Journal of Food Composition and Analysis* 92, 103546.

Barone, G., O'Regan, J., Kelly, A. L., O'Mahony, J. A., 2021. Calcium fortification of a model infant milk formula system using soluble and insoluble calcium salts. *International Dairy Journal* 117, 104951.

Barukčić, I., Božanić, R., Kulozik, U., 2015. Influence of process temperature and microfiltration pre-treatment on flux and fouling intensity during cross-flow ultrafiltration of sweet whey using ceramic membranes. *International Dairy Journal* 51, 1–7.

Bell, D. J., Dunnill, P., 1982. The influence of precipitation reactor configuration on the centrifugal recovery of isoelectric soya protein precipitate. *Biotechnology and Bioengineering* 24, 2319–2336.

Berliner, L. J., Koga, K., Nishikawa, H., Scheffler, J. E., 1987. High-resolution proton and laser photochemically induced dynamic nuclear polarization NMR studies of cation binding to bovine alpha-lactalbumin. *Biochemistry* 26, 5769–5774.

Bernal, V., Jelen, P., 1984. Effect of calcium binding on thermal denaturation of bovine α-lactalbumin. *Journal of Dairy Science* 67, 2452–2454.

Bertrand-Harb, C., Baday, A., Dalgalarrondo, M., Chobert, J.-M., Haertlé, T., 2002. Thermal modifications of structure and codenaturation of α-lactalbumin and β-lactoglobulin induce changes of solubility and susceptibility to proteases. *Food/Nahrung* 46, 283–289.

Beveridge, T., Harrison, J. E., 1995. Juice extraction with the decanter centrifuge: sweet and sour cherries, peaches and apricots. *Food Research International* 28, 173–177.

Beyer, H.-J., 1990. Zum Einfluss der Proteinkonzentration auf das Denaturierungsverhalten der Molkenproteine die damit verbundenen rheologischen Veränderungen, Technische Universität München, München, Germany.

Bhattacharjee, S., Bhattacharjee, C., Datta, S., 2006a. Studies on the fractionation of β-lactoglobulin from casein whey using ultrafiltration and ion-exchange membrane chromatography. *Journal of Membrane Science* 275, 141–150.

Bhattacharjee, S., Ghosh, S., Datta, S., Bhattacharjee, C., 2006b. Studies on ultrafiltration of casein whey using a rotating disk module: effects of pH and membrane disk rotation. *Desalination* 195, 95–108.

Bhatty, J. I., 1986. Clusters formation during sedimentation of dilute suspensions. *Separation Science and Technology* 21, 953–967.

Bickert, G., Stahl, W., 1997. Settling behavior characterization of submicron particles in dilute and concentrated suspensions. *Particle & particle systems characterization* 14, 142–147.

Bonnaillie, L. M., Tomasula, P. M., 2012. Kinetics, aggregation behavior and optimization of the fractionation of whey protein isolate with hydrochloric acid. *Food and bioproducts processing* 90, 737–747.

Booij, L., Merens, W., Markus, C. R., van der Does, A. W., 2006. Diet rich in α-lactalbumin improves memory in unmedicated recovered depressed patients and matched controls. *Journal of Psychopharmacology* 20, 526–535.

Boscaini, S., Cabrera-Rubio, R., Speakman, J. R., Cotter, P. D., Cryan, J. F., Nilaweera, K. N., 2019. Dietary α-lactalbumin alters energy balance, gut microbiota composition and intestinal nutrient transporter expression in high-fat diet-fed mice. *The British journal of nutrition* 121, 1097–1107.

Bouhallab, S., Henry, G., Caussin, F., Croguennec, T., Fauquant, J., Mollé, D., 2004. Copper-catalyzed formation of disulfide-linked dimer of bovine β-lactoglobulin. *Le Lait* 84, 517–525.

Boye, J. I., Alli, I., 2000. Thermal denaturation of mixtures of α-lactalbumin and β-lactoglobulin: a differential scanning calorimetric study. *Food Research International* 33, 673–682.

Boye, J. I., Alli, I., Ismail, A. A., 1997. Use of differential scanning calorimetry and infrared spectroscopy in the study of thermal and structural stability of α-lactalbumin. *Journal of Agricultural and Food Chemistry* 45, 1116–1125.

Boye, J. I., Ma, C. Y., Ismail, A., 2004. Thermal stability of β-lactoglobulins A and B: effect of SDS, urea, cysteine and N-ethylmaleimide. *Journal of Dairy Research* 71, 207–215.

Bramaud, C., Aimar, P., Daufin, G., 1995. Thermal isoelectric precipitation of α-lactalbumin from a whey protein concentrate: Influence of protein–calcium complexation. *Biotechnology and Bioengineering* 47, 121–130.

Bramaud, C., Aimar, P., Daufin, G., 1997a. Optimisation of a whey protein fractionation process based on the selective precipitation of α-lactalbumin. *Le Lait* 77, 411–423.

Bramaud, C., Aimar, P., Daufin, G., 1997b. Whey protein fractionation: Isoelectric precipitation of α-lactalbumin under gentle heat treatment. *Biotechnology and Bioengineering* 56, 391–397.

Brew, K., Hill, R. L., 1975. Lactose biosynthesis. *Reviews of Physiology, Biochemistry and Pharmacology, Volume 72*, 105–158.

Brück, W. M., Kelleher, S. L., Gibson, G. R., Nielsen, K. E., Chatterton, D. E. W., Lönnerdal, B., 2003. rRNA probes used to quantify the effects of glycomacropeptide and

α-lactalbumin supplementation on the predominant groups of intestinal bacteria of infant rhesus monkeys challenged with enteropathogenic Escherichia coli. *Journal of pediatric gastroenterology and nutrition* 37, 273–280.

Bryant, C., Barnett, J., 2020. Consumer acceptance of cultured meat: an updated review (2018–2020). *Applied Sciences* 10, 5201.

Bryant, C. M., McClements, D. J., 1998. Molecular basis of protein functionality with special consideration of cold-set gels derived from heat-denatured whey. *Trends in Food Science & Technology* 9, 143–151.

Buggy, A. K., McManus, J. J., Brodkorb, A., Carthy, N. M., Fenelon, M. A., 2017. Stabilising effect of α-lactalbumin on concentrated infant milk formula emulsions heat treated pre- or post-homogenisation. *Dairy Science & Technology* 96, 845–859.

Burova, T. V., Choiset, Y., Tran, V., Haertlé, T., 1998. Role of free Cys121 in stabilization of bovine beta-lactoglobulin B. *Protein engineering* 11, 1065–1073.

Buscall, R., White, L. R., 1987. The consolidation of concentrated suspensions. Part 1.—The theory of sedimentation. *Journal of the Chemical Society, Faraday Transactions 1: Physical Chemistry in Condensed Phases* 83, 873–891.

Bushmarina, N. A., Blanchet, C. E., Vernier, G., Forge, V., 2006. Cofactor effects on the protein folding reaction: Acceleration of α-lactalbumin refolding by metal ions. *Protein Science* 15, 659–671.

Byrne, E. P., Fitzpatrick, J. J., 2002. Investigation of how agitation during precipitation, and subsequent processing affects the particle size distribution and separation of α-lactalbumin enriched whey protein precipitates. *Biochemical Engineering Journal* 10, 17–25.

Byrne, E. P., Fitzpatrick, J. J., Pampel, L. W., Titchener-Hooker, N. J., 2002. Influence of shear on particle size and fractal dimension of whey protein precipitates: Implications for scale-up and centrifugal clarification efficiency. *Chemical Engineering Science* 57, 3767–3779.

Cacossa, K. F., Vaccari, D. A., 1994. Calibration of a compressive gravity thickening model from a single batch settling curve. *Water Science and Technology* 30, 107.

Calvo, M. M., Leaver, J., Banks, J. M., 1993. Influence of other whey proteins on the heat-induced aggregation of α-lactalbumin. *International Dairy Journal* 3, 719–727.

Carbonaro, M., Nucara, A., 2010. Secondary structure of food proteins by Fourier transform spectroscopy in the mid-infrared region. *Amino acids* 38, 679–690.

Carrère, H., Bascoul, A., Floquet, P., Am Wilhelm, Delmas, H., 1996. Whey proteins extraction by fluidized ion exchange chromatography: simplified modeling and economical optimization. *The Chemical Engineering Journal and The Biochemical Engineering Journal* 64, 307–317.

Carrotta, R., Bauer, R., Waninge, R., Rischel, C., 2001. Conformational characterization of oligomeric intermediates and aggregates in β-lactoglobulin heat aggregation. *Protein Science* 10, 1312–1318.

Casal, E., Montilla, A., Moreno, F. J., Olano, A., Corzo, N., 2006. Use of chitosan for selective removal of β-lactoglobulin from whey. *Journal of Dairy Science* 89, 1384–1389.

Chandra, N., Brew, K., Acharya, K. R., 1998. Structural evidence for the presence of a secondary calcium binding site in human alpha-lactalbumin. *Biochemistry* 37, 4767–4772.

Chang, J.-Y., 2002. The folding pathway of α-lactalbumin elucidated by the technique of disulfide scrambling: Isolation of on-pathway and off-pathway intermediates. *The Journal of biological chemistry* 277, 120–126.

Chang, J.-Y., Li, L., 2002. Pathway of oxidative folding of alpha-lactalbumin: a model for illustrating the diversity of disulfide folding pathways. *Biochemistry* 41, 8405–8413.

Channell, G. M., Zukoski, C. F., 1997. Shear and compressive rheology of aggregated alumina suspensions. *AIChE Journal* 43, 1700–1708.

Chatterton, D. E. W., Smithers, G., Roupas, P., Brodkorb, A., 2006. Bioactivity of β-lactoglobulin and α-lactalbumin—Technological implications for processing. *Technological and Health Aspects of Bioactive Components of Milk Technological and Health Aspects of Bioactive Components of Milk* 16, 1229–1240.

Cheang, B., Zydney, A. L., 2003. Separation of α-lactalbumin and β-lactoglobulin using membrane ultrafiltration. *Biotechnology and Bioengineering* 83, 201–209.

Chedad, A., van Dael, H., 2004. Kinetics of folding and unfolding of goat α-lactalbumin. *Proteins: Structure, Function, and Bioinformatics* 57, 345–356.

Cheison, S. C., Leeb, E., Toro-Sierra, J., Kulozik, U., 2011. Influence of hydrolysis temperature and pH on the selective hydrolysis of whey proteins by trypsin and potential recovery of native alpha-lactalbumin. *International Dairy Journal* 21, 166–171.

Chen, L., Guo, C., Guan, Y., Liu, H., 2007. Isolation of lactoferrin from acid whey by magnetic affinity separation. *Separation and Purification Technology* 56, 168–174.

Christensen, M. L., Keiding, K., Nielsen, P. H., Jørgensen, M. K., 2015. Dewatering in biological wastewater treatment: a review. *Water research* 82, 14–24.

Coe, H. S., 1916. Methods for determining the capacities of slime settling tanks. *Transactions American Institute of Mining Engineerring* 55.

Colby, C. B., O'Neill, B. K., Vaughan, F., Middelberg, A. P. J., 1996. Simulation of Compression Effects during Scaleup of a Commercial Ion-Exchange Process. *Biotechnology progress* 12, 662–681.

Creamer, L. K., Parry, D. A., Malcolm, G. N., 1983. Secondary structure of bovine beta-lactoglobulin B. *Archives of Biochemistry and Biophysics* 227, 98–105.

Croguennec, T., Bouhallab, S., Mollé, D., O'Kennedy, B. T., Mehra, R., 2003. Stable monomeric intermediate with exposed Cys-119 is formed during heat denaturation of β-lactoglobulin. *Biochemical and Biophysical Research Communications* 301, 465–471.

Curvers, D., Saveyn, H., Scales, P. J., van der Meeren, P., 2009. A centrifugation method for the assessment of low pressure compressibility of particulate suspensions. *Chemical Engineering Journal* 148, 405–413.

Dalgleish, D. G., Senaratne, V., Francois, S., 1997. Interactions between α-lactalbumin and β-lactoglobulin in the early stages of heat denaturation. *Journal of Agricultural and Food Chemistry* 45, 3459–3464.

Dannenberg, F., 1986. Zur Reaktionskinetik der Molkendenaturierung und deren technologischer Bedeutung, Technisches Universität München, München, Germany.

Dannenberg, F., Kessler, H.-G., 1988. Reaction Kinetics of the Denaturation of Whey Proteins in Milk. *Journal of Food Science* 53, 258–263.

Das, K. P., Kinsella, J. E., 1989. pH dependent emulsifying properties of b-lactoglobulin. *Journal of Dispersion Science and Technology* 10, 77–102.

Daw, E., Hartel, R. W., 2015. Fat destabilization and melt-down of ice creams with increased protein content. *International Dairy Journal* 43, 33–41.

De Wit, J. N., 1990. Thermal stability and functionality of whey proteins. *Journal of Dairy Science* 73, 3602–3612.

De Wit, J. N., 2009. Thermal behaviour of bovine β-lactoglobulin at temperatures up to 150 °C. a review. *Trends in Food Science & Technology* 20, 27–34.

De Wit, J. N., Klarenbeek, G., 1984. Effects of Various Heat Treatments on Structure and Solubility of Whey Proteins. *Journal of Dairy Science* 67, 2701–2710.

Delgado, Y., Morales-Cruz, M., Figueroa, C. M., Hernández-Román, J., Hernández, G., Griebenow, K., 2015a. The cytotoxicity of BAMLET complexes is due to oleic acid and independent of the α-lactalbumin component. *FEBS open bio* 5, 397–404.

Delgado, Y., Morales-Cruz, M., Hernández-Román, J., Hernández, G., Griebenow, K., 2015b. Development of HAMLET-like cytochrome c-oleic acid nanoparticles for cancer therapy. *Journal of Nanomedicine & Nanotechnology* 6, 1.

Desai, N., Nolting, J. 1995. Microstucture Studies of Reduced-Fat Cheeses Containing Fat Substitute. In Chemistry of Structure-Function Relationships, Springer, Boston, MA, 295–302.

Dickinson, E., Matsumura, Y., 1994. Proteins at liquid interfaces: role of the molten globule state. *Colloids and Surfaces B: Biointerfaces* 3, 1–17.

Dissanayake, M., Ramchandran, L., Donkor, O. N., Vasiljevic, T., 2013a. Denaturation of whey proteins as a function of heat, pH and protein concentration. *International Dairy Journal* 31, 93–99.

Dissanayake, M., Ramchandran, L., Vasiljevic, T., 2013b. Influence of pH and protein concentration on rheological properties of whey protein dispersions. *International Food Research Journal* 20, 2167.

Dobson, C. M., Šali, A., Karplus, M., 1998. Protein folding: a perspective from theory and experiment. *Angewandte Chemie International Edition* 37, 868–893.

Dolgikh, D. A., Gilmanshin, R. I., Brazhnikov, E. V., Bychkova, V. E., Semisotnov, G. V., Venyaminov, S., Ptitsyn, O. B., 1981. Alpha-Lactalbumin: compact state with fluctuating tertiary structure? *FEBS Letters* 136, 311–315.

Dombrowski, J., Gschwendtner, M., Kulozik, U., 2017. Evaluation of structural characteristics determining surface and foaming properties of β-lactoglobulin aggregates. *Colloids and Surfaces A: Physicochemical and Engineering Aspects* 516, 286–295.

Doultani, S., Turhan, K. N., Etzel, M. R., 2004. Fractionation of proteins from whey using cation exchange chromatography. *Process biochemistry* 39, 1737–1743.

Dumpler, J., Wohlschläger, H., Kulozik, U., 2017. Dissociation and coagulation of caseins and whey proteins in concentrated skim milk heated by direct steam injection. *Dairy Science & Technology* 96, 807–826.

El-Sayed, M. M. H., Chase, H. A., 2009. Single and two-component cation-exchange adsorption of the two pure major whey proteins. *Journal of Chromatography A* 1216, 8705–8711.

Erabit, N., Flick, D., Alvarez, G., 2014. Formation of β-lactoglobulin aggregates during thermomechanical treatments under controlled shear and temperature conditions. *Journal of Food Engineering* 120, 57–68.

Erk, A., Luda, B., 2003. Beeinflussung der Schlammkompression in Vollmantelzentrifugen. *Chemie Ingenieur Technik* 75, 1250–1254.

Etzel, M. R., 2004. Manufacture and use of dairy protein fractions. *The Journal of nutrition* 134, 996S-1002S.

Euston, S. R., 2013. Molecular dynamics simulation of the effect of heat on the conformation of bovine β-lactoglobulin A: A comparison of conventional and accelerated methods. *Food Hydrocolloids* 30, 519–530.

Expósito, I. L., Recio, I., 2006. Antibacterial activity of peptides and folding variants from milk proteins. *International Dairy Journal* 16, 1294–1305.

Fernández, A., Menéndez, V., Riera, F. A., 2012. α-Lactalbumin solubilisation from a precipitated whey protein concentrates fraction: pH and calcium concentration effects. *International Journal of Food Science & Technology* 47, 467–474.

Fernández, A., Menéndez, V., Riera, F. A., Álvarez, R., 2011. Caseinomacropeptide behaviour in a whey protein fractionation process based on α-lactalbumin precipitation. *Journal of Dairy Research* 78, 196–202.

Fersht, A. R., 1995. Optimization of rates of protein folding: the nucleation-condensation mechanism and its implications. *Proceedings of the National Academy of Sciences* 92, 10869–10873.

Fitzsimons, S. M., Mulvihill, D. M., Morris, E. R., 2007. Denaturation and aggregation processes in thermal gelation of whey proteins resolved by differential scanning calorimetry. *Food Hydrocolloids* 21, 638–644.

Flashner, M., Ramsden, H., Crane, L. J., 1983. Separation of proteins by high-performance anion-exchange chromatography. *Analytical Biochemistry* 135, 340–344.

Foegeding, E. A., Luck, P. J., Davis, J. P., 2006. Factors determining the physical properties of protein foams. *Food Hydrocolloids* 20, 284–292.

Fox, P. F., Guinee, T. P., Cogan, T. M., McSweeney, P. L. H., 2017. Fundamentals of cheese science, Springer, New York, USA.

Friedman, H. H., Whitney, J. E., Szczesniak, A. S., 1963. The texturometer—a new instrument for objective texture measurement. *Journal of Food Science* 28, 390–396.

Galani, D., Apenten, R. K. O., 1999. Heat-induced denaturation and aggregation of β-Lactoglobulin: kinetics of formation of hydrophobic and disulphide-linked aggregates. *International Journal of Food Science & Technology* 34, 467–476.

Ganju, S., Gogate, P. R., 2017. A review on approaches for efficient recovery of whey proteins from dairy industry effluents. *Journal of Food Engineering* 215, 84–96.

Gast, K., Zirwer, D., Müller-Frohne, M., Damaschun, G., 1998. Compactness of the kinetic molten globule of bovine alpha-lactalbumin: a dynamic light scattering study. *Protein science a publication of the Protein Society* 7, 2004–2011.

Gerberding, S. J., Byers, C. H., 1998. Preparative ion-exchange chromatography of proteins from dairy whey. *Journal of Chromatography A* 808, 141–151.

Gésan-Guiziou, G., Daufin, G., Timmer, M., Allersma, D., van der Horst, C., 1999. Process steps for the preparation of purified fractions of α-lactalbumin and β-lactoglobulin from whey protein concentrates. *Journal of Dairy Research* 66, 225–236.

Gezimati, J., Creamer, L. K., Singh, H., 1997. Heat-induced interactions and gelation of mixtures of β-lactoglobulin and α-lactalbumin. *Journal of Agricultural and Food Chemistry* 45, 1130–1136.

Ghernaout, D., Al-Ghonamy, A. I., Boucherit, A., Ghernaout, B., Naceur, M. W., Messaoudene, N. A., Aichouni, M., Mahjoubi, A. A., Elboughdiri, N. A., 2015. Brownian motion and coagulation process. *American Journal of Environmental Protection* 4, 1–15.

Gimel, J. C., Durand, D., Nicolai, T., 1994. Structure and distribution of aggregates formed after heat-induced denaturation of globular proteins. *Macromolecules* 27, 583–589.

Giraud, I., Franceschi-Messant, S., Perez, E., Lacabanne, C., Dantras, E., 2013. Preparation of aqueous dispersion of thermoplastic sizing agent for carbon fiber by emulsion/solvent evaporation. *Applied Surface Science* 266, 94–99.

Gladman, B., Usher, S. P., Scales, P. J., 2006. Compressive rheology of aggregated particulate suspensions. *Korea-Australia Rheology Journal* 18, 191–197.

Godovac-Zimmermann, J., Krause, I., Baranyi, M., Fischer-Frühholz, S., Juszczak, J., Erhardt, G., Buchberger, J., Klostermeyer, H., 1996. Isolation and rapid sequence characterization of two novel bovine beta-lactoglobulins I and J. *Journal of protein chemistry* 15, 743–750.

Goers, J., Permyakov, S. E., Permyakov, E. A., Uversky, V. N., Fink, A. L., 2002. Conformational prerequisites for α-lactalbumin fibrillation. *Biochemistry* 41, 12546–12551.

Goodall, S., Grandison, A. S., Jauregi, P. J., Price, J., 2008. Selective separation of the major whey proteins using ion exchange membranes. *Journal of Dairy Science* 91, 1–10.

Gottschalk, M., Nilsson, H., Roos, H., Halle, B., 2003. Protein self-association in solution: The bovine β-lactoglobulin dimer and octamer. *Protein science a publication of the Protein Society* 12, 2404–2411.

Grassia, P., Usher, S. P., Scales, P. J., 2008. A simplified parameter extraction technique using batch settling data to estimate suspension material properties in dewatering applications. *Chemical Engineering Science* 63, 1971–1986.

Grassia, P., Usher, S. P., Scales, P. J., 2011. Closed-form solutions for batch settling height from model settling flux functions. *Chemical Engineering Science* 66, 964–972.

Green, M. D., Eberl, M., Landman, K. A., 1996. Compressive yield stress of flocculated suspensions: Determination via experiment. *AIChE Journal* 42, 2308–2318.

Gregory, J., O'Melia, C. R., 1989. Fundamentals of flocculation. *Critical Reviews in Environmental Science and Technology* 19, 185–230.

Grey, V., Mohammed, S. R., Smountas, A. A., Bahlool, R., Lands, L. C., 2003. Improved glutathione status in young adult patients with cystic fibrosis supplemented with whey protein. *Journal of cystic fibrosis official journal of the European Cystic Fibrosis Society* 2, 195–198.

Griffin, W. G., Griffin, M. C. A., Martin, S. R., Price, J., 1993. Molecular basis of thermal aggregation of bovine β-lactoglobulin A. *Journal of the Chemical Society, Faraday Transactions* 89, 3395–3405.

Griko, Y. V., Remeta, D. P., 1999. Energetics of solvent and ligand-induced conformational changes in alpha-lactalbumin. *Protein science a publication of the Protein Society* 8, 554–561.

Guo, M., 2019. Whey protein production, chemistry, functionality, and applications, John Wiley & Sons Ltd, Chichester, UK.

Gurgel, P. V., Carbonell, R. G., Swaisgood, H. E., 2000. Fractionation of whey proteins with a hexapeptide ligand affinity resin. *Bioseparation* 9, 385–392.

Gustafsson, L., Hallgren, O., Mossberg, A.-K., Pettersson, J., Fischer, W., Aronsson, A., Svanborg, C., 2005. HAMLET kills tumor cells by apoptosis: structure, cellular mechanisms, and therapy. *The Journal of nutrition* 135, 1299–1303.

Guyomarc'h, F., Famelart, M.-H., Henry, G., Gulzar, M., Leonil, J., Hamon, P., Bouhallab, S., Croguennec, T., 2015. Current ways to modify the structure of whey proteins for specific functionalities—a review. *Dairy Science & Technology* 95, 795–814.

Hahn, R., Schulz, P. M., Schaupp, C., Jungbauer, A., 1998. Bovine whey fractionation based on cation-exchange chromatography. *Journal of Chromatography A* 795, 277–287.

Håkansson, A., Svensson, M., Mossberg, A.-K., Sabharwal, H., Linse, S., Lazou, I., LoÈnnerdal, B., Svanborg, C., 2000. A folding variant of α-lactalbumin with bactericidal activity against Streptococcus pneumoniae. *Molecular microbiology* 35, 589–600.

Haller, N., Greßlinger, A. S., Kulozik, U., 2021. Separation of aggregated β-lactoglobulin with optimised yield in a decanter centrifuge. *International Dairy Journal* 114, 104918.

Haller, N., Kulozik, U., 2019. Separation of whey protein aggregates by means of continuous centrifugation. *Food and Bioprocess Technology* 12, 1052–1067.

Haller, N., Kulozik, U., 2020. Continuous centrifugal separation of selectively precipitated α-lactalbumin. *International Dairy Journal* 101, 104566.

Hamada, D., Tanaka, T., Tartaglia, G. G., Pawar, A., Vendruscolo, M., Kawamura, M., Tamura, A., Tanaka, N., Dobson, C. M., 2009. Competition between folding, native-state dimerisation and amyloid aggregation in β-lactoglobulin. *Journal of Molecular Biology* 386, 878–890.

Harrison, S. C., Durbin, R., 1985. Is there a single pathway for the folding of a polypeptide chain? *Proceedings of the National Academy of Sciences* 82, 4028–4030.

Havea, P., Singh, H., Creamer, L. K., 2000. Formation of new protein structures in heated mixtures of BSA and α-lactalbumin. *Journal of Agricultural and Food Chemistry* 48, 1548–1556.

Havea, P., Singh, H., Creamer, L. K., 2001. Characterization of heat-induced aggregates of β-lactoglobulin, α-lactalbumin and bovine serum albumin in a whey protein concentrate environment. *Journal of Dairy Research* 68, 483–497.

Heffernan, S. P., Zumaeta, N., Cartland-Glover, G. M., Byrne, E. P., Fitzpatrick, J. J., 2005. Influence of downstream processing on the breakage of whey protein precipitates. *Food and bioproducts processing* 83, 238–244.

Heidebrecht, H.-J., Kulozik, U., 2019. Fractionation of casein micelles and minor proteins by microfiltration in diafiltration mode. Study of the transmission and yield of the immunoglobulins IgG, IgA and IgM. *International Dairy Journal* 93, 1–10.

Heine, W., Radke, M., Wutzke, K. D., Peters, E., Kundt, G., 1996. α-Lactalbumin-enriched low-protein infant formulas: A comparison to breast milk feeding. *Acta Paediatrica* 85, 1024–1028.

Heine, W. E., Klein, P. D., Reeds, P. J., 1991. The importance of alpha-lactalbumin in infant nutrition. *The Journal of nutrition* 121, 277–283.

Hendrix, T., Griko, Y. V., Privalov, P. L., 2000. A calorimetric study of the influence of calcium on the stability of bovine α-lactalbumin. *Biophysical Chemistry* 84, 27–34.

Herceg, Z., Lelas, V., 2005. The influence of temperature and solid matter content on the viscosity of whey protein concentrates and skim milk powder before and after tribomechanical treatment. *Journal of Food Engineering* 66, 433–438.

Hermansson, A.-M., 1975. Functional properties of proteins for foods-flow properties. *Journal of Texture Studies* 5, 425–439.

Hernández-Ledesma, B., Amigo, L., Recio, I., Bartolomé, B., 2007. ACE-inhibitory and radical-scavenging activity of peptides derived from β-lactoglobulin f (19− 25). Interactions with ascorbic acid. *Journal of Agricultural and Food Chemistry* 55, 3392–3397.

Hernández-Ledesma, B., Recio, I., Amigo, L., 2008. β-Lactoglobulin as source of bioactive peptides. *Amino acids* 35, 257–265.

Hillier, R. M., Lyster, R. L. J., 1979. Whey protein denaturation in heated milk and cheese whey. *Journal of Dairy Research* 46, 95–102.

Hinrichs, J., 2001. Incorporation of whey proteins in cheese. *International Dairy Journal* 11, 495–503.

Hiraoka, Y., Segawa, T., Kuwajima, K., Sugai, S., Murai, N., 1980. α-Lactalbumin: A calcium metalloprotein. *Biochemical and Biophysical Research Communications* 95, 1098–1104.

Hirose, M., 1993. Molten globule state of food proteins. *Trends in Food Science & Technology* 4, 48–51.

Hoffmann, M. A. M., van Mil, P. J. J. M., 1997. Heat-Induced Aggregation of β-Lactoglobulin: Role of the Free Thiol Group and Disulfide Bonds. *Journal of Agricultural and Food Chemistry* 45, 2942–2948.

Höfgen, E., Kühne, S., Peuker, U. A., Stickland, A. D., 2019. A comparison of filtration characterisation devices for compressible suspensions using conventional filtration theory and compressional rheology. *Powder Technology* 346, 49–56.

Hogg, R., 2005. Flocculation and dewatering of fine-particle suspensions. *Coagulation and flocculation* 2, 805–849.

Holland, B., Kackmar, J., Corredig, M., 2012. Isolation of a whey fraction rich in α-lactalbumin from skim milk using tangential flow ultrafiltration. *Journal of Dairy Science* 95, 5604–5607.

Hoque, M., Gupta, J., Rabbani, G., Khan, R. H., Saleemuddin, M., 2016. Behaviour of oleic acid-depleted bovine alpha-lactalbumin made LEthal to tumor cells (BAMLET). *Molecular bioSystems* 12, 1871–1880.

Hoque, M., Nanduri, R., Gupta, J., Mahajan, S., Gupta, P., Saleemuddin, M., 2015. Oleic acid complex of bovine α-lactalbumin induces eryptosis in human and other erythrocytes by a Ca2+-independent mechanism. *Biochimica et Biophysica Acta (BBA)-General Subjects* 1850, 1729–1739.

Hosseini-Nia, T., Ismail, A. A., Kubow, S., 2002. Effect of High Hydrostatic Pressure on the Secondary Structures of BSA and Apo-and Holo-α-Lactalbumin Employing Fourier Transform Infrared Spectroscopy. *Journal of Food Science* 67, 1341–1347.

Howells, I., Landman, K. A., Panjkov, A., Sirakoff, C., White, L. R., 1990. Time-dependent batch settling of flocculated suspensions. *Applied Mathematical Modelling* 14, 77–86.

Hsu, D. J., Leshchev, D., Kosheleva, I., Kohlstedt, K. L., Chen, L. X., 2021. Unfolding bovine α-lactalbumin with T-jump: Characterizing disordered intermediates via time-resolved x-ray solution scattering and molecular dynamics simulations. *The Journal of Chemical Physics* 154, 105101.

Hu, H., Wu, J., Li-Chan, E. C. Y., Le Zhu, Zhang, F., Xu, X., Fan, G., Wang, L., Huang, X., Pan, S., 2013. Effects of ultrasound on structural and physical properties of soy protein isolate (SPI) dispersions. *Food Hydrocolloids* 30, 647–655.

Huang, W.-C., Chang, Y.-C., Chen, Y.-M., Hsu, Y.-J., Huang, C.-C., Kan, N.-W., Chen, S.-S., 2017. Whey Protein Improves Marathon-Induced Injury and Exercise Performance in Elite Track Runners. *International journal of medical sciences* 14, 648–654.

Hulmi, J. J., Lockwood, C. M., Stout, J. R., 2010. Effect of protein/essential amino acids and resistance training on skeletal muscle hypertrophy: A case for whey protein. *Nutrition & metabolism* 7, 1–11.

Hussain, R., Gaiani, C., Jeandel, C., Ghanbaja, J., Scher, J., 2012. Combined effect of heat treatment and ionic strength on the functionality of whey proteins. *Journal of Dairy Science* 95, 6260–6273.

Iametti, S., Cairoli, S., Gregori, B. de, Bonomi, F., 1995. Modifications of High-Order Structures upon Heating of. beta.-Lactoglobulin: Dependence on the Protein Concentration. *Journal of Agricultural and Food Chemistry* 43, 53–58.

Ikeda, S., 2003. Atomic force microscopy and Raman scattering spectroscopy studies on heat-induced fibrous aggregates of β-lactoglobulin. *Spectroscopy* 17, 195–202.

Ikeda, S., Morris, V. J., 2002. Fine-Stranded and Particulate Aggregates of Heat-Denatured Whey Proteins Visualized by Atomic Force Microscopy. *Biomacromolecules* 3, 382–389.

Ipsen, R., 2017. Microparticulated whey proteins for improving dairy product texture. *International Dairy Journal* 67, 73–79.

Itzhaki, L. S., Otzen, D. E., Fersht, A. R., 1995. The structure of the transition state for folding of chymotrypsin inhibitor 2 analysed by protein engineering methods: evidence for a nucleation-condensation mechanism for protein folding. *Journal of Molecular Biology* 254, 260–288.

Jabed, A., Wagner, S., McCracken, J., Wells, D. N., Laible, G., 2012. Targeted microRNA expression in dairy cattle directs production of β-lactoglobulin-free, high-casein milk. *Proceedings of the National Academy of Sciences* 109, 16811–16816.

Jakopović, K. L., Cheison, S. C., Kulozik, U., Božanić, R., 2019. Comparison of selective hydrolysis of α-lactalbumin by acid Protease A and Protease M as alternative to pepsin: potential for β-lactoglobulin purification in whey proteins. *The Journal of dairy research* 86, 114–119.

Järvinen, K.-M., Chatchatee, P., Bardina, L., Beyer, K., Sampson, H. A., 2001. IgE and IgG binding epitopes on α-lactalbumin and β-lactoglobulin in cow's milk allergy. *International archives of allergy and immunology* 126, 111–118.

Jaziri, M., Migliore-Samour, D., Casabianca-Pignède, M. R., Keddad, K., Morgat, J. L., Jollès, P., 1992. Specific binding sites on human phagocytic blood cells for Gly-Leu-Phe and Val-Glu-Pro-Ile-Pro-Tyr, immunostimulating peptides from human milk proteins. *Biochimica et biophysica acta* 1160, 251–261.

Jiang, B., Na, J., Wang, L., Li, D., Liu, C., Feng, Z., 2019. Separation and enrichment of antioxidant peptides from whey protein isolate hydrolysate by aqueous two-phase extraction and aqueous two-phase flotation. *Foods* 8, 34.

Jiang, B., Wang, L., Na, J., Zhang, X., Yuan, Y., Liu, C., Feng, Z., 2020. Environmentally-friendly strategy for separation of α-lactalbumin from whey by aqueous two phase flotation. *Arabian Journal of Chemistry* 13, 3391–3402.

Jiang, S., Cheng, J., Jiang, Z., Geng, H., Sun, Y., Sun, C., Hou, J., 2018. Effect of heat treatment on physicochemical and emulsifying properties of polymerized whey protein concentrate and polymerized whey protein isolate. *LWT - Food Science and Technology* 98, 134–140.

Johne, R., 1966. Einfluß der Konzentration einer monodispersen Suspension auf die Sinkgeschwindigkeit ihrer Teilchen. *Chemie Ingenieur Technik* 38, 428–430.

Jost, R., Maire, J.-C., Maynard, F., Secretin, M.-C., 1999. Aspects of whey protein usage in infant nutrition, a brief review. *International Journal of Food Science & Technology* 34, 533–542.

Kalaivani, S., Regupathi, I., 2013. Partitioning studies of α-lactalbumin in environmental friendly poly (ethylene glycol)—citrate salt aqueous two phase systems. *Bioprocess and biosystems engineering* 36, 1475–1483.

Kataoka, M., Kuwajima, K., Tokunaga, F., Goto, Y., 1997. Structural characterization of the molten globule of alpha-lactalbumin by solution X-ray scattering. *Protein science a publication of the Protein Society* 6, 422–430.

Kaye, B. H., Boardman, R. P. 1962. Cluster formation in dilute suspensions. In Proc. Symp. on the Interaction between Fluids and Particles, London, UK, 17–21.

Kehoe, J. J., Wang, L., Morris, E. R., Brodkorb, A., 2011. Formation of non-native β-lactoglobulin during heat-induced denaturation. *Food Biophysics* 6, 487–496.

Kella, N. K. D., Kinsella, J. E., 1988. Enhanced thermodynamic stability of β-lactoglobulin at low pH. A possible mechanism. *Biochemical Journal* 255, 113–118.

Kennel, R., 1994. Hitzeinduzierte Molkenproteinaggregationen-Größenbestimmung und Strukturanalyse, München, Germany.

Keri Marshall, N. D., 2004. Therapeutic applications of whey protein. *Alternative medicine review* 9, 136–156.

Khaldi, M., Croguennec, T., André, C., Ronse, G., Jimenez, M., Bellayer, S., Blanpain-Avet, P., Bouvier, L., Six, T., Bornaz, S., 2018. Effect of the calcium/protein molar ratio on β-lactoglobulin denaturation kinetics and fouling phenomena. *International Dairy Journal* 78, 1–10.

Kiesner, C., Clawin-Rädecker, I., Meisel, H., Buchheim, W., 2000. Manufacturing of α-lactalbumin-enriched whey systems by selective thermal treatment in combination with membrane processes. *Le Lait* 80, 99–111.

Kim, J. I., Du Choi, Y., Row, K. H., 2003. Separation of whey proteins by anion-exchange membranes. *Korean Journal of Chemical Engineering* 20, 538–541.

Kleine, U., Stahl, W., 1989. Model concept of floc disintegration in centrifugal fields. *Chemical Engineering & Technology* 12, 200–204.

Kong, J., Yu, S., 2007. Fourier transform infrared spectroscopic analysis of protein secondary structures. *Acta biochimica et biophysica Sinica* 39, 549–559.

Konrad, G., Kleinschmidt, T., 2008. A new method for isolation of native α-lactalbumin from sweet whey. *International Dairy Journal* 18, 47–54.

Konrad, G., Lieske, B., Faber, W., 2000. A large-scale isolation of native β-lactoglobulin: characterization of physicochemical properties and comparison with other methods. *International Dairy Journal* 10, 713–721.

Koxholt, M., Eisenmann, B., Hinrichs, J., 2000. Effect of process parameters on the structure of ice-cream: possible methods of optimizing traditional freezer technology. *European Dairy Magazine* 12, 27–29.

Koxholt, M., McIntosh, T., Eisenmann, B., 1999. Enhanced stability of ice cream by using particulated whey proteins. *European Dairy Magazine* 10, 14–15.

Krebs, M. R. H., Devlin, G. L., Donald, A. M., 2007. Protein Particulates: Another Generic Form of Protein Aggregation? *Biophysical Journal* 92, 1336–1342.

Krebs, M. R. H., Devlin, G. L., Donald, A. M., 2009. Amyloid fibril-like structure underlies the aggregate structure across the pH range for β-lactoglobulin. *Biophysical Journal* 96, 5013–5019.

Kretser, R. G. de, Boger, D. V., Scales, P. J., 2003. Compressive rheology: an overview. *Rheology reviews*, 125–166.

Kristiansen, K. R., Otte, J., Ipsen, R., Qvist, K. B., 1998. Large-scale preparation of β-lactoglobulin A and B by ultrafiltration and ion-exchange chromatography. *International Dairy Journal* 8, 113–118.

Kroes, M. C. W., van Wingen, G. A., Wittwer, J., Mohajeri, M. H., Kloek, J., Fernández, G., 2014. Food can lift mood by affecting mood-regulating neurocircuits via a serotonergic mechanism. *Neuroimage* 84, 825–832.

Kronman, M. J., Andreotti, R., Vitols, R., 1964. Inter- and intramolecular interactions of alpha-lactalbumin. II. Aggregation reactions at acid pH. *Biochemistry* 3, 1152–1160.

Kronman, M. J., Sinha, S. K., Brew, K., 1981. Characteristics of the binding of Ca2+ and other divalent metal ions to bovine alpha-lactalbumin. *The Journal of biological chemistry* 256, 8582–8587.

Kuhlman, B., Boice, J. A., Wu, W.-J., Fairman, R., Raleigh, D. P., 1997. Calcium binding peptides from α-lactalbumin: Implications for protein folding and stability. *Biochemistry* 36, 4607–4615.

Kuntz, I. D., Kauzmann, W., 1974. Hydration of proteins and polypeptides. *Advances in Protein Chemistry* 28, 239–345.

Kunz, C., Lönnerdal, B., 1989. Human milk proteins: separation of whey proteins and their analysis by polyacrylamide gel electrophoresis, fast protein liquid chromatography (FPLC) gel filtration, and anion-exchange chromatography. *The American journal of clinical nutrition* 49, 464–470.

Kushibiki, S., Hodate, K., Kurisaki, J., Shingu, H., Ueda, Y., Watanabe, A., Shinoda, M., 2001. Effect of beta-lactoglobulin on plasma retinol and triglyceride concentrations, and fatty acid composition in calves. *The Journal of dairy research* 68, 579–586.

Kuwajima, K., 1996. The molten globule state of alpha-lactalbumin. *FASEB journal official publication of the Federation of American Societies for Experimental Biology* 10, 102–109.

Kynch, G. J., 1952. A theory of sedimentation. *Transactions of the Faraday society* 48, 166–176.

Lam, R. S. H., Nickerson, M. T., 2015. The effect of pH and temperature pre-treatments on the physicochemical and emulsifying properties of whey protein isolate. *LWT - Food Science and Technology* 60, 427–434.

Landman, K. A., White, L. R., 1994. Solid/liquid separation of flocculated suspensions. *Advances in Colloid and Interface Science* 51, 175–246.

Langton, M., Hermansson, A.-M., 1992. Fine-stranded and particulate gels of β-lactoglobulin and whey protein at varying pH. *Food Hydrocolloids* 5, 523–539.

Layman, D. K., Lönnerdal, B., Fernstrom, J. D., 2018. Applications for α-lactalbumin in human nutrition. *Nutrition reviews* 76, 444–460.

Le Bon, C., Nicolai, T., Durand, D., 1999. Growth and structure of aggregates of heat-denatured β-Lactoglobulin. *International Journal of Food Science & Technology* 34, 451–465.

Leeb, E., Haller, N., Kulozik, U., 2018. Effect of pH on the reaction mechanism of thermal denaturation and aggregation of bovine β-lactoglobulin. *International Dairy Journal* 78, 103–111.

Lefevre, T., Subirade, M., 2000. Molecular differences in the formation and structure of fine-stranded and particulate β-lactoglobulin gels. *Biopolymers: Original Research on Biomolecules* 54, 578–586.

Leong, Y.-K., Boger, D. V., Scales, P. J., Healy, T. W., Buscall, R., 1993. Control of the rheology of concentrated aqueous colloidal systems by steric and hydrophobic forces. *Journal of the Chemical Society, Chemical Communications*, 639–641.

Lerche, D., Sobisch, T., 2007. Consolidation of concentrated dispersions of nano- and microparticles determined by analytical centrifugation. *Powder Technology* 174, 46–49.

Lerche, D., Sobisch, T., 2014. Evaluation of particle interactions by in situ visualization of separation behaviour. *Colloids and Surfaces A: Physicochemical and Engineering Aspects* 440, 122–130.

Lester, D. R., Usher, S. P., Scales, P. J., 2005. Estimation of the hindered settling function R (φ) from batch-settling tests. *AIChE Journal* 51, 1158–1168.

Levinthal, C (Ed.), 1969. Mossbauer spectroscopy in biological systems.

Lieberman, H. R., Agarwal, S., Fulgoni III, V. L., 2016. Tryptophan intake in the US adult population is not related to liver or kidney function but is associated with depression and sleep outcomes. *The Journal of nutrition* 146, 2609S-2615S.

Lien, E. L., 2003. Infant formulas with increased concentrations of alpha-lactalbumin. *The American journal of clinical nutrition* 77, 1555S-1558S.

Lien, E. L., Davis, A. M., Euler, A. R., Group, M. S., 2004. Growth and safety in term infants fed reduced-protein formula with added bovine alpha-lactalbumin. *Journal of pediatric gastroenterology and nutrition* 38, 170–176.

Lin, M. Y., Lindsay, H._M., Weitz, D. A., Ball, R. C., Klein, R., Meakin, P., 1989. Universality in colloid aggregation. *Nature* 339, 360–362.

Lisak, K., Toro-Sierra, J., Kulozik, U., Božanić, R., Cheison, S. C., 2013. Chymotrypsin selectively digests β-lactoglobulin in whey protein isolate away from enzyme optimal conditions: Potential for native α-lactalbumin purification. *The Journal of dairy research* 80, 14–20.

Loch, J. I., Bonarek, P., Polit, A., Świątek, S., Dziedzicka-Wasylewska, M., Lewiński, K., 2013. The differences in binding 12-carbon aliphatic ligands by bovine β-lactoglobulin isoform A and B studied by isothermal titration calorimetry and X-ray crystallography. *Journal of Molecular Recognition* 26, 357–367.

Loginov, M., Lebovka, N., Vorobiev, E., 2014. Multistage centrifugation method for determination of filtration and consolidation properties of mineral and biological suspensions using the analytical photocentrifuge. *Chemical Engineering Science* 107, 277–289.

Loginov, M., Zierau, A., Kavianpour, D., Lerche, D., Vorobiev, E., Gésan-Guiziou, G., Mahnic-Kalamiza, S., Sobisch, T., 2017. Multistep centrifugal consolidation method for characterization of filterability of aggregated concentrated suspensions. *Separation and Purification Technology* 183, 304–317.

Lönnerdal, B., 2014. Infant formula and infant nutrition: bioactive proteins of human milk and implications for composition of infant formulas. *The American journal of clinical nutrition* 99, 712S-717S.

Lönnerdal, B., Lien, E. L., 2003. Nutritional and physiologic significance of α-lactalbumin in infants. *Nutrition reviews* 61, 295–305.

Lorenzen, P. C., Schrader, K., 2006. A comparative study of the gelation properties of whey protein concentrate and whey protein isolate. *Le Lait* 86, 259–271.

Loveday, S. M., 2016. β-Lactoglobulin heat denaturation: A critical assessment of kinetic modelling. *International Dairy Journal* 52, 92–100.

Lucas, D., Rabiller-Baudry, M., Millesime, L., Chaufer, B., Daufin, G., 1998. Extraction of α-lactalbumin from whey protein concentrate with modified inorganic membranes. *Journal of Membrane Science* 148, 1–12.

Lucena, E. M., Alvarez, S., Menéndez, C., Riera, F. A., Alvarez, R., 2006. Beta-lactoglobulin removal from whey protein concentrates. *Separation and Purification Technology* 52, 310–316.

Lucena, E. M., Alvarez, S., Menéndez, C., Riera, F. A., Alvarez, R., 2007. α-Lactalbumin precipitation from commercial whey protein concentrates. *Separation and Purification Technology* 52, 446–453.

Mailliart, P., Ribadeau-Dumas, B., 1988. Preparation of β-lactoglobulin and p-lactoglobulin-free proteins from whey retentate by NaCl salting out at low pH. *Journal of Food Science* 53, 743–745.

Majekodunmi, S. O., 2015. A review on centrifugation in the pharmaceutical industry. *American Journal of Biomedical Engineering* 5, 67–78.

Majhi, P. R., Ganta, R. R., Vanam, R. P., Seyrek, E., Giger, K., Dubin, P. L., 2006. Electrostatically driven protein aggregation: beta-lactoglobulin at low ionic strength. *Langmuir the ACS journal of surfaces and colloids* 22, 9150–9159.

Mandalari, G., Mackie, A. M., Rigby, N. M., Wickham, M. S. J., Mills, E. N. C., 2009. Physiological phosphatidylcholine protects bovine beta-lactoglobulin from simulated gastrointestinal proteolysis. *Molecular nutrition & food research* 53 Suppl 1, S131-9.

Manderson, G. A., Hardman, M. J., Creamer, L. K., 1999. Effect of heat treatment on bovine beta-lactoglobulin A, B, and C explored using thiol availability and fluorescence. *Journal of Agricultural and Food Chemistry* 47, 3617–3627.

Manji, B., Hill, A., Kakuda, Y., Irvine, D. M., 1985. Rapid separation of milk whey proteins by anion exchange chromatography. *Journal of Dairy Science* 68, 3176–3179.

Marciniak, A., Suwal, S., Brisson, G., Britten, M., Pouliot, Y., Doyen, A., 2019. Evaluation of casein as a binding ligand protein for purification of alpha-lactalbumin from beta-lactoglobulin under high hydrostatic pressure. *Food chmistry* 275, 193–196.

Marella, C., Muthukumarappan, K., Le Metzger, 2011. Evaluation of commercially available, wide-pore ultrafiltration membranes for production of α-lactalbumin–enriched whey protein concentrate. *Journal of Dairy Science* 94, 1165–1175.

Markus, C. R., Jonkman, L. M., Lammers, J. H., Deutz, N. E. P., Messer, M. H., Rigtering, N., 2005. Evening intake of α-lactalbumin increases plasma tryptophan availability and improves morning alertness and brain measures of attention. *The American journal of clinical nutrition* 81, 1026–1033.

Markus, C. R., Olivier, B., Panhuysen, G. E., van der Gugten, J., Alles, M. S., Tuiten, A., Westenberg, H. G., Fekkes, D., Koppeschaar, H. F., Haan, E. E. de, 2000. The bovine protein alpha-lactalbumin increases the plasma ratio of tryptophan to the other large neutral amino acids, and in vulnerable subjects raises brain serotonin activity, reduces

cortisol concentration, and improves mood under stress. *The American journal of clinical nutrition* 71, 1536–1544.

Marshall, A. D., Munro, P. A., Trägårdh, G., 1997. Influence of permeate flux on fouling during the microfiltration of β-lactoglobulin solutions under cross-flow conditions. *Journal of Membrane Science* 130, 23–30.

Martorell-Aragonés, A., Echeverría-Zudaire, L., Alonso-Lebrero, E., Boné-Calvo, J., Martín-Muñoz, M. F., Nevot-Falcó, S., Piquer-Gibert, M., Valdesoiro-Navarrete, L., 2015. Position document: IgE-mediated cow's milk allergy. *Allergologia et immunopathologia* 43, 507–526.

Maté, J. I., Krochta, J. M., 1994. β-Lactoglobulin separation from whey protein isolate on a large scale. *Journal of Food Science* 59, 1111–1114.

Matsudomi, N., Oshita, T., Sasaki, E., Kobayashi, K., 1992. Enhanced heat-induced gelation of β-lactoglobulin by α-lactalbumin. *Bioscience, biotechnology, and biochemistry* 56, 1697–1700.

Maubois, J. L., Pierre, A., Fauquant, J., Piot, M., 1987. Industrial fractionation of main whey proteins. *International Dairy Federation* 212, 154–159.

Maybury, J. P., Hoare, M., Dunnill, P., 2000. The use of laboratory centrifugation studies to predict performance of industrial machines: Studies of shear-insensitive and shear-sensitive materials. *Biotechnology and Bioengineering* 67, 265–273.

McGuffey, M. K., Epting, K. L., Kelly, R. M., Foegeding, E. A., 2005. Denaturation and aggregation of three α-lactalbumin preparations at neutral pH. *Journal of Agricultural and Food Chemistry* 53, 3182–3190.

McIntosh, G. H., Regester, G. O., Le Leu, R. K., Royle, P. J., Smithers, G. W., 1995. Dairy proteins protect against dimethylhydrazine-induced intestinal cancers in rats. *The Journal of nutrition* 125, 809–816.

McKenzie, H. A., 1967. Milk proteins. *Advances in Protein Chemistry* 22, 55–234.

McSwiney, M., Singh, H., Campanella, O., Creamer, L. K., 1994a. Thermal gelation and denaturation of bovine β-lactoglobulins A and B. *Journal of Dairy Research* 61, 221–232.

McSwiney, M., Singh, H., Campanella, O. H., 1994b. Thermal aggregation and gelation of bovine β-lactoglobulin. *Food Hydrocolloids* 8, 441–453.

Mehra, R., Kelly, P. M., 2004. Whey protein fractionation using cascade membrane filtration. *Bulletin-International Dairy Federation*, 40–44.

Menesklou, P., Sinn, T., Nirschl, H., Gleiss, M., 2021. Scale-Up of Decanter Centrifuges for The Particle Separation and Mechanical Dewatering in The Minerals Processing Industry by Means of A Numerical Process Model. *Minerals* 11, 229.

Merkl, R., Steiger, W., 2012. Properties of decanter centrifuges in the mining industry. *Mining, Metallurgy & Exploration* 29, 6–12.

Metsämuuronen, S., Nyström, M., 2009. Enrichment of α-lactalbumin from diluted whey with polymeric ultrafiltration membranes. *Journal of Membrane Science* 337, 248–256.

Meyer, A., Berensmeier, S., Franzreb, M., 2007. Direct capture of lactoferrin from whey using magnetic micro-ion exchangers in combination with high-gradient magnetic separation. *Reactive and Functional Polymers* 67, 1577–1588.

Micke, P., Beeh, K. M., Buhl, R., 2002. Effects of long-term supplementation with whey proteins on plasma glutathione levels of HIV-infected patients. *European journal of nutrition* 41, 12–18.

Mirza, S., Richardson, J. F., 1979. Sedimentation of suspensions of particles of two or more sizes. *Chemical Engineering Science* 34, 447–454.

Montilla, A., Casal, E., Moreno, F. J., Belloque, J., Olano, A., Corzo, N., 2007. Isolation of bovine β-lactoglobulin from complexes with chitosan. *International Dairy Journal* 17, 459–464.

Morison, K. R., Mackay, F. M., 2001. Viscosity of lactose and whey protein solutions. *International Journal of Food Properties* 4, 441–454.

Mourouzidis-Mourouzis, S. A., Karabelas, A. J., 2008. Whey protein fouling of large pore-size ceramic microfiltration membranes at small cross-flow velocity. *Journal of Membrane Science* 323, 17–27.

Mullally, M. M., Meisel, H., FitzGerald, R. J., 1997. Angiotensin-I-converting enzyme inhibitory activities of gastric and pancreatic proteinase digests of whey proteins. *International Dairy Journal* 7, 299–303.

Muller, A., Chaufer, B., Merin, U., Daufin, G., 2003a. Prepurification of α-lactalbumin with ultrafiltration ceramic membranes from acid casein whey: Study of operating conditions. *Le Lait* 83, 111–129.

Muller, A., Chaufer, B., Merin, U., Daufin, G., 2003b. Purification of α-lactalbumin from a prepurified acid whey: Ultrafiltration or precipitation. *Le Lait* 83, 439–451.

Mulvihill, D., Donovan, M., 1987. Whey proteins and their thermal denaturation-a review. *Irish Journal of Food Science and Technology* 11, 43–75.

Mulvihill, D. M., Kinsella, J. E., 1988. Gelation of β-lactoglobulin: effects of sodium chloride and calcium chloride on the rheological and structural properties of gels. *Journal of Food Science* 53, 231–236.

Munro, P. A., van Til, H. J., 1988. Centrifugal dewatering of acid casein curd: Effect of casein manufacturing and centrifugation variables on curd compression in a laboratory centrifuge. *Biotechnology and Bioengineering* 32, 1153–1157.

Muuronen, K., Partanen, R., Heidebrecht, H.-J., Kulozik, U., 2021. Effects of conventional processing methods on whey proteins in production of native whey powder. *International Dairy Journal* 116, 104959.

Nagaoka, S., Futamura, Y., Miwa, K., Awano, T., Yamauchi, K., Kanamaru, Y., Tadashi, K., Kuwata, T., 2001. Identification of novel hypocholesterolemic peptides derived from bovine milk β-lactoglobulin. *Biochemical and Biophysical Research Communications* 281, 11–17.

Nath, A., Zin, M. M., Molnár, M. A., Bánvölgyi, S., Gáspár, I., Vatai, G., Koris, A., 2022. Membrane Chromatography and Fractionation of Proteins from Whey—A Review. *Processes* 10, 1025.

Navis, M., Muncan, V., Sangild, P. T., Møller Willumsen, L., Koelink, P. J., Wildenberg, M. E., Abrahamse, E., Thymann, T., van Elburg, R. M., Renes, I. B., 2020a. Beneficial effect of mildly pasteurized whey protein on intestinal integrity and innate defense in preterm and near-term piglets. *Nutrients* 12, 1125.

Navis, M., Schwebel, L., Soendergaard Kappel, S., Muncan, V., Sangild, P. T., Abrahamse, E., Aunsholt, L., Thymann, T., van Elburg, R. M., Renes, I. B., 2020b. Mildly pasteurized whey protein promotes gut tolerance in immature piglets compared with extensively heated whey protein. *Nutrients* 12, 3391.

Neurath, A. R., Debnath, A. K., Strick, N., Li, Y. Y., Lin, K., Jiang, S., 1997. 3-hydroxy-phthaloyl-β-lactoglobulin. I. Optimization of production and comparison with other compounds considered for chemoprophylaxis of mucosally transmitted human immunodeficiency virus type 1. *Antiviral Chemistry and Chemotherapy* 8, 131–139.

Neyestani, T. R., Djalali, M., Pezeshki, M., 2003. Isolation of α-lactalbumin, β-lactoglobulin, and bovine serum albumin from cow's milk using gel filtration and anion-exchange chromatography including evaluation of their antigenicity. *Protein Expression and Purification* 29, 202–208.

Ng, T. B., Cheung, R. C. F., Wong, J. H., Wang, Y., Ip, D. T. M., Wan, D. C. C., Xia, J., 2015. Antiviral activities of whey proteins. *Applied microbiology and biotechnology* 99, 6997–7008.

Nicolai, T., Britten, M., Schmitt, C., 2011. β-Lactoglobulin and WPI aggregates: Formation, structure and applications. *Food Hydrocolloids* 25, 1945–1962.

Nicorescu, I., Loisel, C., Vial, C., Riaublanc, A., Djelveh, G., Cuvelier, G., Legrand, J., 2008. Combined effect of dynamic heat treatment and ionic strength on denaturation and aggregation of whey proteins – Part I. *Food Research International* 41, 707–713.

Noyelle, K., van Dael, H., 2002. Kinetics of conformational changes induced by the binding of various metal ions to bovine alpha-lactalbumin. *Journal of inorganic biochemistry* 88, 69–76.

Nozaki, Y., Bunville, L. G., Tanford, C., 1959. Hydrogen ion titration curves of β-Lactoglobulin1. *Journal of the American Chemical Society* 81, 5523–5529.

O'Kennedy, B. T., Mounsey, J. S., Murphy, F., Pesquera, L., Mehra, R., 2006. Preferential heat-induced denaturation of bovine β-lactoglobulin variants as influenced by pH. *Milchwissenschaft* 61, 366–369.

Olivares, M. L., Shahrivar, K., Vicente, J. de, 2019. Soft lubrication characteristics of microparticulated whey proteins used as fat replacers in dairy systems. *Journal of Food Engineering* 245, 157–165.

Oliveira, K. M. G., Valente-Mesquita, V. L., Botelho, M. M., Sawyer, L., Ferreira, S. T., Polikarpov, I., 2001. Crystal structures of bovine β-lactoglobulin in the orthorhombic space group C2221: Structural differences between genetic variants A and B and features of the Tanford transition. *European Journal of Biochemistry* 268, 477–484.

O'Loughlin, I. B., Kelly, P. M., Murray, B. A., FitzGerald, R. J., Brodkorb, A., 2015. Concentrated whey protein ingredients: A Fourier transformed infrared spectroscopy investigation of thermally induced denaturation. *International Journal of Dairy Technology* 68, 349–356.

Ortiz-Chao, P., Gómez-Ruiz, J. A., Rastall, R. A., Mills, D., Cramer, R., Pihlanto, A., Korhonen, H., Jauregi, P., 2009. Production of novel ACE inhibitory peptides from β-lactoglobulin using Protease N Amano. *International Dairy Journal* 19, 69–76.

Ounis, W. B., Gauthier, S. F., Turgeon, S. L., Roufik, S., Pouliot, Y., 2008. Separation of minor protein components from whey protein isolates by heparin affinity chromatography. *International Dairy Journal* 18, 1043–1050.

Outinen, M., Tossavainen, O., Syväoja, E.-L., 1996. Chromatographic fractionation of α-lactalbumin and β-lactoglobulin with polystyrenic strongly basic anion exchange resins. *LWT - Food Science and Technology* 29, 340–343.

Ouwehand, A. C., Salminen, S. J., Skurnik, M., Conway, P. L., 1997. Inhibition of pathogen adhesion by β-lactoglobulin. *International Dairy Journal* 7, 685–692.

Pansri, S., 2012. Atomistic Simulations for Investigating Structural Stability and Selecting Initial Adsorption Orientation of Lysozyme and Apo-α-Lactalbumin at Hydrophobic and Hydrophilic Surfaces., Edmonton, Alberta, Canada.

Papiz, M. Z., Sawyer, L., Eliopoulos, E. E., North, A. C., Findlay, J. B., Sivaprasadarao, R., Jones, T. A., Newcomer, M. E., Kraulis, P. J., 1986. The structure of beta-lactoglobulin and its similarity to plasma retinol-binding protein. *Nature* 324, 383–385.

Park, K. H., Lund, D. B., 1984. Calorimetric study of thermal denaturation of β-lactoglobulin. *Journal of Dairy Science* 67, 1699–1706.

Patel, S., 2015. Emerging trends in nutraceutical applications of whey protein and its derivatives. *Journal of food science and technology* 52, 6847–6858.

Patocka, G., Cervenkova, R., Narine, S., Jelen, P., 2006. Rheological behaviour of dairy products as affected by soluble whey protein isolate. *International Dairy Journal* 16, 399–405.

Pearce, R. J., 1983. Thermal separation of [beta]-Lactoglobulin and [alpha]-Lactalbumin in bovine cheddar cheese whey. *Australian Journal of Dairy Technology* 38, 144.

Pearce, R. J., 1987. Fractionation of whey proteins. *Australian Journal of Dairy Technology* 42, 75.

Pearce, R. J., 1991. Applications for cheese whey protein fractions. *Food Research Quarterly* 51, 74–85.

Pedersen, J. B., Fojan, P., Sorensen, J., Petersen, S. B., 2006. Towards control of aggregational behaviour of α-lactalbumin at acidic pH. *Journal of Fluorescence* 16, 611–621.

Pedersen, L., Mollerup, J., Hansen, E., Jungbauer, A., 2003. Whey proteins as a model system for chromatographic separation of proteins. *Journal of chromatography B* 790, 161–173.

Pelegrine, D. H.G., Gasparetto, C. A., 2005. Whey proteins solubility as function of temperature and pH. *LWT - Food Science and Technology* 38, 77–80.

Pellegrini, A., Thomas, U., Bramaz, N., Hunziker, P., Fellenberg, R. von, 1999. Isolation and identification of three bactericidal domains in the bovine α-lactalbumin molecule. *Biochimica et Biophysica Acta (BBA)-General Subjects* 1426, 439–448.

Peng, Z.-y., Wu, L. C., Kim, P. S., 1995. Local Structural Preferences in the. alpha.-Lactalbumin Molten Globule. *Biochemistry* 34, 3248–3252.

Perez, M. D., Sanchez, L., Aranda, P., Ena, J. M., Oria, R., Calvo, M., 1992. Effect of beta-lactoglobulin on the activity of pregastric lipase. A possible role for this protein in ruminant milk. *Biochimica et biophysica acta* 1123, 151–155.

Pérez-Cano, F. J., Marín-Gallén, S., Castell, M., Rodríguez-Palmero, M., Rivero, M., Franch, A., Castellote, C., 2007. Bovine whey protein concentrate supplementation modulates maturation of immune system in suckling rats. *British Journal of Nutrition* 98, S80-S84.

Permyakov, E. A., 2020. α-Lactalbumin, Amazing Calcium-Binding Protein. *Biomolecules* 10, 1210.

Permyakov, E. A., Berliner, L. J., 2000. α-Lactalbumin: Structure and function. *FEBS Letters* 473, 269–274.

Permyakov, E. A., Morozova, L. A., Burstein, E. A., 1985. Cation binding effects on the pH, thermal and urea denaturation transitions in alpha-lactalbumin. *Biophysical Chemistry* 21, 21–31.

Permyakov, E. A., Yarmolenko, V. V., Kalinichenko, L. P., Morozova, L. A., Burstein, E. A., 1981. Calcium binding to alpha-lactalbumin: structural rearrangement and association constant evaluation by means of intrinsic protein fluorescence changes. *Biochemical and Biophysical Research Communications* 100, 191–197.

Péron, N., Heffernan, S. P., Byrne, E. P., Rioual, F., Fitzpatrick, J. J., 2007. Characterization of the fragmentation of protein aggregates in suspension subjected to flow. *Chemical Engineering Science* 62, 6440–6450.

Perreault, V., Rémillard, N., Chabot, D., Morin, P., Pouliot, Y., Britten, M., 2017. Effect of denatured whey protein concentrate and its fractions on cheese composition and rheological properties. *Journal of Dairy Science* 100, 5139–5152.

Petersen, H., Nomayo, A., Zelenka, R., Foster, J., Tvrdík, J., Jochum, F., 2020. Adequacy and safety of α-lactalbumin–enriched low-protein infant formula: A randomized controlled trial. *Nutrition* 74, 110728.

Petit, J., Herbig, A.-L., Moreau, A., Delaplace, G., 2011. Influence of calcium on β-lactoglobulin denaturation kinetics: Implications in unfolding and aggregation mechanisms. *Journal of Dairy Science* 94, 5794–5810.

Petit, J., Moreau, A., Ronse, G., Debreyne, P., Bouvier, L., Blanpain-Avet, P., Jeantet, R., Delaplace, G., 2016. Role of whey components in the kinetics and thermodynamics of β-Lactoglobulin unfolding and aggregation. *Food and Bioprocess Technology* 9, 1367–1379.

Phillips, S. M., Tang, J. E., Moore, D. R., 2009. The role of milk- and soy-based protein in support of muscle protein synthesis and muscle protein accretion in young and elderly persons. *Journal of the American College of Nutrition* 28, 343–354.

Pierre, A., Fauquant, J., 1986. Principes pour un procédé industriel de fractionnement des protéines du lactosérum. *Le Lait* 66, 405–419.

Plock, J., 1994. Zum Einfluß von Lactose auf die Denaturierung von Molkenproteinen in Molkenkonzentrat und auf die Ausbildung thermisch induzierter Gelstrukturen, VDI-Verlag, München, Germany.

Prussick, R., Prussick, L., Gutman, J., 2013. Psoriasis improvement in patients using glutathione-enhancing, nondenatured whey protein isolate: A pilot study. *The Journal of Clinical and Aesthetic Dermatology* 6, 23.

Ptitsyn, O. B., Uversky, V. N., 1994. The molten globule is a third thermodynamical state of protein molecules. *FEBS Letters* 341, 15–18.

Puyol, P., Perez, M. D., Sanchez, L., Ena, J. M., Calvo, M., 1995. Uptake and passage of beta-lactoglobulin, palmitic acid and retinol across the Caco-2 monolayer. *Biochimica et biophysica acta* 1236, 149–154.

Qi, X. L., Holt, C., McNulty, D., CLARKE, D. T., BROWNLOW, S., Jones, G. R., 1997. Effect of temperature on the secondary structure of β-lactoglobulin at pH 6.7, as determined by CD and IR spectroscopy: a test of the molten globule hypothesis. *Biochemical Journal* 324, 341–346.

Qin, B. Y., Bewley, M. C., Creamer, L. K., Baker, H. M., Baker, E. N., Jameson, G. B., 1998. Structural basis of the Tanford transition of bovine beta-lactoglobulin. *Biochemistry* 37, 14014–14023.

Rammer, P., Groth-Pedersen, L., Kirkegaard, T., Daugaard, M., Rytter, A., Szyniarowski, P., Høyer-Hansen, M., Povlsen, L. K., Nylandsted, J., Larsen, J. E., 2010. BAMLET

activates a lysosomal cell death program in cancer cells. *Molecular cancer therapeutics* 9, 24–32.

Ramos, Ó. L., Pereira, J. O., Silva, S. I., Amorim, M. M., Fernandes, J. C., Lopes-da-Silva, J. A., Pintado, M. E., Malcata, F. X., 2012. Effect of composition of commercial whey protein preparations upon gelation at various pH values. *Food Research International* 48, 681–689.

Rantamäki, P., Tossavainen, O., Outinen, M., Tupasela, T., Koskela, P., Kaunismäki, M., 2000. Functional properties of the whey protein fractions produced in pilot scale processes. Foaming, water-holding capacity and gelation. *Milchwissenschaft* 55, 569–572.

Records, A., Sutherland, K., 2001. Decanter centrifuge handbook, Elsevier Advanced Technology, Oxford, UK.

Redfield, C., Schulman, B. A., Milhollen, M. A., Kim, P. S., Dobson, C. M., 1999. Alpha-lactalbumin forms a compact molten globule in the absence of disulfide bonds. *Nature structural biology* 6, 948–952.

Reithel, F. J., Kelly, M. J., 1971. Thermodynamic analysis of the monomer-dimer association of. beta.-lactoglobulin A at the isoelectric point. *Biochemistry* 10, 2639–2644.

Richardson, J. F., Zaki, W. N., 1954. The sedimentation of a suspension of uniform spheres under conditions of viscous flow. *Chemical Engineering Science* 3, 65–73.

Roefs, S. P. F. M., Kruif, K. G. de, 1994. A Model for the Denaturation and Aggregation of β-Lactoglobulin. *European Journal of Biochemistry* 226, 883–889.

Rose, G. D., Geselowitz, A. R., Lesser, G. J., Lee, R. H., Zehfus, M. H., 1985. Hydrophobicity of amino acid residues in globular proteins. *Science* 229, 834–838.

Rösner, H. I., Redfield, C., 2009. The human alpha-lactalbumin molten globule: comparison of structural preferences at pH 2 and pH 7. *Journal of Molecular Biology* 394, 351–362.

Rozé, J.-C., Barbarot, S., Butel, M.-J., Kapel, N., Waligora-Dupriet, A.-J., Montgolfier, I. de, Leblanc, M., Godon, N., Soulaines, P., Darmaun, D., 2012. An α-lactalbumin-enriched and symbiotic-supplemented v. a standard infant formula: a multicentre, double-blind, randomised trial. *British Journal of Nutrition* 107, 1616–1622.

Rumpus, J. M., 1997. Dawatering and scale down of solid recovery in industrial centrifuges, University of London, London, UK.

Russo, E., Scicchitano, F., Citraro, R., Aiello, R., Camastra, C., Mainardi, P., Chimirri, S., Perucca, E., Donato, G., Sarro, G. de, 2012. Protective activity of α-lactoalbumin (ALAC), a whey protein rich in tryptophan, in rodent models of epileptogenesis. *Neuroscience* 226, 282–288.

Ryan, K. N., Vardhanabhuti, B., Jaramillo, D. P., van Zanten, J. H., Coupland, J. N., Foegeding, E. A., 2012. Stability and mechanism of whey protein soluble aggregates thermally treated with salts. *Food Hydrocolloids* 27, 411–420.

Sali, A., Shakhnovich, E., Karplus, M., 1994. How does a protein fold? *Nature* 369, 248–251.

Santos, M. J., Teixeira, J. A., Rodrigues, L. R., 2012. Fractionation of the major whey proteins and isolation of β-Lactoglobulin variants by anion exchange chromatography. *Separation and Purification Technology* 90, 133–139.

Saufi, S. M., Fee, C. J., 2009. Fractionation of β-lactoglobulin from whey by mixed matrix membrane ion exchange chromatography. *Biotechnology and Bioengineering* 103, 138–147.

Saufi, S. M., Fee, C. J., 2011. Simultaneous anion and cation exchange chromatography of whey proteins using a customizable mixed matrix membrane. *Journal of Chromatography A* 1218, 9003–9009.

Sawyer, L., James, M. N. G., 1982. Carboxyl–carboxylate interactions in proteins. *Nature* 295, 79–80.

Sawyer, L., Kontopidis, G., 2000. The core lipocalin, bovine beta-lactoglobulin. *Biochimica et biophysica acta* 1482, 136–148.

Scales, P. J., Johnson, S. B., Healy, T. W., Kapur, P. C., 1998. Shear yield stress of partially flocculated colloidal suspensions. *AIChE Journal* 44, 538–544.

Scales, P. J., Johnson, S. B., Kapur, P. C., 2000. The influence of surface chemistry on the rheology and flow of flocculated particulate suspensions. *Mineral Procesing and Extractive Metallurgy Review* 20, 27–40.

Schmitt, C., Bovay, C., Rouvet, M., Shojaei-Rami, S., Kolodziejczyk, E., 2007. Whey protein soluble aggregates from heating with NaCl: physicochemical, interfacial, and foaming properties. *Langmuir the ACS journal of surfaces and colloids* 23, 4155–4166.

Schmitz-Schug, I., 2014. Improving the nutritional quality of dairy powders–analyzing and modeling lysine loss during spray drying as influenced by drying kinetics, thermal stress, physical state and molecular mobility, Technische Universität München, München, Germany.

Schokker, E. P., Singh, H., Creamer, L. K., 2000. Heat-induced aggregation of β-lactoglobulin A and B with α-lactalbumin. *International Dairy Journal* 10, 843–853.

Schubert, T., Meric, A., Boom, R., Hinrichs, J., Atamer, Z., 2018. Application of a decanter centrifuge for casein fractionation on pilot scale: Effect of operational parameters on total solid, purity and yield in solid discharge. *International Dairy Journal* 84, 6–14.

Schultz, C. P., 2000. Illuminating folding intermediates. *Nature structural biology* 7, 7 -10.

Selo, I., Clément, G., Bernard, H., Chatel, J., Créminon, C., Peltre, G., Wal, J., 1999. Allergy to bovine beta-lactoglobulin: specificity of human IgE to tryptic peptides. *Clinical and experimental allergy: journal of the British Society for Allergy and Clinical Immunology* 29, 1055–1063.

Silber, B. Y., Schmitt, J. A.J., 2010. Effects of tryptophan loading on human cognition, mood, and sleep. *Neuroscience & biobehavioral reviews* 34, 387–407.

Singer, N. S., Dunn, J. M., 1990. Protein microparticulation: the principle and the process. *Journal of the American College of Nutrition* 9, 388–397.

Skinner, S. J., Stickland, A. D., Cavalida, R. G., Usher, S. P., Scales, P. J. Sewage sludge dewatering properties for predicting performance of industrial thickeners, centrifuges and filters. In Asia Pacific Confederation of Chemical Engineering Congress 2015: APCChE 2015, incorporating CHEMECA 2015, Engineers Australia Melbourne, 2174–2185.

Skudder, P. J., 1985. Evaluation of a porous silica-based ion-exchange medium for the production of protein fractions from rennet-and acid-whey. *Journal of Dairy Research* 52, 167–181.

Smith, L. J., Jones, R. M., van Gunsteren, W. F., 2005. Characterization of the denaturation of human alpha-lactalbumin in urea by molecular dynamics simulations. *Proteins* 58, 439–449.

Smithers, G. W., 2008. Whey and whey proteins—From 'gutter-to-gold'. *International Dairy Journal* 18, 695–704.

Smithers, G. W., 2015. Whey-ing up the options–Yesterday, today and tomorrow. *International Dairy Journal* 48, 2–14.

Smoluchowski, M. v., 1918. Versuch einer mathematischen Theorie der Koagulationskinetik kolloider Lösungen. *Zeitschrift für physikalische Chemie* 92, 129–168.

Snijders, T., Res, P. T., Smeets, J. S. J., van Vliet, S., van Kranenburg, J., Maase, K., Kies, A. K., Verdijk, L. B., van Loon, L. J. C., 2015. Protein Ingestion before Sleep Increases Muscle Mass and Strength Gains during Prolonged Resistance-Type Exercise Training in Healthy Young Men. *The Journal of nutrition* 145, 1178–1184.

Sobisch, T., Lerche, D., 2000. Application of a new separation analyzer for the characterization of dispersions stabilized with clay derivatives. *Colloid and Polymer Science* 278, 369–374.

Spiegel, T., 1999a. Thermische Denaturierung und Aggregation von Molkenproteinen in Ultrafiltrationsmolkenkonzentraten: Reaktionskinetik und Pratikulierung im Schabewärmetauscher, Shaker Verlag, Aachen, Germany.

Spiegel, T., 1999b. Whey protein aggregation under shear conditions – effects of lactose and heating temperature on aggregate size and structure. *International Journal of Food Science & Technology* 34, 523–531.

Splitt, H., Mackenstedt, I., Freitag, R., 1996. Preparative membrane adsorber chromatography for the isolation of cow milk components. *Journal of Chromatography A* 729, 87–97.

Stahl, W. H., 2004. Fest-Flüssig-Trennung. 2, Industrie-Zentrifugen. Maschinen-& Verfahrenstechnik, DrM Press, Männedorf, Switzerland.

Stănciuc, N., Aprodu, I., Râpeanu, G., Bahrim, G., 2013. pH-and heat-induced structural changes of bovine α-lactalbumin in response to oleic acid binding. *European Food Research and Technology* 236, 257–266.

Stănciuc, N., Râpeanu, G., 2010. An overview of bovine α-lactalbumin structure and functionality. *The Annals of the University Dunarea de Jos of Galati. Fascicle VI-Food Technology* 34, 82–93.

Stănciuc, N., Râpeanu, G., Bahrim, G., Aprodu, I., 2012. pH and heat-induced structural changes of bovine apo-α-lactalbumin. *Food Chemistry* 131, 956–963.

Steinhauer, T., Marx, M., Bogendörfer, K., Kulozik, U., 2015. Membrane fouling during ultra-and microfiltration of whey and whey proteins at different environmental conditions: The role of aggregated whey proteins as fouling initiators. *Journal of Membrane Science* 489, 20–27.

Stiborsky, M., Herlawanto, R., Rabold, F., 2003. Modeling the drying of granular materials in a decanter. *Chemie Ingenieur Technik* 75, 1259–1264.

Stickland, A. D., Kretser, R. G. de, Scales, P. J., 2005. Nontraditional constant pressure filtration behavior. *AIChE Journal* 51, 2481–2488.

Sturaro, A., Marchi, M. de, Zorzi, E., Cassandro, M., 2015. Effect of microparticulated whey protein concentration and protein-to-fat ratio on Caciotta cheese yield and composition. *International Dairy Journal* 48, 46–52.

Sun, Z., Wang, M., Han, S., Ma, S., Zou, Z., Ding, F., Li, X., Li, L., Tang, B., Wang, H., 2018. Production of hypoallergenic milk from DNA-free beta-lactoglobulin (BLG) gene knockout cow using zinc-finger nucleases mRNA. *Scientific reports* 8, 1–11.

Tanford, C., Bunville, L. G., Nozaki, Y., 1959. The reversible transformation of β-lactoglobulin at pH 7.51. *Journal of the American Chemical Society* 81, 4032–4036.

Tang, Q., Munro, P. A., McCarthy, O. J., 1993. Rheology of whey protein concentrate solutions as a function of concentration, temperature, pH and salt concentration. *Journal of Dairy Research* 60, 349–361.

Tanger, C., Quintana Ramos, P., Kulozik, U., 2021. Comparative assessment of thermal aggregation of whey, potato, and pea protein under shear stress for microparticulation. *ACS Food Science & Technology* 1, 975–985.

Tarapata, J., Dybowska, B. E., Zulewska, J., 2022. Evaluation of fouling during ultrafiltration process of acid and sweet whey. *Journal of Food Engineering* 328, 111059.

Tavel, L., Moreau, C., Bouhallab, S., Li-Chan, E. C. Y., Guichard, E., 2010. Interactions between aroma compounds and β-lactoglobulin in the heat-induced molten globule state. *Food Chemistry* 119, 1550–1556.

Thomas, D. N., Judd, S. J., Fawcett, N., 1999. Flocculation modelling: a review. *Water research* 33, 1579–1592.

Timasheff, S. N., Townend, R., 1964. Structure of the β-lactoglobulin tetramer. *Nature* 203, 517–519.

Tipton, K. D., Elliott, T. A., Cree, M. G., Aarsland, A. A., Sanford, A. P., Wolfe, R. R., 2007. Stimulation of net muscle protein synthesis by whey protein ingestion before and after exercise. *American journal of physiology. Endocrinology and metabolism* 292, E71-6.

Tolkach, A., 2008. Thermisches Denaturierungsverhalten von Molkenproteinfraktionen: selektive Denaturierung-Fraktionierung mit Membranen-Reaktions-, Auffaltungs-und Aggregationskinetik, Verlag Dr. Hut, München, Germany.

Tolkach, A., Kulozik, U., 2008. Kinetic modeling of the thermal denaturation of bovine alpha-Lactalbumin in a acidic pH-region and in the presence of a calcium complexing agent. *Chemie Ingenieur Technik* 80, 1165–1173.

Tolkach, A., Steinle, S., Kulozik, U., 2005. Optimization of Thermal Pretreatment Conditions for the Separation of Native α-Lactalbumin from Whey Protein Concentrates by Means of Selective Denaturation of β-Lactoglobulin. *Journal of Food Science* 70, 557–566.

Toro-Sierra, J., 2016. On the separation, thermal and shear induced modification, and study of the functional properties of the major whey protein fractions, Technische Universität München, München, Germany.

Toro-Sierra, J., Tolkach, A., Kulozik, U., 2013. Fractionation of α-Lactalbumin and β-Lactoglobulin from Whey Protein Isolate Using Selective Thermal Aggregation, an Optimized Membrane Separation Procedure and Resolubilization Techniques at Pilot Plant Scale. *Food and Bioprocess Technology* 6, 1032–1043.

Torres, I. C., Amigo, J. M., Knudsen, J. C., Tolkach, A., Mikkelsen, B. Ø., Ipsen, R., 2018. Rheology and microstructure of low-fat yoghurt produced with whey protein microparticles as fat replacer. *International Dairy Journal* 81, 62–71.

Trabulsi, J., Capeding, R., Lebumfacil, J., Ramanujam, K., Feng, P., McSweeney, S., Harris, B., DeRusso, P., 2011. Effect of an α-lactalbumin-enriched infant formula with lower protein on growth. *European journal of clinical nutrition* 65, 167–174.

Troullier, A., Reinstädler, D., Dupont, Y., Naumann, D., Forge, V., 2000. Transient non-native secondary structures during the refolding of α-lactalbumin detected by infrared spectroscopy. *Nature structural biology* 7, 78–86.

Tunick, M. H. 2008. Whey protein production and utilization: a brief history. In Whey Processing, Wiley & Sons, Ames, Iowa, USA, 1–13.

Turhan, K. N., Etzel, 2004. Whey Protein Isolate and α-Lactalbumin Recovery from Lactic Acid Whey Using Cation-Exchange Chromatography. *Journal of Food Science* 69, fep66-fep70.

Ulrichs, T., Drotleff, A. M., Ternes, W., 2015. Determination of heat-induced changes in the protein secondary structure of reconstituted livetins (water-soluble proteins from hen's egg yolk) by FTIR. *Food Chemistry* 172, 909–920.

Usher, S. P., Scales, P. J., 2005. Steady state thickener modelling from the compressive yield stress and hindered settling function. *Chemical Engineering Journal* 111, 253–261.

Usher, S. P., Studer, L. J., Wall, R. C., Scales, P. J., 2013. Characterisation of dewaterability from equilibrium and transient centrifugation test data. *Chemical Engineering Science* 93, 277–291.

van Dael, H., Tieghem, E., Haezebrouck, P., van Cauwelaert, F., 1992. Conformational aspects of the Cu2+ binding to alpha-lactalbumin. Characterization and stability of the Cu-bound state. *Biophysical Chemistry* 42, 235–242.

van Deventer, B. B. G., Usher, S. P., Kumar, A., Rudman, M., Scales, P. J., 2011. Aggregate densification and batch settling. *Chemical Engineering Journal* 171, 141–151.

Vanderheeren, G., Hanssens, I., 1994. Thermal unfolding of bovine alpha-lactalbumin. Comparison of circular dichroism with hydrophobicity measurements. *The Journal of biological chemistry* 269, 7090–7094.

Vanhooren, A., Chedad, A., Farkas, V., Majer, Z., Joniau, M., van Dael, H., Hanssens, I., 2005. Tryptophan to phenylalanine substitutions allow differentiation of short-and long-range conformational changes during denaturation of goat α-lactalbumin. *Proteins: Structure, Function, and Bioinformatics* 60, 118–130.

Veeken, A. H.M., Hamelers, H. V.M., 1999. Removal of heavy metals from sewage sludge by extraction with organic acids. *Water Science and Technology* 40, 129–136.

Veprintsev, D. B., Permyakov, E. A., Kalinichenko, L. P., Berliner, L. J., 1996. Pb2+ and Hg2+ binding to alpha-lactalbumin. *Biochemistry and molecular biology international* 39, 1255–1265.

Veprintsev, D. B., Permyakov, S. E., Permyakov, E. A., Rogov, V. V., Cawthern, K. M., Berliner, L. J., 1997. Cooperative thermal transitions of bovine and human apo-alpha-lactalbumins: evidence for a new intermediate state. *FEBS Letters* 412, 625–628.

Verheul, M., Roefs, S. P. F. M., Kruif, K. G. de, 1998. Kinetics of heat-induced aggregation of β-lactoglobulin. *Journal of Agricultural and Food Chemistry* 46, 896–903.

Voswinkel, L., Kulozik, U., 2011. Fractionation of whey proteins by means of membrane adsorption chromatography. *Procedia Food Science* 1, 900–907.

Voswinkel, L., Kulozik, U., 2013. Membrane based chromatography creates added value in sweet whey. *European Diary Magazine* 25, 4–6.

Voswinkel, L., Kulozik, U., 2014. Fractionation of all major and minor whey proteins with radial flow membrane adsorption chromatography at lab and pilot scale. *International Dairy Journal* 39, 209–214.

Vyas, H. K., Izco, J. M., Jimenez-Flores, R., 2002. Scale-up of native β-lactoglobulin affinity separation process. *Journal of Dairy Science* 85, 1639–1645.

Wakeman, R. J., 2007. Separation technologies for sludge dewatering. *Journal of Hazardous Materials* 144, 614–619.

Wang, Q., Swaisgood, H. E., 1993. Characteristics of β-lactoglobulin binding to the all-trans-retinal moiety covalently immobilized on Celite™. *Journal of Dairy Science* 76, 1895–1901.

Wang, Y., Zhao, J., Zhang, W., Liu, C., Jauregi, P., Huang, M., 2020. Modification of heat-induced whey protein gels by basic amino acids. *Food Hydrocolloids* 100, 105397.

Ward, P. N., Hoare, M. 1990. The dewatering of biological suspensions in industrial centrifuges. In Separations for Biotechnology 2, Springer, Dordrecht, Netherlands, 93–101.

Weinbrenner, W. F., Etzel, M. R., 1994. Competitive adsorption of α-lactalbumin and bovine serum albumin to a sulfopropyl ion-exchange membrane. *Journal of Chromatography A* 662, 414–419.

Wijesinha-Bettoni, R., Gao, C., Jenkins, J. A., Mackie, A. R., Wilde, P. J., Mills, E. C., Smith, L. J., 2007. Heat treatment of bovine α-lactalbumin results in partially folded, disulfide bond shuffled states with enhanced surface activity. *Biochemistry* 46, 9774–9784.

Wolz, M., Kulozik, U., 2015. Thermal denaturation kinetics of whey proteins at high protein concentrations. *International Dairy Journal* 49, 95–101.

Wyand, M. S., Manson, K. H., Miller, C. J., Neurath, A. R., 1999. Effect of 3-hydroxy-phthaloyl-β-lactoglobulin on vaginal transmission of simian immunodeficiency virus in rhesus monkeys. *Antimicrobial agents and chemotherapy* 43, 978–980.

Xie, D., Bhakuni, V., Freire, E., 1993. Are the molten globule and the unfolded states of apo-alpha-lactalbumin enthalpically equivalent? *Journal of Molecular Biology* 232, 5–8.

Yada, R. Y., 2018. Proteins in food processing. (2 ed.), Woodhead publishing, Elsevier, Duxford, UK.

Yan, Y., Seeman, D., Zheng, B., Kizilay, E., Xu, Y., Dubin, P. L., 2013. pH-Dependent aggregation and disaggregation of native β-lactoglobulin in low salt. *Langmuir the ACS journal of surfaces and colloids* 29, 4584–4593.

Yang, J., Dunker, A. K., Powers, J. R., Clark, S., Swanson, B. G., 2001. β-Lactoglobulin molten globule induced by high pressure. *Journal of Agricultural and Food Chemistry* 49, 3236–3243.

Ye, X., Yoshida, S., Ng, T. B., 2000. Isolation of lactoperoxidase, lactoferrin, α-lactalbumin, β-lactoglobulin B and β-lactoglobulin A from bovine rennet whey using ion exchange chromatography. *The international journal of biochemistry & cell biology* 32, 1143–1150.

Yutani, K., Ogasahara, K., Kuwajima, K., 1992. Absence of the thermal transition in apo-alpha-lactalbumin in the molten globule state. A study by differential scanning microcalorimetry. *Journal of Molecular Biology* 228, 347–350.

Zhong, H., Gilmanshin, R., Callender, R., 1999. An FTIR study of the complex melting behavior of α-lactalbumin. *The Journal of Physical Chemistry B* 103, 3947–3953.

Zumaeta, N., Cartland-Glover, G. M., Heffernan, S. P., Byrne, E. P., Fitzpatrick, J. J., 2005. Breakage model development and application with CFD for predicting breakage of whey protein precipitate particles. *Chemical Engineering Science* 60, 3443–3452.

Zuniga, R. N., Tolkach, A., Kulozik, U., Aguilera, J. M., 2010. Kinetics of formation and physicochemical characterization of thermally-induced β-lactoglobulin aggregates. *Journal of Food Science* 75, E261-E268.